A Concept of Renewable Energy Plant-Storage Capacity Sizing for Integration into Electrical Distribution Network

Von der Fakultät für Maschinenbau, Elektro- und Energiesysteme der Brandenburgischen Technischen Universität Cottbus-Senftenberg zur Erlangung des akademischen Grades eines Doktors der Ingenieurwissenschaften genehmigte

Dissertation

vorgelegt von

Master of Science

Xoese Kobla Nanewortor

geboren am 18. Januar 1983 in Kumasi, Ghana

Vorsitzender:	Prof. Dr. –Ing. Gerhard Lappus
Gutachter:	Gastprofessor Dr. –Ing. Przemyslaw Janik
Gutachter:	Prof. Dr. –Ing. Harald Schwarz

Tag der mündlichen Prüfung:	15. Juni 2016

Abstract

Energy demand of continents, countries, communities and individuals will continue to increase in the phase of increasing population and improvement in the living standards of people. The attempt to meet this ever increasing demand and at the same time protect the environment has resulted in the fast growth of power generation from renewable sources of energy especially from wind through wind power plants and solar through photovoltaic power plants. This growth has been facilitated by various support schemes such as feed-in-tariff scheme, feed-in-premium and quota scheme. Further growth is expected in the future. This is because of the existing support schemes and the expectation of the emergence of improved technologies for harvesting renewable energy.

This development of power generation from renewable sources of energy although positive also lead to some distinctive negative effects on the existing electrical network to which they are connected. These negative effects are known and well documented. The fluctuating nature of wind and solar radiation at any given location over a given period of observation is seen to translate into the power they feed into the power network. This fluctuating infeed requires more active management of the network by system operators so as to ensure continuous reliable power generation and delivery. The management process sometimes lead to non-utilization of power produced by the renewables sources. Secondly, expansion and reinforcement of some existing networks are needed in other to accommodate renewable power generators. These come at a cost. Many studies and researches have been dedicated to finding solutions to these issues.

This work agrees with the use of storage systems as means of solving these issues but the question that remains unanswered is what the optimal way is. There is also a further push given to the view of installing renewable energy plants together with storage systems as a unit in this work. The main task presented in this work, however, is a concept of sizing renewable energy plant and storage systems as a unit. The resulting renewable energy plant-storage unit has the objective of supporting the electrical network to which it will be connected. Firstly the support should be by reducing the fluctuating effect from renewable

production. Secondly by helping improve the load hosting capacity of the electrical network. This will be by supplying the part of the load demand leading to the reduction of the overall power drawn by connected loads from the electrical power network.

Historic data of renewable resource and also the load demand at the point or bus of connection are the drivers of this concept. With the earlier mentioned objectives and random or stochastic nature of data involved, particle swarm optimization method is employed in implementing the concept of sizing to arrive at an optimal solution of required sizes of the renewable energy plant-storage system.

The concept of sizing is based on proposing an ideal load demand that can be supplied by a utility under normal operating condition at all time. It follows that any extra demand should be supplied by the optimally sized renewable energy plant-storage unit. In this work sizing results of three scenarios presented. A single node network with three different types of the load was used in testing the effect of optimally sized renewable energy plant-storage system on an electrical network. The outcome of this test showed that the optimally sized renewable energy storage-system improved the ability of the test electrical network to support additional load hence load hosting capacity of test network was improved. The process required modelling and simulation all of which were carried out using MATLAB Simulink software.

keywords: Renewable Energy, Wind Power Plant, Photovoltaics, Particle Swam Optimization, Load hosting capacity, MATLAB Simulink

Abstrakt

Der Energiebedarf von Kontinenten, Ländern, Gemeinden und Einzelpersonen wird sich mit wachsender Bevölkerungszahl und steigendem Lebensstandard auch weiterhin erhöhen. Das Vorhaben, dieser ständig zunehmenden Nachfrage gerecht zu werden und zugleich die Umwelt zu schützen, hat zum schnellen Wachstum der Stromerzeugung aus erneuerbaren Energiequellen geführt. Die Nutzung von Windenergie mit Hilfe von Windkraftanlagen und von Solarenergie durch Photovoltaikanlagen ist dabei von besonderer Bedeutung. Dieses Wachstum wurde unterstützt durch verschiedene Förderregelungen wie dem Feed-in Tariffs scheme, dem Feed-in Premium und der Quotenregelungen. Für die Zukunft wird eine weitere Steigerung für diesen Bereich prognostiziert. Die bestehenden Förderregelungen und die zu erwartenden Verbesserungen in den Technologien zur Gewinnung erneuerbarer Energie legen dies nahe.

Diese generell positive Entwicklung der Stromerzeugung aus erneuerbaren Energiequellen führt jedoch auch zu einigen markanten negativen Auswirkungen auf das bestehende elektrische Netz. Diese negativen Effekte sind bekannt und gut dokumentiert. Durch die über einen bestimmten Beobachtungszeitraum durchgeführte Aufzeichnung der fluktuierenden Charakteristik von Windgeschwindigkeiten und Sonneneinstrahlung kann für einen beliebigen Ort die entsprechende in das Stromnetz eingespeiste Energiemenge bestimmt werden. Diese zeitlich variierende Einspeisung erfordert in höherem Maße eine aktive Überwachung bzw. Steuerung des Netzes durch die Netzbetreiber um die kontinuierliche zuverlässige Stromerzeugung und -lieferung zu gewährleisten. Der Steuerungsprozess führt in einigen Fällen zur Nichtnutzung des durch erneuerbare Energien erzeugten Stroms. Des Weiteren wird die Erweiterung und Verstärkung einiger bestehender Netze benötigt um weitere erneuerbare Energieerzeuger einzubinden. Dieser Ausbau verursacht Kosten. Viele Forschungsstudien arbeiten an den Lösungen für diese Herausforderungen.

Das Ergebnis dieser Arbeit bestätigt die Verwendung von Speichersystemen als ein Mittel

zur Lösung der aufgeführten Probleme, beantwortet jedoch nicht die Frage nach dem optimalen Weg. Die Installation von Anlagen zur Erzeugung erneuerbarer Energie und deren Kopplung mit Speichersystemen wird in der Arbeit aufgegriffen. Das Hauptaugenmerk liegt hierbei auf einem Konzept zur Dimensionierung der Einheit aus erneuerbaren Energieanlagen und Speichersystemen. Die sich daraus ergebende erneuerbare Energieanlage-Speicher-Einheit hat das Ziel, das mit ihr verbundene Stromnetz zu unterstützen. Dies wird erstens durch die Reduzierung des fluktuierenden Effektes der erneuerbaren Energie-Produktion und zweitens durch die Verbesserung der Netzkapazität erreicht. Dieses geschieht indem ein Teil der benötigten Energiemenge durch angeschlossene Speicher bereitgestellt wird, wodurch der Leistungsbezug aus dem Stromnetz reduziert wird.

Historische Daten der erneuerbaren Energiequellen und auch der Energienachfrage an Verbindungspunkten oder –leitungen sind grundlegend für dieses Konzept Mittels den zuvor genannten Angaben und dem Einsatz zufälliger oder stochastischer Daten, sowie der Anwendung der „particle swarm“-Optimierung, welches ein stochastisches Verfahren ist, kann ein Konzept zur Berechnung der optimalen Lösung der erforderlichen Größen des REP-S-System erlangt werden.

Das Konzept der Optimierung basiert auf der Annahme eines idealisierten Energiebedarfs unter normalen Betriebsbedingungen. Diese Daten können vom Energieversorger bereitgestellt werden. Weiterer Energiebedarf soll durch die optimale Größe der REP-S-Einheit geliefert werden. In dieser Arbeit werden Sizing Optimierungs-Ergebnisse von drei Szenarien dargestellt. Ein einzelnes Knotennetz mit drei verschiedenen Arten des Energiebedarfes wurde genutzt um die Wirkung der optimierten Größe des REP-S-System auf ein elektrisches Netz zu prüfen. Das Ergebnis dieses Tests zeigte, dass die optimale Größe des REP-S-Systems die Fähigkeit des Testnetzes zusätzlichen Bedarf zu auszugleichen steigert und somit die Kapazität des Testnetzes verbessert wurde. Unter Verwendung von MATLAB Simulink-Software wurden die für den Prozess notwendigen Simulationen und Modellierungen durchgeführt.

Stichworte: Erneuerbare Energie, Windkraftanlagen, Photovoltaik, Particle Swarm Optimierung, Lastaufnahmekapazität, MATLAB Simulink

List of Acronyms and Abbreviations

RES	Renewable Energy Source
OECD	Organization for Economic Co-operation and Development
EC	European Commission
IEA	International Energy Agency
GW	Gigawatt
TWh	Tera-watthour
EU	European Union
UN	United Nations
RES-E	Electricity from Renewable Energy Source
MV	Medium Voltage
LV	Low Voltage
PV	Photovoltaic
REP	Renewable Energy Plant
FIT	Feed-in-Tariffs
FIP	Feed-in-Premiums
KfW	Kreditanstalt für Wiederaufbau
DG	Decentralized Generation
EEG	Erneuerbare-Energie-Gesetz
REP-S	Renewable Energy-Storage
TSOs	Transmission System Operators
DSOs	Distribution System Operators
EESS	Electrical Energy Storage System
SM	Smart Meters
AMI	Artificial Metering Infrastructure
ENEL	Ente Nazionale per L'energia Elettrica
EnWG	Energie Wirtshaftgesetz (German Energy Industry Act)
kWh	Kilowatthour

V2G	Vehicle-to-Grid
SG	Smart Grid
MW	Megawatt
CIGRE	Conseil International des Grands Réseaux Électriques (International Council on Large Electric Systems)
ADNs	Active Distribution Networks
ADSs	Active Distribution Systems
DERs	Distributed Energy Resources
Tx	Transformer
Kn	Electrical Network Bus
VDE	Verband der Elektrotechnik, Elektronik und Informationstechnik
SERF	Solar Energy Research Field
BTU	Brandenburg University of Technology
kW	Kilowatt
DWD	Deutscher Wetterdienst
FMPA	Forschungs- und Materialprüfanstalt
DIN	Deutsches Institut für Normung
IEC	International Electrotechnical Commission
PCC	Point of Common Coupling
GA	Genetic Algorithm
PSO	Particle Swan Optimization

Table of Content

1. Introduction

1.1 Developing Trend in primary energy source for Electricity Generation

The conventional way of generating electricity is by an electro-mechanical generator which is usually driven by steam generated by fossil or nuclear source of energy.The modern steam turbine invented in 1884 by Sir Charles Parsons still generates up to about 80 % of the world's electricity [1], [2]. Environmental concerns of the present day resulting in change in energy policy direction of organizations, unions and countries has led to the ever increasing share of generation from alternative and renewable sources of primary energy. Some of these primary sources such as hydro; extracting energy from water at a height, wind; extracting energy from volume of moving air and solar; by extracting heat energy, nowadays drive electro – mechanical generators. Another contributing factor to the above mentioned observation has been as a result of available technologies for the extraction process and the reasonable economic returns. For instance increasing capacities of wind turbine can attributed to increase in rotor diameter. Wider rotor diameter is due to newly found strong but light materials (carbon fibre).

The generation of electricity over the past three decades has also seen generation from photovoltaics, biomass, geothermal and tidal waves as a result of above mentioned reasons Figure 1-1, Figure 1-2, Figure 1-3 and Figure 1-4 show the trends in installed capacity of power plants and electricity production by fuel types in Germany and the European Union (Data from [3], [4]).

The above mentioned development is expected to continue in the in the decades to come. This is because discussions on the further integration of environmentally friendly renewable energy sources (RES) into the electrical energy mix with the aim of reducing electricity from conventional non-environmentally friendly sources is ongoing. The electricity sector is and will continue to play a major role through the integration of renewable energy sources [5].

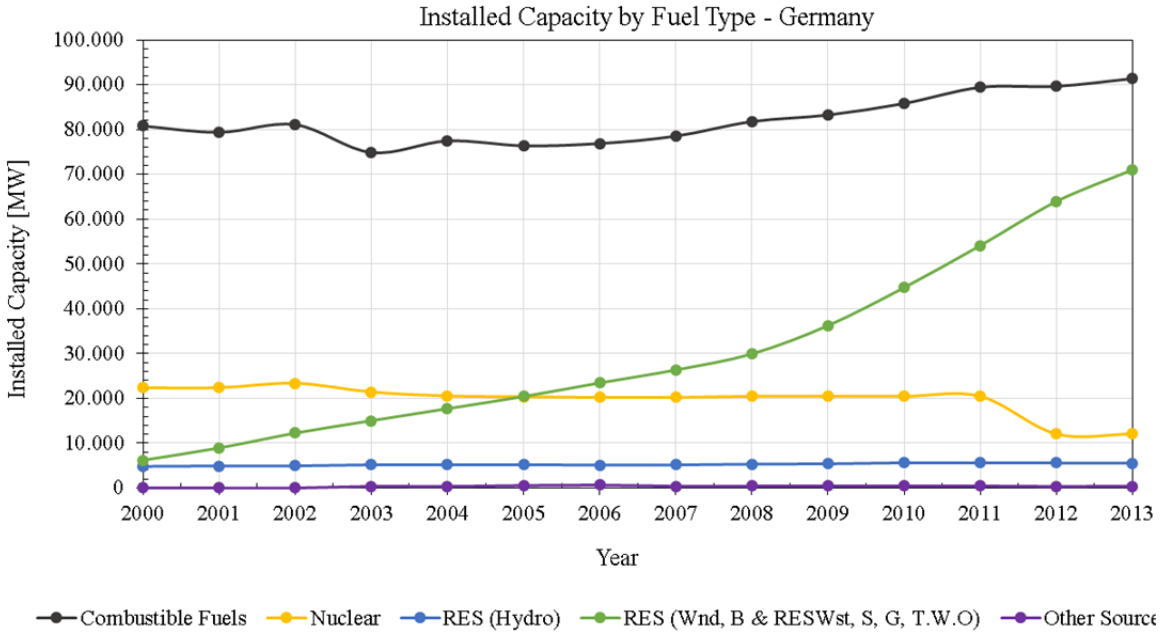

Figure 1-1: Total Installed Capacity by fuel type for Germany (Data from [3], [4]; Plot by Author)

This evolving landscape observed is also seen to be driven by these factors:

- security of supply for the respective economy and consumers
- energy price affordability and
- Climate protection policy adoption.

For instance, countries in the European Union import more than half total energy consumed in a year. This includes a portion of primary energy that will be used in the production of electricity. To safeguard the supply of electricity, the EU came up with some obligations. This is the *"Directive 2005/89/EC"*. Diversity in electricity generation which sees the introduction of RES generators, promotion of energy efficiency technologies, expansion of transmission and distribution networks are parts of the directives to ensure security of supply [6], [7].

According to [3], the estimated share of RES (hydro and non-hydro) stood at 22.9 % by end of 2014. Compared with year 2013, an increment of 2.9 % was seen to have resulted. Data from the International Energy Agency (IEA) showing total yearly electricity production by fuel type for countries of Organisation for Economic Co-operation and Development

(OECD) listed 671 TWh as electricity produce from non-hydro RES at the end of 2014. This accounted for about 6.6 % of production [4].

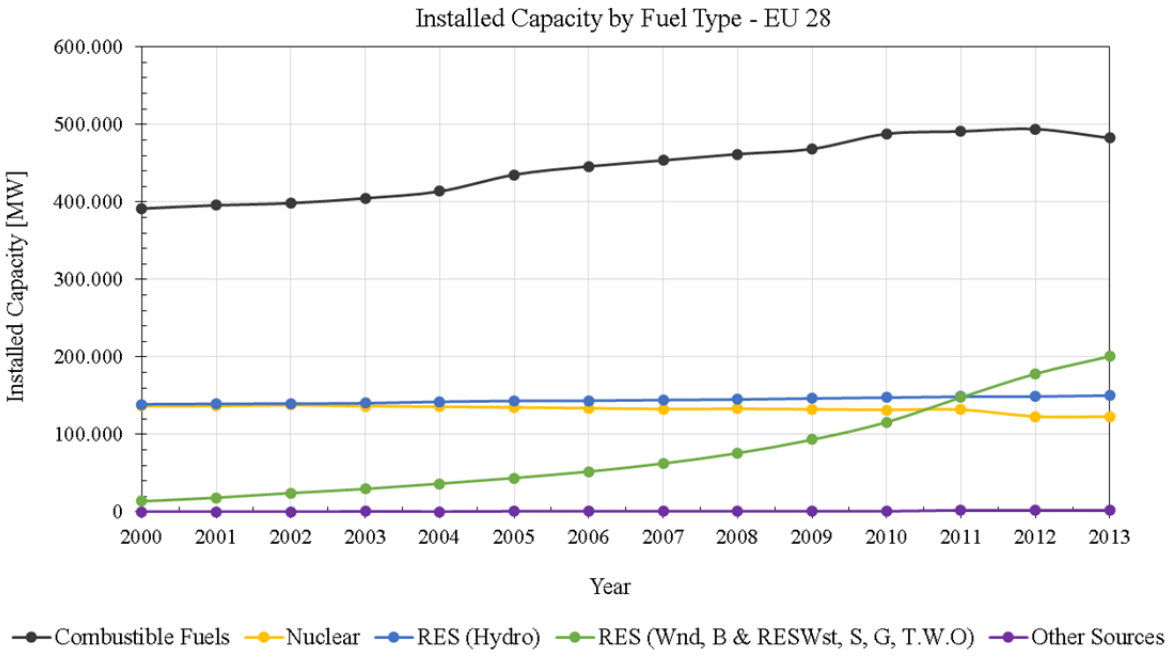

Figure 1-2: Cumulative Installed Capacity by fuel type for the EU (Data from [3], [4]; Plot by Author)

A total electricity of about 484 TWh and 129 TWh form non-hydro RES accounting for about 15 % and 20 % of total generated electricity was recorded in 2013 for EU 28 and Germany respectively [4], [8], [9].

The observed increment in electricity production is parallel to increased installed capacity of RES power plant over a period of thirteen year as seen. As seen in Figure 1-1 and Figure 1-2, the installed capacity for non-Hydro RES power plants stood at about 200.8 GW and 71 GW for EU 28 and Germany respectively by the end of 2013. The two most important RES sources (Wind and Solar) driving the RES industry contributes substantially to the share of RES in electricity production. The share of wind power plants stood at 117.9 GW (58.7 % of total installed capacity of non-Hydro RES power) for EU 28 and 34.7 GW (48.8 % of total installed capacity of non-Hydro RES power) for Germany. On the other hand solar contributed 79.6 GW (39.6 %) and 36.3 GW (51.2 %) of installed non-hydro RE power plants for EU and Germany respectively [9], [10].

The increasing trends observed in plots of Figure 1-1 to Figure 1-4 are as already mentioned a result of policy directions and targets of unions and organizations such as the EU, United Nations (UN) and individual countries such as Germany, Japan, United States of America etc. For instance, the EU in accordance with Directive 2009/28/EC has set a 20/20/20 target with timeline spanning up to 2020.This target simply means consuming 20 % of final energy from RES, reducing greenhouse gas emissions by 20 % and achieving 20 % energy savings.

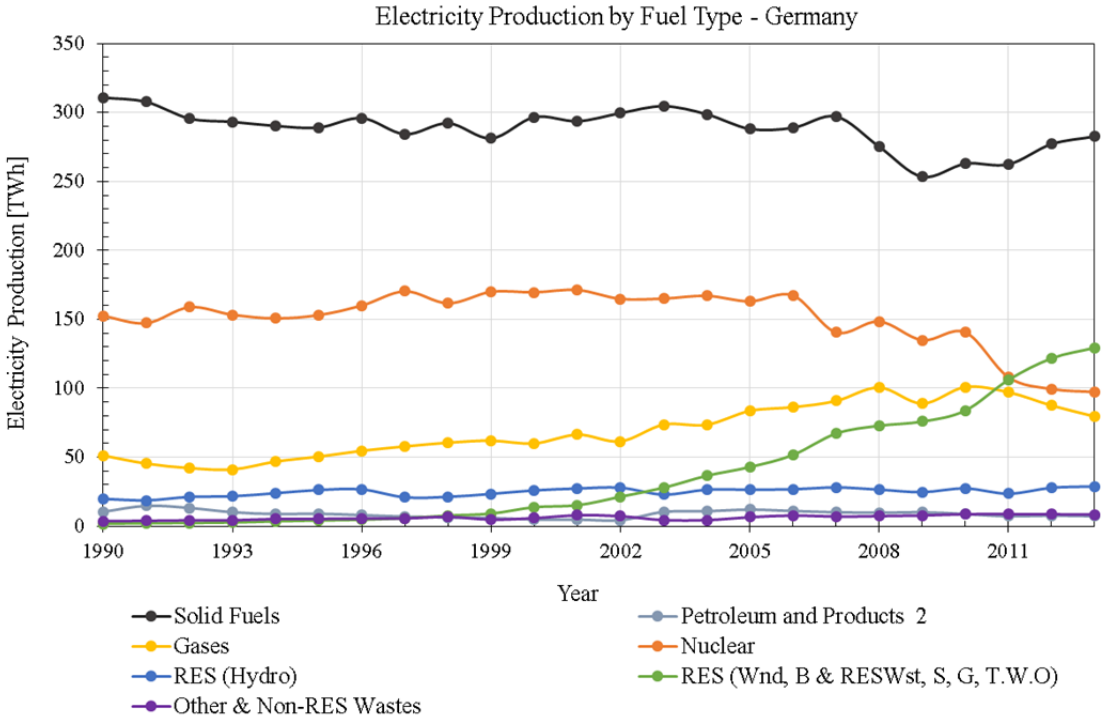

Figure 1-3: Total Electricity production by fuel type for Germany (Data from [3], [4]; Plot by Author)

To achieve this set target EU Member States submitted documents stating their expected forecast ranging from 10 % to 49 % of final energy consumption [9], [11]. A status report indicated that, the efforts of Member States will result in exceeding the 20 % target by 0.3 % Ten Member States including Germany and Spain are expecting surplus (2 % of needed RES) while five expects deficit by 2020 compared with binding target set by them. EU countries have agreed on new target of cutting in greenhouse gas emissions by 40 % requiring increase of RES shares in final energy consumption to 27 % and level of energy savings to 25 % by 2030 [11]. Saudi Arabia among other countries has formulated energy policy that has a goal of increasing the share of installed capacity of electricity from

renewable energy sources (RES-E) to 54 GW by 2032 [12].

Increase in energy consumption or demand requires the production of energy of equal proportion. This may sometimes require the addition of generation capacity. This increasing trend in energy consumption observed in preceding figures is evident of the fact that more and more countries are faced with the reality of meeting increasing energy demand. The increase consumption of electronic gadgets ranging from mobile phones to electronic books, electronic toothbrushes to game consoles etc. and in the area of mobility ranging from electric bicycles to electric cars, increases with population hence increase in energy demand.

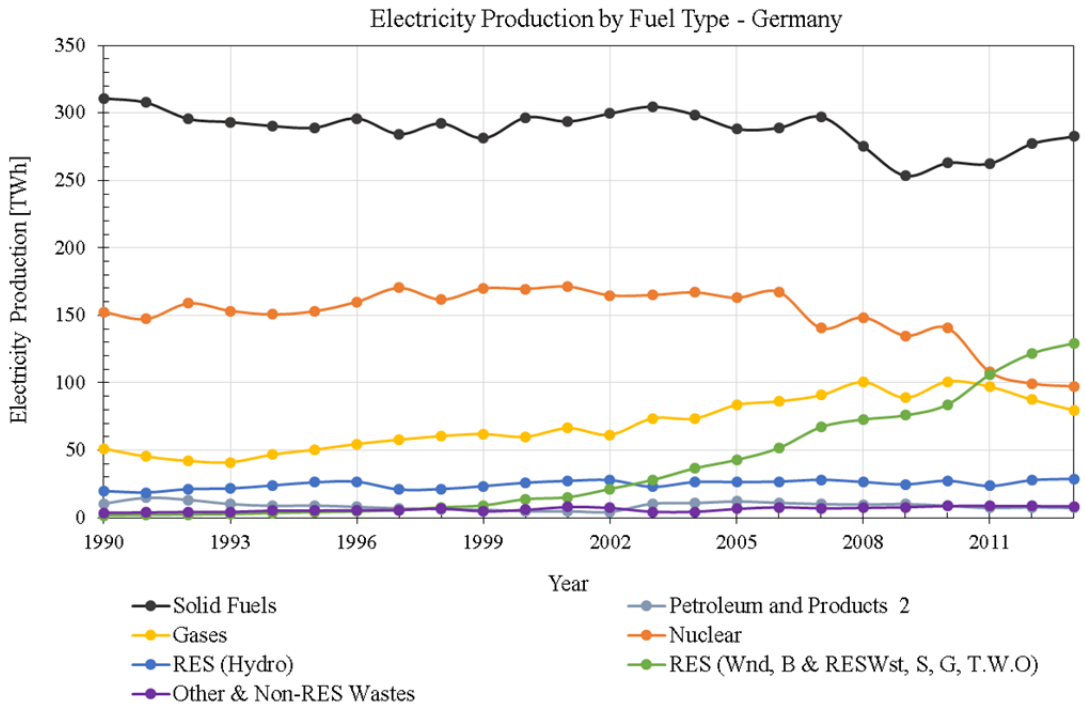

Figure 1-4: Total Electricity production by fuel type for EU 28 (Data from [3], [4]; Plot by Author)

In 2009, V. Fthenakis together with his collaborators published a Solar Grand Plan that demonstrated the feasibility of renewable energy supplying the US with 69% of electricity demand by 2050. This when implemented or followed could result in the reduction of CO_2 by about 60 % of levels observed in 2005 [13].

1.2 RES in Distribution Network

Higher proportion of RES power plant installations are located at medium to low voltage levels of the electric network. As at the end of 2012, the total installed RES power plants in Germany totalled 69.6 GW and distributed among the four Transmission system operators as depicted in Table 1-1. About 21.18 GW (30.4 %) of the total sum is located in the 50 Hertz transmission controlled area.

Table 1-1: Installed Capacity of RES in Germany by end of 2012

German TSO	PV [MW]	Wind [MW] (Onshore)	Wind[MW] (Offshore)	Hydro [MW]	Biomass[MW]	Total [GW]
50 Hertz	6.755	12.620	48	159	1.585	21.167
Amprion	7.323	5.511	0	369	1.108	14.311
TenneT	12.827	12.112	220	576	2.423	28.158
TransnetBW	4.493	586	0	302	626	6.007
Total	31.398	30.829	268	1.406	5.742	69.643

The updated value of total installed RES plant in 50 Hertz transmission control area in 2014 was about 24.13 GW. About 51 % of these located in the medium voltage (MV) and Low voltage (LV) levels. Based on data from [14] resulting in plot found in Figure 1-5, about 81 % of installed RES power plants are located in MV and LV level. A look at share of RES on the bases of type revealed that, Wind and PV power plants in the 50 Hertz control area contributed a total of 22.14 GW of power amounting a percentage value 92 % of total RES installed as seen in Figure 1-6. In Figure 1-7 and Figure 1-8, about 31 % of total installed Wind power and 76 % of total PV power are located at MV and LV levels combined. About 3,609 out of 9,021 Wind Plant and 125,211 out of 125,697 PV plants are installed at the medium and low voltage levels.

Table 1-2 show the number of RES plants by type in Cottbus and its immediate surrounding settlements. According to data from [14], out of the total of 890 RES plants 32 are wind power plants all of which were located in the High voltage level of the network with total installed capacity of about 64 MW. Out of the total of 849 PV plants, 19 are located in MV level having total capacity of about 30.69 MW while the remaining in the LV level with total installed capacity of 10.65 MW. The locations of much renewable energy plants (REP) in MV and LV level of the electrical networks have contributed to the changed in the

direction of power and current flow in the network. The flows are now bi-directional; power and current flow from high to low voltage levels, from low level to higher voltage levels and lateral within same voltage levels.

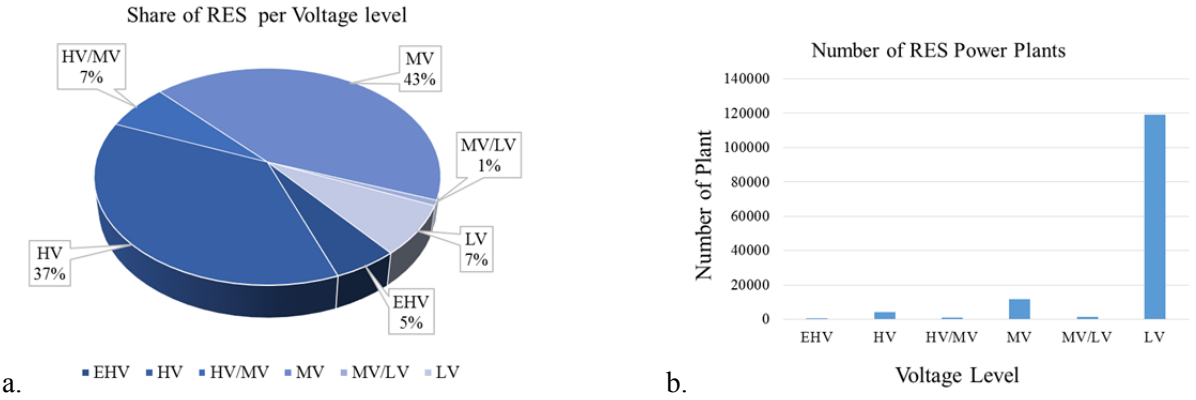

Figure 1-5: Share of RES Power plant in 50 Hertz Transmission Control area; (a) is the percentage share of installed capacity at each voltage level within the area, (b) is the number of plants at each voltage level with the area (Data from [14]).

Most RES at LV level are owned by power consumers themselves. These consumers therefore serve as power producers as well. Such consumers are referred to as prosumers.

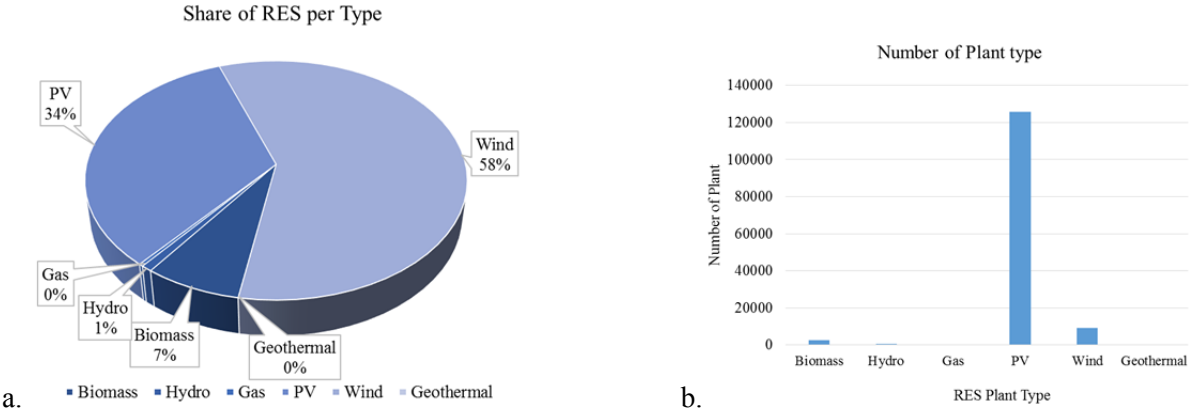

Figure 1-6: Share of RES Power plant in 50 Hertz transmission Control area; (a) is the percentage share of installed capacity per type of RES power plant, (b) is the number of RES plant type (Data from [14]).

This phenomena is expected to increase as a result of continuing support policies and fall in cost of per kilowatt installed RES power plant.

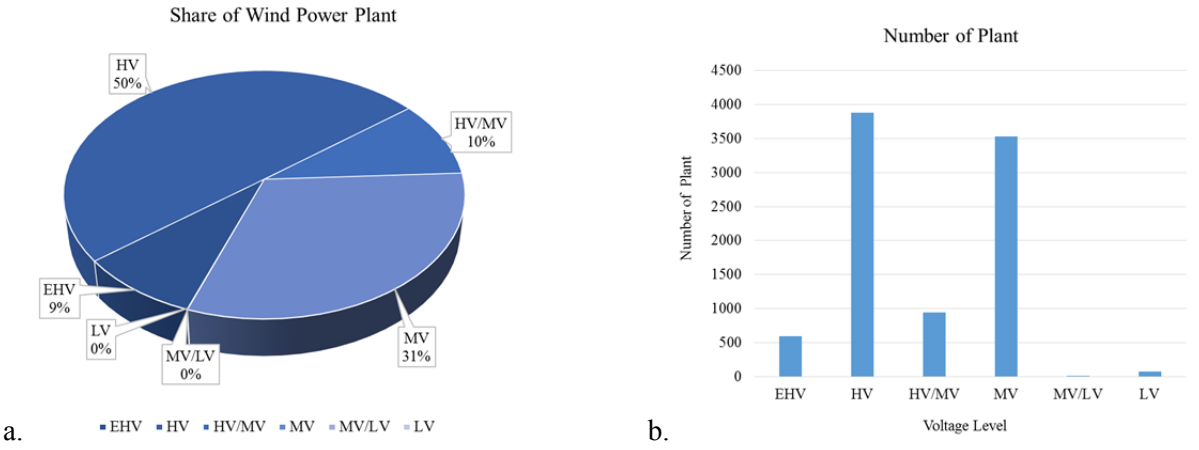

Figure 1-7: Share of Wind Power plants in 50 Hertz Transmission control area.; (a) is percentage share of installed capacity of Wind Power plant at voltage levels, (b) is the share of PV plant by number that voltage levels (Data from [14])

This rather positive development comes with some operational related problems. These problems are managed by the utility (network operator). The fluctuating nature of especially wind and solar renewable sources results in constant voltage variations. Another know problem associated with power from RES especially Wind and PV is that unlike conventional power sources, they cannot be dispatched due to the nature of the resource.

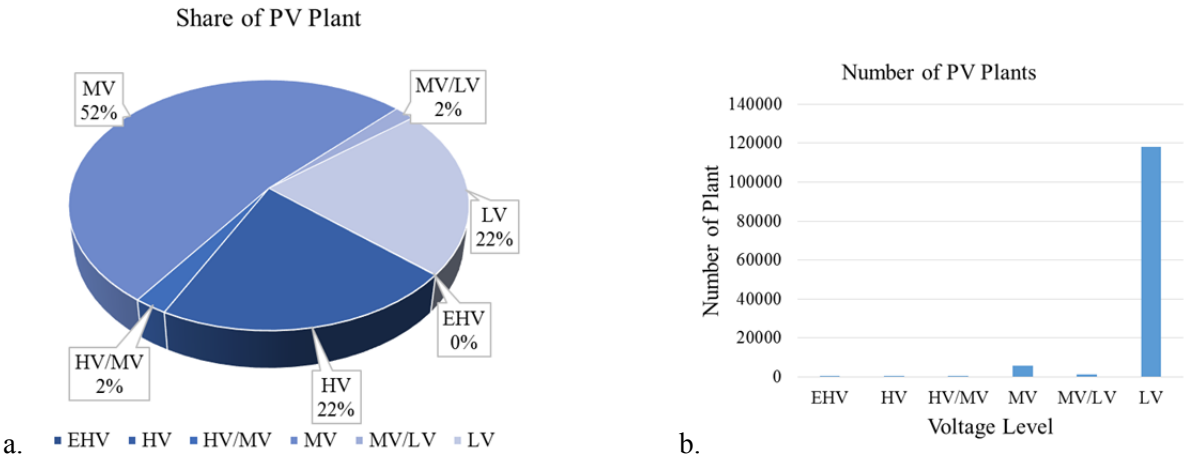

Figure 1-8: Share of PV Power plants in 50 Hertz Transmission control area.; (a) is percentage share of installed capacity of PV at voltage levels, (b) is the share of PV plant by number at voltage levels

Table 1-2: Share of RES Plants in Cottbus in 2014 (Data from [14])

Type of RES	Total Installed Capacity [MW]	Number of Units
Gas	1.31	4
Biomass	0.48	4
PV	41.34	849
Water	0.28	1
Wind	64.03	32
Total	107.44	890

1.3 Frameworks Supporting RES Integration

Developed countries have since the early 90's supported the RES Electricity (RES-E) industry through various support mechanisms. These mechanisms are either regulatory or voluntary, investment focused or generation focused, direct or indirect and finally either price-driven or quantity driven [15]. The most commonly adapted include feed-in tariffs, feed-in premiums, tax exemptions, tender investments and quota obligations [9], [16]. A location specific case study conducted and presented in [17] indicates the need for governments in developing countries to support the RES-E industry. Increase in renewable energy plants results in a corresponding decrease in electricity from conventional sources especially from nuclear as depicted in Figure 1-1 to Figure 1-4.

1.3.1 Feed-in-Tariffs (FIT)

This is a generation-based, price driven incentive or support scheme under which eligible electricity generators using RES receive a guaranteed price for generated electricity for a period of time. That is this scheme offers long-term purchase agreements for RE electricity sales. The buyer is most often the utilities or grid operators. This price normally depend on the eligible technology used by the producer. Some technologies include wind power plant, photovoltaic systems, hydropower systems and biomass power plants. FIT scheme has been applied in the German model of support where grid operators enter into long-term contracts at specified price rates with eligible[1] RE producers. The rates are fixed for a period after which a digression factor which tends to reduce price per unit power produced is applied for

[1] Eligible RE producers include homeowners, business and farm owners and could also be private investers

the rest of the period (Table 1-3). These rates are normally higher than existing retail electricity price. This scheme has the advantage of supporting new market entrants by lowering cost of capital investments [16], [18], [19].

Table 1-3: Feed – in Tariffs for Germany since 2014 (Data source [18])

Technology	Feed – in tariff	Digression factor
PV System	11.49	0.5 % from 01.09.2014
Onshore Wind	8.9	0.4 % from 01.01.2016
Geothermal	25.20	5 % from 01.01.2016
Biomass	11.78	0.5 % from 01.01.2016

Feed-in tariff are characterised by three main features:

1. guaranteed access to electrical grid;
2. stable, long term electricity purchase agreements usually spanning a period of 15 to 20 years;
3. payments based on costs of RES plant under consideration.

To enable producers to actively participate in the energy market, FIT could be tailored towards market price signals such as feed in premiums [20].

1.3.2 Feed-In-Premiums (FIP)

Feed-in-Premiums are considered to have evolved from the FIT system. Unlike FIT, Feed-in-Premiums policies offer a premium above the available average spot electricity market price. FIP schemes are therefore dependent on market price for electricity. Electricity from the RES is therefore sold on the spot market in contrast to a more purchase guaranteed FIT approach [20]. FIP can foster competiveness and encourage innovation when well designed.

1.3.3 Quota Scheme

This scheme requires energy supplier to buy a set quota of energy from RES. This is in the form of green certificates indicating production of energy from RES. This scheme exposes producer to market prices and puts investment in RES on the same level with other forms of

energy generation investment [19], [20].

1.3.4 Investment Support and Tax Exemptions

Investments support are generally upfront support that could include tax exemptions. The generally covered capital costs can be assessed through grants, tax reduction and some preferential loans. Tax exemptions or reduction as a support scheme are used to incentivise private and household RES installations such as rooftops and biofuels [19], [20].

1.3.5 Kreditanstalt für Wiederaufbau (KfW) 275

In May 2013, the KfW 275 storage subsidy scheme came into force in Germany. This scheme supports the new installation of both photovoltaic systems combined with storage and also stationary storage systems through financial support. There is a guarantee of low-interest loan for the overall investment and also bonus payment on storage financing by the German Federal Environment Ministry as result of the scheme [21], [22].

1.4 Outline of Thesis

Chapter one of this thesis start with a brief introduction into the general trend in the use of primary energy for electricity generation with the share of renewable energies. This is followed by the discussion on share of renewable energy in the electrical network and some support schemes and frameworks that support renewable energy.

Chapter two is dedicated to bringing out the motivation of the work through the discussion of some problems associated with renewable energy integration into the network and some possible developments that can help solve these problems.

Chapter three describes the study network and data used in this work.

In chapter four, simulation on the study network are conducted to establish the state of the network with and without renewable energy source. This is considered as the base case

scenario without any support for voltage and reactive power to the network.

The concept of sizing renewable energy plant and storage as a unit is described in chapter five. The concept proposes the use of historic data of renewable energy resources and load demand of a location with the aid of stochastic method of optimization to size a renewable energy plant – storage unit. Also described are sample cases (scenario) that are then used in implementing the proposed method of sizing.

The results of the sizing process are presented in chapter 6. Also, the effect of the result of the optimally sized unit on the study network is discussed.

Chapter seven summarises the thesis. The scope of future work on this thesis is also presented in this chapter.

2. Motivation

In this chapter the motivation and objectives of this thesis is discussed. This is divided into problems discussed as challenges and opportunities leading to the solutions. The problems are associated with the increasing development of renewable energy integration into the network. The problems are explored for possible opportunities.

As already indicated, available data, studies by various institutions, individuals and organisation points to RES as the future technology for electricity production. The future will therefore see more and more Wind and PV plants at all voltage levels hence future electrical networks will be powered by more distributed generators. Much of this will be made of RE plants or installations. The support schemes and policies set by governments and other global bodies and organizations mentioned earlier are expected to support the development of RES power plant installation until set targets or goals are met.

2.1 Challenges

In this section three main challenges associated with the integration of RES into electrical power networks are mentioned and briefly described.

The integration of RES into the grid helps reduce the introduction of end products of hydrocarbons such as CO_2; a major contribution to greenhouse gasses. Technically, RES can also help improve voltage profiles at the bus or feeder they are coupled to or in electrical networks in which they are installed. DG from PV have been shown to improve voltage profiles and reduce systems loss to about 44% by works carried out in [23]. The share of wind and solar generated electric power are set to increase in the network. Their share to the overall REP generated power is therefore expected to be significant. However, the significant contribution mentioned above could result in a significant manifestation of associated problems of power quality, energy reliability and frequency deviation that is seen with the integration REP into the network [24], [25]. The three main challenges considered

as motivating factor for this work are;

a) residual power (energy) flow in the network

b) wastage or losses in power (energy) as a result of unutilized power generated from RES plants.

c) cost due to grid expansion and reinforcement

2.1.1 Residual Power (Energy)

The presence of RE from wind and solar PV also results in a residual power profile at point of connection. The instantaneous residual power could either be surplus or deficit. Surplus in this case refers to more production than required by total load in the system network. These surplus powers which are intermittent in nature (Figure 2-1) are either fed into the network or discarded to avoid grid congestion or in other words maintain network stability. The deficit power is therefore the extra power to be produced to meet load demand in instance of inadequate production from RES. This deficit is usually covered by the network and sometimes possess a problem to the network.

2.1.2 Losses due to Unutilized Power from REP

Increase in contribution of REP to the network will almost directly increase the magnitudes and rate of change of residual power. Figure 2-1 depicts the already stated problems. Steep increases and decreases of REP infeed (yellow in (a) and green in (b)) as observed in both plots need to be compensated by the utility (blue plot) in other to always match generation with demand (orange plot). Existing power plants cannot react to fluctuating residual loads. This is because some change are too rapid for them to follow. The priority to always operate and keep network under stable condition also presents a limitation. This limitation is observed through occasional disconnection or reduction of production from RE plants when network stability issues may arise. Hence large amount of produced energy can be lost during fluctuation from RES source.

Performance ratio[2] of RES from wind and solar are less than 1. A Performance ratio from 0.7 to 0.9 is estimated for PV installations in Germany [26]. To ensure a smoother running of the electrical network, a statutory regulation that stipulate ways of regulating infeed from REP came into enforcement in Germany in 2012. This is the "*Erneuerbare Energiens Gesetz*" EEG Feed-in-management[3] with different requirements according to plant power [27], [28], [26]. This regulation stipulates the following;

- PV plants with power less than 30 kW can choose to provide possibility for system operators to remotely reduce feed-in power in case of looming system overload else permanently limit active power production of plant to 70 % of installed capacity. Though not much, excess produced active power above this limit need to be discarded.

- PV plants with installed capacity of 30 up to 100 kW must provide remote control access for power system operators. This gives system operators the permanent ability for continuous monitoring and regulation of power output in event of pending system overload.

- All other plants including PV with installed capacity above 100 kW must provide the capability for power system operators to remotely control their power output in event of pending system overload.

2.1.3 Cost of Grid Expansion and Reinforcement

A recall of an earlier statement on the fact REP integration will continue also bring to fore grid expansion as well as reinforcement projects that are been undertaken by system operators within Germany and other countries. These expansions occurring in both transmission and distribution levels are to enhance the transfer of RES power from

[2] Performance ratio is independent of irradiation and is considered to be the ratio between actual yield of electricity and the expected electricity yield.

[3] EGG Feed-in-management is a guideline that clarifies the other in which grid operators can take over technical control of RE sources to avoid grid congestions.

distribution levels where they are been produced in excess to where they are needed. These developments come with a cost.

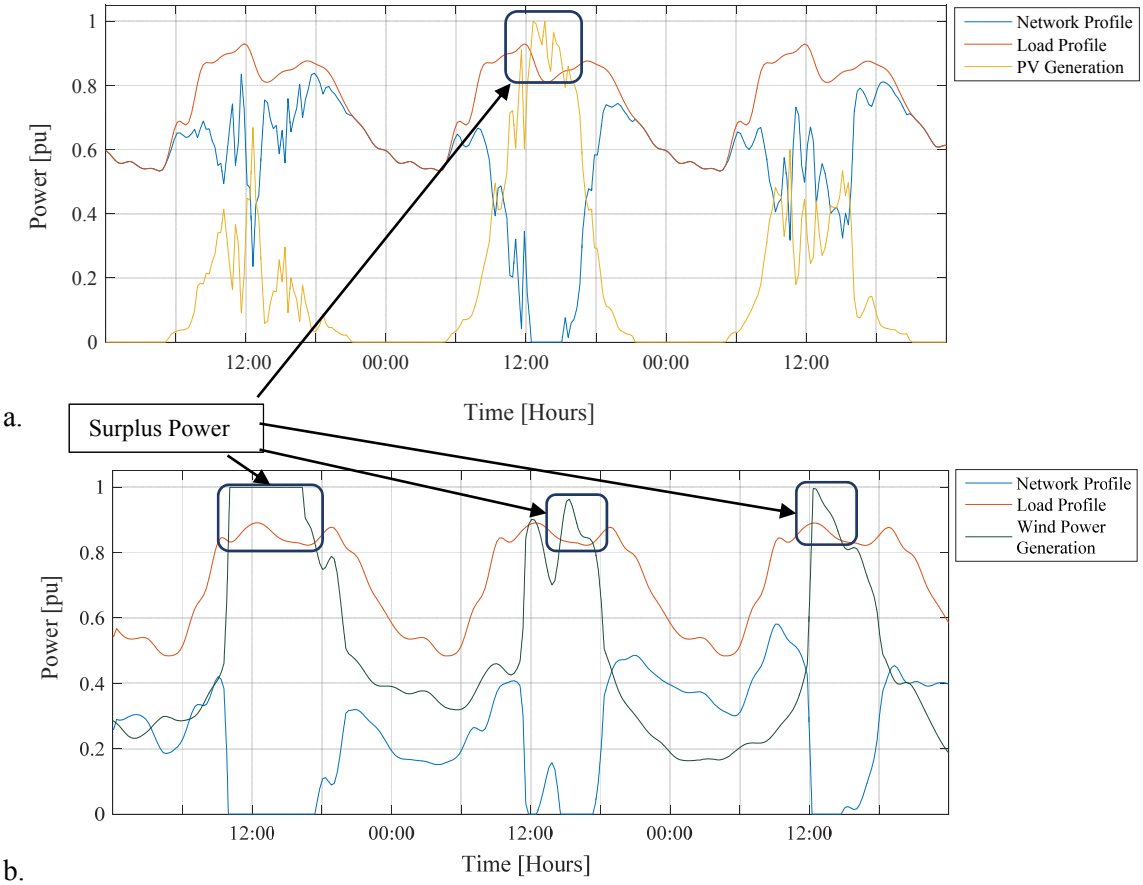

Figure 2-1: Load and generation profile; plot depicting typical behaviour of power output from RES and corresponding effect on power supply pattern for at a node (graph plotted with historic PV power output, historic Wind data and standard load profile). Data of the best periods of production in the year were selected for the plot above

2.2 Opportunities and Solution

Recent developments in electrical energy flow monitoring, data acquisition and storage and energy storage technologies presents some opportunities to solving the challenges presented in section 2.1. This section briefly discusses these developments, the opportunity thereof and the resulting solution.

2.2.1 Potentials in Residual and Unutilized power

To reduce the residual effect of REP on electrical network, excess energy from positive residual power could be stored and later discharged to offset arising deficit that arises. Sudden increases in REP production and ramping down of demand in the midst of high production from REP could be directly stored by storage systems. This will then be used at a later time when needed. The application of a storage system therefore will help to reduce the fluctuating effect and losses.

In other to cover both residual and losses mentioned above, REP and storage systems can be used to supply up to a specific percentage of load demand. That is REP and storage systems could be sized to always supply a percentage of load demand either at a main supply feeder (utility application) of a utility or at the location of a specific consumer. REP-Storage system as a unit should be integrated into the network instead of REP systems only. This is the option adopted in this work. However finding the size of the respective systems of the REP-S unit is not a straight forward. The nature of sizing which seeks to find the best size makes the process of sizing REP-S unit an optimization problem.This is describes in chapter 5. The amount of power drawn from the utility will be reduce up to the amount to be supported by REP-Storage system.

The effort to support the network could be done locally or within the immediate vicinity of installed REP at the distribution level by identifying and exploring opportunities that may be available. The goal of the REP-Storage unit in this work, is to support the immediate network to which they are connected (Figure 2-2c). That is;

- The outcome of this integration is to as much as possible reduce number of times and level to which the network operator would have to compensate both technically and economically for deficit or surplus of power from REP within the system.
- The gradient of fluctuation in power output of REP power generation, frequency of occurrence or magnitude of power quantity or all should reduce.
- There should be reduction in levels of unutilized power or energy generated from the

REP plants.

The combined effect of the above supports will be the increased improvement of load hosting capacity of the network. That is, more load could be in connected to the network. Figure 2-2a and Figure 2-2b shows the contrast. The feeder linking the consumer to the utility network is assumed to be the same in both cases. In the latter figure, power from the utility network is seen to decrease as represented by *light red* arrow coming from the network compared with the former with complete demand (dark red) met by utility network.

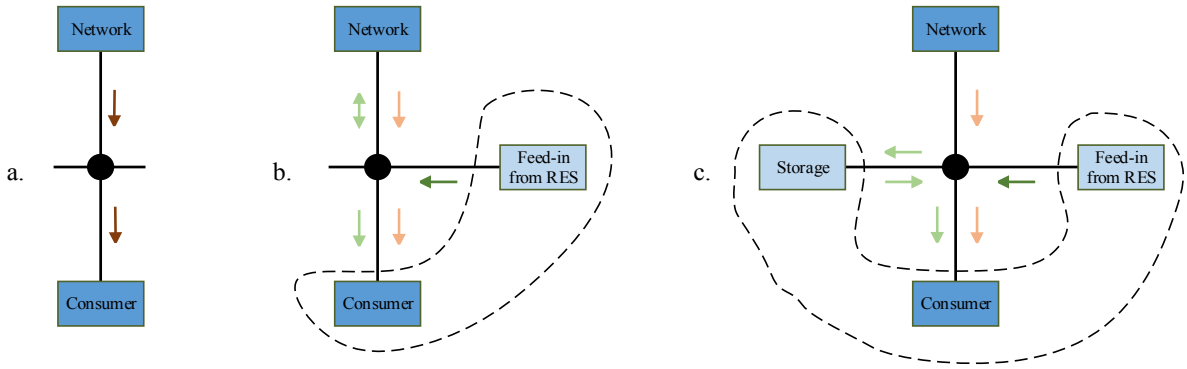

Figure 2-2: Illustration of power balance at point of common coupling (PCC) of system component. Darker shades of colour implies total power while the converse implies part of the total power; (a) PCC with only network and consumer. Whole power demand by consumer provided by network (b) RES connects to PCC. Demand supported by both RES and network with surplus RES fed into network. (c) Addition of Storage system which serves as buffer for excess power from RES.

As per Kirchhoff's current law, energy injected at any time of production by RES reduces the net power coming from the utility to the immediate network it belongs to (Figure 2-2b). The Figure 2-2a shows the initial situation of demand been entirely supplied through the electrical network by conventional plant in a top-down manner. In Figure 2-2b, is a simple topology that depicts demand been supported by additional supply from RES For installation up to a few megawatt, Figure 2-2b can be said to represent or illustrate prosumers. This set-up has been the practice for REP integration. Figure 2-2c represents demand been supported by both REP and Storage system. And on a smaller scale, it also depicts prosumers with storage systems. This arrangement is gradually becoming popular in integrating REP into electrical networks. As earlier stated, the introduction of REP to support load at a point of common coupling results in the reduction total energy drawn from the network. With the

addition of a storage system, the total amount of energy from utility will be expected to further reduce. This expected reduction is dependent on the size and capacity of REP-S system installed. The reduction in energy from utility at this bus will;

- Provide the opportunity for utility to extend their feeders and add new consumers.
- Provide the opportunity to postpone system reinforcement since more REP energy management will be done within the immediate network they belong to. This is illustrated in Figure 2-2c.

The REP-S system been able to provide the above mentioned opportunities would have succeeded in expanding the ability of its hosting network to support more consumers. The load hosting capacity of the network would have been therefore improved.

The rule of thumb for sizing RES is that, maximum size of RES for network integration should not exceed the ratio of maximum power demand to the minimum power factor of loads at the point of common coupling. This is especially stipulated in a technical guideline provided in Germany by the Bundesverband der Energie und Wasserwirtschaft e.V (BDEW) [29].This means that irrespective of the size of RES to be constructed, if technical guidelines in [29] should be observed in agreements with TSOs and DSOs before construction, commissioning and production of power. Details of such technical guideline used in Germany can be found in [29].

As will be seen later in this work, the proposed option described in this work seeks to emphasize the need for taking into account the operational impact of RES on the network as mentioned in section 2.1. Storage systems are a key component in the implementation of a solution to the problems stated in section 2.1. The charge and discharge function of storages will assist in reducing the effect of residual power in the network hence reducing the magnitude of unutilized over produced power or energy.

There are two fundamental characteristics of electricity generation and distribution that makes the need for electrical energy storage systems (EESS) in the presence of RES important.

1. In the first instance, generated electricity must be consumed at the same instance (equation 2-1 and Figure 2-2); a balance in supply and demand of electricity.

$$Electricity(Wh)_{generated} = Electricity(Wh)_{consumed} \quad (2\text{-}1)$$

A short period of imbalance ($Electricity(Wh)_{generated} \neq Electricity(Wh)_{consumed}$) lasting some few seconds may result in system instability [30]. A reduction in the quality of power supply will results. This could have cost implications. As a solution EESS can provide ancillary services such as voltage and frequency control support.

2. The second instance is the transport of generated electricity over long distance to demand location. With new demand locations further away, the distance of electricity transport also increases. Existing transmission lines and cables may need to be upgraded in other to support the extra load and to also reduce system transmission losses. Storage systems with decentralized RES power plants can help mitigate overload conditions [31] and in effect postpone in some instances transmission line and cable upgrade projects. Storage systems can therefore be used to indirectly control electrical network congestion and as a consequence reduce network loss.

For the proposed solution mentioned in this work, an effective REP-S systems requires adequate sizing. Adequate sizing in this instance implies an REP-S unit that would result in the reduction of residual power to a minimum. The sizing of REP and storage requires optimization process which generally not straight forward. This is evident through various studies aimed at finding effective ways of sizing and placement that have been conducted and still ongoing. These studies employs various methods that are either deterministic, analytical or stochastic. For example genetic algorithm optimization was used in sizing storage systems in works presented in [32], [33]. Stochastic optimization[4] method where historic data are used as input variables is employed in this thesis.

[4] Stochastic optimization methods minimize or maximize optimization problems with either the input or variables, search method or both subject to randomness [64], [65].

The sections that follows briefly describes two phenomenon that will contribute to the implementation of proposed solution briefly mentioned in this section

2.2.2 Big Data and Smart Metering

Society as a whole has experience digitalization in the past few decades. This is coupled with the introduction of sensing, monitoring and data acquisition equipment that are getting cheaper and improved by the day. These two occurrences have led to the explosion in the availability of historic data, a phenomenon referred to as *"Big Data"*. The electrical energy generation, transmission and distribution sector has experienced their fair share of the above mentioned phenomenon through various Supervisory Control and data acquisition systems, automatic meter reading systems and of recent smart metering systems.

Over 100 million smart meters (SM) which forms part of the developing artificial metering infrastructure (AMI) have been installed worldwide in the past decade either directly as new or as a replacement of traditional analog meters.Information show that over 50 million smart meters were deployed as of July 2014 in the United States of America (USA) amounting to about 43 % of household consumers in the USA [34]. The traditional meters as well established only tracked consumption with reading conducted on an average of 12 times in a year. Depending on their technical capabilities and choice, smart meters provides readings from 1 seconds to 15 minutes time intervals and with reading not only limited to consumption of energy but voltage, current, power factor, power flow etc. Other capabilities of SM are:

- the real time logging of the above mention quantities for both consumption and generation in the case of decentralized energy sources.
- the possibility of cutting or reducing electricity supply as measure of ensuring systems stability.
- the possibility of logging in data from DG units connected.

Utility companies in different countries introduced smart meters for various reasons. ENEL

in Italy introduce smart meters in anticipation of savings in areas of field customer service, operations and protection against revenue collection fraud. While in the state of California in the US, smart metering was introduced to increase reliability through demand peak reduction [35]. In Germany, the introduction of smart meters are to enable possibility of consumers to actively participate in the electricity supply market. The introduction was backed by the German Energy Industry Act (EnWG) in 2011 and aimed at equipping 80 % of energy consumers with smart meters by 2020, a process which is part of meeting the EU Directive 2009/72/EC. The EU has set a goal to replace at least 80 % existing meters with smart meters by 2020. The amounts to about 200 million smart meters for electricity and 45 million for gas. The cost of implementation was estimated to be on average between 200 and 250 € per installation [36]. A conclusion from a report on an analysis conducted in Germany advocated for a rollout tailored and complaint with national the energy reforms rather than a large scale roll-out advocated by the EU. It found large scale roll-out of smart metering infrastructure rather economically unfavourable for consumers with low annual energy consumption. The current German legislative instrument encourages roll out of smart meters for users with consumption upward from 6000 kWh, for RES generation facilities and new consumers. The report therefore suggested an improvement of this legislative instrument and the use of upgradable electronic meters that can be interfaced with smart metering infrastructure in the future. Implementation and ownership are not exclusive to DSOs. The implementation and ownership are exclusive to DSOs in Poland. Analysis by Poland concluded that, large scale role out will be cost beneficial to both consumers the energy systems as whole. The result of the ongoing amendment of Polish Energy Law is expected to favour a large-scale roll out of smart meters to cover 80 % of consumers. However there must be a financial scheme that will provide incentives for the DSOs. The cost of rolling out smart meters in the UK will be covered by energy suppliers of this service. The suppliers, apart from been responsible for installation are also the owners. A report on cost benefit analysis presented to the EU indicated that, the United Kingdom stand to gain from a large scale roll-out envisaged to complete by the end of 2020. In France, a recommendation have been given for a national roll-out of smart meters. This recommendation was based on the positive financial cost-benefit analysis that was carried out coupled with the fact that consumers will be empowered while the grid supported due to

smart meter implementation. This is a win-win situation. DSO are implementers and owners of the smart meters provided to consumers. As at 2013, there were 1.63 million smart metering points due to voluntary roll-out led by DSOs. A long term economic evaluation carried out on 1.38 million out 1.63 million points yielded positive outcome. However a law introduced in 2013 mandated DSO to fully roll-out smart meters from 2014 to 2020.

The information provided above points out the initiatives taken by countries in other to have smart meters in their energy infrastructure. It is an indication of a bright future of smart meters and for more data acquisition

The influx of present data obtained from smart meters provides lots of opportunity for electrical energy consumers, producers, suppliers, network operators etc. An important opportunity is the facilitation of load shifting or time shifting of demand due to real time information on tariffs provided by smart meters. These data also form the foundation for a more accurate load forecasting, load planning and further analysis for network expansion and planning of new networks of similar load demand.

Smart Meters

In the electrical energy industry, smart meters also known as advanced electronic meters are measurement devices used by energy utility companies to record and transfer customer energy consumption information for the purpose of billing. Information that facilitates the smooth operation of systems of utilities are also obtained from smart meters. As compared to the traditional analog meters, smart meters are electronics devices which employs microprocessors in the process of metering. As a result they deliver relatively more accurate data. In addition, there exist a two-way communication between smart meters and central system of utility involved for remote reporting and monitoring.

Essential to smart meter systems as mentioned earlier is the existence of two-way communication between the electronic metering devices of consumers and a central system of a utility. This system is used for the purposes of information gathering, monitoring and control of demand consumption where necessary. Prior to the onset of the smart grid initiative, the advanced metering infrastructure (AMI) has been in existance. Smart metering

system forms an integral part of the future smart grid systems due to its real time monitoring and communication capabilities and as source of historic data on system behaviour.

As depicted in Figure 2-3, the smart metering infrastructure at the moment communicate with central monitoring systems, the load centres where the consumers have real time access and also with generating units and distribution system. The consumer get awareness on their consumption patterns and are therefore provided with the opportunity of changing their energy consumption behaviour. This they may do by manually and intentionally shifting some consumption to off-peak periods of the day. Alternatively, the use automated system that continuously monitor real energy prices can be employed to control load system appropriately. The urgency of power demand by consumer should be one among additional factors that should be considered in either decreasing or increasing amount of power drawn from network.

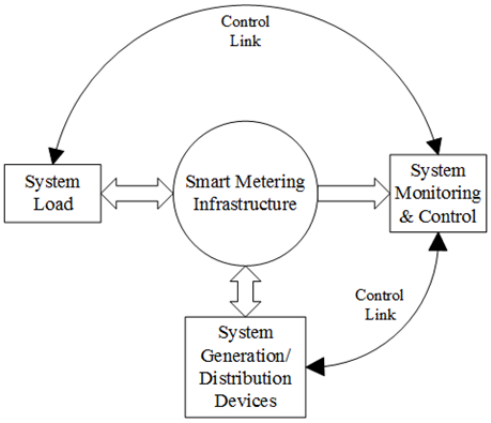

Figure 2-3: Simple presentation of Smart metering infrastructure central role in electrical network

More real-time consumption data at regular intervals (some few seconds to 15 minutes) including the voltage levels on distribution lines increases quality of information received by utilities or third party monitoring system. The monitoring system can in effect send ramping signals in event power imbalances to controllable system load and generating units when this capability is activated in the future and only if need arises.

The trend as can be observed is the increasing integration REP especially by PV for household, commercial, institutions and industrial application and wind power plants into the distribution. This is gradually changing and in some countries (eg. Germany) changed

the nature of electrical network from the traditional top (Generation) – bottom (Load) operation to a bi-directional operational network. A situation that has given rise to prosumers. Smart meters could in the form integral part in the acquisition of data. The accumulating bulk of data arising from deployed smart meters and those that shall arise in the future will provide as stock of information for systems development.In a similar manner, data that will be obtained from RES will enrich data base for a more accurate and realistic prediction and production planning.

In view of the above, assumptions for implementing the concept are partly drawn from the hypothetical existence or possibility of constantly obtaining adequate data from smart meters and other sources in the future. This will help produce more realistic results from sizing process of REP-Storage system capacities

2.2.3 Storage system

Storage systems are considered as a vital piece of the puzzle of finding solution to the problems associated with REP integration described in Section 2.1. A simple illustration of the role played by storage system in the integration of RES into electrical networks is shown in Figure 2-4. As can be seen, storage systems are useful for implementing off-grid RES power system. Their support features ensures the use of energy from RES for longer period of time in the day. For grid connected RES, storage systems has the ability to support RES integration by smoothing out fluctuations experienced by the electrical network and also supports time shifting of generation from renewable energy source. Electrical storage systems have been used as reserves for system regulation and spinning service allowing grid operators to overcome some bottlenecks associated with transmission and distribution. Examples are Bath County Hydroelectric pumped storage in the USA, Goldisthal Pumped-Storage in Germany, Compressed Air Energy Storage in Huntorf Germany and 12 MW Li-ion Battery Storage in Los Andes Chile [37], [38], [39]. The present growing interest is how to utilize electricity storage systems or technologies to enhance the controllability and be able to dispatch a rather irregular RESs has resulted in numerous studies. That is, applicability for responds to system support requirement from some milliseconds to bulk supply for some hours.

Ordinarily, higher integration of supply from RESs require corresponding large energy storage to support variation of supply. The general practice is sizing storage system to be able to produce maximum instantaneous power as RE power plant when required and for a stipulated time period. What is left to be answered is amount of energy that is optimal and how this capacity can be calculated. In [40], the potential of using energy storage in coordination with Smart PV inverters much of which will be seen in the future is investigated with positive results of improved demand management.A study in [41] proposes a method of sizing storage to increase wind penetration as limited by grid frequency. In this, power spectral density theorem was used to model the stochastic characteristics of wind power fluctuations with frequency response characteristics of the power grid under study taken into account. In [42], pattern search optimization techniques is used to optimally size wind generation, PV generation and storage capacity of a hybrid power system taking into consideration load shifting capability of the systems. A suggested form of storage is through the use of Vehicle-to-grid (V2G) concept where the storage systems (battery) of electric vehicles serves as an energy sink to help improve the stability of the grid. Some studies have been carried on to investigate this possibility. V2G capacity has been estimated to be about 9 MW in 2013.

Low capacity storage can be used to support standby generator operation especially where there is need for low capacity supply. Storage systems can be used to support weak networks that are sometimes observed at point of direct connection of the grid with wind turbines or wind farms with squirrel cage induction generators.

Storage can also be used in smart grid (SG) application of which distributed generation (DG) comprising of RES is part. Studies in [43] shows that outage probability in SG decreases exponentially with the square of storage capacity.In [44], the use of storage systems together with smart PV inverter for the purpose of peak shaving and voltage regulation in systems having high PV penetration is presented. An optimization process with focused on minimizing cost of ESS installation shows improvement in voltage profile and reduction in size of ESS needed.

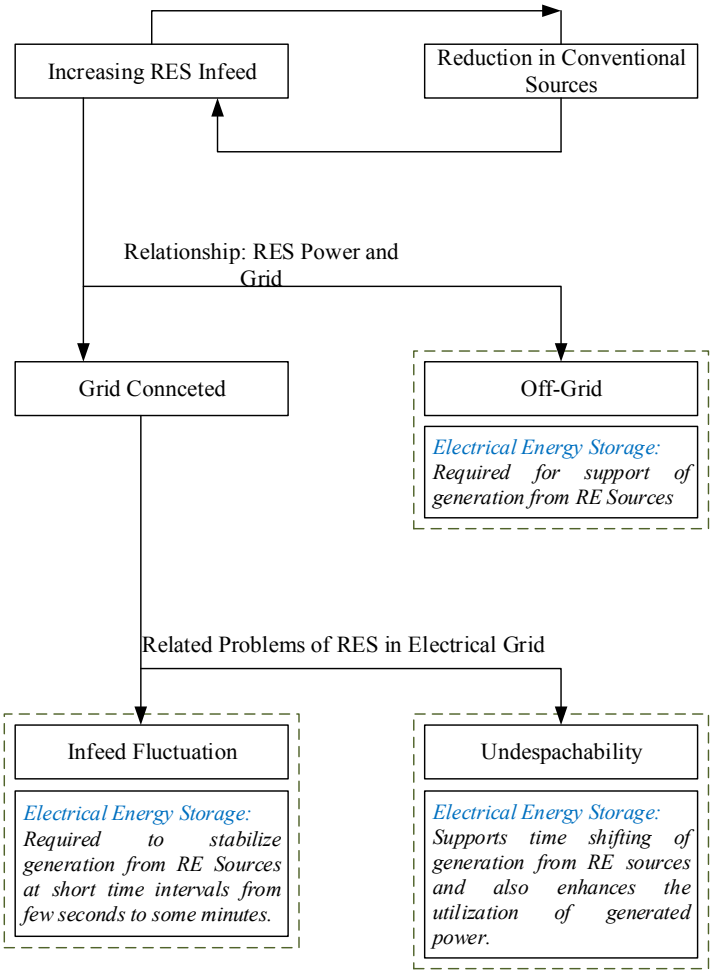

Figure 2-4: Storage usage in RES integrated system

The CIGRE C6.19 Working Group who convened in August 2010, have been working on planning and optimization of active distribution systems (ADSs). ADSs are composed of distributed energy resources (DERs), load and storages. Their target is based on recommendations of CIGRE WG C6.11 whose focus was on development and operation of active distribution networks (ADNs). Probabilistic base and multi-objective optimization approaches are two approaches identified as for the planning of ADSs as opposed to traditional deterministic approaches. This is due to the uncertainties that can be associated with future load demand, the intermittent generation of RE and future storage system integration [45] [46]. Different storage technologies existing have been classified according to the wide range of application and potentials that exists.

2.2.3.1. Classification of Electrical Storage

The main classification criterion for ESS is based on the form of energy as storage medium or storage technology employed. ESS are also classified or compared based on application range in an electrical network as depicted in Table 2-1. On the basis of storage technology used, electrical system storage could be said to be of mechanical, electrochemical, chemical thermal and electrical in nature. Energy from all types except electrical undergo energy conversion process in other to utilize stored energy in the form of electricity. Figure 2-5 shows examples of storages under each of the technologies mentioned. Some classification are also based on a combination of maximum available rated power, storage capacity and rate of charge and discharge. The authors in [37] did such comparison in their work. This is seen in Figure 2-6. Further important criteria are their respective responds time, power and energy density.

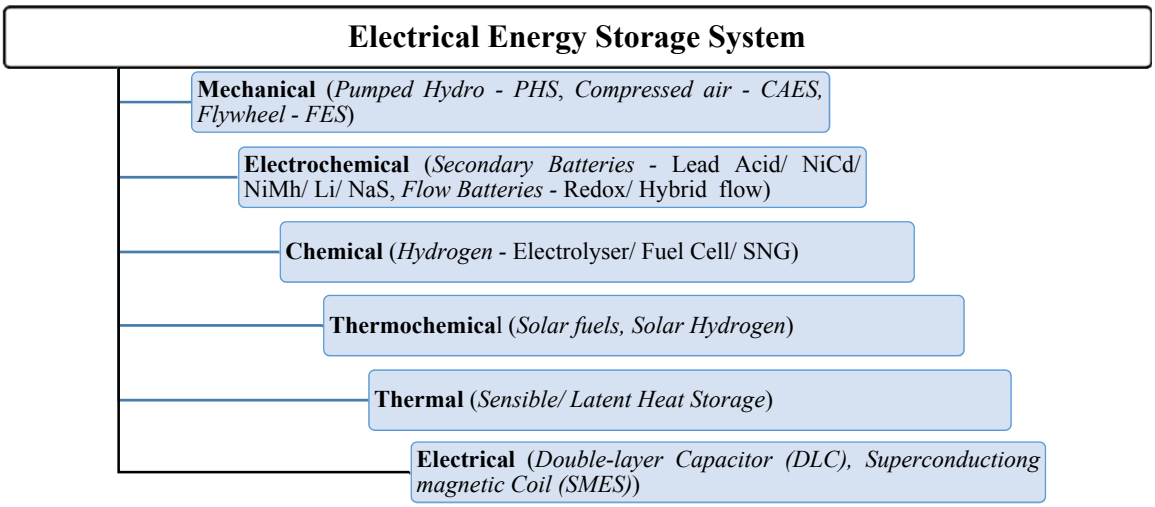

Figure 2-5: Classification of electrical energy storage based on form of storage [37], [38].

There are therefore large capacity storage systems such as pump hydro in the gigawatt range and compressed air energy storage systems up to about a few gigawatt of installation [47], [48].

These capacity of storage find their application in the high voltage network and sometimes in the medium voltage depending on their size. Their size makes them suitable for application in reserve and timeshift supply mode.

Table 2-1: Range of storage system application [38]

		Duration						
		Seconds			Minutes		Hours	
		0.1	1	15	1	15	1	8
Number of Use	1/month	Reserve Supply						
	1/day					Timeshift		
	12/day		Primary Regulation					
	30/h							
	30/min	Power Quality						
	5/sec							

Flywheels, Batteries, Fuel cells and Capacitors are storage systems that can aid in the improvement of power quality, providing energy for primary regulation and reserve supply. Power quality support is mainly due to their fast responds time. Flywheels for instance have responds time to full capacity of less than four seconds normally considered as instant. Batteries and capacitors also have responds time of few milliseconds and also considered as instant responds. They are suitable for network frequency regulation. They are also used in reserve and timeshift supply mode. These systems ranges from a few kilowatts to some megawatts [48], [49].

The mentioned storage systems in the previous paragraph find their application in medium and low voltages of the network due to their possible installed capacities.

Developments in electrical energy storage technology has resulted in modular and movable storage systems. Their energy capacity ranges from some kWh to 6 MWh and can be deployed in low and medium voltage network (up to 24 kV). They can be aggregated to achieve higher energy capacity. A major limitation to aggregating modular storage is the cost. Movable storages ranges from batteries in electric vehicles to batteries built into a container. Modular are normally permanently installed at location. In Figure 2-7 are pictures of modular storage unit from ABB and Siemens

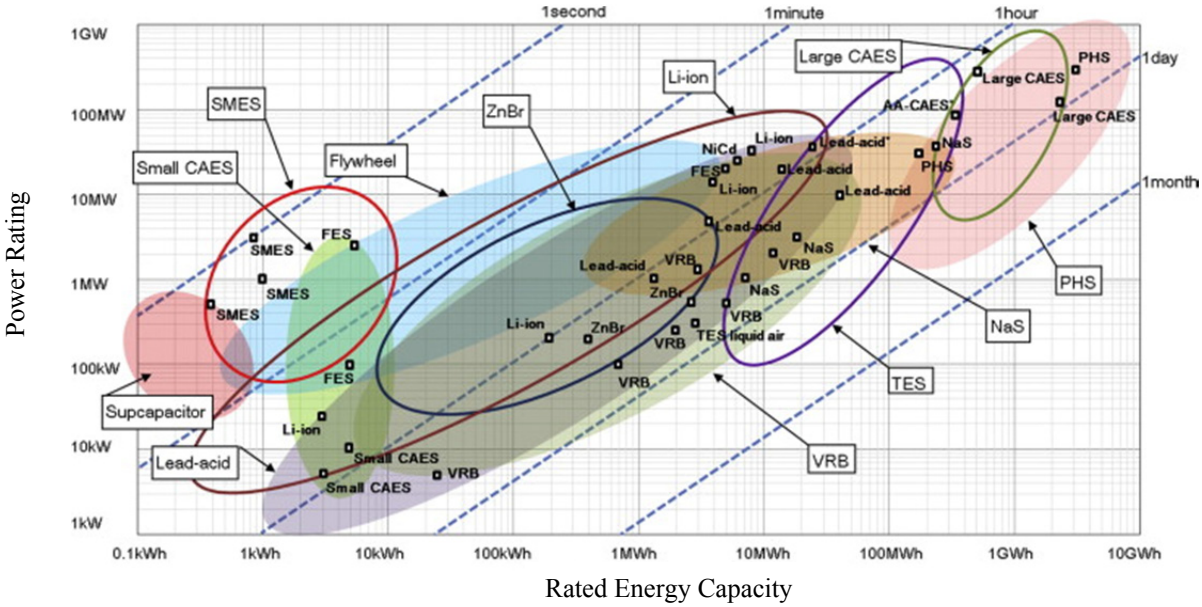

Figure 2-6: Comparison of power rating and rated energy capacity with discharge duration at power rating [37].

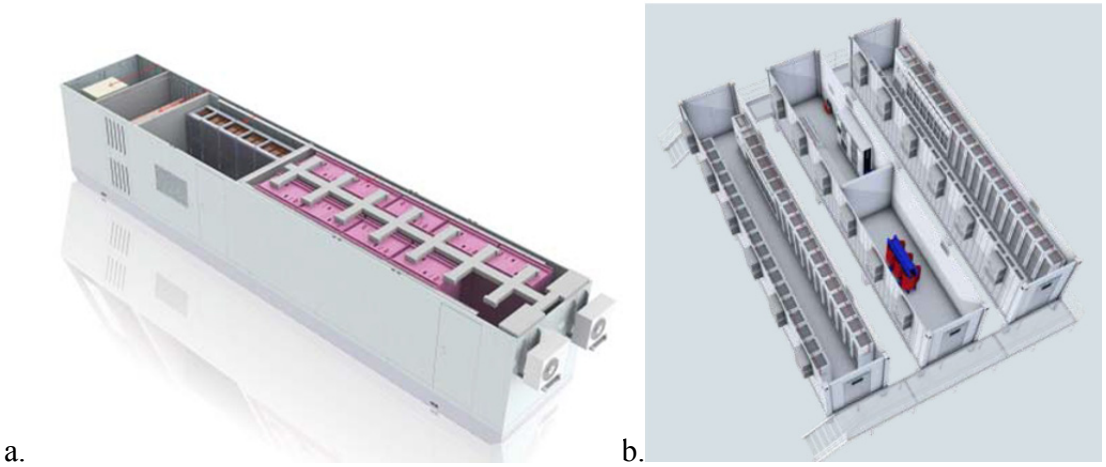

Figure 2-7: Modular storage systems; a. Modular Storage system from ABB and b. Modular Storage system from Siemens [50], [51].

2.2.3.2. Storage System Implementation

In Figure 2-8 are simple illustrations in radial topology of RES - Storage systems integration into an electrical network. These illustrations are but a few of numerous possibilities. Figure 2-8c can be considered as a scaled up version of single consumer units in the topology

presented in Figure 2-8a. That is, one consumer unit is analogous to the assumed aggregated consumers in Figure 2-8c and the individual REP-S units in Figure 2-8a are analogous to REP–S system in Figure 2-8c.

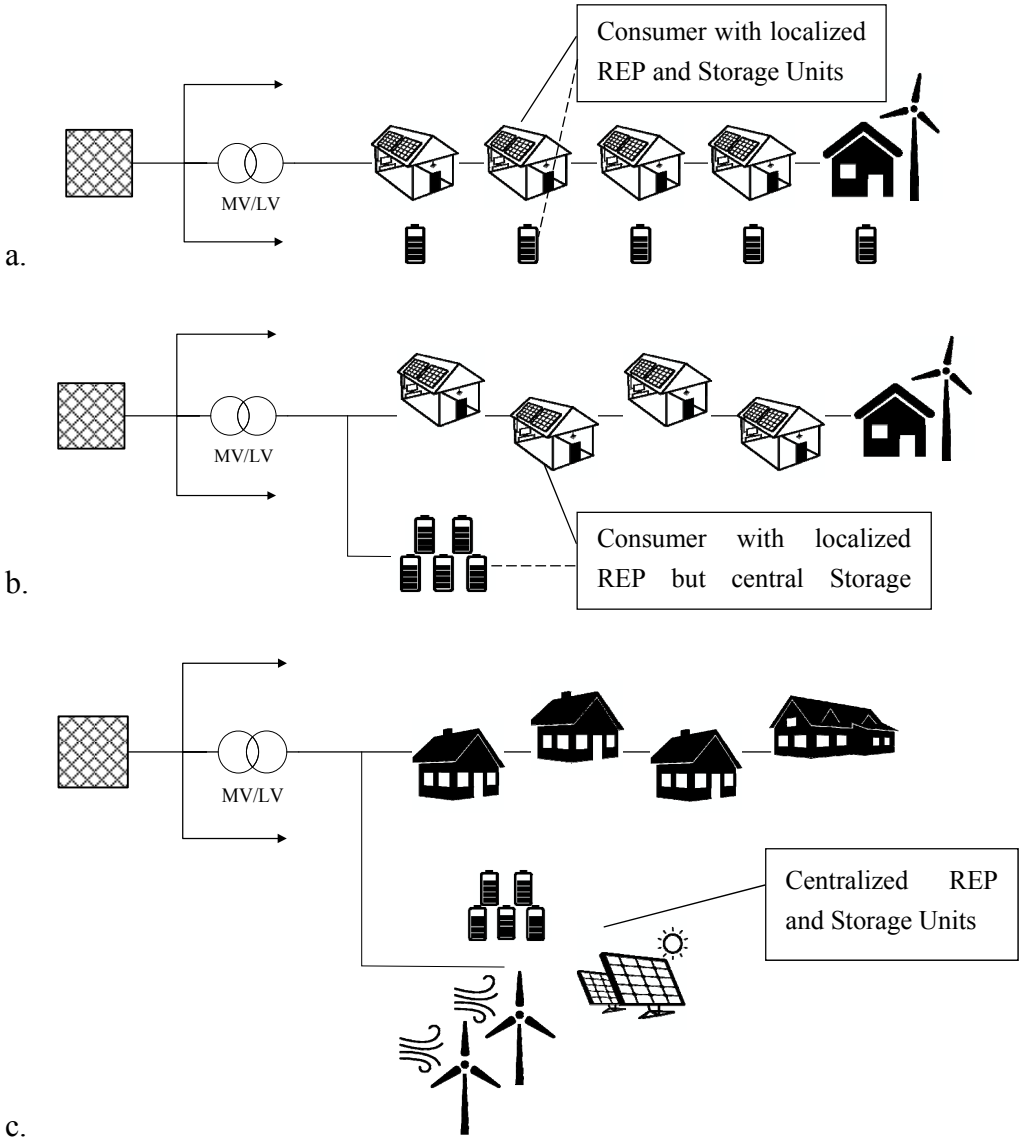

Figure 2-8: Modes of storage integration. (a) each consumer with RES has a corresponding storage system, (b) corresponding central storage system for combined installed RES. (c) RES – Storage system as a unit.

The location of storage system and REP – Storage system in Figure 2-8b and Figure 2-8c can be determined based on prevailing conditions of the hosting network. Different options are therefore possible. A variation of Figure 2-8b could be one with the storage system located at the end of the network feeder, in the middle of the feeder or divided into cluster

of storages with varying storage capacity and power rating. Decision such as this are not straight forward and therefore require some step by step analysis.

The successful implementation of a REP–Storage system proposed will be partly dependent on the supporting infrastructure for monitoring and controlling and storage of electrical energy. The present telecommunication platform available provide suitable link for obtaining real time data that will aid in the monitoring and controlling of such systems.

2.3 Aims and Objectives

The sections preceding this section stated the challenges associated with the introduction of RES into electrical network. The potentials that exists from these challenges and solution to tackling the challenges were also mentioned. This was followed some technological advancements that will contribute to the implementation of proposed solution.

In summary of the above sections, the main aim of this work is to present a concept of optimally sizing renewable energy plant-storage (REP-S) system as a unit for integration into an electrical network. This concept depends on historic data of renewable resource and of the network. The result of sizing aims at supporting the load hosting capacity of the network by reducing residual power and losses due to unutilized power from RES plants. That is, the power or energy that contributes to residual power or loss will be harnessed and fed to the load.

The concept of sizing as per the brief description above poses an optimization problem. Historic data of wind, solar and demand profile are to be used as the main input parameters. These data are random, therefore stochastic optimization method will be employed in determining the optimal size of RES-S unit. This method is general and returns unique results per network location under consideration. This means different results will be obtained for different geographical locations since each geographical location in the network has unique sets of data. That is renewable energy resource data at different location are different. Also load consumption profiles differ for individual consumers and also for different substations and feeders representing consumer communities in the network.

To start with, the objective function or procedure and sets of constraints variable that describes the problems stated in section 2.1 will be presented together with sets of rules that will guide the process to arrive at the solution of optimal size of RES-S unit. A series of test analysis based on different scenarios using historic data of renewable energy resource and load consumption profile will be conducted and presented.

The problems stated are observe in electrical network. The description of assumptions and parameters of a test electrical distribution network that serves a work bench will therefore be presented.

The outcome of these analysis which for each scenario will be the size of RES-S unit will be integrated into the test electrical network. The possibility and extent of supporting the load hosting capacity of feeders in the study or test network and finally the entire network will be presented per scenario. The hosting capacity relates to the amount of load and/or decentralized energy sources a feeder or network can support without changing the existing topology, configuration and physical response characteristics [52], [53]. The following network characteristics will be compared;

- The voltage profile at buses before and after the integration of optimally sized REP-Storage unit
- Loading of lines and transformers before and after the integration of REP-Storage unit.

This is to help determine the extent to which optimally sized REP–Storage unit could support the electrical network (study network) of given parameters and data set. Also to be determined is whether the network will operate within operational conditions such as voltage and thermal limit of lines, cables and transformers for a given optimal REP–Storage unit.

3. Study Network and Data

In other to implement and test the outcome of the concept of sizing proposed in this work, an electrical network is required. In the previous chapter, mention was also made of historic data as a requirement in the implementation of the proposed concept. This chapter describes the selected network that was modelled and some of its components and parameters.A description of data used in this work and their pre-processing steps are also given.The RES data used was location specific (Cottbus in Brandenburg Germany).Some evaluations to determine the potential in renewable resource are made and presented in this chapter as well.

3.1 General Overview Test Network

For the purpose of unanimity and simplicity a 30 bus standard Medium Voltage(MV) network is selected. This is shown in Figure 3-1. This network is based on work from CIGRE Task Force C6.04.02 which is affiliated with CIGRE Study Committee C6. The CIGRE 30 bus distribution benchmark model has characteristic similar to most networks in Europe and adapted from the German MV distribution network [54], [55], [56].

In [54], a 14 bus network extracted from the original 30 bus network was used to develop a benchmark model for investigating DG integration into medium voltage distribution. The study in [54] was focused on the impact of DG units on power flow and voltage profile within the network. A general improvement in voltage profile was observed in this study.

3.1.1 CIGRE 30 bus Benchmark Network

The network in Figure 3-1 (a) comprises of two main separate subnetworks (Subnetwork 1 and Subnetwork 2) supplied by an Overlay Network through two 110/20 kV transformers (Tx1 and Tx2 respectively). The nodes Kn01 and Kn23 represents the substations that steps down voltage from the transmission level to the medium voltage distribution level for subnetwork 1 and subnetwork 2 respectively. These are the starting points of the feeders of

these respective subnetwork. The node or buses number Kn02 to Kn24 represent substations that supply their respective connected loads at medium voltage level or at a stepped down low voltage level. These loads could be;

- a big single loads such as industries, institutions, commercial centres such as big shopping arcades etc.
- comprising of different loads aggregating into one lumped load. Examples are a community of household consumers with few shops or a few light industrial and commercial loads.

The network shown in Figure 3-1 (b) is an example of a possible scenarios seen at the nodes Kn02 to Kn24. The rated voltage of each subnetworks is 20 kV but supplied by 110 kV network through Tx1 and Tx2.

In [54] and [55], the benchmark network together with its parameter represents to a large extent what is seen in practice. The benchmark network therefore provides the opportunity to conduct different scenario that could be observed in MV networks. It can be used to conduct studies on the impact of DG units on power flow, impact of DG on voltage profiles, energy management systems for DG, power quality issues such as harmonics, flicker, voltage and frequency variations, voltage stability issues, impact of DG on transmission capability and also protection of MW networks [54]. In [56], the benchmark network is used to undertake a study that also took into consideration future growth of RE integration and related cost implications. In view of this, the benchmark network will therefore provide the platform to study REP-Storage System integration into a distribution network.

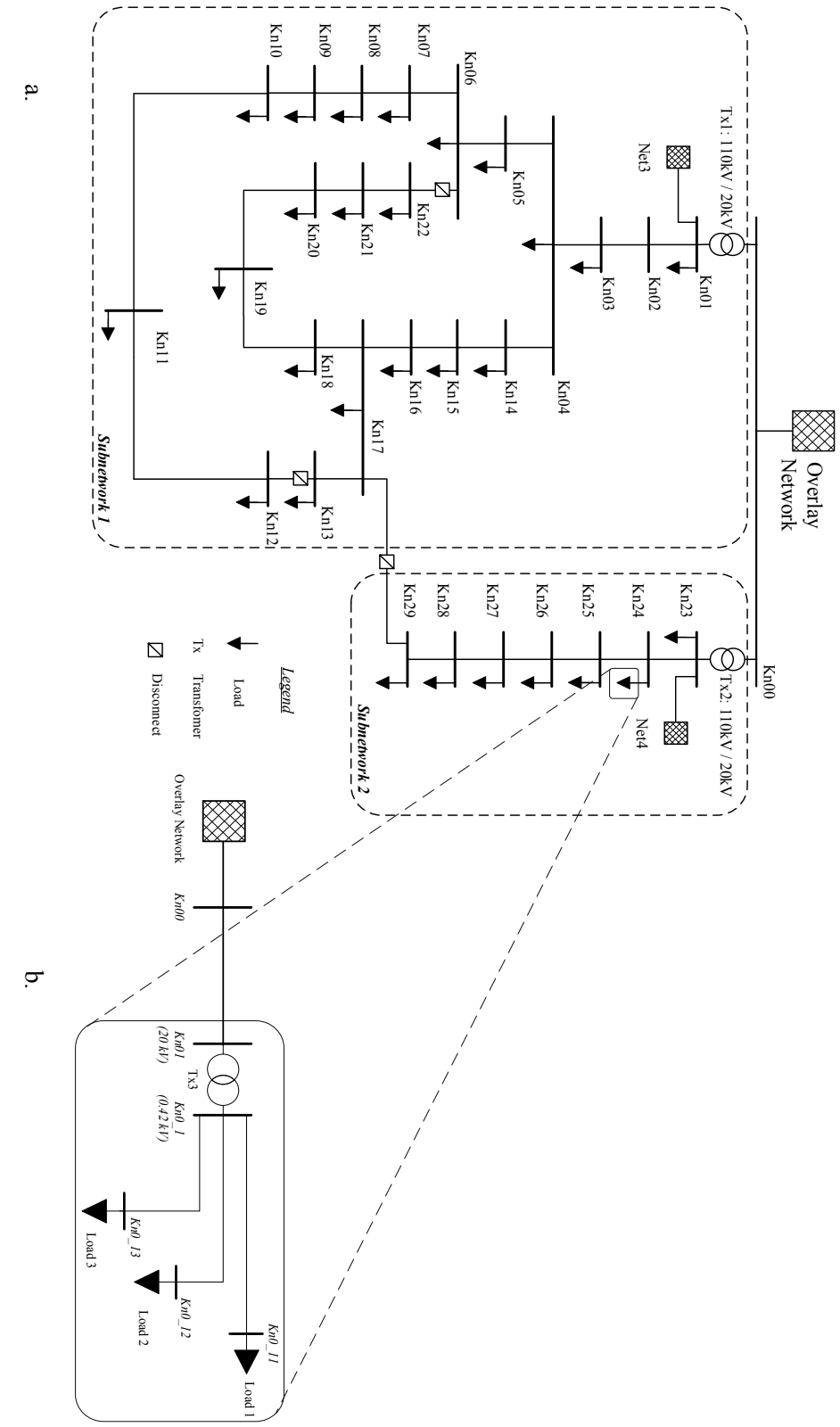

Figure 3-1: Selected electrical Network (a) One-line diagram of 30 bus MV benchmark distribution network from CIGRE. (b) One-line diagram for a single node consideration: simple radial with loads having a common bus

3.1.2 Single Node Network

In Figure 2-2 the basic concept for the analysis of the power and energy flow at a single node is illustrated. More often than not, changes in voltage level, increase in demand and disturbances observed in entire electrical networks are aggregates of similar events occurring at several single nodes of the network. A single node is therefore used as a reference point to size, integrate and study the effect of REP - Storage system integration into electrical distribution networks. In Figure 3-1(b) is the single line adopted single node network. This could represent any of the 28 loads in Figure 3-1(a). Analysis with scaled up results from sizing will be conducted on 30 bus network.

3.1.3 Network Components

The networks model in Figure 3-1 are implemented and simulated in MATLAB Simulink. MATLAB Simulink has a dedicated library called *SimPowerSystems*. This library contains various blocks that represent electrical network components such as transmission lines,cables, transformers etc. This made the implementation of electrical networks in Figure 3-1 possible. Each component requires appropriate and adequate data for all respective parameters that describe them.While some components use static or constant data, some require dynamic data for simulation. In this work the dynamic data which were usually a time series data that respective blocks read during simulation or evaluation were used. Some components of the selected networks are as follows.

3.1.3.1. Transformers (Tx1, Tx2 and Tx3)

The transformer used in the model in Figure 3-1(a) is a tap changing transformer with setting of ± 10 % of secondary voltage and tap steps of 0.0625 % [56]. The MVA rating of both transformers are chosen to be 40 MVA. The transformers are labelled in Figure 3-1(a) as Tx1 and Tx2. As earlier stated, power demand for Subnetwork 1 is supplied through Tx1, likewise demand for Subnetwork 2 supplied through Tx2. Total active power demand on both transformers is 60 MW.Transformer Tx2 supplies a total active load demand of 25 MW hence the total active load demand of Subnetwork 1 is 35 MW.

The transformer in Figure 3-1(b), (Tx3) on the other hand has a rating of 2 MVA and support a total active power demand of 1.735 MW. Its primary and secondary voltage ratings are 20 kV and 0.42 kV respectively.

3.1.3.2. Transmission Lines

The transmission lines in this model are characterised predominantly by underground cables since that is the practice in both urban and most rural networks. The parameters of the underground cable PROTOTHEN-X (NA2XS2Y) were adapted. The feeders spans a total distance of about 15 km and 8 km for Subnetwork 1 and Subnetwork 2 respectively. Table 3-1 show the basic but relevant parameter of the cable used. A table showing the length of each transmission line of the network can be found in Table A-1 in the Appendix. The cable are sized according to VDE 0276 – 1000 to be able to stand 0.76 of full load [57].

Table 3-2 show distribution cables in Figure 3-1(b) with respective parameters. The cables selected are copper conductors and XPLE insulated.

Table 3-1: Basic Parameters of Cable used in model

Cable Type	Current Carrying Capacity [A]	Resistance at 20°C [ohm/km]	Inductance [mH/km]	Capacitance [µm/km]
NA2XS2Y 3 x 1 x 150/25	319	0.206	0.386	0.249
NA2XS2Y 3 x 1 x 120/16	285	0.253	0.399	0.231

Table 3-2: Cable parameters of single node model presented in Figure 3-1(b)

Cable	Current Carrying Capacity [A]	Resistance at 90°C [ohm/km]	Inductance [mH/km]	Capacitance [µm/km]	Length [km]
Kn00 – Kn01	172	0.8250	0.460	0.171	1.00
Kn01_1 – Kn01_11	538	0.0536	0.226	0.269	0.25
Kn01_1 – Kn01_12	538	0.0536	0.226	0.269	0.35
Kn01_1 – Kn01_13	538	0.0536	0.226	0.269	0.15

3.1.3.3. Loads

The loads in networks presented in Figure 3-1 are considered as lumped up loads.That is each load is a cluster of consumers comprising various types. The types of load are based on standard load profiles. In this thesis, four load types out of existing standard load profiles are

combined differently to form each load cluster. This will be seen later in the work. In Table A-2 are the installed load capacity at each bus in Figure 3-1(a). Each lumped load has corresponding power factor (pf) as a result of its constituent load type. A list of power factor per lumped load is seen in Table A-3 in the Appendix. Similar to loads in Figure 3-1(a), loads in Figure 3-1(b) are considered to be a lumped combination of selected standard load profiles of different load types. The maximum apparent power ratings of loads in Figure 3-1(b) are 850 kVA (Load 1), 650 kVA (Load 2) and 450 kVA (Load 3) respectively. Load 1 is a combination of residential and industrial load profile at power factor of 0.85,Load 2 represent a combination of commercial/institutional and residential load at power of 0.90 while Load 3 is assume to operate at a power factor 0f 0.95 and only comprising of residential load characteristic profile [56].

3.1.4 System Nodes (Buses)

As already mentioned the nodes as seen in Figure 3-1 feed corresponding loads. The loads are a combination of MV and low voltage (LV) electrical networks and could be of different topologies. They are MW loads in case feeder from the respective bus feed industrial loads and or rural load. In the case of LV loads, they feed households, small industrial and commercial loads [57]. The main topologies that are employed are either radial, ring.

Topologies

The 30 bus network used in this thesis employ the radial topology (Subnetwork 2) and ring topology (Subnetwork 1) which could also be changed into a radial network depending on scenario.

Radial Topology

This topology is mainly applied in MV and LV levels of a network. The implementation of this topology is illustrated in Figure 3-2(a) below. The feeders are connected to a main station (such as Kn01, Kn03… Kn29 main stations) with consumers (loads) branching off. Branch offs as seen in Figure 3-2b also exists and are suitable at low density areas and for feeding

bulk loads. With the disconnect switches in the open position during operation, the adopted CIGRE network in Figure 3-1(a) can be operated a radial system.

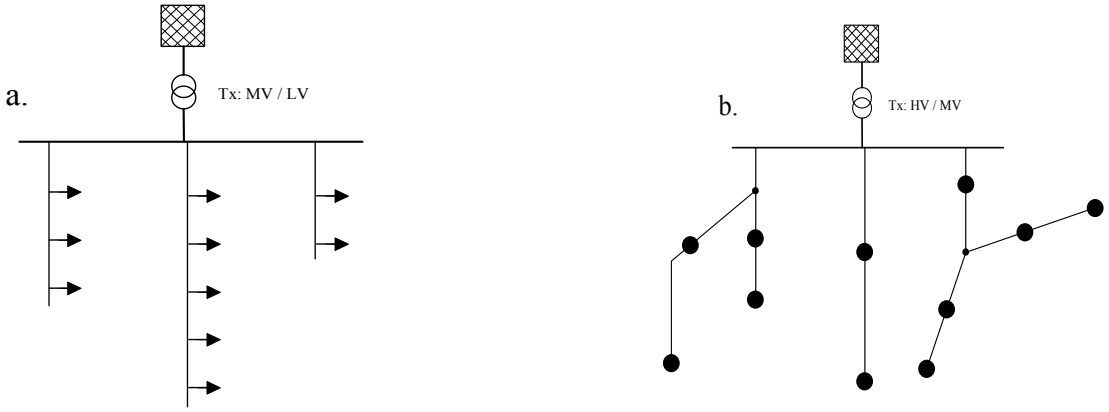

Figure 3-2: Radial Topology. (a) Simple Radial Structure; (b) Radial Structure with branch lines

The single node mentioned and shown in Figure 3-1(b) also adapts the radial topology in Figure 3-2(a) with three lumped load loads connected to a hypothetical node at the low voltage level.

Ring Main Topology

There are variations in this topology which starts as a radial type topology. As seen in the simple form represented in Figure 3-3 a ring topology is formed by connecting line ends back to the feeding station. This system is usually operated with the switch (disconnection point) in normally open position. The ring main form shown in Figure 3-3 is the simple topology. Some other forms of the ring topology are;

- **ring-main system with remote station without supply** where receiving ends of individual feeders are connected to station with no supply
- **ring-main system with feeding remote station** where receiving ends of individual feeders are connected to station with supply
- **ring-main system with reserve line** where a separate line which does not feed any load is constructed between the feeding station and remote station

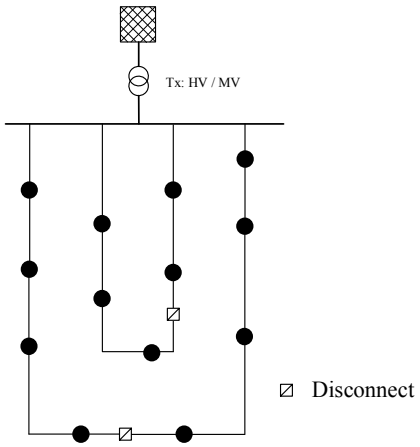

Figure 3-3: Ring Main System simple topology

The network in Figure 3-1(a) can be operated as a ring-main network with all disconnect switches in the closed position.

3.2 Data and Components of Study Network

The outcome of implementing the concept of sizing REP-Storage system proposed in this work is to have an optimally sized unit (REP-S). The consideration of parameters and characteristic of the hosting network reflects in the outcome. The method of optimization to be used as already stated is a stochastic optimization method that depends on historic data. There are numerous ways to obtain data in recent times. Utilities have stockpile of data that span years. These accumulated data could be of help in future implementation of proposed concept of this work. These data include various power consumption patterns based on consumer types. With numerous weather stations and data centres of research institutes and RES installations,data on RES are available to make this method of sizing possible.Modelling and approximation methods could also be used for generating data based on historic data of demand curves and RES resource already available. In this work, data was taken from:

1. MITNETZ STROM[5] [58]; dataset on different consumer types,

[5] MITNETZ STROM is a regional power utility company responsible for distribution networks spanning four network region of Germany. The regions are part of Brandenburg, Saxony-Anhalt, Southern Saxony and Western Saxony. They make available to the public achieved standardized historic demand profiles of different loads for each year.

2. Deutsher Wetterdient[6] [59]; Historic Wind speed data from a weather station in Cottbus and

3. Solar Energy Research Field of the Brandenburg University of Technology (SERF-BTU); Historic power output data from rooftop photovoltaic plant installation.

The emergence of modern sensors, fast and efficient communication links to smart meters as already discussed are means of obtaining continuous data at desired time intervals. This trend is expected to facilitate the near Smart Grid of the future which is expected to gradually replace the unidirectional electric grid of the twentieth century. Smart metering does and will continue to facilitate the collection of data that could help RES-Storage sizing in the future.

The modelling of the electrical network used in the study as well as scripts for implementing the proposed method of sizing RES-Storage system were implemented on the MATLAB/Simulink software platform.

MATLAB/Simulink comprises of two main parts; the language of Technical Computing (MATLAB) and the Simulation and Model-Based design (SIMULINK). The technical computing language part is useful for solving problems in mathematics, statistics, data approximation and optimization. SIMULINK is useful for physical modelling such as power system, electronics, mechanics etc.

In the work, data approximation, optimization and statistic tools were useful.As earlier stated, *SimPowerSystem* toolbox of SIMULINK was useful in implementing and simulating electrical network models shown in Figure 3-1.

The subsections that follows briefly describes the pre-processing of each data and block models used in implementing the study networks shown in Figure 3-1.

[6] Deutscher Wetterdienst (Germany's National Meteorological Service) is a public institution with partial legal capacity under the department of the Federal Ministry of Transport and Digital Infrastructure. They hold, achieve and document metrological data and products the public and individual customers and users.

3.2.1 Load (Consumption) data

A description of load types and the respective Simulink block used for their representation are briefly presented in the section. A description of consideration for and pre-processing of relevant data to be used in the simulation is also presented.

The load component of the network in Figure 3-1 is implemented with the Simulink block for three phase dynamic loads.

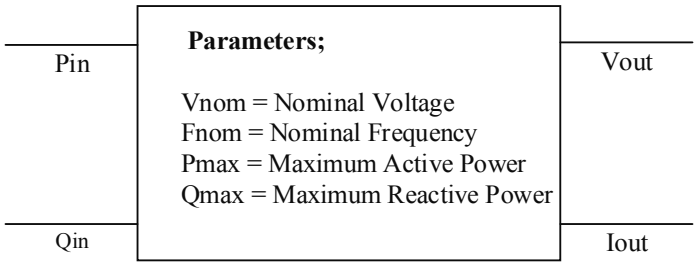

Figure 3-4: Symbolic representation of dynamic load block.

This block represents an uncontrollable load. As parameters, voltage, frequency, active and reactive power values of load to be implemented is given.The block take two dynamic signals for simulation. These signal are the active power (Pin) and reactive power (Qin).The resulting voltage (Vout) and current (Iout) are monitored and recorded from a bus to which the load is connected. The active power (Pin) infeed signal for the dynamic load block is the generated load profile according to (3-6) in section 3.2.1.1. The reactive power (Qin) on the other hand is generated according to (3-7). These two set of data are very important aspect of the load model and to successfully size RES-Storage for integration and simulation of the modelled network seen in Figure 3-1. As a result, constantly varying loads pattern that depict demand as seen in real situation is used. The data taken from the *Download – Center* of MITNETZ STROM served this purpose [58]. These data are standard load profiles available to the public and based on yearly obtained consumptions of consumers.

As seen in Figure 3-1(a), there are 28 lumped loads in the networks each supplied from a corresponding substation represented by buses (Kn01, Kn03, Kn04,..., Kn29). For the purpose of this work, a mixture of different standard load profile data were aggregated into the lump loads in the adapted model. Four out of a total of fourteen standard profiles found in the data

from [58] are used. The four profiles are;

1. Household Load Profile (H0)
2. General Commercial Load Profile (G0)
3. Industrial Load Profile (G3)
4. Agricultural (Farmland) Load Profile (L0)

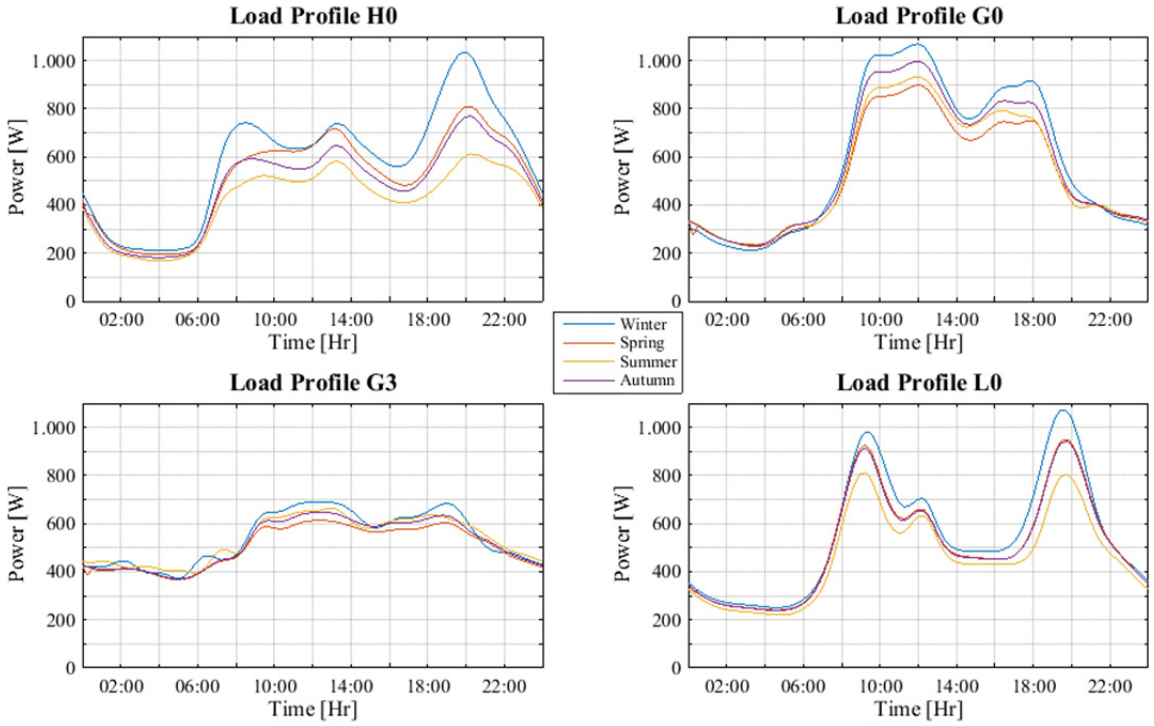

Figure 3-5: Selected load profiles for typical days of the seasons of the year 2013 [Data from MITNETZ)

The data is for the year 2013 and are in 15 minutes time steps. The initial data was a vector energy values per 15 minutes. This was converted into a vector of instantaneous power values spanning the year 2013. The conversion was done using the expression below.

$$P_{15\min\_i} = \frac{E_{15\min\_i}}{0.25\ hours}\ kW, \quad \{i = 1, 2, ..., n:\ n = 35040\} \tag{3-1}$$

where

$P_{15\min\_i}$ is instantaneous power for corresponding energy per 15 minutes ($E_{15\min\_i}$). The multiplication factor "0.25 hours" converts the entire vector energy values into power.

This factor indicates the fact that energy values are at every 15 minutes.

3.2.1.1. New Load Profile Generation

In Figure 3-5, the plot of the selected standard load profiles are depicted for a typical work day in each season of 2013. As expected, winter season shows a higher profile while summer on the other hand shows a relatively lower profile comparatively.

Table 3-3 : Allocation burden of load in pu

Load Type	G3	H0	G0	L0
Allocation factor [pu]	0.4	0.3	0.2	0.1

To have a common reference, all load profiles normalized to 1. The resultant of combination of two or more load types at bus is also referenced to 1. The contribution of each load type is based on its allocation factor seen in Table 3-3. The allocation factor is a weight defining an approximate contribution of each of the four selected loads per unit installation at bus.

- If the load consists of all four selected load types, each will contribute to the total demand in the proportion (allocation burden) shown in Table 3-3. These ideas was adopted from work presented in [56].

- However if the load consists of any number of combination other than four, the reference sum of the factors is rebased according to the load types within this combination.

The allocation factor could be expanded to include other load types. Both assumptions are summarised in (3-3).

To start with, the initial standard loads are normalized according to (3-2) to obtain a vector of normalized standard load profile. For network buses with just one load type, the new profile is obtained from the product of allocated load demand and appropriate normalized vector according to (3-4). That is $\mathbf{P_b} = \mathbf{X}'_j$ in the application of (3-4).

For network buses with combined load types, a new normalized profile is obtained by

combining individual normalized profiles of each load type according to (3-3). The product of this new vector and installed demand at node as represented by (3-4), gives the new load profile.

$$\mathbf{X}'_{\mathbf{j}} = \frac{\mathbf{X}_{\mathbf{j}}}{\left\|\mathbf{X}_{\mathbf{j}}\right\|}, \quad \{j = 1, \ldots, n\} \tag{3-2}$$

$$\mathbf{P}_{\mathbf{b}} = \frac{\sum_{j=1}^{n} c_j \mathbf{X}'_{\mathbf{j}}}{\sum_{j=1}^{n} c_j} \tag{3-3}$$

$$\mathbf{P}_b^{\mathbf{profile}} = \mathbf{P}_b C_b^{ins.}, \{b = 1, 2, 3, \ldots, 29\} \tag{3-4}$$

where

n is number of load types (could be 1 up to 4)

$\mathbf{P}_b^{profile}$ is vector of new generated load profile at each node or bus $'b'$

$\mathbf{P}_b$ is resultant normalized per bus $'b'$

c_j is the allocation factor of the jth load type (profile) depending on profiles selected for respective node $'b'$

$\mathbf{X}_j$ is the vector of jth load type (profile) depending on profiles selected for respective node $'b'$

$\mathbf{X}'_j$ is the normalized jth load type (profile)

C_b^{ins} is the installed load demand at node (bus) $'b'$

In Figure 3-6, a plot of normalized ($\mathbf{P}_{24}$) and actual ($\mathbf{P}_{24}^{profile}$) profile of combined load types; H0, G0 and L0 at system node Kn24 is shown. This profile is for a 24 hour period. This process is replicated for all 28 nodes with load attached to them. For the 28 loads, the time range of data spans a period of one year.

With reference to Table A-2 in the Appendix, H0, G3, G0 and L0 are estimated to contribute about 49.32 %, 27.98 %, 17.84 % and 4.86 % of the total active load demand in the model presented in Figure 3-1 (a) respectively.

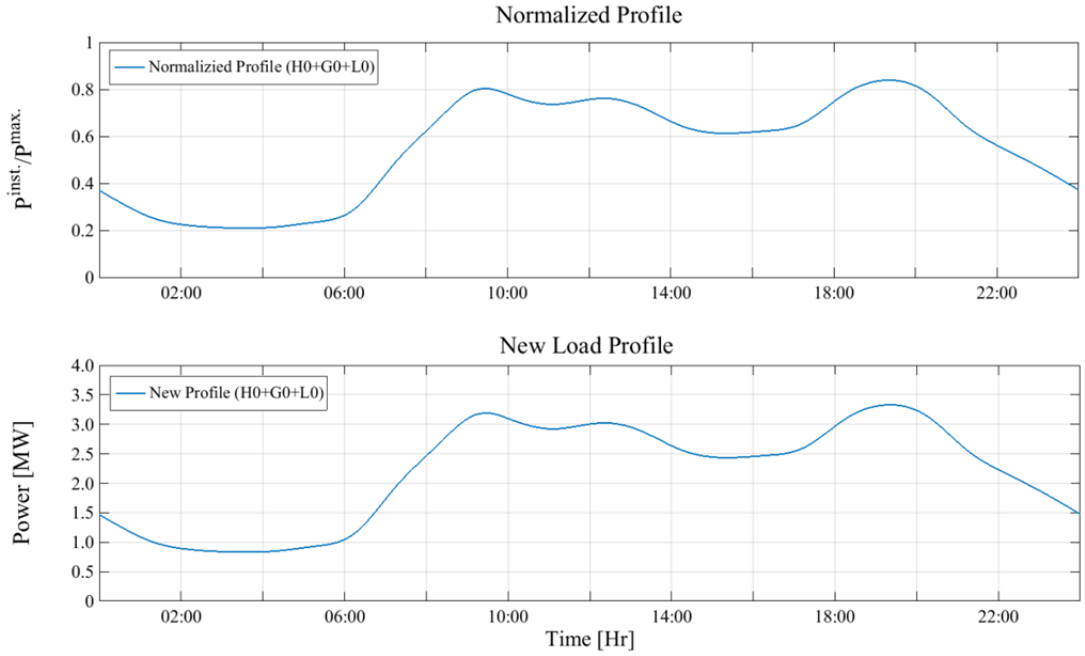

Figure 3-6: Profile of normalized and real combined load types H0, G0 and L0 for a 24 hour period

The load data whose pre-processing steps have been discussed up until now are all a representation of the active power profile of respective loads. The next step is to approximate corresponding reactive power. To do so, the power formula in which reactive power is expressed as a function of power factor is used. The equation for estimating reactive power is shown in (3-5). Base on literature review, the average power factor of commercial loads and industrial loads was considered to be 0.85. That of residential loads and agricultural loads were considered 0.9 and 0.95 respectively [56]. The resulting table of power factors have already been mentioned to be in the appendix (Table A-3). The active power data together with power factor per node is used in the approximation of reactive power requirement at each node according to the expression shown in (3-5). The result of this step results in the second dynamic signal required by all load during simulation.

$$Q_b = P_b \left[1 - \frac{1}{pf_b^{\,2}} \right]^{\frac{1}{2}} \quad kVA \tag{3-5}$$

where,

Q_b, P_b, pf_b are the reactive power, new active power as per equation (3-4) and power

factor at network node $'b'$ respectively.

3.2.1.2. Seasonal Analysis of Load

A brief analysis is conducted on load type G3 which is a generalized standard profile for industrial loads. This analysis is conducted as a general step to know and establish some facts about load connected to bus to which optimally sized RES-Storage system will be installed.

As a start, a power duration curve is generated from available data. The duration is over a period of one year as seen in Figure 3-7. About 2 % of the period is observed to have power demand above 90 % of maximum load. That is about 250 hours of 8760 hours. Further analysis is conducted to estimate the energy usage of load type G3. This is organized into seasonal energy consumption and shown in Table 3-4 and Table 3-5.

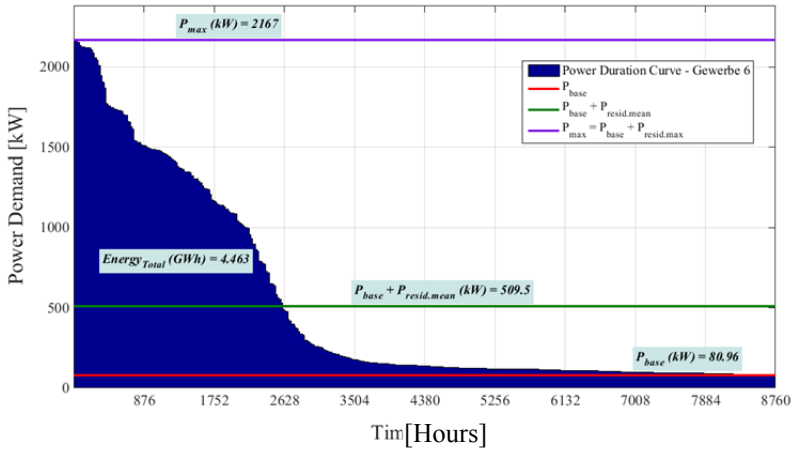

Figure 3-7: Load duration curve for Load type G3. Data source [58].

As can be seen from Table 3-4 and Table 3-5 a maximum power demand and maximum total daily energy of 2.167 MW and 19.31 MWh is estimated respectively. Similar maximum daily energy consumption is observed for the seasons of Spring, Autumn and Winter. This is because standard load profile has in some instances similar profile for all three seasons.

Table 3-4: G3 Power and Energy analysis by seasons.

Month	P_{base}	$P_{resid.average}$	$P_{resid.max}$	Total Energy	Total Energy $_{Base}$	Total Energy$_{Resid}$
	kW			MWh		
Spring	80.96	410.01	2086.4	1084.1	178.76	905.31
Summer	81.40	357.75	1428.1	969.7	179.74	789.92
Autumn	80.96	446.45	2086.4	1151.9	176.82	975.05
Winter	104.1	477.77	2062.9	1257.5	225.52	1032.00

From Table 3-4 the total energy consumed by load over the year is estimated to be about 4.463 GWh. Table 3-5 shows maximum, minimum and average energy consumption per day for each season. A maximum of 19.31 MWh was calculated

Table 3-5: Energy Consumption per day for each season

Energy Min (Daily Total)	**Energy Max (Daily Total)**	**Average Energy**
Spring Energy Data (MWh)		
2.18	19.31	11.81
Summer Energy Data (MWh)		
2.38	13.85	10.56
Autumn Energy Data (MWh)		
2.18	19.31	12.68
Winter Energy Data (MWh)		
3.11	19.31	14.00

3.2.2 Renewable Energy Source (RES) Data

The renewable infeed is represented by data signals with fixed time stamps with no focus on. This is because the focus of this work was not on the transient behaviour and dynamics of the RES plants involved but on the on the output power profile.

Energy from wind and solar are the sources of renewable energy (RE) used in this work hence a description of data use. A detailed description of respective data and its preparation before use is given.

3.2.2.1. Wind Speed Data

Wind data for the year 2013 was taken from the *Deutscher Wetterdienst (DWD)*. The data taken from the DWD was at one hour interval and taken at a height of ten metres. That is

each day had 24 data points. The recorded data is from weather station with identification number 880 located in Cottbus [59]. This kind of weather data among others for various locations around the globe can be obtained for locations specific analysis and implementation of the REP-S system sizing concept introduced in this work.

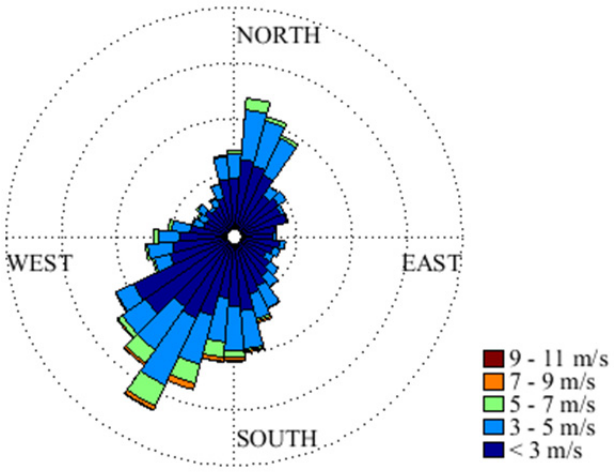

Figure 3-8: Wind Rose of hourly data from DWD for weather station 880 in Cottbus

For the purpose of time synchronisation, the hour-interval wind data was converted into a 15 minutes interval data for further analysis and estimation such as power and energy. This was done using MATLAB implemented spline interpolation function. Upon a simple analysis, much of wind measured is observed to have come from the South-West direction (Figure 3-8) with a mean wind speed of 2.64 ms^{-1} (Figure 3-9). This observation will differ from location to location.

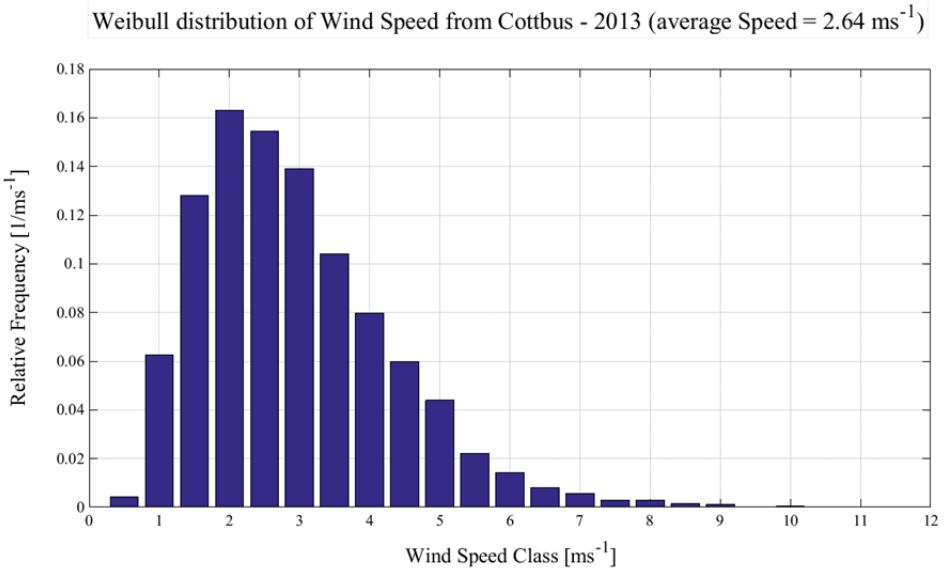

Figure 3-9: Weibull distribution plot of data from DWD for Cottbus

This mean speed of 2.6 ms^{-1} lower than cut in wind speed of most commercial wind turbine in use. This however might not be a problem in the future especially for small wind turbines for households due to innovations. Examples are the Onipko [60] and Vortex Wind turbines, both of which can be brought into operation at wind speeds less than 3 ms^{-1}. Both are still in the prototype stage.

In other to analyse with commercial turbines, the data is adapted to varying heights from 20 meter to about 100 meters using the *logarithmic height formula* shown in (3-6) [61] [62].

$$v = v_{ref} \times \frac{\ln \frac{h}{z_0}}{\ln \frac{h_{ref}}{z_0}} \tag{3-6}$$

where,

v wind speed at height h in ms^{-1},

v_{ref} is wind speed at reference elevation h_{ref} in ms^{-1}

z_0 is the roughness length of area.

The roughness length describes the extent of existence of obstacle in an area under observation. The obtained data sample represent the reference wind speed at 10m. A

roughness length of 0.3 synonymous to obstacles in *Built-up* terrains is used. A result of conversion is seen in Table 3-6.

Table 3-6: Wind Speed at different heights

Height (h) [m]	Minimum Velocity [ms^{-1}]	Maximum Velocity [ms^{-1}]	Average Velocity [ms^{-1}]
10	0.19	10.9	2.64
20	0.22	13.05	3.16
30	0.25	14.32	3.47
40	0.26	15.21	3.69
50	0.27	15.90	3.86
60	0.28	16.47	3.99
70	0.29	16.95	4.11
80	0.30	17.36	4.21
90	0.30	17.73	4.30
100	0.31	18.06	4.38

Mean speed of resulting data obtained at all height are seen to be lower than $5ms^{-1}$. Wind turbine with 1000 kW rated power is considered. The power and coefficient (c_p) curve the turbine is shown in Figure 3-10. The result of estimated energy yield based on above assumption is presented in Table 3-7.

The result present in Table 3-7 were obtained from simulation with generalized wind turbine model in MATLAB Simulink. The estimation gives an overview of how much could be produced from wind turbines of up 1000 kW with data similar to that obtained for the area of Cottbus.

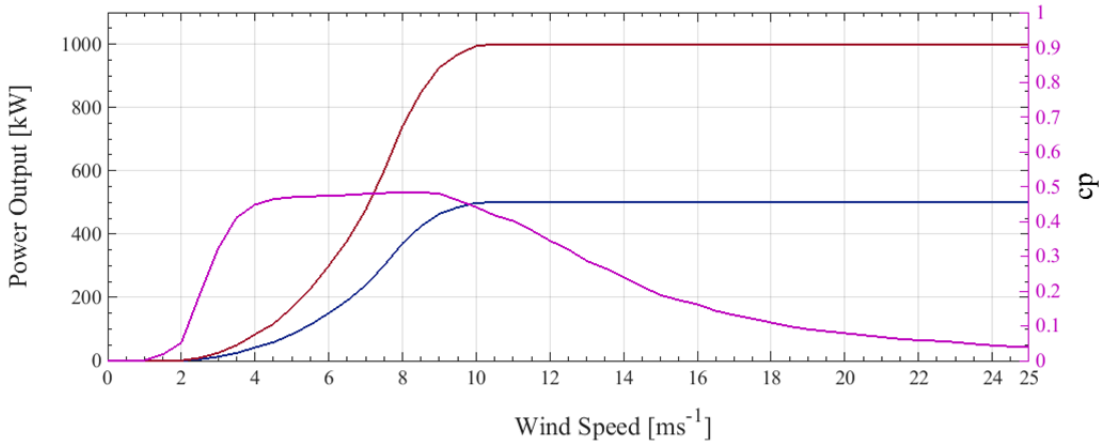

Figure 3-10: Power and Power coefficient Curve for a 500 kW (blue) and 1000 kW (red) wind Turbine

Table 3-7: Estimated energy yield

Height [m]	Estimated Energy [MWh] – 1000 kW
10	372.92
20	668.23
30	880.05
40	1046.90
50	1185.30
60	1303.70
70	1407.00
80	1498.90
90	1581.30
100	1655.90

The total energy at 100 m amounts to about 37 % of total estimated energy consumed by load shown in Table 3-4. This value can be scaled up by multiplying with required factors as required.

$$E_{new}[kWh] = z \times E_{1000}; \quad E_{1000} = 1655.90 \text{ `} \tag{3-7}$$

z is a scaler multiple referenced to 1000 kW

For instance total energy for a 2500 kW Wind turbine at 100 m high will be 4139.75 MWh.

3.2.2.2. Solar Data

The solar power data used in this work was obtained from the Solar Energy Research Field (SERF) of the Brandenburg University of Technology, Cottbus – Senftenberg. The SERF has a photovoltaic (PV) plant comprising of 530 polycrystalline PV modules installed on the roof of the Laboratories of Research and Material Testing (FMPA) of the BTU Cottbus-Senftenberg. Each modules has a nominal voltage of 27.22 V, a nominal current of 8.22 A, module efficiency of about 14.9 % and a peak power rating of about 220 Watts amounting to about 116.6 kW peak power in total. The surface area per PV module is 1.667 m², therefore a total of 833 m² for the total plant. Out of 530, 162 of the modules are installed at an angle 70° while the remaining are at angle of 30°.

The FMPA building has orientation of about 12° towards south-west and is located at

51°46'04.89"N and 14°19'21.83"E. The total roof area of the FMPA building is estimated to be about 4000 m².

The data obtained are originally recorded and stored as 1 second values. The values are then converted to 15 minutes values using simple averaging of second data values spanning equivalent time of 15 minutes. As a result 96 data sample per day instead of 86400 is seen. In Figure 3-11, an example of average data compared with original 1second data for a typical summer day (June 5, 2013) is shown.

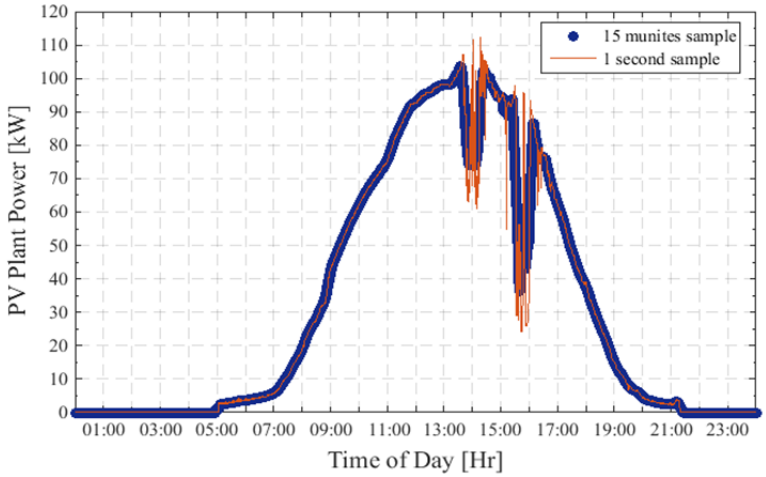

Figure 3-11: Solar power output for a typical summer day.

As seen in Figure 3-11, some information is lost during conversion from 1second data samples to 15 minutes data samples. Deviations as high as about +93.7 kW and low as -86.2 kW are observed when 15 minutes data samples were compared with the original data sample over the entire period.

For the year 2013, a total amount of 101.7 MWh energy was generated. A maximum of peak power of 112.9 kW and average of 15.19 kW was observed from data (Table 3-8). As expected the lowest energy production data is observed for the winter period with total energy of about 6.35 MWh (Table 3-9).

Table 3-8: Power and Energy from SERF – BTU Cottbus, 2013

Installed Capacity	Inst. $P_{average}$	Inst. P_{max}	Total Energy	Average Daily Energy
kW			MWh	
116.6	15.19	112.9	101.7	0.279

The BTU central campus in Cottbus covers an area of about 300,000 m², 27.3% of which is covered with structures. The percentage covered with structures amount to about 82,000 m². A simple direct proportional relation shown in (3-7) is used to estimate the possible maximum PV power that can be installed on BTU Cottbus Campus. The estimation is based strictly on the rated values of PV modules used by SERF. The PV plant covered between about 45 – 50 % of estimated FMPA roof area of 4000[7] m². An assumption that between 50 – 60 % of roof surface could be used for PV was made.

$$P_{peak\_new}^{pv} = \frac{116.6 \times A_{new}^{roof}}{4000 \times 0.45}\ kW \tag{3-8}$$

where,

$P_{peak\_new}^{pv}$ is peak power for PV plant covering new roof area of A_{new}^{roof} .

Table 3-9: Energy Supply by Seasons from SERF for 2013

Total Energy	Energy Min (Daily Total)	Energy Max (Daily Total)	Average Energy
Spring Energy Data (MWh)			
32.27	0.019	0.771	0.355
Summer Energy Data (MWh)			
41.10	0.033	0.769	0.457
Autumn Energy Data (MWh)			
21.93	0.017	0.660	0.244
Winter Energy Data (MWh)			
6.35	0.00712	0.389	0.0723

Based on the aforementioned considerations and assumptions and with a total area of structures of 82,000 m², estimated feasible A_{new}^{roof} to be covered by PV plant is 36,900 m². This results in a $P_{peak\_new}^{pv}$ of 2,390.3 kW. A rounded up figure of 2.5 MW is therefore used for estimation. A total energy of about 2.19 GWh is estimated for a period of one year. Table 3-10 shows a seasonal break down in the estimated energy production. This amount is about 49 % of estimated energy consumption presented in Table 3-4.

The above analysis was made in other to have an overview of the potential of RES energy

[7] The roof area was estimated using ARCGIS and Google Earth

in form of electricity that can be produced from institution, industrial complexes and commercial establishments alike.

In summary some industrial, commercial and institutions have the space to produce up to half their energy consumption in the year. However installing such capacities of REP might not guarantee maximum yield due to earlier mentioned bottlenecks that may be encountered.

Table 3-10: Estimated Energy Supply by Seasons for an estimated installed capacity of 2.5 MW

Total Energy	$Energy_{Min}$ (Daily Total)	$Energy_{Max}$ (Daily Total)	$Energy_{Average}$
Spring Energy Data (MWh)			
695.57	0.418	16.619	7.644
Summer Energy Data (MWh)			
885.81	0.709	16.582	9.842
Autumn Energy Data (MWh)			
472.78	0.357	14.224	5.253
Winter Energy Data (MWh)			
136.88	0.154	8.394	1.555

4. Load flow and Base Case Simulations

In this chapter, the base case states of the study network are established using Load flow analysis. The base case is describes the study networks without RES and RES-Storage systems. Both static and dynamic load flow analysis will be conducted. The result of the base case analysis serves as a reference. The states of the networks under with RES and RES-Storage system are compare with this reference. Figure 4-1 shows the general steps followed when evaluating the electrical network with RES-Storage system. The assumptions and scenarios are described. Results of static load flow analysis followed by that of dynamic load flow analysis are presented.

After establishing the base case states, the states of the study network with only RES with also be established. That is the first two steps are presented in this chapter. Steps 3 and 4 are described in chapter 5. Step 1, Step 2 and Step 4 are process conducted with power flow analysis. Step 3 is done using optimization process.

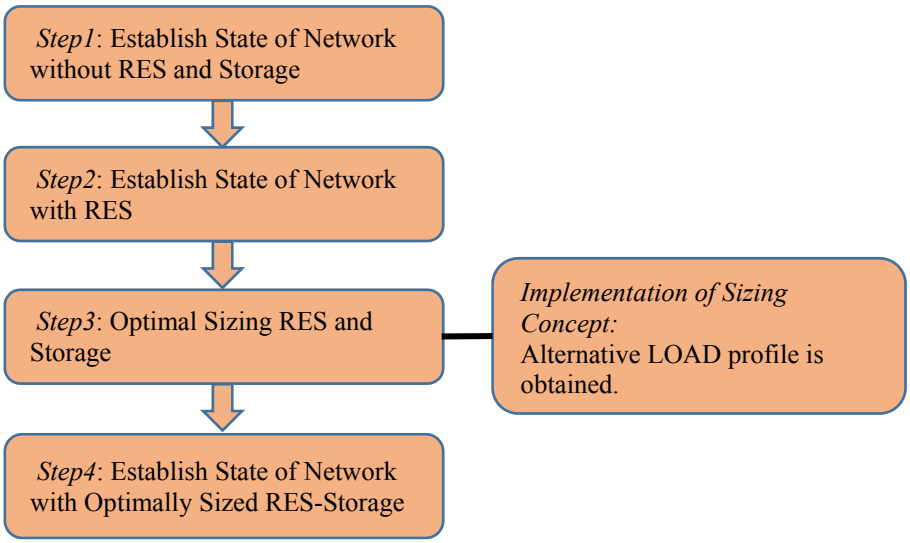

Figure 4-1: General steps of evaluating sizing system with RES-Storage system integration

With reference to Figure 4-2, load flow analysis helps to establish the voltage drops at each bus in study network according (4-1). The voltage values obtained are analysed to ascertain

their conformity with voltage limit according to IEC 60038.

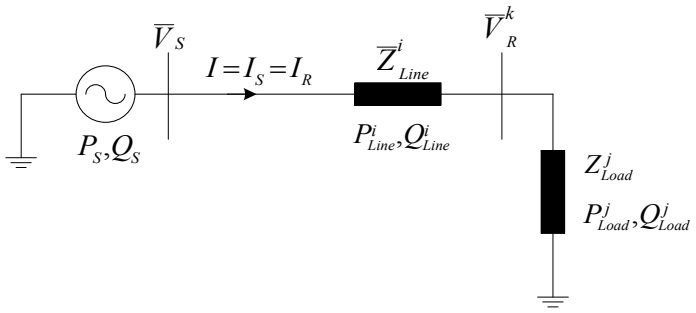

Figure 4-2: Simple single line model of electrical network (source, transmission line, load and buses)

$$\overline{V}^k_R = \overline{V}_s - I\overline{Z}^i_{Line} \tag{4-1}$$

P^i_{Line} and Q^i_{Line} of all i branches helps in determining currents through respective branches are also determined. In other words, the current *"I*" through all branches are monitored and analysed. P^j_{Load} and Q^j_{Load} of all j loads within the network are known at the beginning of the analysis. Finally the total network loss is determined.

In other to conduct the analysis, the software MATLAB was adopted though there are numerous software dedicated to load flow analysis. The choice of MATLAB is due to the flexibility it provides its users to model in this case electrical power networks and process large data. Within the same platform results of simulation can be analysed, edited and reprocessed for simulation of various scenario. In Figure 4-3 are snapshots of implemented CIGRE 30 bus network in MATLAB Simulink environment; (a) shows the network with the two subnetworks separated into two subsystems, (b) is subnetwork 1, (c) is subnetwork 2.

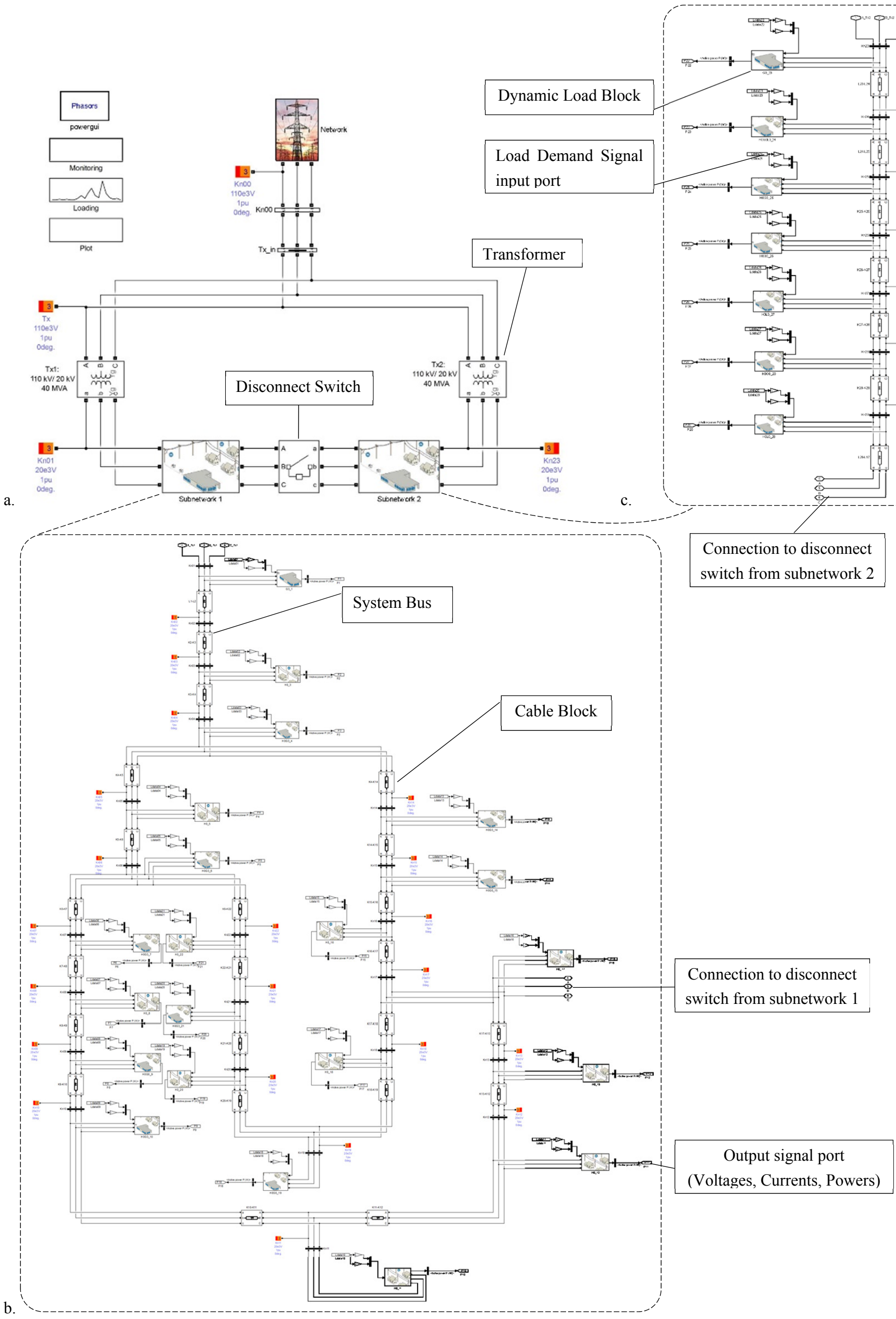

Figure 4-3: Model of 30 bus network in MATLAB Simulink: a. Overview of network showing subnetworks with and disconnect switch; b. Expansion showing elements of subnetwork 1; c. Expansion showing elements of subnetwork 2

4.1 Static Load Flow analysis

A static load flow analysis basically happens to be a snap-shot of the state of an electrical network at an instance. This is a numerical analysis of the flow of electrical power in an electrical power network or system.

4.1.1 Base Case for 30 Bus Network

To conduct analysis for to establish the base state for the 30 bus network shown in Figure 3-1, the scenarios summarised in Table 4-1 are considered. The disconnect switch is kept open and then closed for analysis at various loading percentage levels.

Table 4-1: Difference Scenarios for establishing base state of 30 bus network

Disconnect Switch State	Open	Closed
Loading condition at buses [%]	25 % of Installed Capacity	
	50 % of Installed Capacity	
	90 of Installed Capacity	
	100 of Installed Capacity	

The open state of the disconnect switch separates both subnetworks from each other. In this state, the respective transformers are solely responsible for networks connected to them.There are no voltage support within the network. With closed disconnect switch, there should be redistribution of current flows leading to changes in voltage levels when analysis at same voltage levels are compared.

Results of Analysis

The voltage at all buses are recorded and tabulated for each load flow analysis. A screen shot of a typical load flow analysis is shown in Figure 4-4. This is for the scenario where the disconnect switch is opened and all load are assume to be drawing 25 % of their installed capacity from the network.

	Block type	Bus type	Bus ID	Vbase (kV)	Vref (pu)	Vangle (deg)	P (MW)	Q (Mvar)	Qmin (Mvar)	Qmax (Mvar)	V_LF (pu)	Vangle_LF (deg)	P_LF (MW)	Q_LF (Mvar)	Block Name
1	Vsrc	swing	Kn00	110.00	1.0400	0.00	0.00	0.00	-Inf	Inf	1.0400	0.00	31.71	13.49	Network/Overlay Network
2	DYN load	PQ	Kn01	20.00	1	0.00	1.52	0.94	-Inf	Inf	1.1053	-4.60	1.52	0.94	Subnetwork 1/G3_1
3	DYN load	PQ	Kn23	20.00	1	0.00	1.75	1.08	-Inf	Inf	1.1185	-3.10	1.75	1.08	Subnetwork 2/G3_23
4	Bus	-	Tx	110.00	1	0.00	0.00	0.00	0.00	0.00	1.0400	0.00	0.00	0.00	Load Flow Bus3
5	Bus	-	Kn02	20.00	1	0.00	0.00	0.00	0.00	0.00	1.0824	-4.88	0.00	0.00	Subnetwork 1/Load Flow Bus1
6	DYN load	PQ	Kn11	20.00	1	0.00	0.31	0.10	-Inf	Inf	1.0217	-5.38	0.31	0.10	Subnetwork 1/HO_11
7	DYN load	PQ	Kn12	20.00	1	0.00	0.23	0.08	-Inf	Inf	1.0219	-5.38	0.23	0.08	Subnetwork 1/HO_12
8	DYN load	PQ	Kn13	20.00	1	0.00	0.26	0.09	-Inf	Inf	1.0220	-5.38	0.26	0.09	Subnetwork 1/HO_13
9	DYN load	PQ	Kn14	20.00	1	0.00	1.28	0.42	-Inf	Inf	1.0258	-5.35	1.28	0.42	Subnetwork 1/HOG3_14
10	DYN load	PQ	Kn15	20.00	1	0.00	1.53	0.51	-Inf	Inf	1.0248	-5.36	1.53	0.51	Subnetwork 1/HOGO_15
11	DYN load	PQ	Kn16	20.00	1	0.00	0.26	0.08	-Inf	Inf	1.0240	-5.36	0.26	0.08	Subnetwork 1/HO_16
12	DYN load	PQ	Kn17	20.00	1	0.00	0.35	0.12	-Inf	Inf	1.0233	-5.37	0.35	0.12	Subnetwork 1/HO_17
13	DYN load	PQ	Kn18	20.00	1	0.00	0.23	0.08	-Inf	Inf	1.0231	-5.37	0.23	0.08	Subnetwork 1/HO_18
14	DYN load	PQ	Kn19	20.00	1	0.00	1.44	0.48	-Inf	Inf	1.0230	-5.37	1.44	0.48	Subnetwork 1/HOGO_19
15	DYN load	PQ	Kn20	20.00	1	0.00	0.25	0.08	-Inf	Inf	1.0231	-5.37	0.25	0.08	Subnetwork 1/HO_20
16	DYN load	PQ	Kn03	20.00	1	0.00	0.26	0.08	-Inf	Inf	1.0549	-5.10	0.26	0.08	Subnetwork 1/HO_3
17	DYN load	PQ	Kn21	20.00	1	0.00	1.18	0.39	-Inf	Inf	1.0232	-5.37	1.18	0.39	Subnetwork 1/HOG3_21
18	DYN load	PQ	Kn22	20.00	1	0.00	0.24	0.08	-Inf	Inf	1.0237	-5.37	0.24	0.08	Subnetwork 1/HO_22
19	DYN load	PQ	Kn04	20.00	1	0.00	1.38	0.45	-Inf	Inf	1.0278	-5.33	1.38	0.45	Subnetwork 1/HOG3_4
20	DYN load	PQ	Kn05	20.00	1	0.00	0.31	0.15	-Inf	Inf	1.0259	-5.35	0.31	0.15	Subnetwork 1/HO_5
21	DYN load	PQ	Kn06	20.00	1	0.00	1.81	0.59	-Inf	Inf	1.0241	-5.36	1.81	0.59	Subnetwork 1/HOG3_6
22	DYN load	PQ	Kn07	20.00	1	0.00	0.96	0.31	-Inf	Inf	1.0233	-5.37	0.96	0.31	Subnetwork 1/HOG3_7
23	DYN load	PQ	Kn08	20.00	1	0.00	0.37	0.12	-Inf	Inf	1.0226	-5.38	0.37	0.12	Subnetwork 1/HO_8
24	DYN load	PQ	Kn09	20.00	1	0.00	1.46	0.49	-Inf	Inf	1.0219	-5.38	1.46	0.49	Subnetwork 1/HOGO_9
25	DYN load	PQ	Kn10	20.00	1	0.00	1.86	0.61	-Inf	Inf	1.0216	-5.38	1.86	0.61	Subnetwork 1/HOG3_10
26	DYN load	PQ	Kn24	20.00	1	0.00	1.98	0.65	-Inf	Inf	1.0951	-3.39	1.98	0.65	Subnetwork 2/HOGOLO_24
27	DYN load	PQ	Kn25	20.00	1	0.00	2.07	0.68	-Inf	Inf	1.0927	-3.42	2.07	0.68	Subnetwork 2/HOG3_25
28	DYN load	PQ	Kn26	20.00	1	0.00	2.07	0.68	-Inf	Inf	1.0909	-3.45	2.07	0.68	Subnetwork 2/HOG3_26
29	DYN load	PQ	Kn27	20.00	1	0.00	1.79	0.59	-Inf	Inf	1.0899	-3.46	1.79	0.59	Subnetwork 2/HOLO_27
30	DYN load	PQ	Kn28	20.00	1	0.00	1.15	0.38	-Inf	Inf	1.0893	-3.47	1.15	0.38	Subnetwork 2/HOGO_28
31	DYN load	PQ	Kn29	20.00	1	0.00	1.69	0.55	-Inf	Inf	1.0873	-3.50	1.69	0.55	Subnetwork 2/HOLO_29
32	Bus	-	*1*	20.00	1	0.00	0.00	0.00	0.00	0.00	1.0873	-3.50	0.00	0.00	Subnetwork 2/L29-L17

Figure 4-4: Screenshot of Results of load flow analysis for the scenario – open disconnect switch at 25 %loading of all loads connected to network

The result of voltages for analysis conducted on the network with opened disconnect switch is plotted and shown in Figure 4-5.Information about voltage profiles of buses Kn07 to Kn12, Kn18 to Kn21 and from Kn24 to Kn28 were omitted since the trend and main information can been with the presented plot. The complete plot can be found in Figure B- 1 in the appendix. A decrease in voltage as load levels increases is observed at all buses. The lowest is voltage of about 0.815 pu is observe at bus Kn013 when the load draws full capacity from network. This observation was made for opened and closed disconnect switch.

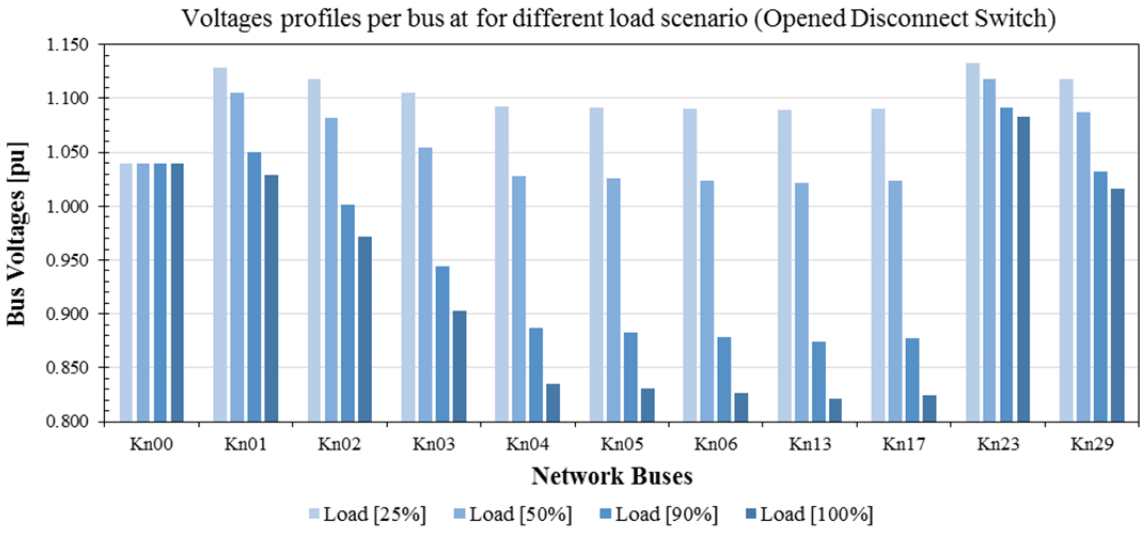

Figure 4-5: Voltage profile per bus under opened switch condition

Depicted in Figure 4-6 is the trend of voltage at all buses at the four load levels presented in Table 4-1 under closed condition of disconnect switch. The profile of all 30 buses can be seen in the appendix in Figure B- 2. A similar trend of decreasing voltage level with increasing system load is observed. The lowest voltage is about 0.93 pu is observed at bus Kn13. This occurs when a demand of 100 % of installed load capacity been drawn from each bus of the network.

The voltage profile of the entire 30 bus network is observed to be better when the switch is closed than when it was opened. Voltages of buses Kn04 to Kn22 fall below 0.9 pu when switch is kept open for loading of 50 % to 100 % of installed capacity of load. These values fell below the allowable stipulated voltage operating tolerance of $\pm 10\%$ less or greater than nominal voltage (V_{rT}).

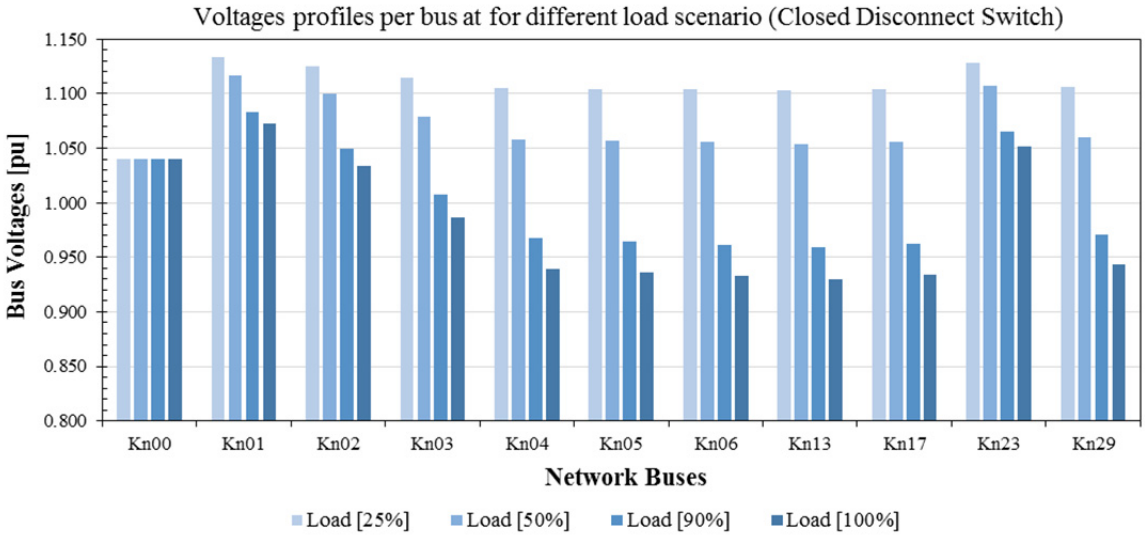

Figure 4-6: Voltage profile per bus under closed switch condition

The total losses of the network for each scenario is presented in Table 4-2 . A general trend of losses increasing with increasing load demand was obsersed. On the hand, relatively higher overall system losses were observed when disconnect switches are opened then when kept closed.

Table 4-2: Total network losses at different load demand level

Load Level [%]	25		50		90		100	
Disconnect switch condition	Open	Closed	Open	Closed	Open	Closed	Open	Closed
Total Losses [MW]	0.34	0.29	1.53	1.29	6.55	5.02	9.02	6.57

4.1.2 Base Case for Single Node network

The base case scenario for the single node network is the network without RES or RES-Storage systems connected to it. Load hosting capacity of components in the electrical network and network as a whole takes into consideration two main parameters that should not be violated during operation. These main parameters are the voltage levels at buses and thermal rating or limits of components characterised by their current currying capacities. The connection of REP-storage system into a network will effectively alter current characteristics both in magnitude and direction in the network.This effect could be beneficial to the network. Based on the parameters and maximum possible demand of study network, preliminary

hosting capacity level can be determined. Equation 4-2 is used to find maximum demand and rated currents of loads and the transformer seen in Table 4-3 and Table 4-4. Equation 4-3 shows the acceptable operational voltage limit expected at buses in the network.

$$I_{rT} = \frac{S_{rT}}{\sqrt{3}.V_{rT}} \tag{4-2}$$

where

I_{rT} =rated current, V_{rT} =rated voltage, S_{rT} =rated apparent power

$$V_{\min} \le V_{rT} \le V_{\max}, \{V_{\min} = 0.9 \times V_{rT}, V_{\max} = 1.1 \times V_{rT}\} \tag{4-3}$$

where

$V_{\min}$ =lower voltage limit, $V_{\max}$ = higher voltage limit,

Table 4-3: Rated power Cable parameters of modified single node model

Network Load	Rated Apparent Power Demand [kVA]	Maximum Demand Current [A]
Load 1	850	1226.9
Load 2	650	938.2
Load 3	450	649.5
Total Load	1950	2814.6

The maximum current demands seen in Table 4-3 are seen to be greater than the current carrying capacity of their respective cables presented in

Table 3-2. Therefore 3, 2 and 2 cable sets were used in the model for cable link Kn01_1 – Kn01_11, Kn01_1 – Kn01_12 and Kn01_1 – Kn01_13 respectively for network in Figure 3-1 (b). This implies that the cable links now have combined current carrying capacity of 1614, 1076 and 1076 amperes respectively amounting to a total of 3766 amperes.

Table 4-4: Transformer and Network rated parameters.

Component	Rated Power [kVA]	Rated Current 1°Side [A]	Rated Current 2° Side [A]
Transformer	2000	57.7	2886.8
	Short Circuit Level [kVA]		
Overlay Network	100000		

Comparing the total maximum demand current with transformer rated current results in a

difference of about 72.2 ampere. Referring the 72.2 ampere to transformer rated current gives a percentage value of about 2.5 %. Per this analysis, only a load of about 72 ampere rated current extra can be connected to this transformer. This is in spite of the fact that the cables can still allow current in excess of 387 A, 138 A and 427 A for Kn01_1 – Kn01_11, Kn01_1 – Kn01_12 and Kn01_1 – Kn01_13 respectively. Theoretically and as already known, the injection of current at a bus improves the voltage at the bus. The hosting capacities at the buses Kn01_11 to Kn01_13 are values of infeed at which the upper voltage operational limit is reached.

Results of Analysis

To establish the state of the network under base case scenario, load flow analysis of the single node network is conducted. The network at base case as already stated is the network without REP-Storage system and without voltage supports. Initial results of this load flow analysis for the base case single node network in is shown in Table 4-5. The worse voltage of 0.92 pu was observed at bus Kn01_12. However, this value falls within the allowable stipulated voltage operating tolerance of $\pm 10\%$ less of nominal voltage (V_{rT}). This tolerance limit is specified in the DIN IEC 60038 and EN 50160 standards. From this same table, the highest real power losses of 63.15 kW is observed for 100 % loading.

Table 4-5: Results of load flow analysis for single node model in Figure 3-1 (b) at varying percentage of loading

100 % Loading							
Bus ID	V_{rT} [kV]	V_{rT} [pu]	V [pu]	V_angle		P [kW]	Q [kVar]
Kn00	20.00	1.00	1.00	0.00		- 1798.15	- 1211.72
Kn01	20.00	1.00	0.99	0.11		0.00	0.00
Kn01_1	0.40	1.00	0.96	-6.94		0.00	0.00
Kn01_11	0.40	1.00	0.93	-7.61		722.50	447.77
Kn01_12	0.40	1.00	0.92	-8.17		585.00	283.33
Kn01_13	0.40	1.00	0.95	-7.61		427.50	140.51
					Losses	-63.15	-340.11
90 % Loading							
Bus ID	V_{rT} [kV]	V_{rT} [pu]	V [pu]	V_angle		P [kW]	Q [kVar]
Kn00	20.00	1.00	1.00	0.00		- 1612.46	- 1050.20
Kn01	20.00	1.00	0.99	0.09		0.00	0.00
Kn01_1	0.40	1.00	0.98	-6.16		0.00	0.00
Kn01_11	0.40	1.00	0.95	-6.76		650.25	402.99
Kn01_12	0.40	1.00	0.94	-7.24		526.50	255.00
Kn01_13	0.40	1.00	0.96	-6.75		384.75	126.46
					Losses	- 50.96	- 265.75
50 % Loading							
Bus ID	V_{rT} [kV]	V_{rT} [pu]	V [pu]	V_angle		P [kW]	Q [kVar]
Kn00	20.00	1.00	1.00	0.00		- 887.80	- 500.70
Kn01	20.00	1.00	0.99	0.04		0.00	0.00
Kn01_1	0.40	1.00	1.01	-3.27		0.00	0.00
Kn01_11	0.40	1.00	0.99	-3.57		361.25	223.88
Kn01_12	0.40	1.00	0.99	-3.81		292.50	141.66
Kn01_13	0.40	1.00	1.01	-3.57		213.75	70.26
					Losses	-20.3	-64.9
25 % Loading							
Bus ID	V_{rT} [kV]	V_{rT} [pu]	V [pu]	V_angle		P [kW]	Q [kVar]
Kn00	20.00	1.00	1.00	0.00		- 465.51	- 234.48
Kn01	20.00	1.00	0.99	0.02		0.00	0.00
Kn01_1	0.40	1.00	1.03	-1.68		0.00	0.00
Kn01_11	0.40	1.00	1.02	-1.83		180.62	111.94
Kn01_12	0.40	1.00	1.02	-1.95		146.25	70.83
Kn01_13	0.40	1.00	1.03	-1.83		106.88	35.13
					Losses	-31.76	-16.58

4.2 Dynamic Load Flow analysis

The dynamic load flow analysis is first carried out on the study network without any voltage support scheme during the simulation. Tap changer were used in only two stages where they were either set at maximum or neutral. The full impact of the load due to the demand characteristics will be more pronounced in this case.

4.2.1 Base Case for 30 Bus Network

For the dynamic analysis, the 30 bus network model is simulated for a year period with measurement taken at 15 minutes time intervals. As stated earlier, tap changing transformers are used in the 30 bus network. The load flow analysis over the period of one year was therefore conducted for scenarios where tap changers are assumed to be on neutral and maximum position in combination with open and closed disconnect switch positions. In Figure 4-7, average of most bus voltages for Subnetwork 1 is observed to be around 0.84 pu and 0.93 pu for Subnetwork 2 with lowest voltages observed to be about 0.66 pu at bus 10 and 0.87 pu at bus 29.

The condition as expected is seen to improve when disconnect switch is closed. This is seen in Figure 4-9 where average bus voltages are seen to be around 0.95 pu and 1.03 pu for subnetwork 1 and subnetwork 2 respectively.

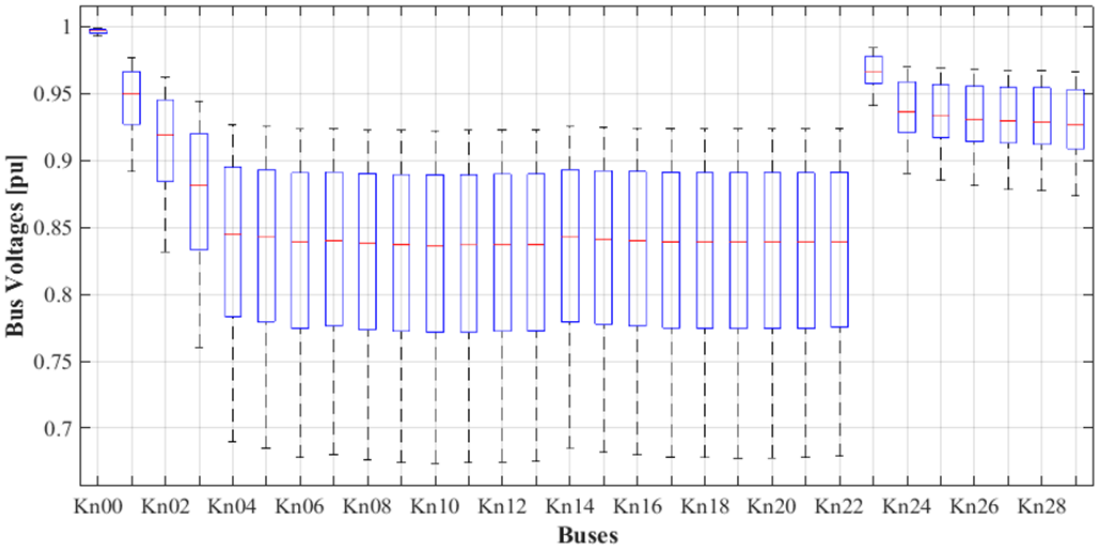

Figure 4-7: Boxplot of voltage profile for 30 bus network in Figure 3-1 (a) with opened disconnect switch and transformer tap changers set to neutral

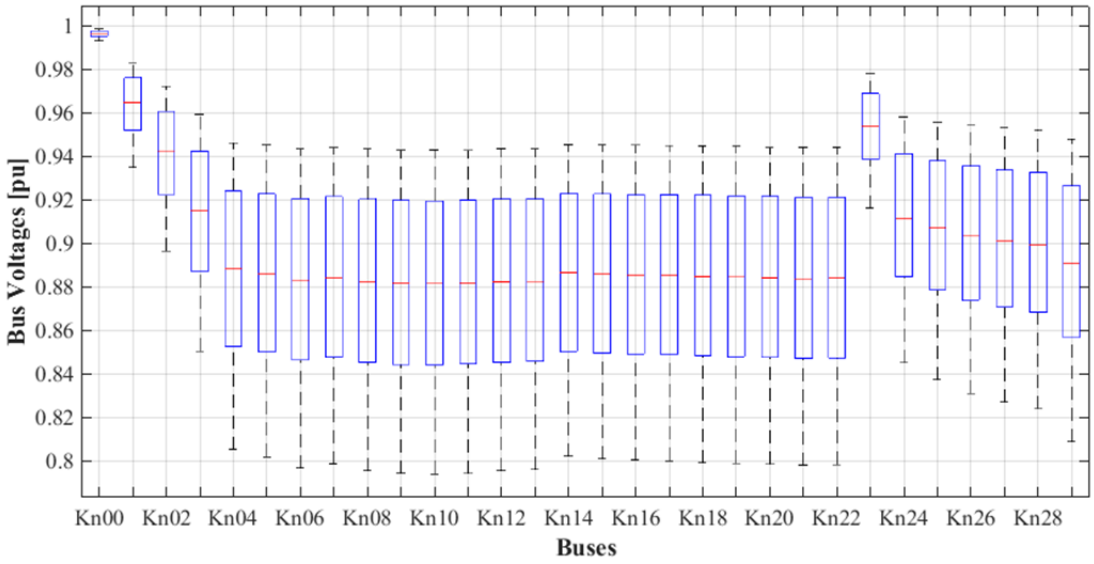

Figure 4-8: Boxplot of voltage profile 30 bus network in Figure 3-1(a) with closed disconnect switch with transformer tap changers set to neutral

Minimum voltages observed are 0.81 pu and about 0.95 pu for subnetwork 1 and subnetwork 2. Both values are lower that the stipulated acceptable voltage range.

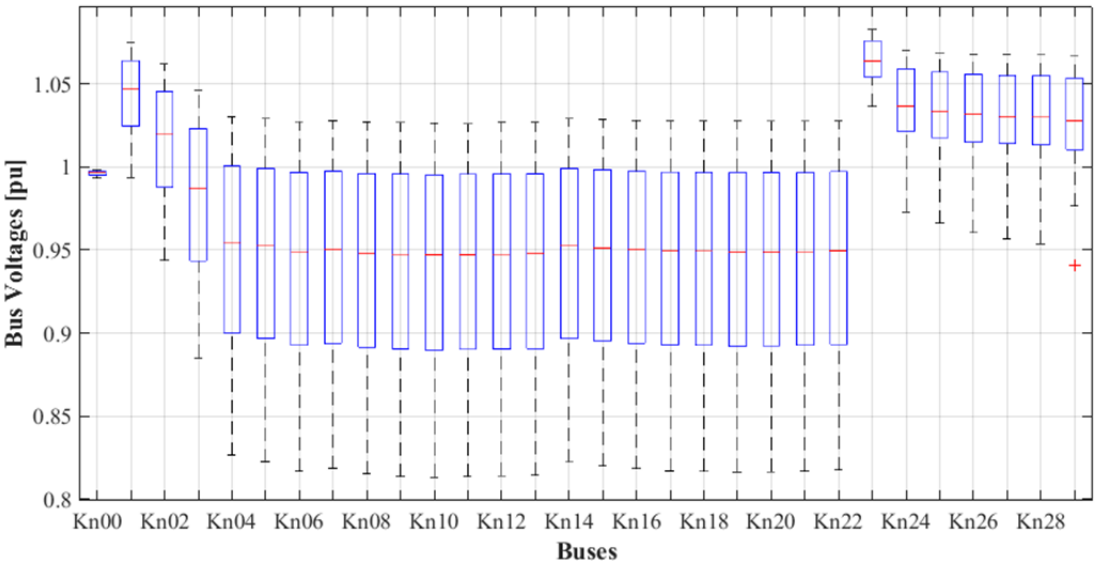

Figure 4-9: Boxplot of voltage profile 30 bus network in Figure 3-1(a) with opened disconnect switch and transformer tap changers set to a maximum

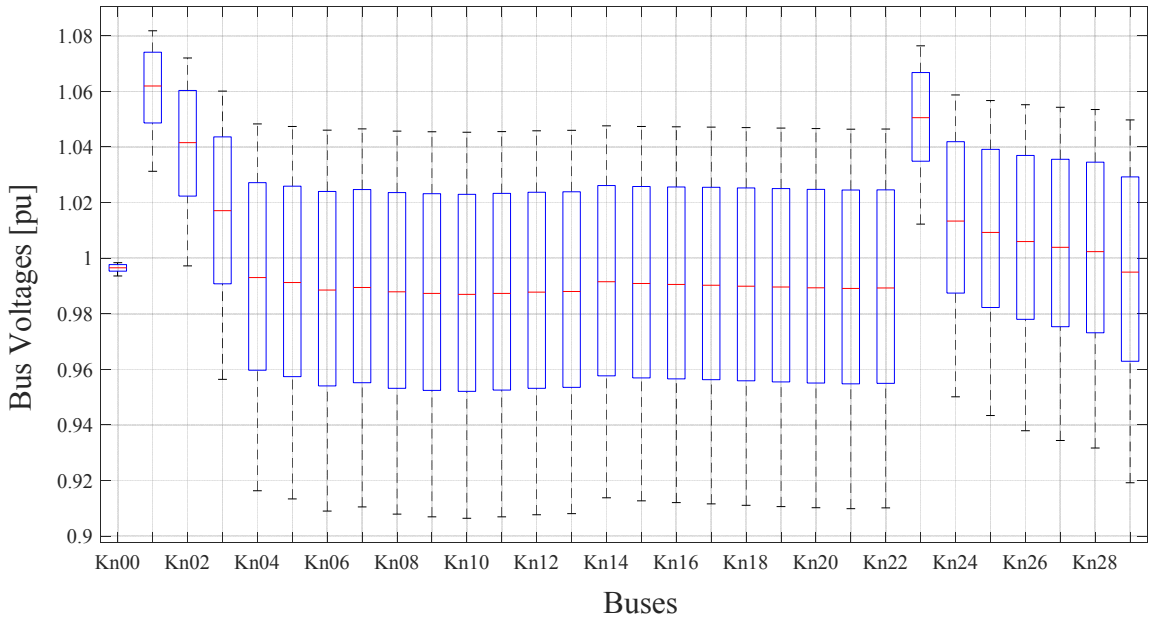

Figure 4-10: Boxplot of voltage profile for 30 bus network in Figure 3-1 (a) with closed disconnect switch with transformer tap changers set to maximum

Comparison of the above Figure 4-7 and Figure 4-9 reveal that, voltage profile of subnetwork 2 reduces as the profile of subnetwork 1 increases for closed disconnect switch. This is due to the redistribution power (current) flow through the network.

In analysis conducted for the network with closed disconnect switch with transformer tap changer set to neutral resulted,minimum voltage level observed are about 0.79 pu and 0.81 pu in Subnetwork 1 and Subnetwork 2 respectively. The average values however, are seen to be about 0.88 pu and 0.91 pu as seen in Figure 4-8. The result on the other hand observed in Figure 4-10 where transformer tap changers are set maximum with closed disconnect switch, shows a relatively higher average overall voltage level of about 0.99 pu and 1.01 pu for the two subnetworks. The minimum voltage levels are 0.905 pu and 0.92 pu in the two subnetworks.

4.2.2 Base Case for Single Node network

A boxplot of bus voltages is presented in Figure 4-11. This is the result of dynamic simulation analysis conducted on single node network shown in Figure 3-1 (b) with load profile of load with installed capacities present in chapter 3. Similar to its static load flow analysis, all

voltages appear to fall with the allowable tolerance as stipulated in the DIN IEC 60038 and EN 50160 standards. A seen the lowest voltage is observed at bus Kn0_12 with value about 0.922 pu.

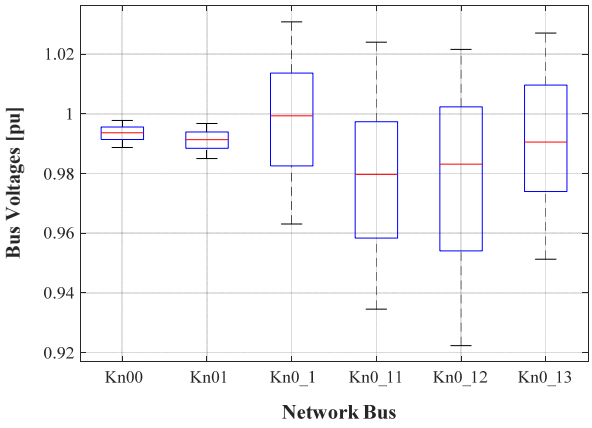

Figure 4-11: Boxplot of voltage profile for single node network presented in Figure 3-1 (b)

Table 4-6: Summery of Voltages and Currents at bus of network in Figure 3-1 (b) simulated with only load profile

Dynamic Modelling						
Bus ID	V_max [pu]	V_min [pu]	V_mean [pu]	I_max [A]	I_min [A]	I_mean [A]
Kn00	1.00	0.99	0.99	55.80	17.55	34.89
Kn01	1.00	0.99	0.99	56.15	17.86	35.21
Kn01_1	1.02	0.96	1.00	2664.6	841.25	1667.8
Kn01_11	1.01	0.93	0.98	1307.8	580.23	904.61
Kn01_12	1.02	0.92	0.98	1017.2	168.25	488.69
Kn01_13	1.02	0.95	0.99	673.79	86.90	280.91

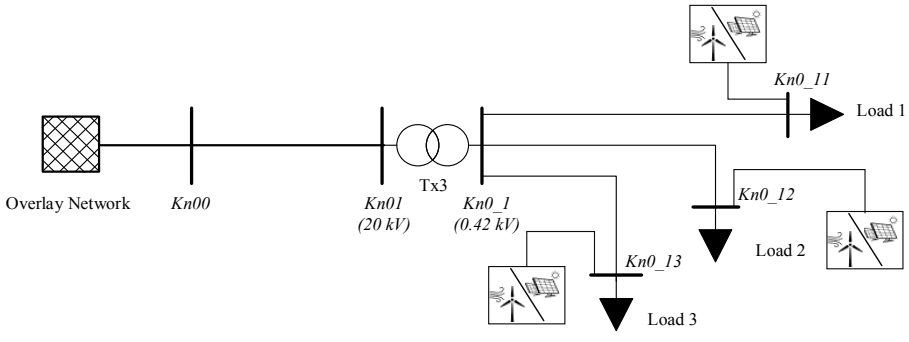

Figure 4-12: Single node network with RES integration; Configuration to assess impact of only RES integration into the single node network.

The dynamic simulation is also conduction for with Wind and PV integrated at the integrated at each of the buses of network in Figure 4-12 separately.

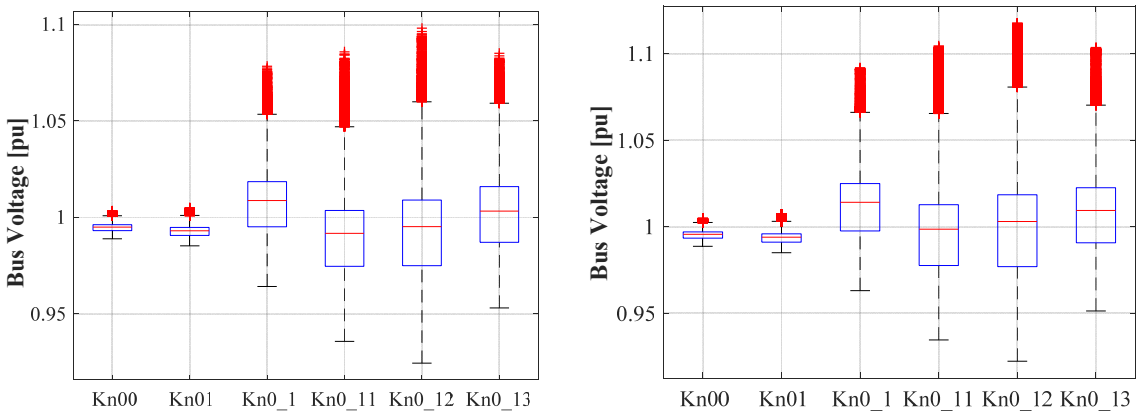

Figure 4-13: Boxplot of voltages at buses in in single node model; (a) integration with PV (b) integration with Wind power

The maximum capacity of each renewable plant were set to the rated load capacity at the respective buses. That is each REP had has rated power of 722.5 kW, 585 kW and 427.5 kW respectively.

Table 4-7: Summery of Voltages and Currents at bus of network in Figure 3-1 (b) simulated with PV and Wind integration.

PV						
Bus ID	V_max [pu]	V_min [pu]	V_mean [pu]	I_max [A]	I_min [A]	I_mean [A]
Kn00	1.00	0.99	0.99	55.02	0.10	28.73
Kn01	1.001	0.99	0.99	55.36	0.14	29.04
Kn01_1	1.08	0.96	1.01	2627.4	1.69	1374.2
Kn01_11	1.09	0.94	0.99	1307.8	0.065	766.45
Kn01_12	1.10	0.92	0.99	1002.4	0.073	394.85
Kn01_13	1.09	0.95	1.00	673.79	0.016	231.85
Wind						
Bus ID	V_max [pu]	V_min [pu]	V_mean [pu]	I_max [A]	I_min [A]	I_mean [A]
Kn00	1.00	0.99	1.00	55.80	0.057	26.03
Kn01	1.01	0.99	0.99	56.14	0.099	26.31
Kn01_1	1.09	0.96	1.01	2664.5	4.09	1245.1
Kn01_11	1.10	0.93	0.99	1307.7	0.018	697.07
Kn01_12	1.12	0.92	1.00	1017.2	0.043	361.17
Kn01_13	1.04	0.95	1.00	669.01	0.027	205.27

5. Renewable Energy Plant-Storage system Sizing Concept

This chapter describes the proposed method of sizing Renewable Energy Plant-Storage (REP-S). A brief description of how REPs are sized is presented. The theory of optimization is also briefly described to justify why a specific optimization method was chosen for implementing the concept.

REP-S system as has been used in preceding chapter of this thesis is a made up word used to represent a combination of a renewable energy powered power plant and any form of storage system as a unit. This name is backed by the idea that renewable energy source plants should be designed, sized and installed together with storage as a unit. This unit can be considered as a "real unit" or as a virtual unit. A real unit in this instance represents the situation where both renewable energy plant (REP) and storage are in close proximity sharing a common point of common coupling. A virtual unit on the other hand will consists REPs and storage systems distributed at different locations within the distribution network. In the sense of a virtual unit, there should be central command and control centre responsible for monitoring as oppose to the former with individual or decentralized monitoring and control.

The nature of the major contributors to REP connected to the distribution networks as well as their operation modes could cause higher loading in network equipment. Higher loading in network equipment translates into higher loading of immediate hosting network. As already mentioned in chapter 2, electrical network system operators are allowed to reduce power output from REP when a network overloading situation is foreseen.

This thesis is proposing that the installation of REP with storage component should be encouraged. The KfW 275 and similar incentives are schemes that can support this concept. Some RES power producers and consumers with rooftop installation already have storage components as part of the entire system. A key point of this proposal is that an agreed upon reference power should be made available by utility to the consumer at all time.

There are technical requirements that need to be considered before connecting REP to network. Two main requirement relevant to this work are;

a. plant dimension or size

b. admissible voltage change or variation

In Germany, the Bundesverband der Energie und Wasserwirtschaft e.V (BDEW) has provided technical guidelines in this respect. A summary of guidelines for the above stated requirement are as follows;

- the maximum apparent power of an REP ($S_{REP}^{\max}$) connecting into the medium voltage network is given by;

$$S_{REP}^{\max} = \frac{\sum P_{Load}^{rated}}{pf_{\min}} \tag{5-1}$$

where, $\sum P_{Load}^{rated}$ is the sum of active power of all load connected to the same point of common coupling (PCC) or busbar under consideration and $pf_{\min}$ minimum power factor at the same bus.The maximum apparent power is therefore based on the thermal loading of the as seen from the PCC.

- the admissible voltage change (δv) is the difference in voltage that is observed at the PCC before and after the integration of a REP. This value should not exceed 2 % of former voltage. That is

$$\delta v \leq \pm 0.02 V_{PCC}^{old} \tag{5-2}$$

The main aim of this work is to explore the option of supporting existing network. This is by means of utilizing more efficiently the hosting capacity through the use REP-S systems. Figure 5-1 is a simplified one-line diagram illustrating REP-Storage system integration into the study network. Unlike going by the assumption of installing as much REP capacity as the network or section of the network can support, REP-Storage systems is optimally sized for a specific point of connection in the network.The pivot of this sizing concept is the historic data

of RE resource and power or energy demand profile. The classical theories of stochastic optimization methods is employed in the sizing process.

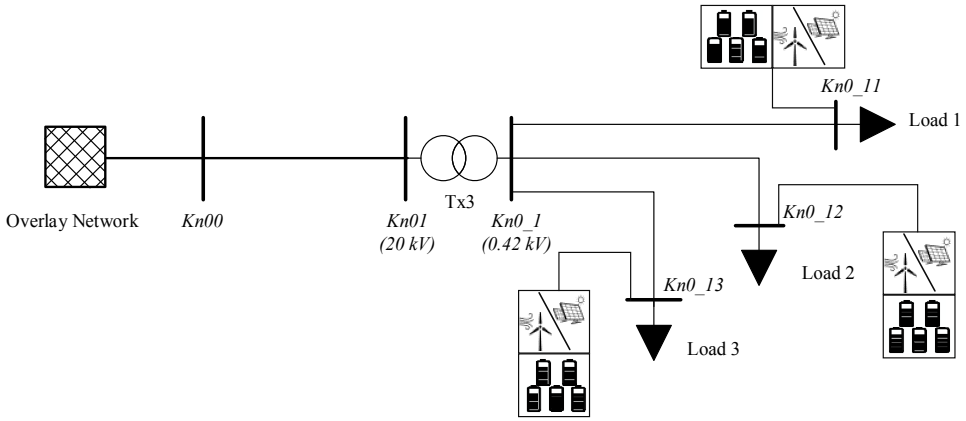

Figure 5-1: Single node model with RES – Storage integration.

5.1 Optimization Theory

The oxford dictionary defines optimization as “The action of making the best or most of a situation or resource”. Other definitions in summary, refers to optimization as the process of making best amid other alternatives or choices. This can be done through trial and error or by an iterative process. The process of optimization is evident in our everyday decision making either consciously or subconsciously with task of choosing among alternatives guided by ones desire to make the best choice [63], [64]. A simplified iterative process that can be seen in optimization is depicted in Figure 5-2 where the process starts with initial options with defined problem at hand. When outcome after considered options or alternatives is not desired, the options are reviewed, changes made and the process repeated until desired outcome to be implemented is obtained. Stochastic optimization methods are basically optimization methods that finds best solution of random objective function using random variables.

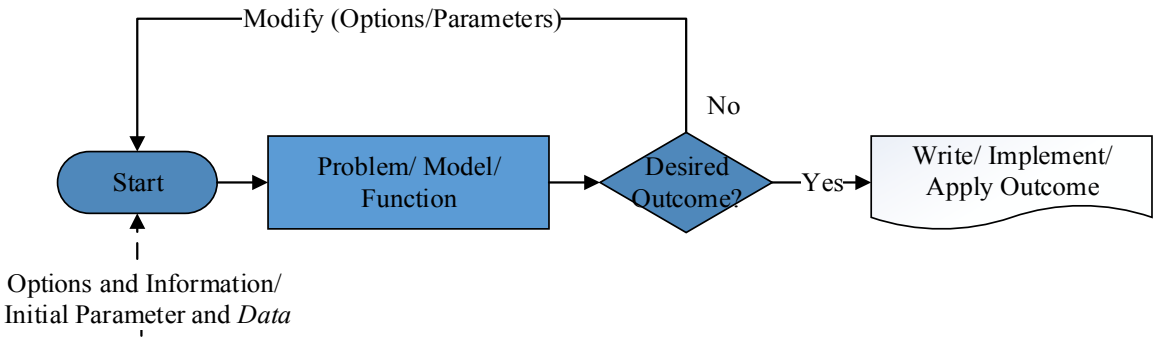

Figure 5-2: Basic depiction of an Iterative procedure

5.1.1 Mathematical Description

Mathematically, the measure of how best a choice is, is based on the outcome of a model or function called the objective function denoted as f . Optimization theory and methods deals with the selection of best alternative based on a given objective function. This function, also called the mathematical model is also referred to as the optimization problem and describes usually an existing problem or intended system to be optimized. When the optimization problem consist of more than one objective function, the problem is termed a multi-objective optimization problem. The function value depends on sets of variables which change over the search for a suitable outcome. These variables are referred to as the decision variables. Variable are usually denoted $x_1, x_2, x_3, ..., x_n$, where n is the number of variable.The objective function may also depend on set of constant parameters $p_1, p_2, p_3, ..., p_q$, where q is the number of parameters. Generally, the objective function is represented as cost or loss function where a non-desired quantity is minimized. It can also be presented as a utility or fitness function where a desired quantity is maximized. The outcome or solution of the objective function is a value or set of values at which the function is said to be minimized or maximized. To help in the decision process, the objective function (optimization problem) could either be subject to constrains or in some instances without constrains.

Therefore the objective function f and dependent variable translates into the following;

Minimize $f(\mathbf{x})$ (5-3)

subject to $\mathbf{x}=\Omega$ (5-4)

Where the function $f:\mathbb{R}^n \to \mathbb{R}$ is a real-valued function that is to be minimized. The vector $\mathbf{x}$ is a vector of *n* variables denoted by

$$\mathbf{x} = \left[x_1, \quad x_2, \quad x_3, \quad . \quad . \quad ., \quad x_n\right]^T \in \mathbb{R}^n \tag{5-5}$$

Therefore (5-4) becomes;

$$\text{minimize } f(\mathbf{x}) = f(x_1, x_2, x_3, ...x_n)$$

The problem represent by (5-1) is an unconstrained optimization problem if $\Omega \in \mathbb{R}^n$. Equation 5-1 is on the other hand a constrained optimization problem when only (5-3) called the constraint set holds. The constraint set are called functional constraints and is either;

$$\Omega = \left\{\mathbf{x} : \mathbf{h(x)} = \mathbf{0}\right\} \tag{5-6}$$

is equality constraint where the function $\mathbf{h}$ is denoted by

$\mathbf{h}(\mathbf{x}) = \left[h_1, \quad h_2, \quad h_3, \quad . \quad . \quad ., \quad h_l\right]^T$, and $l < n$

$$\begin{aligned} &h_1(x_1, x_2, x_3, ...x_n) = 0 \\ &h_2(x_1, x_2, x_3, ...x_n) = 0 \\ &h_3(x_1, x_2, x_3, ...x_n) = 0 \\ &\qquad . \\ &\qquad . \\ &\qquad . \\ &h_l(x_1, x_2, x_3, ...x_n) = 0 \end{aligned} \tag{5-7}$$

or

$$\Omega = \left\{\mathbf{x} : \mathbf{g(x)} \le \mathbf{0}\right\} \tag{5-8}$$

inequality constraint where the function $\mathbf{g}$ is denoted by

$$g(\mathbf{x}) = \left[g_1, \quad g_2, \quad g_3, \quad . \quad . \quad ., \quad g_m\right]^T$$

$$
\begin{aligned}
&g_1(x_1, x_2, x_3, \ldots x_n) \le 0 \\
&g_2(x_1, x_2, x_3, \ldots x_n) \le 0 \\
&g_3(x_1, x_2, x_3, \ldots x_n) \le 0 \\
&\quad . \\
&\quad . \\
&\quad . \\
&g_m(x_1, x_2, x_3, \ldots x_n) \le 0
\end{aligned}
\tag{5-9}
$$

The inequalities constraint are usually $\leq$ or $\geq$. As already stated the solution of the objective function is the desired outcome. Be it the minimizer or maximize. There are various methods and algorithms that are used in finding this solution.

5.1.2 Global Methods and Search Algorithms

The methods for solving optimization problems ranges from simple one-dimensional iterative search methods to methods that are considered to be global in nature. The former include golden search and Newton's method which normally require first and sometimes second derivatives of the objective function. They start with an initial candidate solution say $x^{(k)}$ followed by iterates of $x^{(k+1)}$ each of which depends on previous $x^{(k)}$ and $f(\mathbf{x})$.

The later however, attempts to find solution by searching the entire feasible set and require no derivatives. For this reason, this method is applied in this work. Examples of global search method include Particle Swam Algorithm (PSO), Genetic Algorithm (GA) which will be briefly discussed in the section that follows. Other global search method include Nelder-Mead Simplex Algorithm and Simulated Annealing [63], [65]. PSO and GA are also classified as stochastic optimization algorithms [66].

5.1.3 Stochastic Optimization

Stochastic optimization has been described as methods that provide means of copping with inherent noise in a system and with models or systems that are considered inappropriate for classical deterministic methods of optimization in [66]. These systems are considered to be high dimensional and highly nonlinear. It was simply described as a collection of methods of

optimization for minimizing or maximizing an objective function when randomness is present in [67]. The randomness comes into the problem either through the objective function itself, the constraint set or both.

The method of stochastic optimization thrives on data. Large sets of data spanning longer period of time should therefore result in a more accurate and better solution. As will be seen later in this chapter, the nature of RES data used are random in nature. The decision and outcome space are given in other to limit search space of the optimal sizing process.

5.1.3.1. Particle Swam algorithm

The particle swam optimization (PSO) algorithm deals with updating a set (population) of candidate solutions called a swarm at each iteration step. Each element of the swarm is referred to as a particle. This is an attempt at improving the set towards the optimized solution which is achieved when a stopping criteria is met. It is a randomized search technique that tends to mimic the social behaviour or movement of birds, fishes or bees in flock, schools or swarm respectively [65].

The process of optimization (minimization) of an objective function f over $\mathbb{R}^n$ (ie $f:\mathbb{R}^n \to \mathbb{R}$) will typically start with a randomly generated initial set of points in $\mathbb{R}^n$, where each point is assigned a velocity vector as is analogous to movements of birds or bees. The objective function will then be evaluated at each point of the set. The solution is the basis upon which new set of points and corresponding velocity vectors are created. The update of velocity of each particle is according to its 'best-so-far' position (*pbsest*) and the 'best-so-far' position of members of the entire set (*gbest*). A solution is reached when a defined stopping criteria is satisfied. This is either after reaching a certain number of iterative step or when the solution obtained do not change significantly per subsequent iterative steps. Detailed explanation of this algorithm be found in [63], [65].

5.1.3.2. Genetic Algorithm

Considering the problem

minimize $f(x)$

subject to $x \in \Omega$

The Genetic Algorithm (GA) method use stochastic search process to finding an optimal solution for a problem. It is population base with roots in the principle of genetics. Similar to PSO, GA moves from one solution population to the next based on defined search operator until a stopping criteria is satisfied. GA applies search operators such as crossover and mutation to generate new solution set which are evaluated for the better solution sets. This better solutions form the next generation set.

This method of optimization escapes the consideration of convexity, concavity and continuity of functions and suitable for hand dynamic or real time problems. Also because of its capability of simultaneous optimization of conflicting objective function in a single run, GA is suitable for multi-objective optimization problems. These reference have detailed text on this topic [63], [64], [65], [68].

5.2 The Sizing Concept

In this section the concept of sizing REP-Storage system as a unit is described. This is aimed at utilizing as much as possible, losses that arise from the unused generated power from RES plants in event of system stability. The end result will be the support of network the REP-Storage system belongs to in the form of improved hosting capacity. The sizing process is an optimization problem. The resulting size of the components of the REP-Storage system is dependent on an ideal power demand (P_{Load}^{ideal}) which in practice will be agreed upon with the utility. The ideal load demand is considered as a renegotiated contracted power demand required by consumer.

The optimal sizes should contribute to minimizing as much as possible extra power (energy) other than agreed upon drawn from utility. The net unused power (energy) from RES should also be at a minimum as a result of the optimal size of REP-S unit. This will support the hosting capacity of the network and reduce the fluctuating effect of REP power production on

the network.

Measured and standardized historic data is used in this work. These data include historic load demand of loads connected to respective PCC with their corresponding historic data on the respective renewable energy source used. To test the outcome of sizing procedure, a standard 30 bus network and a simple nodal network with three different load alternatives are adopted.

5.2.1 Description of Sizing Concept

As stated in section 2.2, supporting the hosting capacity is a by-product of a successful implementation of the proposed REP-Storage system to be discussed. The concept starts with a basic assumption. This assumption is that, load profile seen by network of utilities should as much as possible not exceed an agreed upon ideal reference value (P_{Load}^{ideal}). The ideal reference level is represented by the black dashed-line in Figure 5-3.

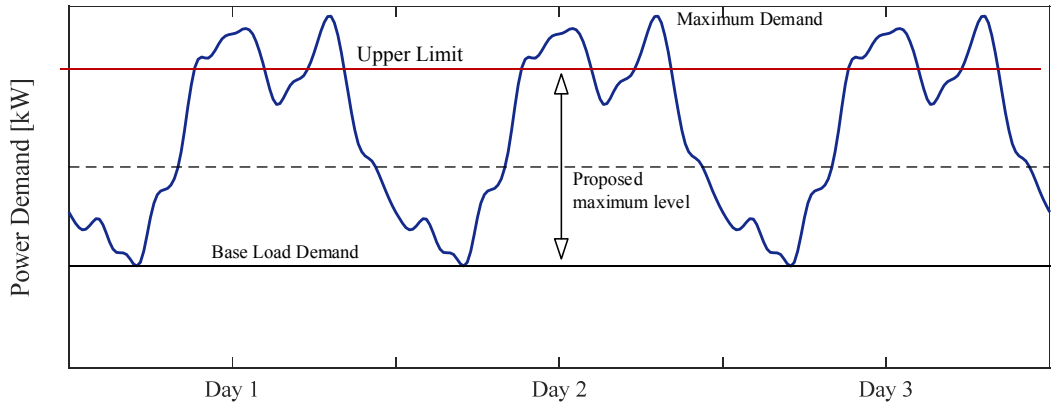

Figure 5-3: Illustration of maximum level setting for utilities. The arrow indicates the range where level can be set and the dashed lines indicates the level.

As stated earlier, with respect ordinary consumers and single large loads, the ideal reference load level is synonymous to contracted power agreed upon by consumer and utility. For instance a consumers who want to generate part of their power demand would renegotiate for a new lower maximum power demand than there was. This is then the new maximum instantaneous power demand the consumer can draw from the utility. This demand level is within the demand level covered continuously by utility and should theoretically pose no

problem. Power demand up to P_{Load}^{ideal} should be supplied by the utility at all times.

The P_{Load}^{ideal} is a reference value for the sizing of RES-Storage system. In practice the ideal power demand will be the reference value for any control and monitoring systems that will manage a Load and RES-Storage system in an electric network. Additional demand should be covered to a large extent by REP-Storage system. The question that stands out is what the value of this ideal P_{Load}^{ideal} should be and how it should be determined. Also how big should the RES-Storage be and how the required size be achieved. This is an ideal consideration hence the possible best set of solution tend to be the sort after solution.

The objective function describing the problem of this thesis is based on the following preambles which are a summary of discussions in preceding chapters.

- There exist an agreed ideal load demand (ideal reference demand) P_{Load}^{ideal}.
- The network (utility) is required to always supply demand up to this reference value.
- It is only when demand exceed this level that the load draws energy from the REP–S system to meet the resulting extra demand.
- Energy or power can be drawn from the network when combined energy from REP–Storage System is insufficient for the extra power demand needed by consumer.
- The storage is charge only when there is excess production from RES
- In event that the storage is fully charged, no excess energy should be fed into the network.
- The ideal is to have the sum of all power or energy at the end of the each iteration step equalling to zero as described by equation 5-10.

$$0 = P_{Load}^{actual.demand}(t) - [P_{Load}^{ideal}(t) + P_{RES}(t) + P_{storage}(t) + P_{network}^{extra}(t)] \quad (5\text{-}10)$$

It follows from equation 5-10 that, the set of sizes at which the solution of equation 5-8 is the

nearest in magnitude to zero is the set of optimal size of the REP-S system. The terms in equation 5-10 are defined as follows.

$P_{Load}^{ideal}, E_{Load}^{ideal}$ as already mentioned the ideal power demand (maximum possible power) or ideal energy demand proposed.

$P_{Load}^{extra.need}, E_{Load}^{extra.need}$ is the instantaneous extra power demand or extra energy demand over a period(15 minutes in this work).

$P_{Load}^{actual.demand}, E_{Load}^{actual.demand}$ is the actual instantaneous power demand or actual energy demand over a period(15 minutes in this work).This is arithmetical sum of $P_{Load}^{ideal}, E_{Load}^{ideal}$ and $P_{Load}^{extra.need}, E_{Load}^{extra.need}$.

$P_{storage}, E_{storage}$ is the power or energy supply drawn from the storage.

$P_{network}, E_{network}$ is the power or energy supply from overlay network

P_{RES}, E_{RES} be power or energy supply from renewable energy source

$P_{network}^{extra}, E_{network}^{extra}$ is the extra power or energy drawn from the network in event of inadequate supply from RES-S unit to meet extra demand

Steps of Sizing process

The objective function for sizing is presented as a management flow chat shown in Figure 5-4. This flow chat implements a set of decision that helps manage the flow of power between the load, network, REP and storage system. This flow chat is implemented as a function in MATLAB. Figure 5-4(a) is the overview of complete REP-S sizing process.

It starts with the upload of data pre-processed as shown in section 3.2. As already seen the input are series of time dependent data. This is followed by sets of constraints which provide the space or ranges within which to search for the solution to the problem. The constraints conditions are discussed in the section that follows. A combination of several *"if ... else"*

statements help to manage the flow power for the period under consideration. When demand exceed the P_{Load}^{ideal}, the subroutine *"Extra demand"* is comes in to manage RES-S power to meet excess demand else demand is supplied by the utility. That is;

If

$P_{Load}^{\text{actual.demand}} \leq P_{Load}^{ideal}$, at a time instance (t) over the period under consideration is true,

$P_{Load}^{actual.\text{demand}} = P_{network}$ at the time (t).

Power is first drawn from RES when it is producing power. Power is then drawn from storage unit in event of insufficient or no production from RES. In situations of insufficient power from renewable source and storage system, the network comes in to make up for the deficit with $P_{network}^{extra}$ as seen after the third if decision block in Figure 5-4(b). That is;

If

$P_{Load}^{actual.demand} > P_{Load}^{ideal}$, is rather true

$P_{Load}^{extra.need} = P_{Load}^{actual.demand} - P_{Load}^{ideal}$ should be provided by RES, storage and utility. That is, power is provided by P_{RES}, $P_{storage}$, $P_{network}^{extra}$ in that order

The extra supply from the network ($P_{network}^{extra}, E_{network}^{extra}$) is stored at each time instant just as the other data observed. The above sub-routine also return the level of storage and the value of excess power from RES. These information are used by the next sub-routine responsible for charging the storage system.

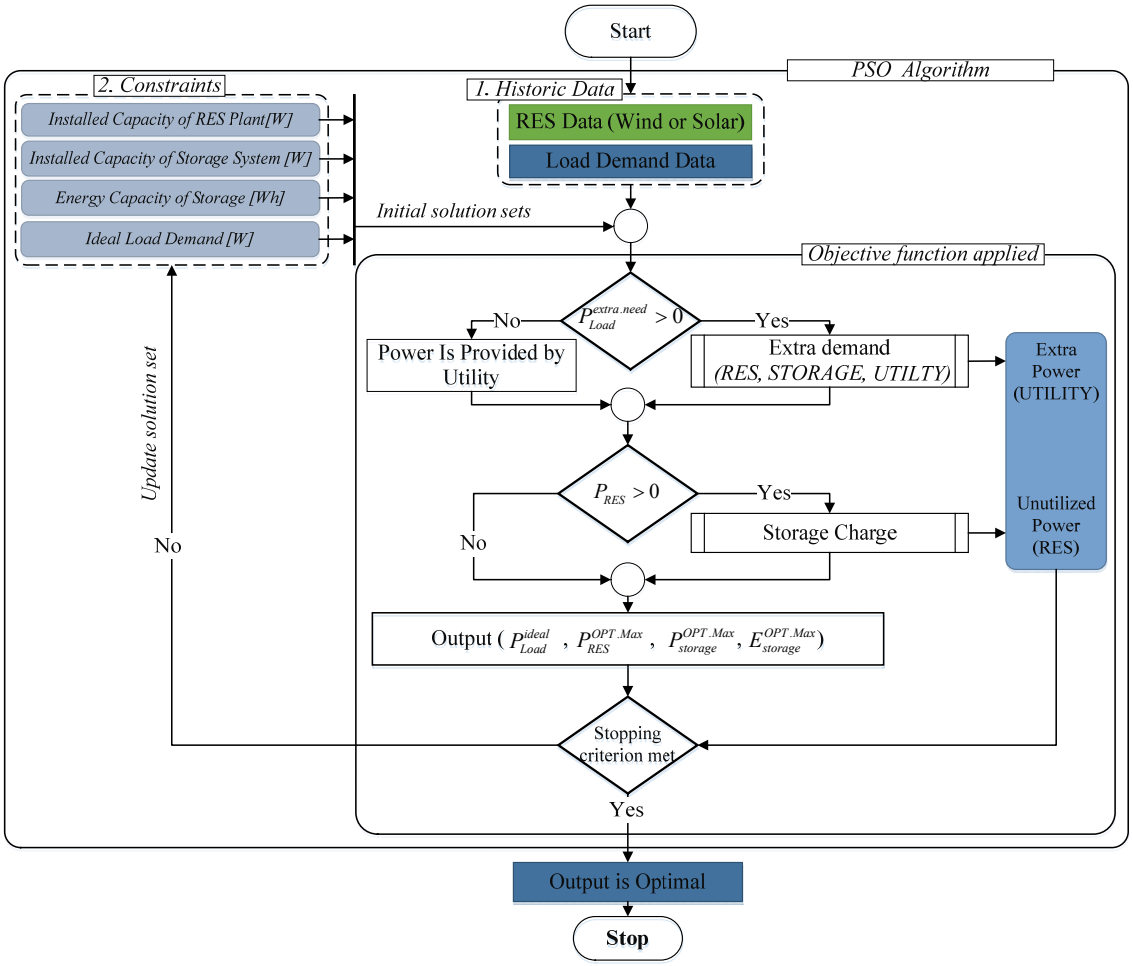
Start
PSO Algorithm
2. Constraints
Installed Capacity of RES Plant[W]
Installed Capacity of Storage System [W]
Energy Capacity of Storage [Wh]
Ideal Load Demand [W]
1. Historic Data
RES Data (Wind or Solar)
Load Demand Data
Initial solution sets
Objective function applied
$P_{Load}^{extra.need} > 0$
No
Yes
Power Is Provided by Utility
Extra demand (RES, STORAGE, UTILTY)
Extra Power (UTILITY)
$P_{RES} > 0$
Yes
No
Storage Charge
Unutilized Power (RES)
Output (P_{Load}^{ideal} , $P_{RES}^{OPT.Max}$, $P_{storage}^{OPT.Max}$, $E_{storage}^{OPT.Max}$)
Update solution set
No
Stopping criterion met
Yes
Output is Optimal
Stop

a.

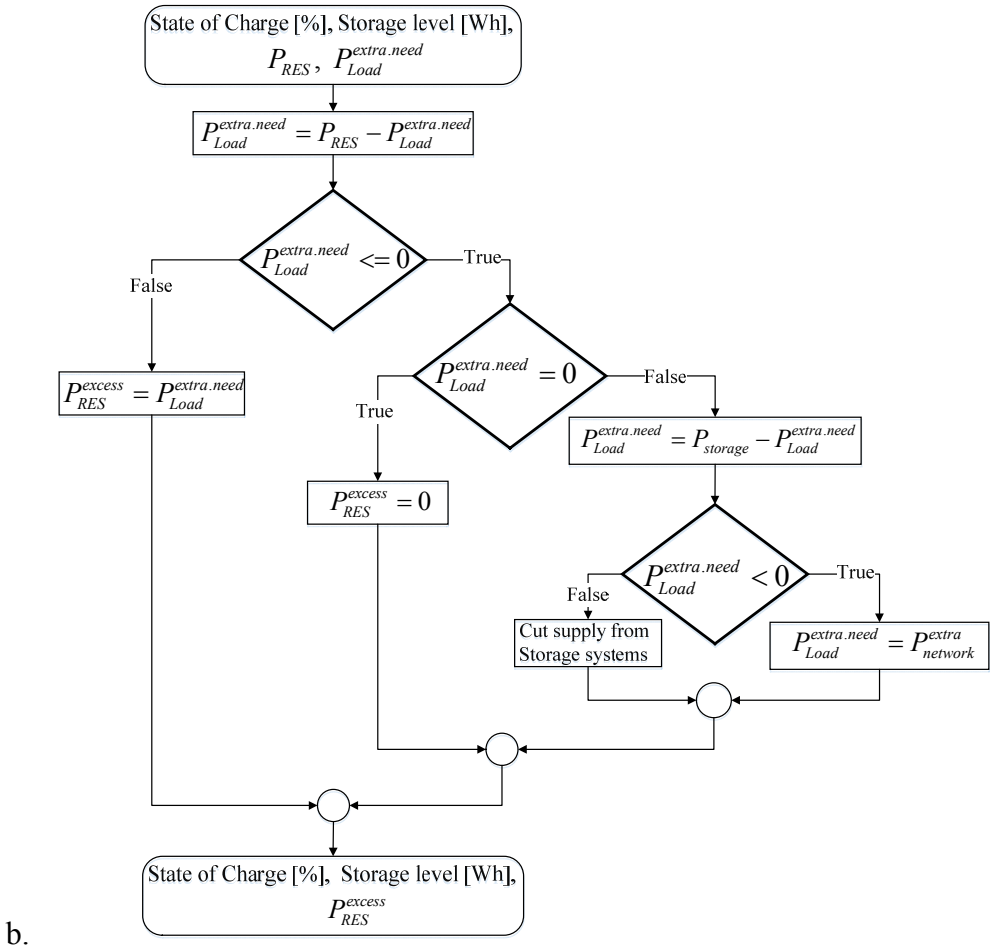

b.

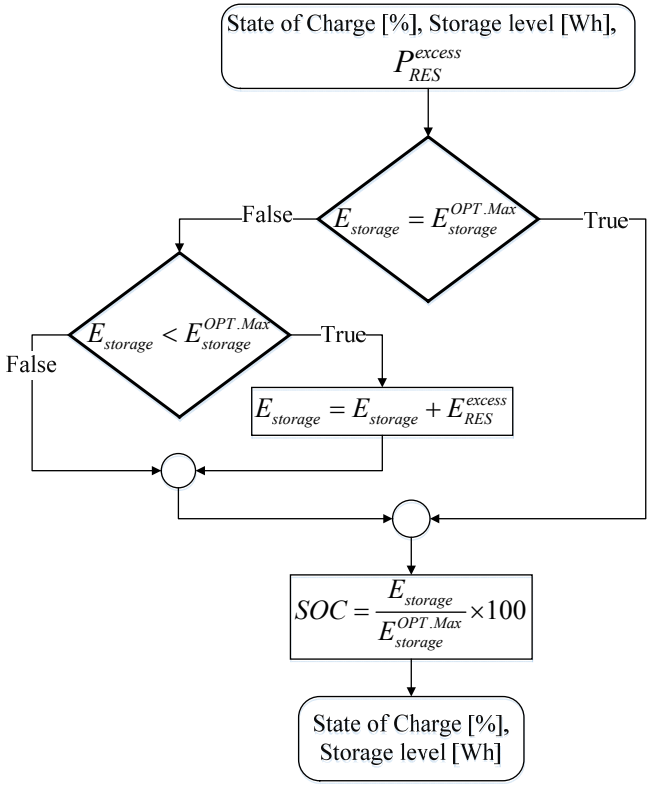

c.

Figure 5-4: Flow chat of *REP-S* objective function: (a) Overall flow chat of Objective function for sizing; (b) Flow chat for the subroutine "Extra demand" of objective function; (c) Flow chat for the subroutine "Storage Charge" of Objective function

The sub-routine *"Storage Charge"* presented in Figure 5-4(c) monitors and implement storage charging process when there is availability excess power from the RES (P_{RES}^{excess}). Either of these two conditions when enable storage charging;

- RES is producing power and extra load demand is zero. That is

$$P_{RES} > 0, P_{Load}^{extra.need} = 0$$

- RES is producing more power than needed to support extra demanded power.

$$P_{RES} > P_{Load}^{extra.need}$$

The state of charge or level of energy remaining in the storage is determined in the presence of excess power from RES. The storage is charge when found not to be fully charged (at $E_{storage}^{OPT.\max}$).Power from RES is unutilized when full charge of storage is attained. Equation 5-10 is verified at the end of every iterative process.

As previously indicated, the nature of power from RES is intermittent hence there could be time instances of no power from RES. Intuitively, supply should be provided by storage and then with or by network if storage cannot support total demand or empty. Though the storage have been prioritised to provide extra need power before the network, there is a limit to which power can be drawn due to rated power of the storage ($P_{storage}^{rated.Max}$). This condition is also considered in the process of sizing.

There will be time instances where there is abundance of generation from REP but low demand and no storage space to absorb the production. REP should then cease to feed power into the node. This implies the network should not take surplus power from the RES since a key aim is to eliminate the fluctuating effect of REP on the network as well. It is therefore apparent that some amount of power from REP will not be used. The optimal sizing process therefore has the task of finding a solution that provides low levels of unutilized power from RES ($P_{RES}^{Loss.mean}$). Also required from sizing is that an optimally sized RES-S should be obtained with low extra power ($P_{network}^{extra.mean}$) taken from the utilities' network.

The equations and steps shown in the flow chats make up the objective function that is implemented as MATLAB script. With the appropriate sets of initial starting points and search region, the function is evaluated for the optimal outcome.

In Figure 5-3, a new desired demand profile that will be seen by utility as a result of the agreed upon ideal load demand P_{Load}^{ideal} is illustrated. It should ideally follow the original load profile (blue line) but should not exceed the maximum proposed level (dashed lines) when relevant condition load demand not exceeding P_{Load}^{ideal} is met.

In an attempt of meeting this ideal situation as much as possible, different scenarios for sizing are considered for both wind and solar RE sources. The scenarios considered for the optimization process of sizing in this work are discussed in the section that follows. The output per scenario are a set of optimal sizes of RES and Storage of the RES-S system needed and a series of time dependent profiles (load, RES power and storage) corresponding to the optimal sizes. The set of optimal sizes ($RES\_S_{sizes}^{OPT}$) include the element as seen in equation 5-11and the output block of the flow chat in Figure 5-4(a). These are the set of values at which the objective function represented by equation 5-10 and flow chat in Figure 5-4(a) is minimized. That is the sum of elements in equation 5-10 is nearest to zero.

$$RES\_S_{sizes}^{OPT} = [P_{Load}^{ideal}, P_{RES}^{OPT.Max}, P_{storage}^{OPT.Max}, E_{storage}^{OPT.Max}] \tag{5-11}$$

where;

P_{Load}^{ideal} stands as previously defined

$P_{RES}^{OPT.\mathrm{Max}}$ is the optimal installed capacity of REP needed

$P_{storage}^{OPT.Max}$ is the optimal installed capacity of storage system needed

$E_{storage}^{OPT.Max}$ is the optimal energy capacity of storage needed

The resulting load profile will be used as input data in running simulations of network shown in Figure 3-1(b). The outcome of the simulation will be analysed for the extent to which the hosting capacity of the network is supported.

5.2.2 Scenarios for Sizing RES-Storage System

The proposed method of sizing RES-S system using available historic data that are random in nature and a stochastic optimization method can be applied with data from any RES and demand profile. In the category RES, two scenarios were considered. They are power production from photovoltaic and from wind.

The output of the proposed methods as seen in Figure 5-4(a) are four. They are the same number of constraint variables for solving the objective function. The constraints variable are therefore sets of boundaries for ideal load demand, installed capacity of REP, installed capacity of storage system and energy capacity storage system. Depending on a peculiar situation, some of the constraints could be fixed or could be varied. For instance, a location with already installed REP will have $P_{RES}^{OPT.\mathrm{Max}}$ already defined and therefore the constraint for installed capacity for REP will be fixed (constant) for the sizing. The remaining three parameters could be set as bounded constraints.

In the category of constraint variables three main scenarios or cases were used in this thesis. The three main scenarios are describes in this section. This is to illustrate the generality of proposed concept. Each scenario or case comprises of four rules. The four rules defines how each constraints should be set. Some of the rules are the same for two or all the three cases. The scenarios and set of rules are shown in Figure 5-5. The scenarios considered are tested with wind and PV data discussed in chapter 3. This is in combination with the different loads types or mixtures connected to the study networks shown in Figure 3-1(a). For each of the two RESs (Wind and Solar) considered in this work, the sizing of REP-S system is carried out according to three sets of boundary conditions or cases illustrated in Figure 5-5. In all cases, the rated active power (P_{Load}^{rated}) of all loads at network bus where the RES-S unit is to be installed are established since the boundary conditions are related to it. The description of the cases are as follows.

Case 1

a. The first statement requires the establishment of “n” set of ranges or boundaries

within which to search for the optimal installed capacity of the REP. This is to illustrate the possibility of setting ones constraints within limited available RES. The set boundary is ($0 \le P_{RES}^{\mathrm{OPT}.Max} \le P_{RES}^{\mathrm{Limit\_Up}}$) for finding the optimal maximum rated capacity of RES to be installed. The upper limit $P_{RES}^{Limit\_Up}$ is a factor multiple of rated active power of the load connected to the network bus under consideration. That is; $P_{RES}^{Limit\_Up} = q_n.P_{Load}^{rated}$, where q_n is a set multiplication factor with "n" elements.

b. The second statement states the establishment of the rated power of storage system. This is to be done arbitrary to emulate a situation where there is a limitation of storage rated power to specific values. Rated active power of desired storage system ($P_{storage}^{rated.Max}$) is fixed in during each sizing process. This is the maximum instantaneous power that can be drawn from the storage system when in operation.

c. The boundary within which to find the optimal energy capacity of storage system ($E_{storage}^{\mathrm{OPT}.Max}$) is given by ($E_{storage}^{\mathrm{Limit\_low.max}} \le E_{storage}^{\mathrm{OPT}.Max} \le E_{storage}^{\mathrm{Limit\_Up.max}}$). The lower and upper limits ($E_{storage}^{\mathrm{Limit\_low.max}}$ and $E_{storage}^{\mathrm{Limit\_Up.max}}$) of this boundary is estimated from load demand characteristics of the network bus under consideration.

d. The fourth statement in

e. Figure 5-5 indicates the establishment of a series of ideal load demands. This is given by;

   $P_{Load}^{ideal} = k_{pr.fact}^{m}.P_{Load}^{rated}$, where $k_{pr.fact}^{m}$ is a multiplication factor

   According to the illustration in Figure 5-3 however, the resulting P_{Load}^{ideal} should be between the base demand and a value not more that 85 % of the rated load demand at the network bus under consideration. The constraint in this case is predefined.

The solution of the optimization process is expected to return the two values $P_{RES}^{\mathrm{OPT}.Max}$ and $E_{storage}^{\mathrm{OPT}.Max}$. As will be seen later, the result of this process as stated in the preceding section takes into consideration the solution that also returns the lowest mean loss of utilized power

from RES ($P_{RES}^{Loss.mean}$) in combination with the lowest mean of extra power drawn from utility ($P_{network}^{extra.mean}$) over the period of consideration.

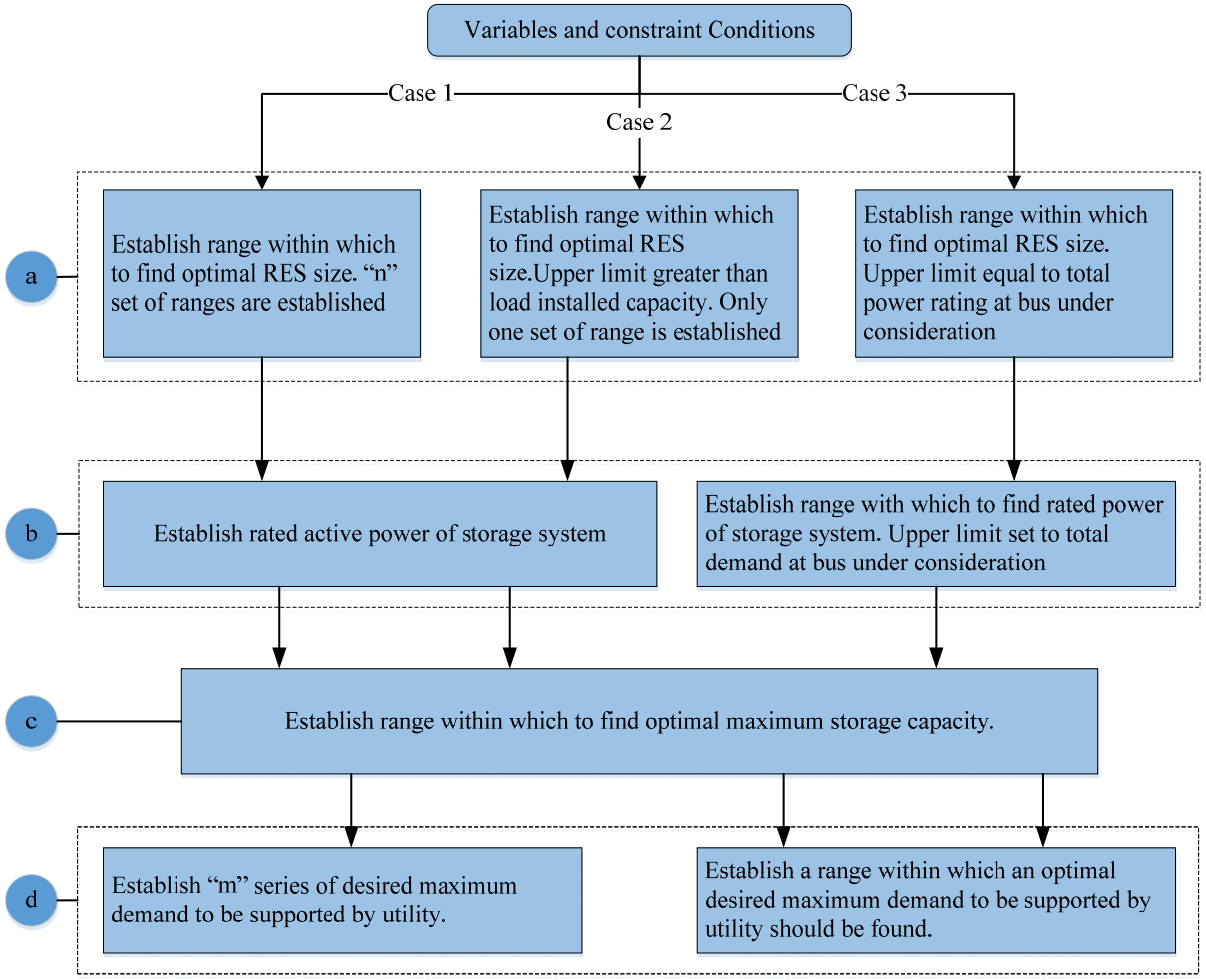

Figure 5-5: Boundary conditions for optimal sizing of RES-Storage systems.

Case 2

Some rules given for "Case 1" are applicable for this case too. The conditions are as follows.

a. The rule indicates the definition of a boundary for finding $P_{RES}^{OPT.Max}$ with upper limit greater than P_{Load}^{rated}. As a rule of thumb and general practice in Germany, The maximum REP to be connected to a node in a network according to equation 5-1 is

more or less the same as P_{Load}^{rated} connected to that node. This is without the consideration storage which can serve a consumer and producer. This rule seeks to explore the introduction of storage system to increase set limit. The boundary in this case is ($0 \le P_{RES}^{\mathrm{OPT}.Max} \le P_{RES}^{\mathrm{Limit\_Up}}$) as seen in Case 1. The upper limit however is greater than the rated installed load capacity. That is;

$$P_{RES}^{\mathrm{Limit\_Up}} > P_{Load}^{rated}$$

b. The second rule is the same as seen in Case 1. That is rated active power of desired storage system ($P_{storage}^{rated.Max}$) is fixed in during each sizing process.

c. This rule is also the same as in the case of Case 1. The boundary for finding the optimal energy capacity of the storage system is ($E_{storage}^{\mathrm{Limit\_low.max}} \le E_{storage}^{\mathrm{OPT}.Max} \le E_{storage}^{\mathrm{Limit\_Up.max}}$)

d. This rule indicates that a boundary within which P_{Load}^{ideal} be found should be defined. This is contrary to the situation in Case 1 where P_{Load}^{ideal} is predetermined. The search for P_{Load}^{ideal} is part of the sizing process. According to Figure 5-3 the boundary is ($P_{Load}^{demand.base} < P_{Load}^{ideal} \le 0.85 P_{Load}^{rated}$).

The solution of the process under this the above set of conditions is expected to return a single set of $P_{RES}^{\mathrm{OPT}.Max}$, $E_{storage}^{\mathrm{OPT}.Max}$ and P_{Load}^{ideal}. Thant three optimal sizes instead unlike two in the preceding case. Once again the final result (optimal sizes) are the set of results that returns the lowest average of unutilized RES power ($P_{RES}^{Loss.mean}$) in combination with the lowest mean of extra power drawn from utility ($P_{network}^{extra.mean}$) over the period of consideration.

Case 3

With reference to Figure 5-5 the first two rules are different from those given under Case 2. The remaining two however are the same as those stated Case 2". The conditions are as follows.

a. The upper limit of the boundary within which to find $P_{RES}^{\mathrm{OPT}.Max}$ is set to be equal to the maximum installed load capacity as indicated by equation 5-1. The boundary is ($0 \le P_{RES}^{\mathrm{OPT}.Max} \le P_{RES}^{\mathrm{Limit\_Up}}$), with upper limit given by; $P_{RES}^{\mathrm{Limit\_Up}} = P_{Load}^{rated}$.

b. The second rule for this case indicates that a boundary for finding optimal storage capacity should be defined contrary to predefined values seen in Case 1 and Case 2. The upper limit should be equal to maximum installed load capacity. The boundary for finding the value of the optimal storage installed capacity is ($0 \le P_{storage}^{OPT.Max} \le P_{storage}^{Limit\_Up}$). The upper limit is given by; $P_{storage}^{Limit\_Up} = P_{Load}^{rated}$

c. The boundary for finding optimal storage energy capacity is the same as seen in Case 1 and Case 2. That is ($E_{storage}^{\mathrm{Limit\_low.max}} \le E_{storage}^{\mathrm{OPT}.Max} \le E_{storage}^{\mathrm{Limit\_Up.max}}$) is the boundary.

d. Similar to the rule given Case 2, the boundary for finding the ideal power demand is ($P_{Load}^{demand.base} < P_{Load}^{ideal} \le 0.85 P_{Load}^{rated}$).

The solution of the process of sizing under this the above set of conditions of Case 3 returns a single set of $P_{RES}^{\mathrm{OPT}.Max}$, $P_{storage}^{\mathrm{OPT}.Max}$, $P_{storage}^{Limit\_Up} = P_{Load}^{rated}$ and P_{Load}^{ideal}. That is all four components are optimally sized through implementing the proposed method of sizing.

5.2.3 Scenario Implementation

In this section, the scenarios discussed in the previous section are used to test on the sizing concept of using historic RES and load demand data to size REP-S system as a unit using stochastic optimization method. Calculations and assumption that had to be done are presented where required. The focus is on the single node network shown in Figure 5-1.In simple terms, the boundary conditions described earlier are actualized with real values from the single node model in Figure 3-1(b) and then used to run the optimal sizing process. The boundary conditions are applied in sizing REP-S systems for PV and wind infeed at all bus (Kn0_11, Kn0_12 and Kn0_13) seen in the single node network under consideration (Figure 3-1(b)). A recall from preceding chapters established the installed active power capacity of

each load at respective buses as 722.5 kW, 585 kW and 427.5 kW respectively. The boundaries of all the three cases are based on the above established active power capacities.

Constraint "a" - Installed Capacity of RES

Base on this data, Table 5-1 which shows the five upper limits ($P_{RES}^{Limit\_Up}$) according rule "a" of Case 1 for each bus is obtained. For simplicity, the multiplication factor q was set to per unit value of 0.5 to 1.5 at 0.25 intervals. That is; $q = \{0.5, 0.75, ..., 1.5\}$, and therefore the resulting Table 5-1.

Table 5-1: Upper limits for RE installed capacity for Condition set 1

q_n	$P_{RES}^{Limit\_Up} = q_n.P_{Load}^{rated}$ [kW] at buses		
	Kn0_11 (P_{Load}^{rated} = 722.5)	Kn0_12 (P_{Load}^{rated} = 585)	Kn0_13 (P_{Load}^{rated} = 427.5)
0.50	361.25	292.50	213.75
0.75	541.88	438.75	320.63
1.00	722.50	585.00	427.50
1.25	903.13	731.25	534.38
1.50	1083.75	877.50	641.25

On the other hand, Table 5-2 is generated for Case 2 with the same installed load active power capacity values satisfying the first rule "a". The upper limit of the boundary was set to be 1.5 times more than the rated installed capacity of Load at respective buses. Five sets of ranges per bus results from Table 5-1 while only one range per bus results from Table 5-2 under rule "a". Table 5-3 is the table showing the upper limits of the boundary condition as per rule "a" for Case 3. There is also only one set of condition per bus. The upper limit of the boundary at each bus is the maximum rated power of load installed at that bus.

Table 5-2: Upper limits for RE installed capacity for Condition set 2

q	$P_{RES}^{Limit\_Up} = q.P_{Load}^{rated}$ [kW] at buses		
	Kn0_11 (P_{Load}^{rated} = 722.5)	Kn0_12 (P_{Load}^{rated} = 585)	Kn0_13 (P_{Load}^{rated} = 427.5)
1.50	1083.75	877.50	641.25

Table 5-3: Upper limits for RE installed capacity for Condition set 3

$P_{RES}^{Limit\_Up} = P_{Load}^{rated}$ [kW] at buses		
Kn0_11 (P_{Load}^{rated} = 722.5)	Kn0_12 (P_{Load}^{rated} = 585)	Kn0_13 (P_{Load}^{rated} = 427.5)
722.5	585	427.5

Constraint "b" - Installed Capacity of Storage

The rated active power of the desired storages ($P_{storage}^{rated.Max}$) at each bus is set to the 300 kW. This satisfies constraint "b" for Case 1 and Case 2. There is one boundary per bus according to $0 \le P_{storage}^{OPT.Max} \le P_{storage}^{Limit\_Up}$, where $P_{storage}^{Limit\_Up} = P_{Load}^{rated}$ for Case 3 hence the following;

$$0 \le P_{storage}^{OPT.Max} \le 722.5 \text{ kW at bus Kn0\_11}$$

$$0 \le P_{storage}^{OPT.Max} \le 585 \text{ kW at bus Kn0\_12}$$

$$0 \le P_{storage}^{OPT.Max} \le 427.5 \text{ kW at bus Kn0\_13}$$

An optimal rated power of storage system ($P_{storage}^{OPT.Max}$) will be in the set of values at which of the objective function was minimized.

Constraint "c" - Storage Energy Capacity

The location (urban, rural or remote) and type of load or part of the network to be supported by the REP-S, will inform the settings limits of the boundary for storage energy capacity. This is because factors such as cost and how much stand-by is needed among other factors would have to be considered. In this work the lower and upper limits of the maximum storage energy capacity, $E_{storage}^{\text{Limit\_low.max}}$ and $E_{storage}^{\text{Limit\_Up.max}}$ are ambitiously chosen to cover an average energy demand of four days and seven days respectively.

A total of about 4.54 GWh of energy is estimated to be consumed by Load 1 per year according to standard load profile adapted. This amount to about 10.24 MWh per day and 71.68 MWh for a week on average. For load 2 and load 3, the total energy consumed according to their respective load profiles amounted to about 2.57 GWh and 1.88 GWh.

Their corresponding average daily and weekly consumption are estimated to be about 7.05 MWh and 49.37 MWh and then about 5.15 MWh and 36.05 MWh respectively. The lower and upper limits are therefore set to 45 MWh and 75 MWh for storage to be connected at bus Kn0_11, 30 MWh and 50 MWh for connection at bus Kn0_12 and 21 MWh and 37 MWh for storage integration at bus Kn0_13. Hence according to $E_{storage}^{\text{Limit\_low.max}} \le E_{storage}^{\text{OPT.}Max} \le E_{storage}^{\text{Limit\_Up.max}}$, the boundaries per are;

$45 \le E_{storage}^{\text{OPT.}Max} \le 75$ MWh at Kn0_11

$30 \le E_{storage}^{rated.Max} \le 50$ MWh at Kn0_12

$21 \le E_{storage}^{rated.Max} \le 37$ MWh at Kn0_13

The above boundaries are used for the sizing processes under all Cases.

Constraint "d" Ideal load demand

For Case 1, there are fixed predetermined ideal load demand. The set of factors $k_{pr.fact}^{m} = \{0.55, 0.60, 0.65, 0.70, 0.75, 0.80, 0.85\}$ is used in this work. Therefore at each bus, seven levels of fixed ideal load demand are fixed based the factor $k_{pr.fact}^{m}$ and according to the expression $P_{Load}^{ideal} = k_{pr.fact}^{m}.P_{Load}^{rated}$. These values are shown in Table 5-4. For both Case 2 and Case 3, the boundary $P_{Load}^{demand.base} < P_{Load}^{ideal} \le 0.85 P_{Load}^{rated}$ is applied. The base load demand ($P_{Load}^{demand.base}$) for the three loads are first determined to be 345.28 kW for Load 1, 106.70 kW for Load 2 and 77.98 kW for Load 3 respectively. On the other hand, the resultant boundaries for all buses within which the ideal power demand for Case 2 and Case 3 can be found are;

$345.28 < P_{Load}^{ideal} \le 614.13$ kW for bus Kn0_11

$106.70 < P_{Load}^{ideal} \le 497.25$ kW for bus Kn0_12

$77.98 < P_{Load}^{ideal} \le 363.38$ kW for bus Kn0_13

Table 5-4: Fixed proposed P_{Load}^{ideal} Case 1

	Fixed P_{Load}^{ideal} at buses[kW]		
$k_{pr.fact}^{m}$	Kn0_11 (P_{Load}^{rated} = 722.5)	Kn0_12 (P_{Load}^{rated} = 585)	Kn0_13 (P_{Load}^{rated} = 427.5)
0.55	397.37	321.75	235.13
0.60	433.50	351.00	256.50
0.65	469.63	380.25	277.88
0.70	505.75	409.50	299.25
0.75	541.88	438.75	320.63
0.80	578.00	468.00	342.00
0.85	614.13	497.25	363.38

The outlined boundaries and parameters based on the 3 sets of conditions are the variable and constraint for the objective function implemented using MATLAB script. As illustrated in the snapshot of Figure 5-6, the boundaries are separated into two input vectors (lower and upper limit vectors) for the MATLAB script. For instance the upper limit of boundary for installed capacity of REP ($P_{RES}^{Limit\_Up}$) for $q = 1$ is 722.5 kW at bus Kn0_11. This is seen occupying the first position of the row vector "UB" in Figure 5-6. The established lower and upper limits of $45 \le E_{storage}^{\mathrm{OPT}.Max} \le 75$ MWh within which optimal maximum storage should be found is also seen to occupy the second position of the vectors "LB" and "UB" respectively. Apart from either of the above mentioned sets of conditions as input, additional data for specific load and RES are loaded as input as well. This is illustrated in the flow chat in Figure 5-4(a).

Due to the nature of objective function and data a stochastic optimization method was used. The particle swarm optimization (PSO) method was used. This algorithm is part of MATLAB optimization tool box. An initial test was conducted with both genetic algorithm (GA) and PSO. Though almost similar result were obtained PSO was chosen because it was quite fast compared with the other algorithms for this particular problem. The Table 5-5 below shows the result of both runs. As can be seen there was time difference of about 5.3 minutes in favour of PSO.

Table 5-5: Comparison between PSO and GA algorithm on objective function.

	$P_{RES}^{\mathrm{OPT}.Max}$ [kW]	$E_{storage}^{\mathrm{OPT}.Max}$ [kWh]	$P_{storage}^{rated.Max}$ [kW] - fixed	P_{Load}^{ideal} [kW] - fixed	Time [s]
PSO	339	74483	300	505.75	582
GA	339	73428	300	505.75	900

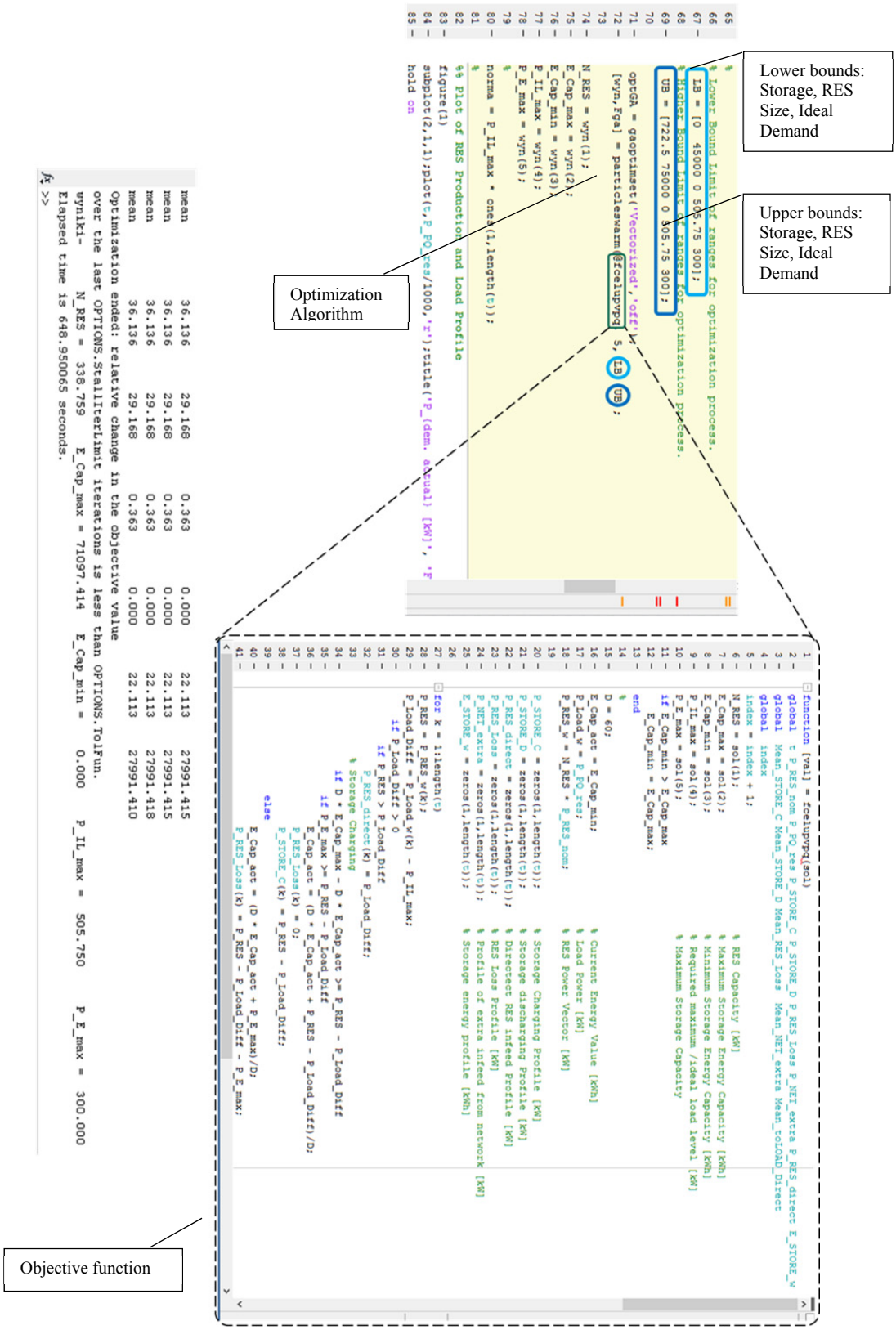

Figure 5-6: Snapshot of parametrization part of MATLAB script for optimal sizing of RES-Storage system

6. Results and Discussions

The results of sizing is discussed in the chapter. For single node network, results of optimal sizing and resulting profiles based on all three scenarios and load are presented. Fourteen buses of the 30 bus benchmark network are connected with REP-S system. The result of this simulation is also present. The impact of REP-Storage system on the network is also presented

6.1 Single Node Network

In this section the results of optimal sizing RES-Storage system for integration into the Single Node network is presented. The documentation of results on sizing are organized according to the three main scenarios (Cases) described in section 5.2 per system bus and for Wind REP and Photovoltaic (PV) REP. That is, for each bus all three cases will be discussed. A few plots are used to facilitate the description of the results in a simple manner. Further plots on the results can be found in the appendix section of the thesis for further understanding of the results. Presentation of results according to the load buses of the network are as follows.

6.1.1 Sizing at Bus Kn0_11

This bus has a maximum installed active load capacity of 722.5 kW. From section 5.2.2 and section 5.2.3, the three cases presented and implemented lead to the results that are to be discussed.

Case 1

For this case, there were five boundaries for installed capacity of RES, one boundary for storage energy capacity, one predetermined installed capacity of storage system and seven predetermined ideal levels of load demand. The predetermined installed storage capacity is

$P_{storage}^{rated.Max} =$ 300 kW whiles the boundary for storage energy capacity is $45 \leq E_{storage}^{\mathrm{OPT}.Max} \leq 75$ MWh. This conditions apply for both Wind and PV plants.

Photovoltaic

Table 6-1 shows the optimal installed REP and storage energy capacity that is required for all boundaries and predetermined ideal load demand for a Photovoltaic-Storage (PV-S) system. Focus is now shifted to results of sizing for q = 1 ($P_{RES}^{Limit\_Up} =$ 722.5 kW) and $P_{Load}^{ideal} = k_{pr.fact}^{m}.P_{Load}^{rated} = 505.75$ kW. Therefore for q = 1 ($P_{RES}^{Limit\_Up} =$ 722.5 kW) and $P_{Load}^{ideal} = k_{pr.fact}^{m}.P_{Load}^{rated} = 505.75$ kW, the sizing process returned the optimal REP installed and storage energy capacity are about 409.5 kW and 75 MWh respectively for the PV-S system. This is over a period of one year. As stated in earlier, the results also return a series of new profiles including load profile the will be seen by the network as a result of REP-S system. The series of figures, Figure 6-1, Figure 6-2 and Figure 6-3 are plots of various profiles obtained together with the optimal sizes. The new load profile is the blue plot of Figure 6-1 superimposed on the initial load profile plotted with red.

Table 6-1: Optimal Storage Capacities with corresponding optimal PV Power capacity at varying P_{Load}^{ideal} and $P_{RES}^{Limit\_Up}$ at Kn0_11

P_{Load}^{ideal} [kW]	Optimal Storage ($E_{storage}^{rated.Max}$) and PV rated capacity ($P_{RES}^{\mathrm{OPT}.Max}$) at different $P_{RES}^{Limit\_Up} = q_n.P_{Load}^{rated}$									
	q = 0.50 (361.3 kW)		q = 0.75 (541.9 kW)		q = 1.00 (722.5 kW)		q = 1.25 (903.1 kW)		q = 1.50 (1083.8 kW)	
	$P_{RES}^{OPT.Ma}$ [kW]	$E_{storage}^{rated.Max}$ [kWh]	$P_{RES}^{OPT.Max}$ [kW]	$E_{storage}^{rated.Max}$ [kWh]	$P_{RES}^{OPT.Max}$ [kW]	$E_{storage}^{rated.Max}$ [kWh]	$P_{RES}^{OPT.Max}$ [kW]	$E_{storage}^{rated.Max}$ [kWh]	$P_{RES}^{OPT.Max}$ [kW]	$E_{storage}^{rated.Max}$ [kWh]
614.13	126.93	75000	126.93	75000	126.93	75000	126.93	75000	126.92	75000
578.00	200.21	75000	200.21	75000	200.21	75000	200.21	75000	200.21	75000
541.88	298.81	75000	298.81	75000	298.81	75000	298.81	75000	298.81	75000
505.75	361.25	45000	409.54	75000	409.54	75000	409.54	75000	409.54	75000
469.63	361.25	75000	541.88	71950	552.26	75000	552.26	75000	552.26	75000
433.50	361.25	75000	541.88	49210	722.50	70140	737.91	75000	737.91	75000
397.38	361.25	47450	541.88	49360	722.50	59690	903.13	61860	1002.9	75000

The optimal values were arrived at after 2250 iterative steps with average unutilized PV generated power ($P_{RES}^{Loss.mean}$) and average extra infeed from utility ($P_{network}^{extra.mean}$) of 0.13 kW and 10.41 kW over twelve months period respectively. This can be seen in

Figure 6-4 and Table 6-3. These values translate to energy values of 1.14 MWh and 91.19 MWh respectively.

With the above resulting optimal sizes and available data used, it is observed that, excess power demand can be supported by PV-S system for a period of about nine and half months (Figure 6-1 and Figure 6-3). The extra power of about 217 kW peak other than agreed upon 505.75 kW is therefore drawn from utility for a period of about 3 months. The storage energy profile in MWh of the supposed PV-S system is shown in Figure 6-2. The storage system is assumed to be empty of usable energy from the beginning of the period. This can be observed at the initial stages of the profile zero energy. For the first two and half months, the storage system remained empty. This is because as per the optimal size of RES, there was not enough power to supply both extra load and charge the battery. The profile is seen to increase over the period with occasional discharge.

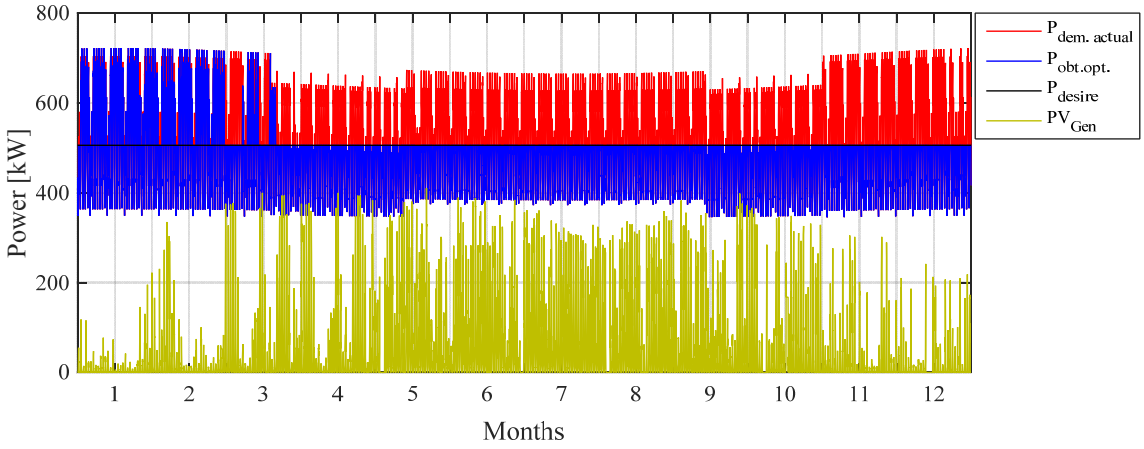

Figure 6-1: Plot of power profiles at Kn0_11 for P_{Load}^{ideal} = 505.75 kW: Actual load profile (red), desired maximum demand utility should support P_{Load}^{ideal} (black), resulting profile of supply from utility (blue), power generation from PV(yellow)

The profile decreases after the tenth month but does not deplete completely by the end of the period. That is, usable storage is not fully discharged at the end of the year. There is therefore some energy for the year that follows.

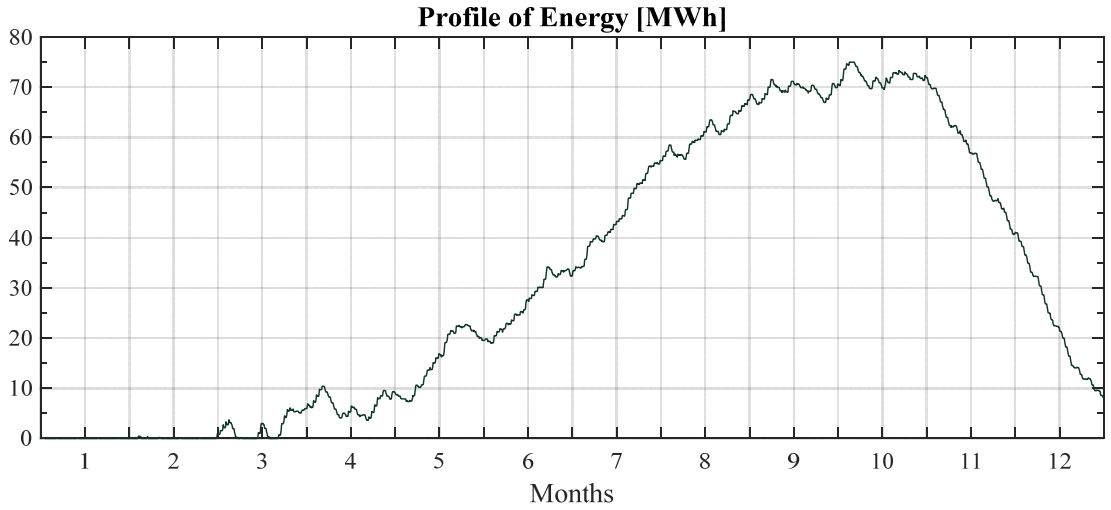

Figure 6-2: Plot of charge and discharge profile of energy storage system over the year for PV-Storage system at Kn0_11 for P_{Load}^{ideal} = 505.75 kW. The value on the ordinate is energy

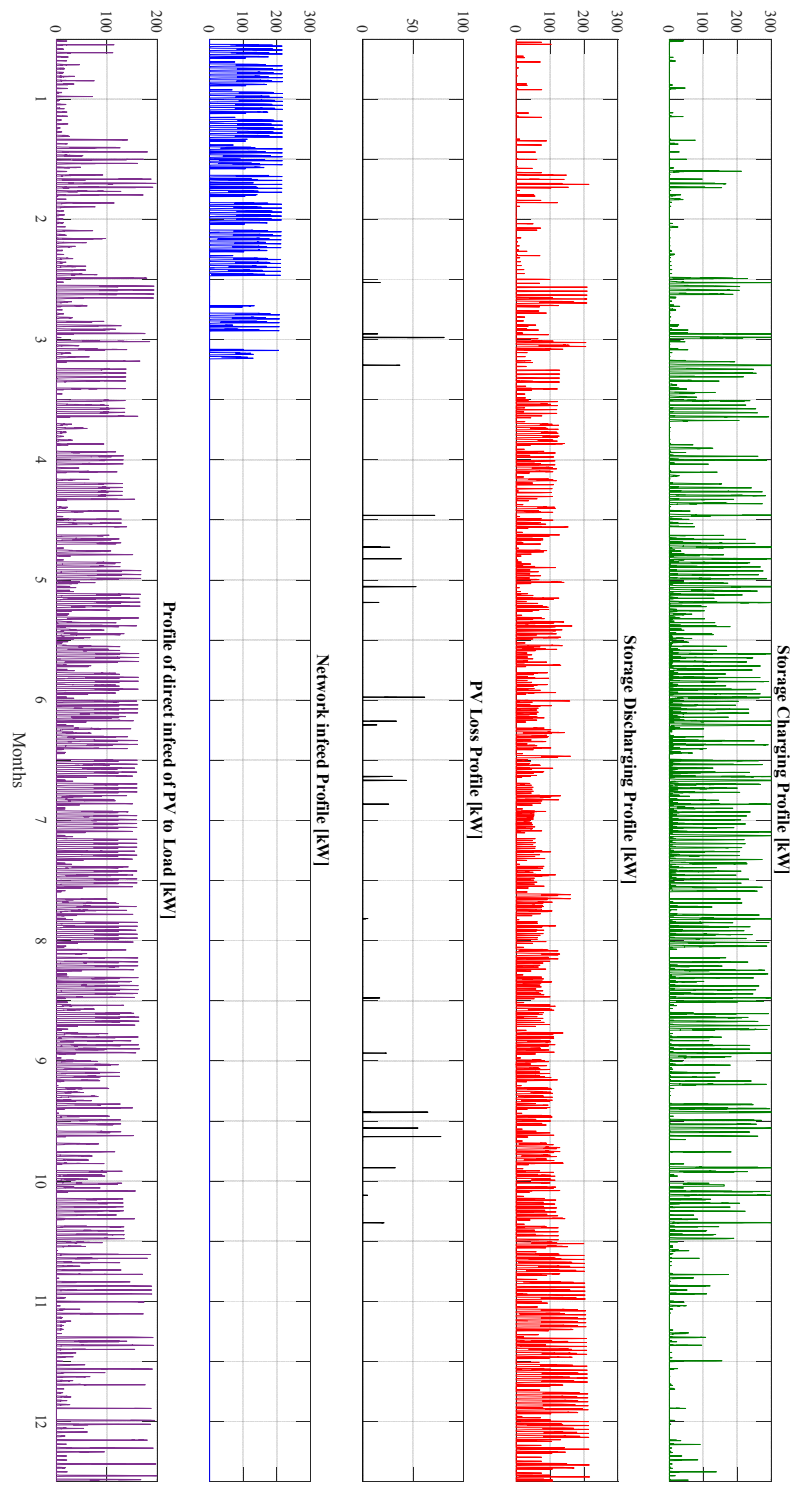

Figure 6-3: Plot of power profiles at Kn0_11 for P_{Load}^{ideal} = 505.75 kW: Storage charging in the presence of PV generation (green), Storage discharge in instance of need (red), unutilized power from PV generator at instance of fully charged battery or higher power output than rated power of storage (black), extra needed demand other than agreed P_{Load}^{ideal} supplied by utility (blue), direct supply from PV generator to load when demand exceed P_{Load}^{ideal}

Figure 6-3 shows various power plots ranging from the charged and discharge of storage system, the loss of PV generated power and extra power drawn from network the network,

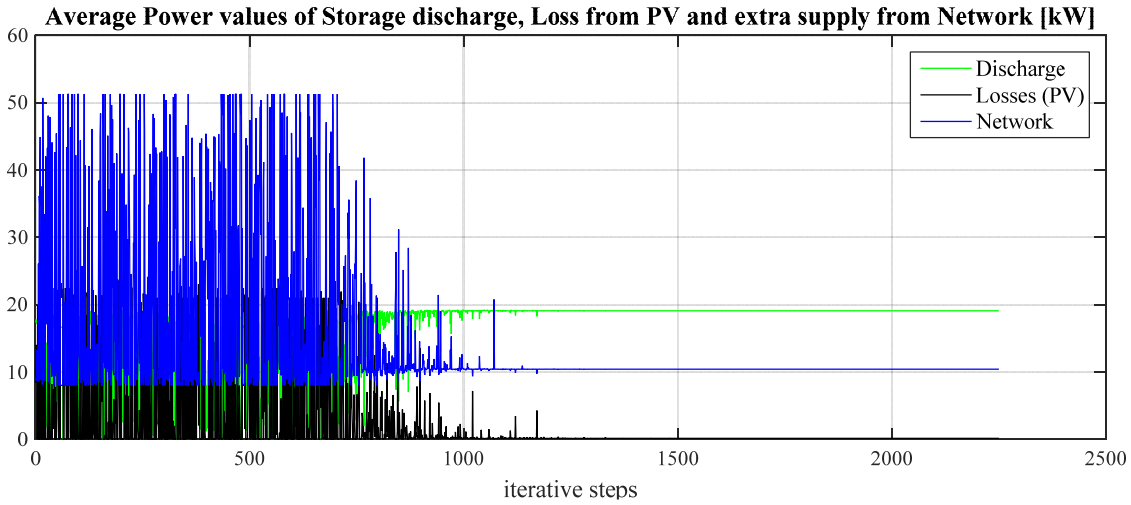

Figure 6-4: Average power values per optimal sizing iterative step (2250 steps) at Kn0_11 for P_{Load}^{ideal} = 505.75 kW: Infeed from network to load (blue), Storage discharge (green) and unutilized power from PV (black).

The solution for optimal sizing is seen in Table 6-1. Out of Table 6-1a function that describes the relationship between optimal PV capacities, multiplication factor (q) that sets the upper limit of PV capacity and maximum demand that utility should always support is obtained with the help of MATLAB curve fitting tool (Figure 6-5).

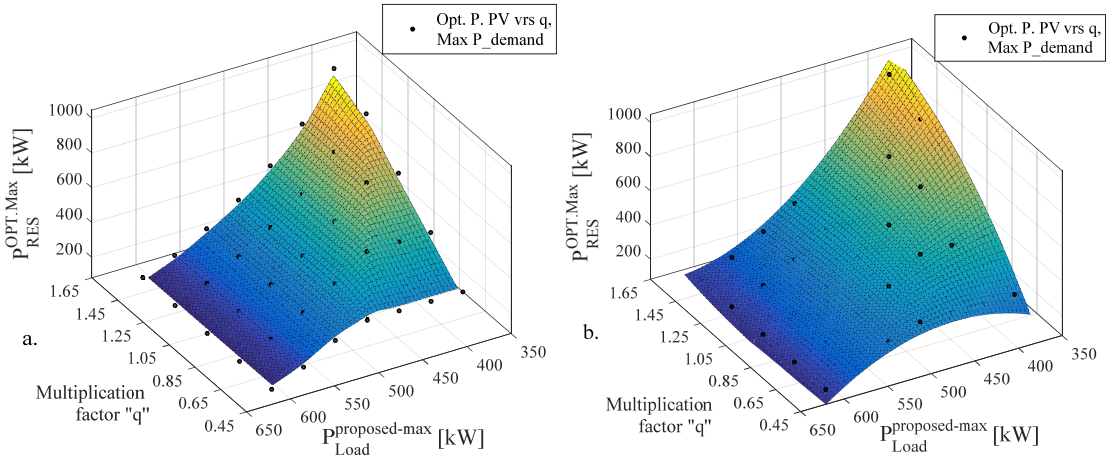

Figure 6-5: Curve fitting plot of $P_{RES}^{OPT.Max}$ versus "q" and fixed P_{Load}^{ideal} for PV-Storage system at bus Kn0_11; (a) is the interpolated surface fit of result in Table 6-1, (b) is the polynomial surface approximation with two variables.

The best approximation fit function which resulted in the lowest root mean square error (RMSE) of 27.17 can be seen in equation 6-1. With this function the optimal installed capacity of REP can be estimated when the multiplication factor "q" and ideal power demand (P_{Load}^{ideal}) is known.

$$f(x_1, x_2) = c_1 + c_2 x_1 + c_3 x_2 + c_4 x_1^2 + c_5 x_1 x_2 + c_6 x_2^2 + c_7 x_1^3 + c_8 x_1^2 x_2 + c_9 x_1 x_2^2 \quad (6\text{-}1)$$

where,

$$f(x_1, x_2) = P_{RES}^{OPT.Max},\ x_1 = \text{the multiplication factor } "q" \text{ and } x_2 = P_{Load}^{ideal}.$$

The coefficients and confidence bounds the function in equation 6-1shown in Table 6-2.

Table 6-2: Coefficient and confidence bounds valid for polynomial surface fit shown in Figure 6-5

Coefficient		Confidence bounds	
		Lower	Upper
C_1	-6791	-8492	-5089
C_2	10530	8329	12730
C_3	25.32	18.88	31.76
C_4	-1560	-2804	-315.4
C_5	-31.75	-38.24	-25.26
C_6	-0.02307	-0.02934	-0.0681
C_7	93.16	-262.8	449.2
C_8	2.158	0.9084	3.407
C_9	0.0243	0.01839	0.0302

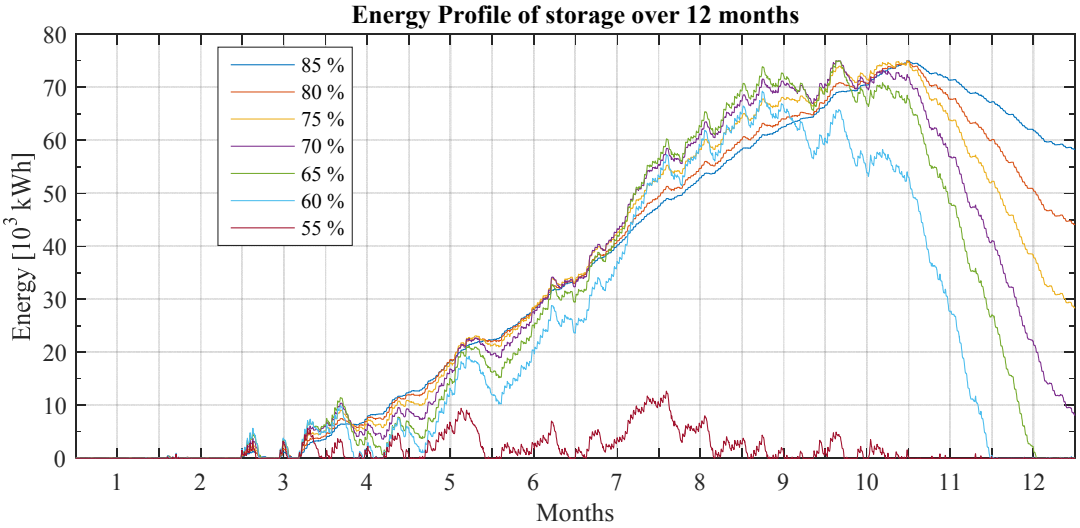

Figure 6-6: Energy profile for storage at different desire maximum demand for PV power for q = 1 at bus Kn0_11. – Case 1

In Figure 6-6, the plot of storage profiles arising from each sizing process with all seven ideal power demand (P_{Load}^{ideal}) and $P_{RES}^{Limit\_Up}$ = 722.5 kW is shown. That is, each of the plots is the storage profile of respective ideal load demand (P_{Load}^{ideal}). For instance the purple plot (at 70 %) is the profile for P_{Load}^{ideal} = 505.25 kW. Data used span a period of one year. The plot revels that from P_{Load}^{ideal} equal to 70 % of P_{Load}^{rated} (505.75 kW), the level of amount of energy of storage systems that is not utilized by the end of the 12 month period increases. The average extra infeed from utility is observed in Table 6-3 to inversely reduce. Plots at the remaining $P_{RES}^{Limit\_Up}$ are shown in Figure C- 1 to Figure C- 4 in Appendix B.

Table 6-3: Average Loss in power from PV and average extra power infeed for varying values of desired maximum demand at Kn0_11 – Case 1

P_{Load}^{ideal} [kW]	Average loss of PV power and average extra infeed from Utility [kW] at Bus Kn0_11									
	q = 0.50 (361.3 kW)		q = 0.75 (541.9 kW)		q = 1.00 (722.5 kW)		q = 1.25 (903.1 kW)		q = 1.50 (1083.8 kW)	
	Loss	Infeed	Loss	Infeed	Loss	Infeed	Loss	Infeed	Loss	Infeed
614.13	0	2.85	0	2.85	0	2.85	0	2.85	0	2.85
578.00	0	5.14	0	5.14	0	5.14	0	5.14	0	5.14
541.88	0	7.62	0	7.62	0	7.62	0	7.62	0	7.61
505.75	0.02	14.26	0.13	10.41	0.13	10.41	0.13	10.41	0.13	10.41
469.63	0.01	34.02	0.99	16.47	1.13	15.60	1.14	15.60	1.14	15.75
433.50	0	57.87	0.57	39.90	4.04	24.85	4.52	23.75	4.52	23.75
397.38	0	86.28	0.28	68.03	2.70	51.93	8.76	39.45	13.36	33.78

Wind

The same values of $P_{RES}^{Limit\_Up}$, $P_{storage}^{rated.Max}$, P_{Load}^{ideal} and within range $45 \le E_{storage}^{\mathrm{OPT}.Max} \le 75$ MWh when applied for optimal sizing of a Wind Power-Storage system at the bus Kn0_11 gave a solution set of 338.76 kW and 71.54 MWh after for $P_{RES}^{\mathrm{OPT}.Max}$ and $E_{storage}^{\mathrm{OPT}.Max}$ respectively (Table 6-4).

It is also observed that, for the available wind speed and demand data, the Wind Power-Storage system with the above optimal size can support power demand above P_{Load}^{ideal} for the 12 month period considered.

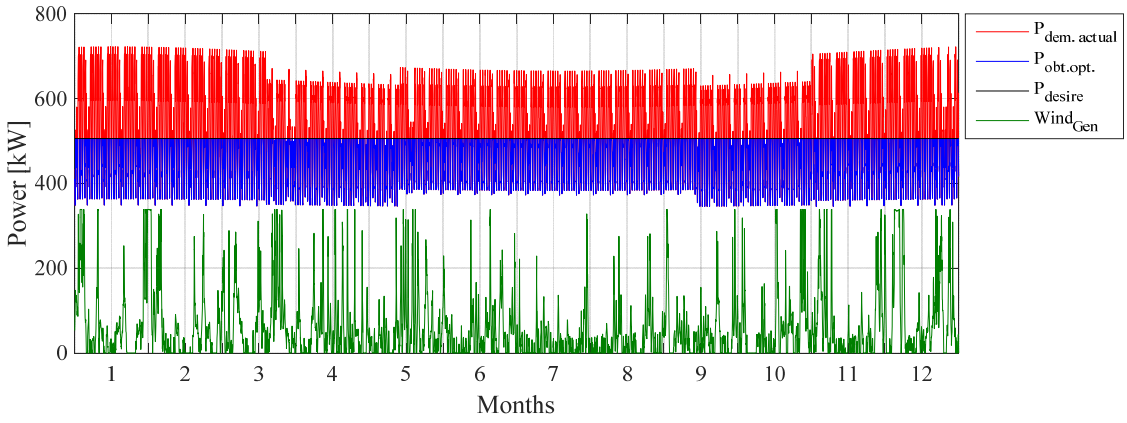

Figure 6-7: Plot of power profiles at Kn0_11 for P_{Load}^{ideal} = 505.75 kW: Actual load profile (red), desired maximum demand utility should support P_{Load}^{ideal} (black), resulting profile of supply from utility (blue), power generation from Wind Plant(green) – Case 1.

This observation is evident in Figure 6-7 where the resulting supply profile has maximum of 505.75 kW peak power and in Figure 6-9 with zero plot for extra demand support from network.

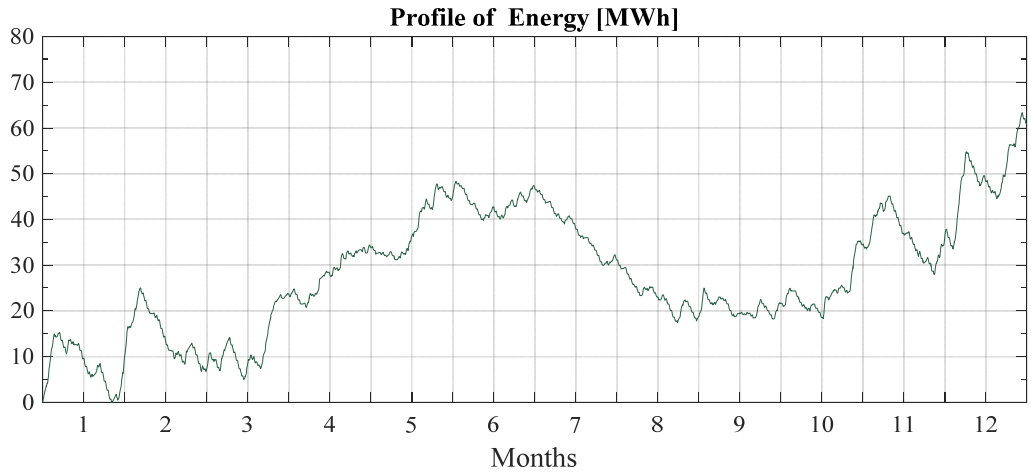

Figure 6-8: Plot of charge and discharge profile of energy storage system over the year for Wind Power-Storage System at Kn0_11 for P_{Load}^{ideal} = 505.75 kW – Case 1

At the end of the period under consideration, the storage system has about 84.56 % of usable energy available for use in the next year cycle (Figure 6-8). The $P_{RES}^{Loss\_mean}$ from wind power generation for the optimal solution is about 0.36 kW after 1941 iterative steps. This is illustrated in Figure 6-10 and amounts to about 3.15 MWh of energy lost during the one year period considered.

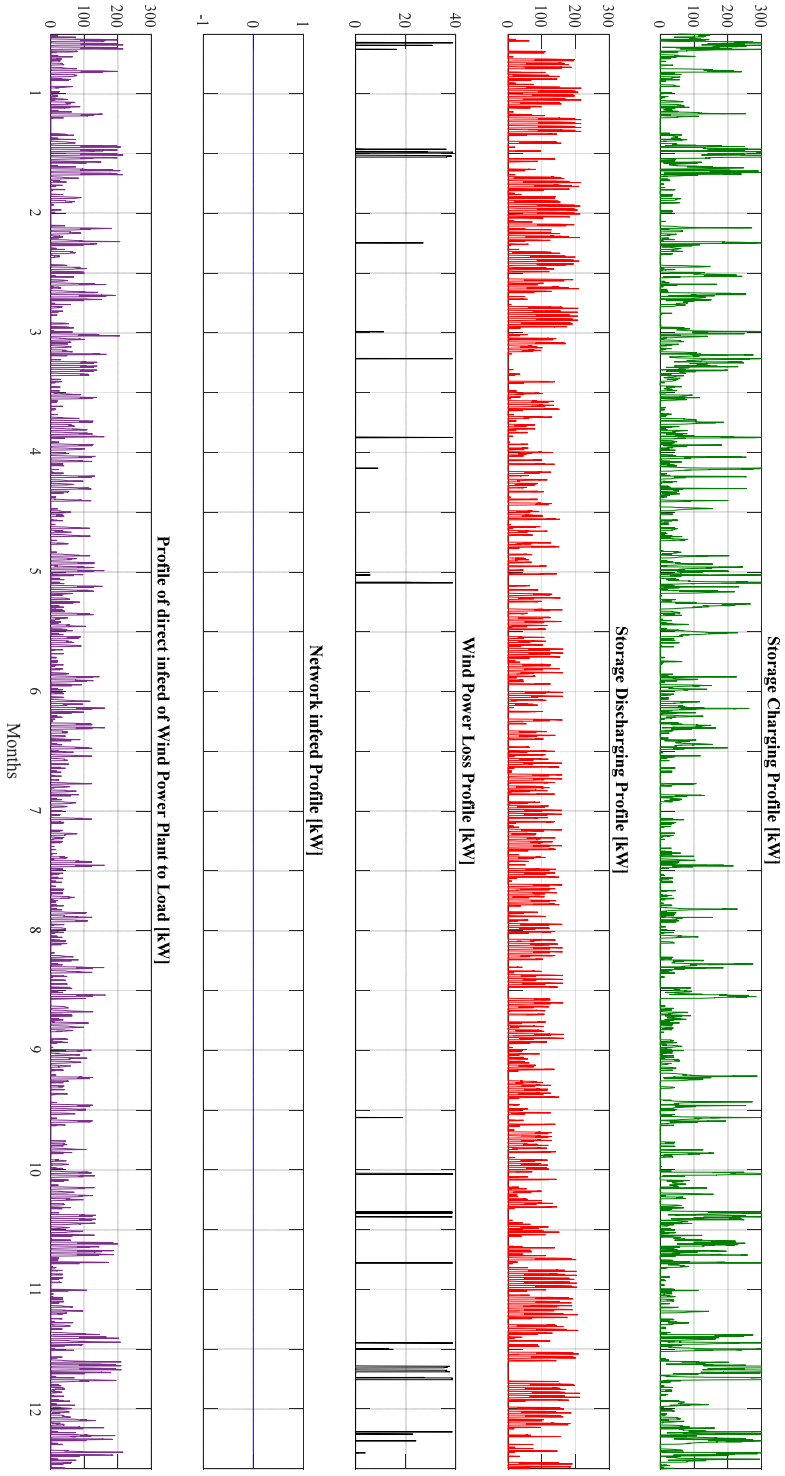

Figure 6-9: Plot of power profiles at Kn0_11 for P_{Load}^{ideal} = 505.75 - kW: Storage charging in the presence of Wind Power generation (green), Storage discharge in instance of need (red), unutilized power from Wind Power generator at instance of fully charged battery or higher power output than rated power of storage (black), extra needed demand other than agreed P_{Load}^{ideal} supplied by utility (blue), direct supply from Wind Power generator to load when demand exceed P_{Load}^{ideal}

A function that describes the relationship between optimal Wind Power capacities, multiplication factor (q) that sets the upper limit of Wind Power capacity and maximum demand that utility should always support is obtained from Table 6-4. This function is similar to the one seen in equation 6-1 except for the resulting unique coefficients and confidence bounds shown in Table 6-5. The surface approximation fit of this function is shown in Figure 6-11 and has RMSE of 22.05.

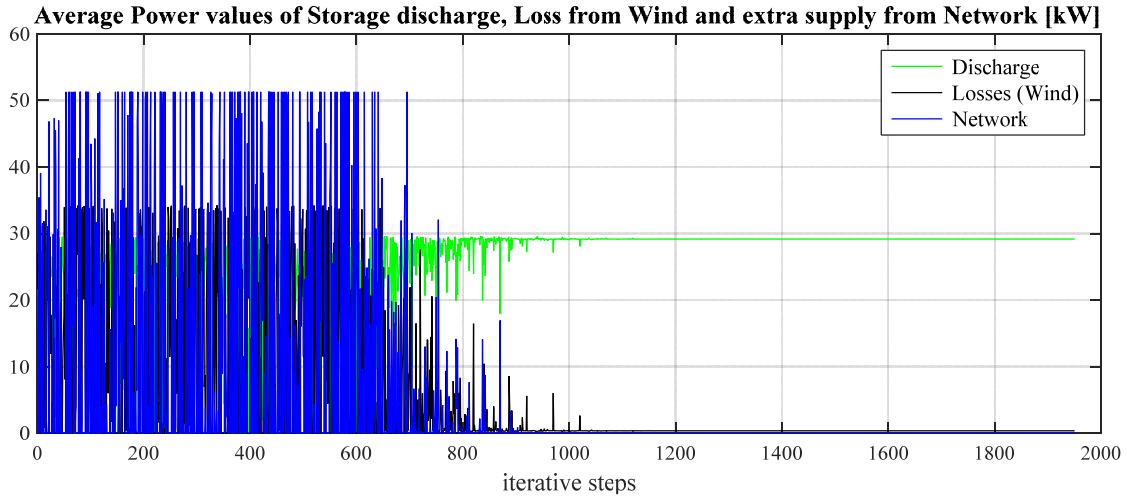

Figure 6-10: Average power values per optimal sizing iterative step (1941 steps): Infeed from network to load (blue), Storage discharge (green) and unutilized power from Wind (black).

Table 6-4: Optimal Storage Capacities with corresponding optimal Wind Power capacity at varying P_{Load}^{ideal} and $P_{RES}^{Limit\_Up}$ at Kn0_11

P_{Load}^{ideal} [kW]	Optimal Storage ($E_{storage}^{rated.Max}$) and Wind rated capacity ($P_{RES}^{OPT.Max}$) at different $P_{RES}^{Limit\_Up} = q_n.P_{Load}^{rated}$									
	q = 0.50 (361.3 kW)		q = 0.75 (541.9 kW)		q = 1.00 (722.5 kW)		q = 1.25 (903.1 kW)		q = 1.50 (1083.8 kW)	
	$P_{RES}^{OPT.Max}$ [kW]	$E_{storage}^{rated.Max}$ [kWh]	$P_{RES}^{OPT.Max}$ [kW]	$E_{storage}^{rated.Max}$ [kWh]	$P_{RES}^{OPT.Max}$ [kW]	$E_{storage}^{rated.Max}$ [kWh]	$P_{RES}^{OPT.Max}$ [kW]	$E_{storage}^{rated.Max}$ [kWh]	$P_{RES}^{OPT.Max}$ [kW]	$E_{storage}^{rated.Max}$ [kWh]
614.13	00.95	74050	101.61	74720	100.63	74980	100.64	73750	100.74	75000
578.00	169.36	75000	169.36	75000	169.36	75000	169.36	75000	169.36	75000
541.88	249.18	73020	249.81	75000	250.26	75000	249.22	74200	249.29	73290
505.75	338.76	65160	338.76	75000	338.76	71540	338.76	66560	338.76	64510
469.63	361.25	64690	456.25	60890	456.25	64700	456.25	73530	456.25	57200
433.50	361.25	57680	541.88	63120	640.26	73770	640.26	74410	640.26	74530
397.38	361.25	55550	541.88	52810	722.5	66540	852.40	75000	852.40	75000

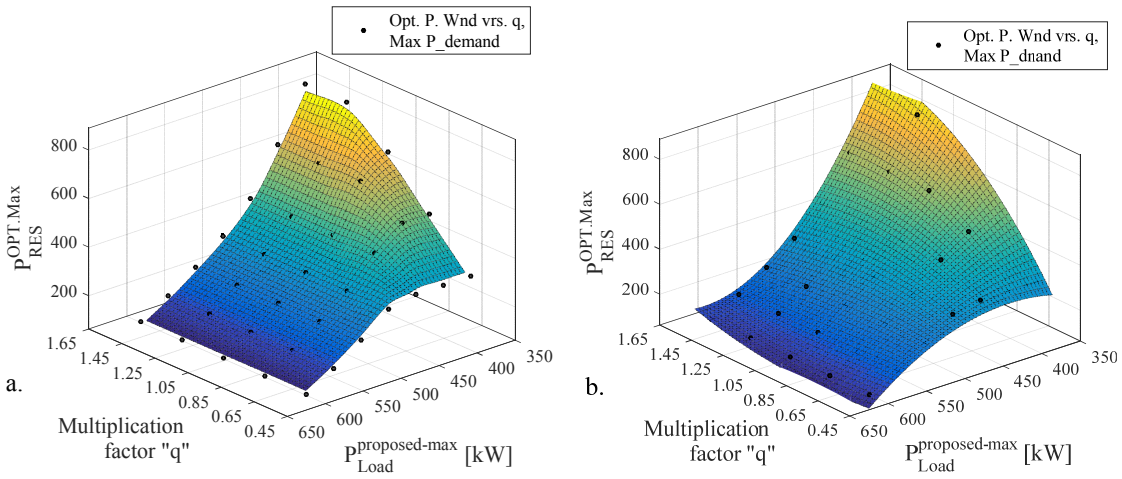

Figure 6-11: Curve fitting plot of $P_{RES}^{OPT.Max}$ versus "q" and fixed P_{Load}^{ideal} for Wind Power-Storage system at bus Kn0_11; 'a' is the interpolated surface fit of result in Table 6-4, 'b' is the polynomial surface approximation with two variables.

Table 6-5: Coefficient and confidence bounds valid for polynomial surface fit in shown in Figure 6-11

Coefficient		Confidence bounds	
		Lower	Upper
C_1	-5279	-6660	-3898
C_2	9714	7929	11500
C_3	19.66	14.43	24.89
C_4	-1627	-2637	-617.4
C_5	-29.16	-34.42	-23.89
C_6	-0.017667	-0.02274	-0.01257
C_7	38.38	-250.6	327.4
C_8	2.646	1.632	3.66
C_9	0.02149	0.01669	0.02628

In Figure 6-12 is a plot of energy profile for storages over the 12 months for Wind-Storage system connected to bus Kn0_11 with different P_{Load}^{ideal} that utility should support but with the same $P_{RES}^{Limit\_Up}$ at q = 1. Each of the plots is the storage profile of respective ideal load demand (P_{Load}^{ideal}). For instance the purple plot (at 70 %) is the profile for P_{Load}^{ideal} = 505.25 kW. None of the storage systems were completely depleted at the end of the year. There was however extra support from utility at an average of about 14.21 kW over the year for P_{Load}^{ideal} = 397.38 kW but zero for P_{Load}^{ideal} = 505.25 kW as compared with the case of PV-S system. This comparison can be made from Table 6-3 and Table 6-6. The plot at other 'q' values can be found in the appendix.

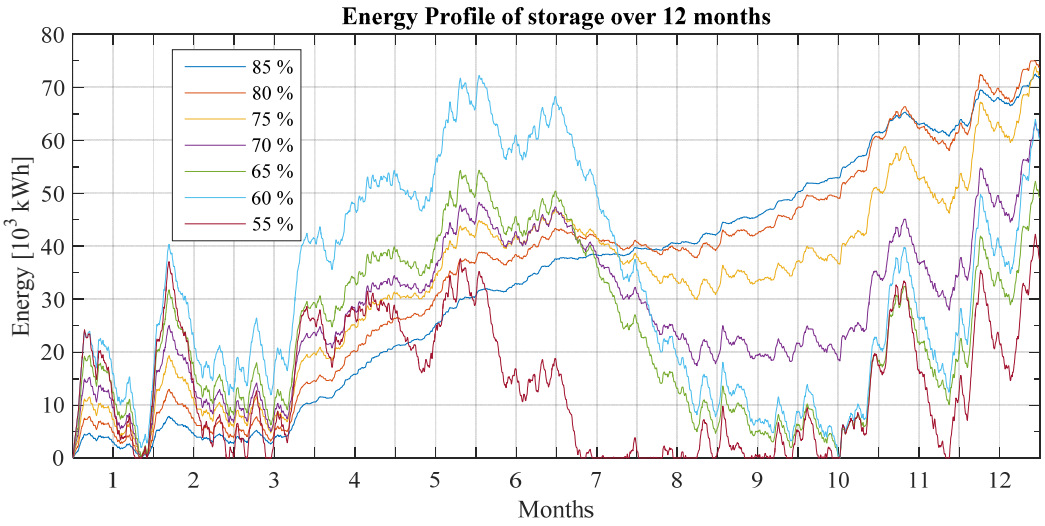

Figure 6-12: Energy profile for storage at different desired maximum demand for Wind Power for q = 1.0 at bus Kn0_11 for P_{Load}^{ideal} =505.75 kW.

For all PV plant sizes, the average losses of unused power and average extra power that will be taken from the utility are shown in Table 6-3. As desired P_{Load}^{ideal} decreases, loss in utilization of PV power as well infeed of average extra power from utility increases.

In the case of Wind plant, the average extra infeed from utility generally decreases with increasing P_{Load}^{ideal}. Likewise the average loss of power from wind decreases with increasing ideal load demand. The average loss of wind power however increase with increase in 'q' values. The above observations can be seen in Table 6-6.

Table 6-6: Average Loss in power from Wind and average extra power infeed for varying values of desired maximum demand at Kn0_11.

P_{Load}^{ideal} [kW]	Average loss of Wind power and average extra infeed from Utility [kW] at Bus Kn0_11									
	q = 0.50 (361.3 kW)		q = 0.75 (541.9 kW)		q = 1.00 (722.5 kW)		q = 1.25 (903.1 kW)		q = 1.50 (1083.8 kW)	
	Loss	Infeed	Loss	Infeed	Loss	Infeed	Loss	Infeed	Loss	Infeed
614.13	0	0	0	0	0	0	0	0	0	0
578.00	0	0	0	0	0	0	0	0	0	0
541.88	0	0	0	0	0	0	0	0	0	0
505.75	0.36	0	0.36	0	0.36	0	0.36	0	0.45	0
469.63	0.52	11.57	2.27	0	2.27	0	2.27	0	2.27	0
433.50	0.37	33.07	4.29	9.47	8.90	0	8.90	0	8.90	0
397.38	0.23	61.16	3.15	34.28	11.63	14.21	19.78	2.61	19.78	2.61

Case 2

For case two, only rated installed capacity of storage system ($P_{storage}^{rated}$) is predetermined. The corresponding optimal rated installed capacity of RES, optimal storage energy capacity and ideal load demand are to be sized by the process. The result for finding optimal size of RES-Storage systems at bus Kn0_11under Case 2 is shown in Table 6-7. For both PV and Wind Power, utility feeds in extra power to support extra demand.

Table 6-7: Summary of result for optimal sizing of PV – Storage and Wind-Storage system at bus Kn0_11 under Case 2.

RES Power Source	Optimal Size of $P_{RES}^{rated.Max}$, P_{Load}^{ideal} and $E_{storage}^{rated.Max}$			$P_{RES}^{Loss.mean}$ [kW]	$P_{network}^{extra.mean}$ [kW]
	$P_{RES}^{OPT.Max}$ [kW]	P_{Load}^{ideal} [kW]	$E_{storage}^{rated.Max}$ [kWh]		
PV	839.68	417.82	75000	7.60	27.87
Wind Power	1083.75	364.50	75000	33.72	6.78

The optimal P_{Load}^{ideal} for Wind-Storage system when compared with values in Table 6-4 is observed to be lower than ideal load demand value equal 55 % of P_{Load}^{rated} (397.38 kW). That is 364.5 kW is lower than $P_{Load}^{ideal} = 0.55\,P_{Load}^{rated}$ at Kn0_11. That of PV-Storage system however, is higher. The optimal storage capacity for both systems is seen to be 75 MWh. It is also observed the storage system for Wind-Storage system is not completely depleted at the end of the one year period under consideration unlike that of PV-Storage system which is completely depleted. This can be observed in Figure 6-16.Also noticeable is the fact that, there seems to be more storage activity with respect to Wind-S system. Observing Figure 6-13 and Figure 6-14, there are more instances of unutilized power (black plots) produced from both PV and wind plants for this *"Case"* compared with Case 1. There are also more instance of utility producing extra power to support load (blue plots). This observation is evident in $P_{RES}^{loss.mean}$ and $P_{network}^{extra.mean}$ in Table 6-7 which generally larger than those obtained from the single scenario studied under *"Case 1"*. However, again comparing with results from *"Case 1"*, relatively higher $P_{RES}^{OPT.Max}$ values were obtained. The values are indicated in Table 6-7 and evident in Figure 6-15 (yellow plot for solar and green plot for Wind).

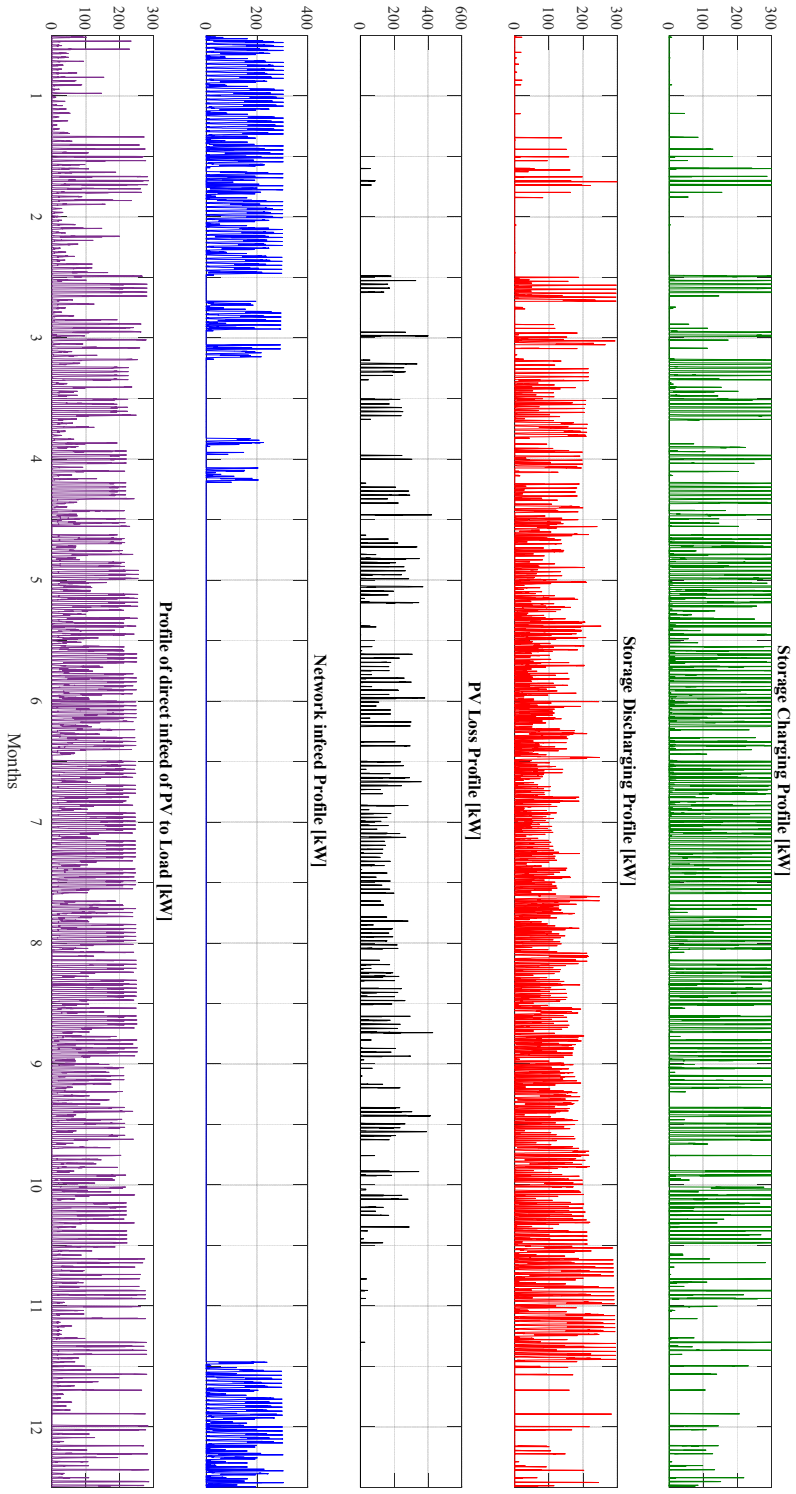

Figure 6-13: Plot of power profiles under Case 2 at Kn0_11: Storage charging in the presence of PV generation (green), Storage discharge in instance of need (red), unutilized power from PV Power generator at instance of fully charged battery or higher power output than rated power of storage (black), extra needed demand other than agreed P_{Load}^{ideal} supplied by utility (blue), direct supply from Wind Power generator to load when demand exceed P_{Load}^{ideal}

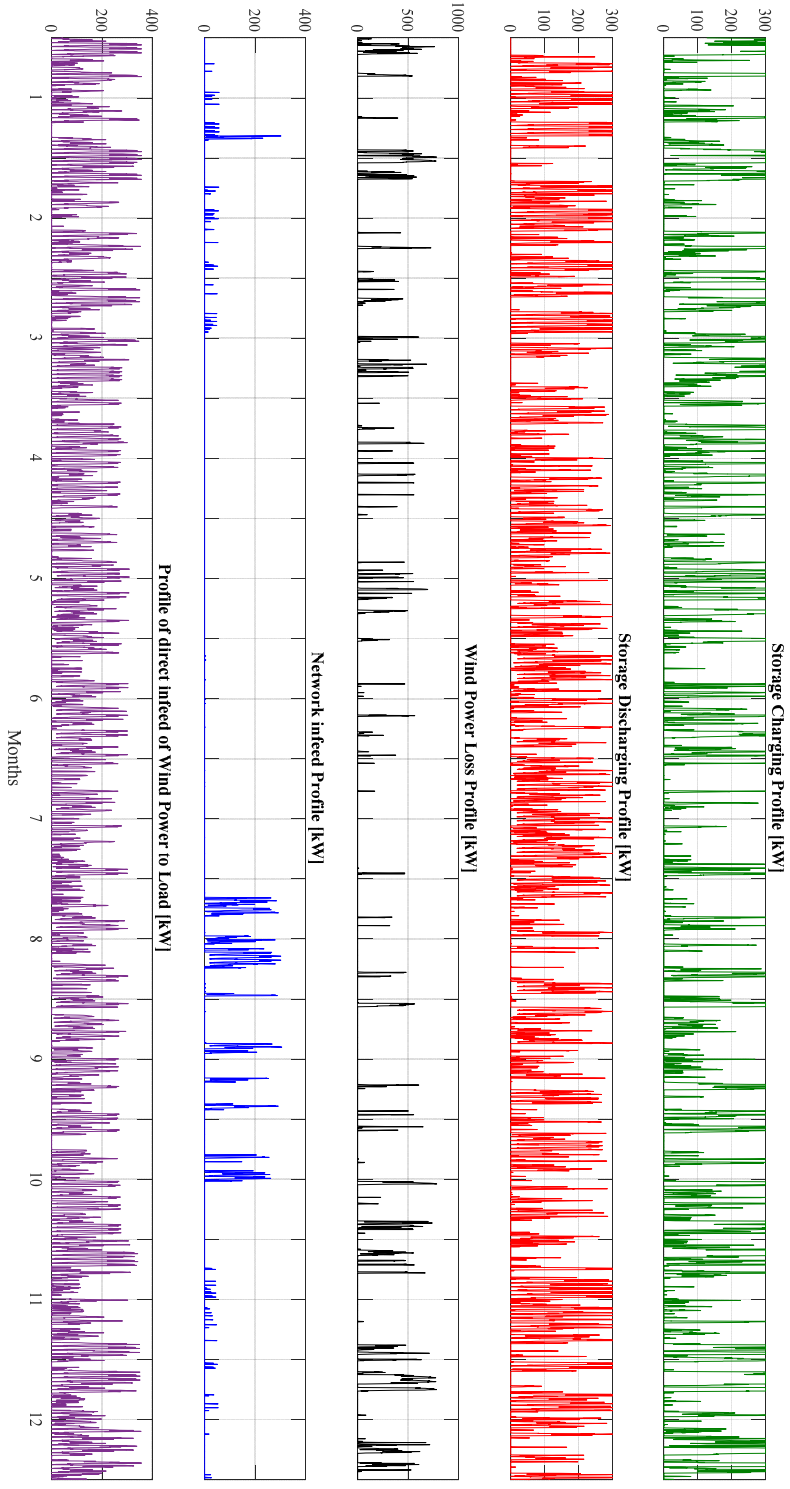

Figure 6-14: Plot of power profiles for Case 2 at Kn0_11: Storage charging in the presence of Wind Power generation (green), Storage discharge in instance of need (red), unutilized power from Wind Power generator at instance of fully charged battery or higher power output than rated power of storage (black), extra needed demand other than agreed P_{Load}^{ideal} supplied by utility (blue), direct supply from Wind Power generator to load when demand exceed P_{Load}^{ideal}

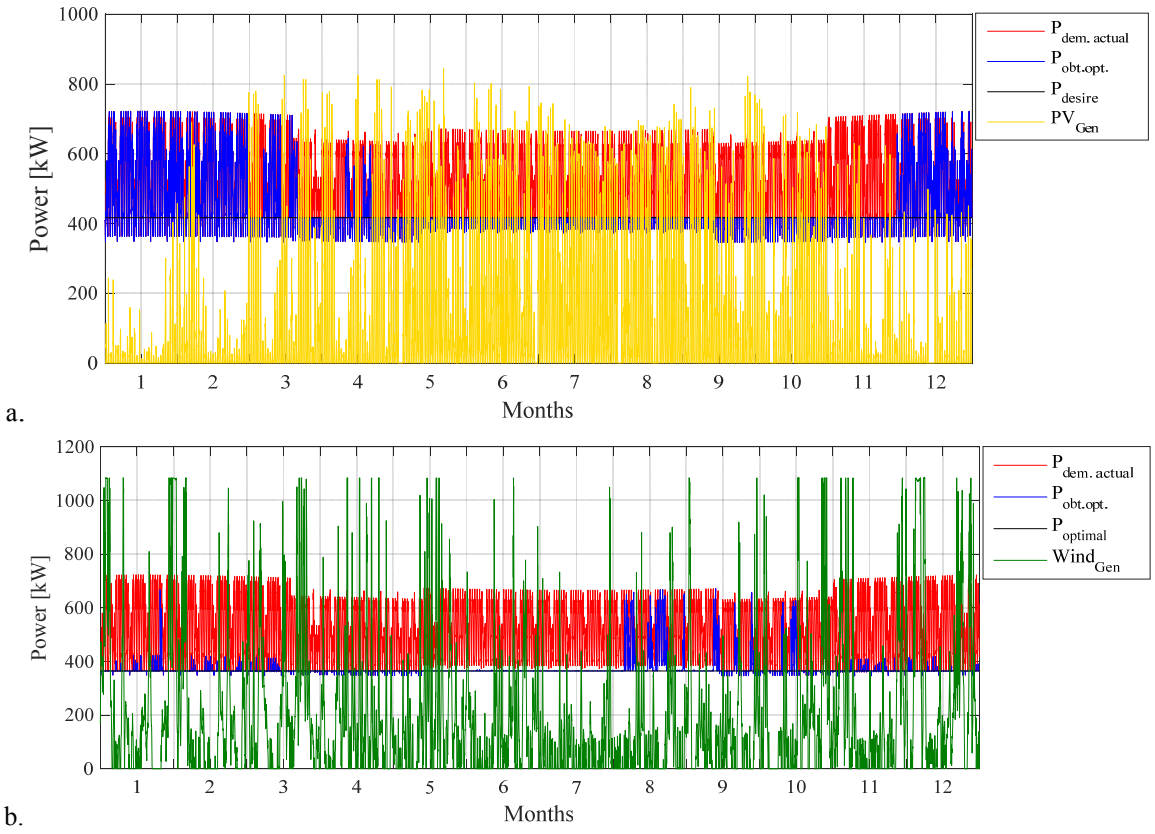

Figure 6-15: Plot of power profiles for Case 2 : Actual load profile (red), Optimal maximum demand utility should support P_{Load}^{ideal} (black), resulting profile of supply from utility (blue), power generation from PV(yellow) in (a), power generation from Wind Plant(green) in (b)

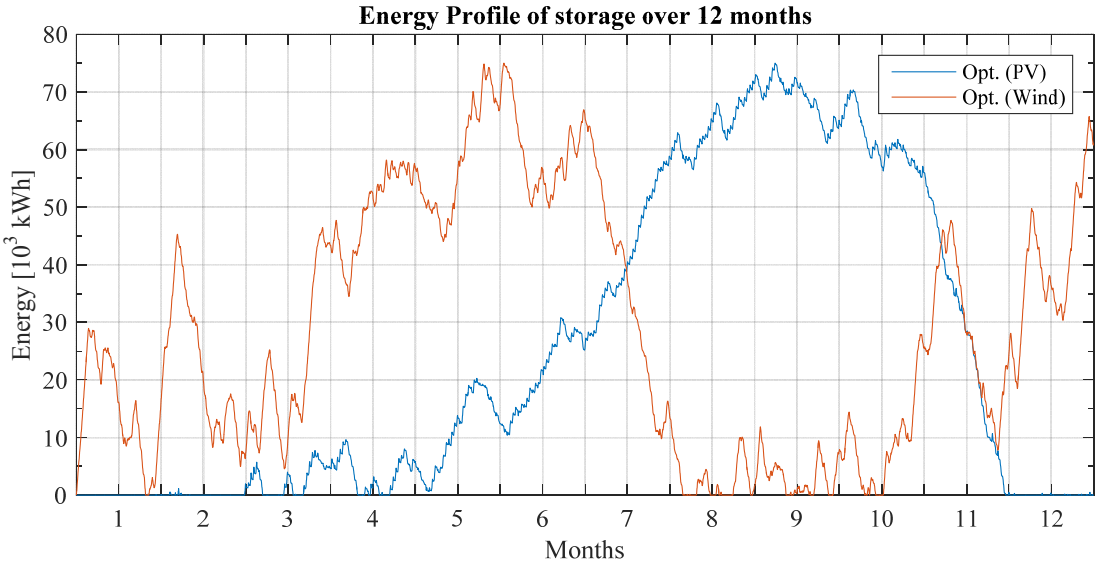

Figure 6-16: Energy profile for storage for PV and Wind Power at bus Kn0_11 for Case2.

Case 3

This case has no predetermined or fixed constraint. The sizing process is to determine the optimal value of all parameters with respect to the search space provided by their boundary conditions. Table 6-8 is a summary of the results from optimally sizing all four parameter of the REP-S system. For Case 3, P_{Load}^{ideal} is seen to increase when compare with results from the former (*Case 2*). The magnitude of $P_{storage}^{OPT.Max}$ is seen to be close to the rated power of load at the same bus. The optimal values of energy capacity of both RES-S system is seen to be the upper limit of the boundary condition given. This almost the same situation as observed in "*Case 1*" and "*Case 2*". The rated capacity of storage is also seen to be close to the installed capacity of the load at bus Kn0_11 and equal as well.

Average unutilized RES went to zero for PV and reduced by 96.1 % for wind compared with the "*Case 2*". Average extra power drown from utility reduced by 9.4 % and 17.8 % for PV and Wind respectively. The dependency on network for extra support is seen to be relatively higher in this case compared with what was observed in "*Case 1*". These observed reduction are also evident in the less to zero activities observed for Wind and PV loss plots in Figure 6-17 and Figure 6-18 respectively.

Table 6-8: Summary of result for optimal sizing of PV-Storage and Wind-Storage system at bus Kn0_11 under Case 3.

RES Power Source	Optimal Size of $P_{RES}^{rated.Max}$, P_{Load}^{ideal} and $E_{storage}^{rated.Max}$				$P_{RES}^{Loss.mean}$ [kW]	$P_{network}^{extra.mean}$ [kW]
	$P_{RES}^{OPT.Max}$ [kW]	P_{Load}^{ideal} [kW]	$E_{storage}^{rated.Max}$ [kWh]	$P_{storage}^{rated.Max}$ [kW]		
PV	722.5	427.44	75000	722.27	0	25.25
Wind Power	722.5	400.26	75000	722.18	1.34	5.57

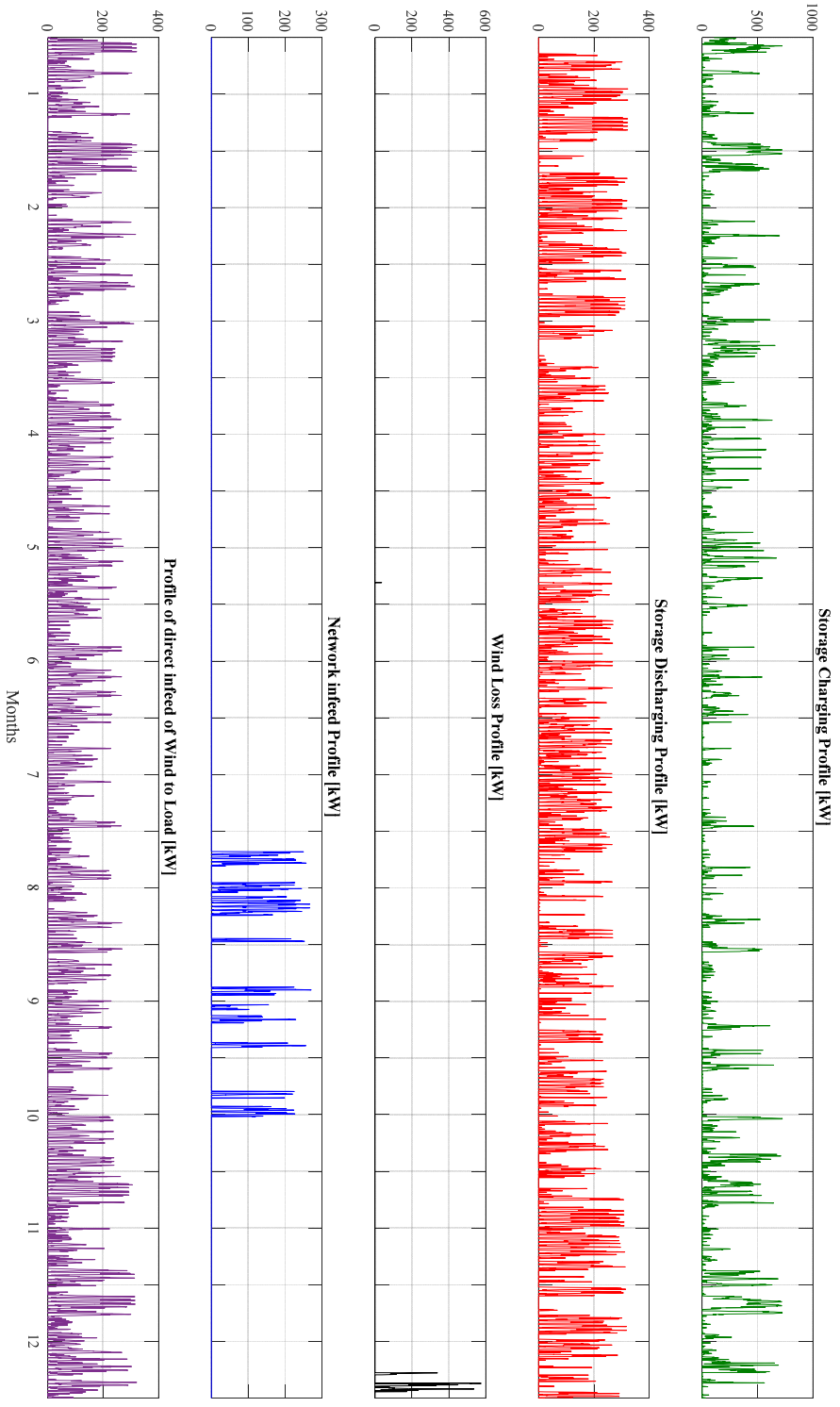

Figure 6-17: Plot of power profiles for Case 3 at Kn0_11: Storage charging with Wind Power generation (green), Storage discharge in instance of need (red), unutilized power from Wind Power generator at instance of fully charged battery or higher power output than rated power of storage (black), extra needed demand other than agreed P_{Load}^{ideal} supplied by utility (blue), direct supply from Wind Power generator to load when demand exceed P_{Load}^{ideal}

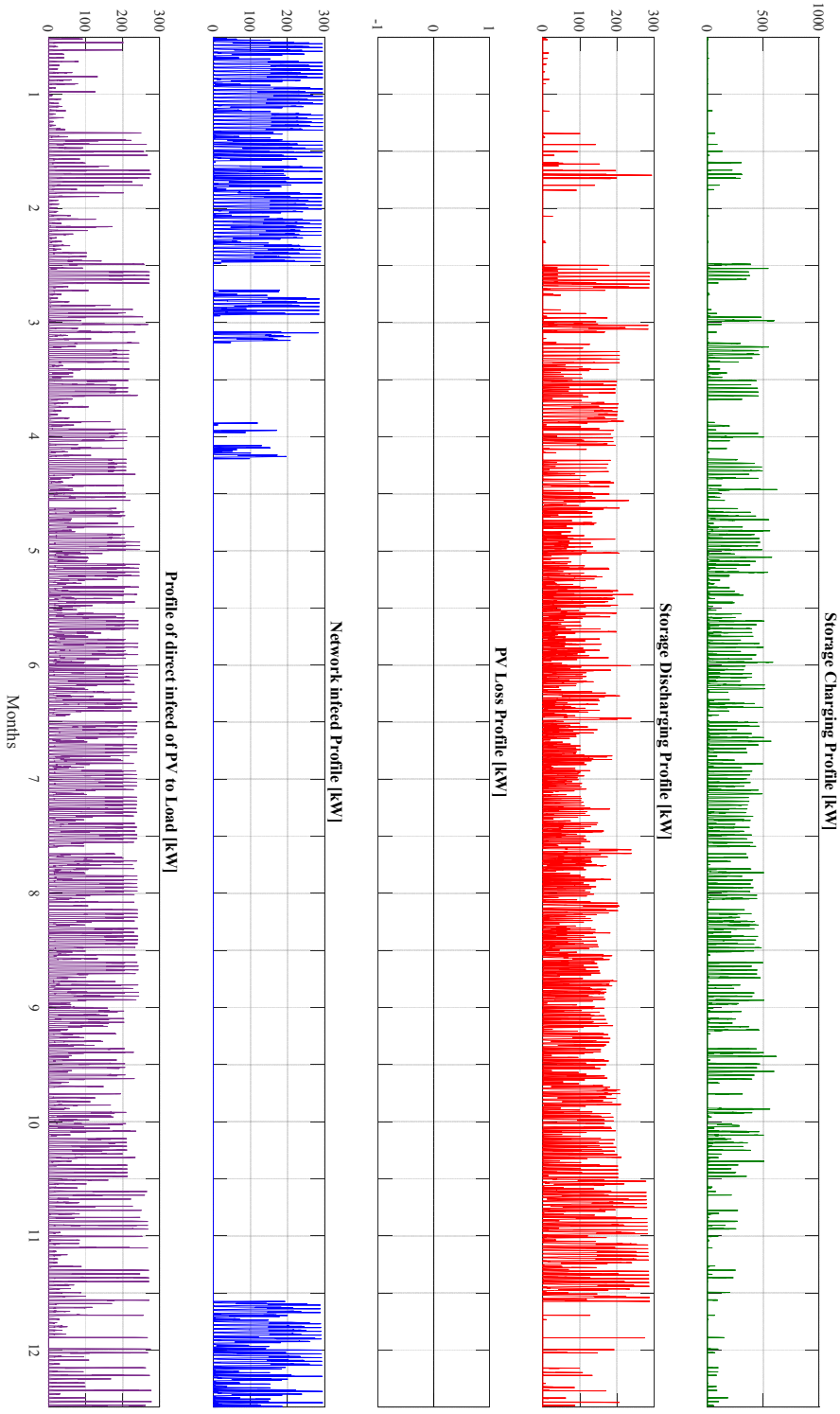

Figure 6-18: Plot of power profiles for Case 3 at Kn0_11: Storage charging with PV Power generation (green), Storage discharge in instance of need (red), unutilized power from PV Power generator at instance of fully charged battery or higher power output than rated power of storage (black), extra needed demand other than agreed P_{Load}^{ideal} supplied by utility (blue), direct supply from Wind Power generator to load when demand exceed P_{Load}^{ideal}

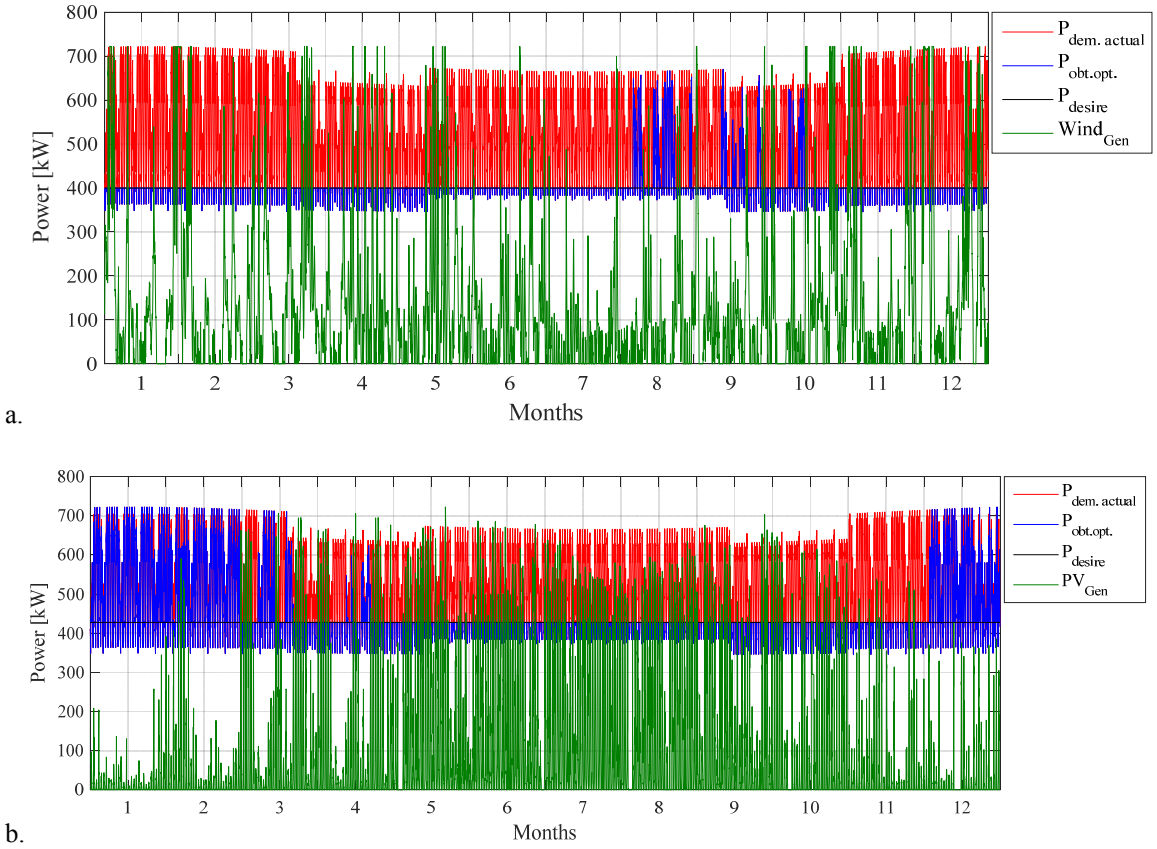

Figure 6-19: Plot of power profiles for Case 3 at bus Kn01_11: Actual load profile (red), Optimal maximum demand utility should support P_{Load}^{ideal} (black), resulting profile of supply from utility (blue), power generation from PV(green) in (a), power generation from Wind Plant (green) in (b)

6.1.2 Sizing at bus Kn0_12

The installed capacity of load (P_{Load}^{rated}) connected at bus Kn0_12 is 585 kW as established earlier in the work. This load is relative smaller in installed capacity when compared with load at bus Kn0_11. It however has a different consumption pattern which is expected to have a different effect on the outcome of the sizing process.

Case 1

Similar to Case 1 for bus Kn0_11, the focus will be on q = 1 and $k_{pr.fact}^{m}$ = 0.70. That is $P_{RES}^{Limit\_Up} = qP_{Load}^{rated}$, $P_{Load}^{ideal} = k_{pr.fact}^{m} P_{Load}^{rated}$ which are 585 kW and 409.5 kW respectively. The boundary conditions for storage energy capacity is $30 \leq E_{storage}^{OPT.Max} \leq 50$ MWh and rated power

of 300 kW as already established in section 5.2.3. The results as per RES are as follows.

Photovoltaic

The optimal solution set that resulted for a PV – Storage system is $P_{RES}^{\mathrm{OPT}.Max}$=172.18 kW and $E_{storage}^{\mathrm{OPT}.Max}$ = 50MWh as can be seen in Table 6-9. This is arrived at after 2050 iterative steps and returned $P_{RES}^{\mathrm{loss}.\mathrm{mean}}$ from PV and $P_{network}^{\mathrm{extra}\_mean}$ of 0.05 kW and 5.62 kW respectively. These loss values can be seen in Table 6-10. This equates to energy values of 0.438 MWh and 49.23 MWh respectively.

Table 6-9: Optimal Storage Capacities with corresponding optimal PV Power capacity at varying P_{Load}^{ideal} and $P_{RES}^{Limit\_Up}$ at Kn0_12

$P_{\mathrm{Load}}^{ideal}$ [kW]	Optimal Storage ($E_{storage}^{\mathrm{OPT}.Max}$) and PV rated capacity ($P_{RES}^{\mathrm{OPT}.Max}$) at different $P_{RES}^{Limit\_Up} = q_n.P_{Load}^{rated}$									
	q = 0.50 (292.5 kW)		q = 0.75 (438.8 kW)		q = 1.00 (585 kW)		q = 1.25 (731.3 kW)		q = 1.50 (877.5)	
	$P_{\mathrm{RES}}^{\mathrm{OPT}.\mathrm{Max}}$ [kW]	$E_{\mathrm{storage}}^{\mathrm{rated}.\mathrm{Max}}$ [kWh]	$P_{\mathrm{RES}}^{\mathrm{OPT}.\mathrm{Max}}$ [kW]	$E_{\mathrm{storage}}^{\mathrm{rated}.\mathrm{Max}}$ [kWh]	$P_{\mathrm{RES}}^{\mathrm{OPT}.\mathrm{Max}}$ [kW]	$E_{\mathrm{storage}}^{\mathrm{rated}.\mathrm{Max}}$ [kWh]	$P_{\mathrm{RES}}^{\mathrm{OPT}.\mathrm{Max}}$ [kW]	$E_{\mathrm{storage}}^{\mathrm{rated}.\mathrm{Max}}$ [kWh]	$P_{\mathrm{RES}}^{\mathrm{OPT}.\mathrm{Max}}$ [kW]	$E_{\mathrm{storage}}^{\mathrm{rated}.\mathrm{Ma}}$ [kWh]
497.25	87.09	50000	87.09	50000	87.09	50000	87.09	50000	87.09	50000
468.00	147.31	50000	147.31	50000	147.31	50000	147.31	50000	147.31	50000
438.75	186.78	50000	186.78	50000	186.78	50000	186.78	50000	186.78	50000
409.50	172.17	50000	172.17	50000	172.18	50000	172.17	50000	172.17	50000
380.25	243.69	50000	243.69	50000	243.69	50000	243.69	50000	243.69	50000
351.00	292.50	50000	403.55	50000	403.55	50000	403.55	50000	403.55	50000
321.75	292.50	37590	412.98	50000	478.31	50000	478.31	50000	478.31	50000

Table 6-10: Average Loss in power from PV and average extra power infeed for varying values of desired maximum demand at Kn0_12.

$P_{\mathrm{Load}}^{ideal}$ [kW]	Average loss of PV power and average extra infeed from Utility [kW] at Bus Kn0_12									
	q = 0.50 (292.5 kW)		q = 0.75 (438.8 kW)		q = 1.00 (585 kW)		q = 1.25 (731.3 kW)		q = 1.50 (877.5 kW)	
	Loss	Infeed	Loss	Infeed	Loss	Infeed	Loss	Infeed	Loss	Infeed
497.25	0.05	1.11	0.06	1.11	0.06	1.11	0.06	1.11	0.06	1.11
468.00	0.51	1.95	0.51	1.95	0.51	1.95	0.51	1.95	0.51	1.95
438.75	0.79	3.32	0.78	3.32	0.78	3.32	0.78	3.32	0.78	3.32
409.50	0.05	5.62	0.05	5.62	0.05	5.62	0.05	5.62	0.05	5.62
380.25	0.43	7.25	0.43	7.25	0.43	7.25	0.43	7.25	0.43	7.25
351.00	0.09	11.15	4.13	8.28	4.13	8.28	4.13	8.28	4.13	8.28
321.75	0	21.05	1.85	13.13	4.46	11.73	4.46	11.73	4.46	11.73

As can be observed in Figure 6-20, the PV - Storage system can support extra demand for about nine months (plot at 70 %). From P_{Load}^{ideal} equal to 65 % of P_{Load}^{rated} (380.25 kW), the

storage is not completely depleted at the end of the 12 month period considered. Plots of storage profiles for other 'q' values can be seen in Appendix.

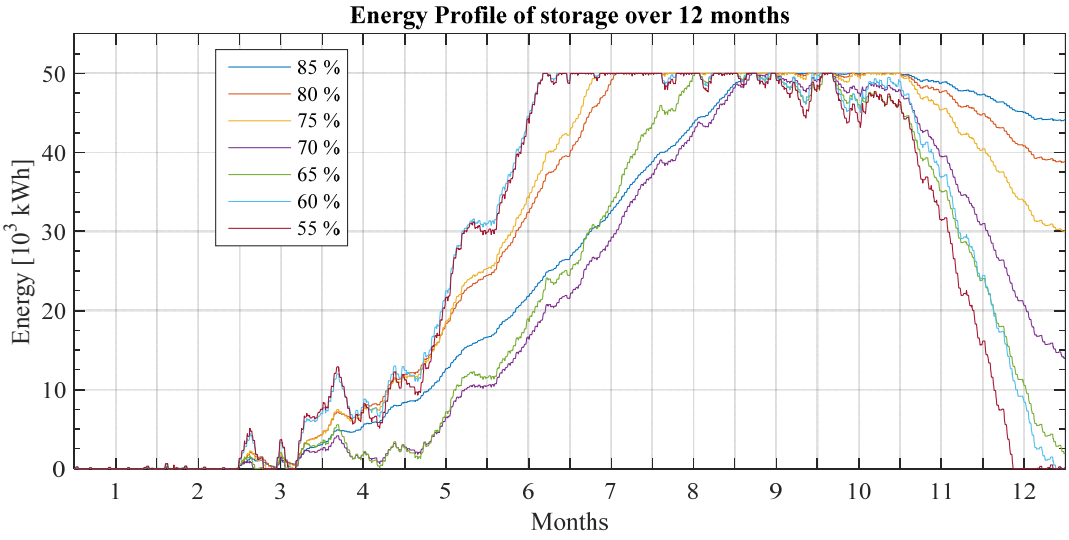

Figure 6-20: Energy profile for storage at different desire maximum demand for PV – Storage system under q = 1.0 at bus Kn0_12

Wind

The solution set for a Wind-Storage system for the same $P_{RES}^{Limit\_Up}$ and P_{Load}^{ideal} above shown together with results of other parameters in Table 6-11 is $P_{RES}^{OPT.Max}$ = 160.9 kW and $E_{storage}^{OPT.Max}$ = 50 MWh. The number of iteration steps is 2300. The $P_{RES}^{Loss\_mean}$ from Wind power and $P_{network}^{extra\_mean}$ obtained are 0.08 kW and 0.18 kW amounting to energy values of 0.70 MWh and 1.40 MWh. The loss values can be seen in Table 6-12. It is observed that optimal storage sizes obtained were on the average close to or the upper limit of the range provided (50 MWh). The energy values 49.23 MWh and 1.40 MWh indicates that both PV – Storage and Wind – Storage system cannot support fully the extra demand that arise.

The storage profile in Figure 6-21 for a Wind-Storage system shows at the end to the 12 months period, about 90 % of total energy remains for future use when needed. The nature of the graphs needs some further test. An attempt to find a function that correlates P_{Load}^{ideal} and q with $P_{RES}^{OPT.Max}$ resulted in a function similar to the one in equation 6-1 for PV-Storage and

Wind-Storage system connected to bus Kn0_12.

Table 6-11: Optimal Storage Capacities with corresponding optimal Wind Power capacity at varying P_{Load}^{ideal} and $P_{RES}^{Limit\_Up}$ at Kn0_12

P_{Load}^{ideal} [kW]	Optimal Storage ($E_{storage}^{rated.Max}$) and PV rated capacity ($P_{RES}^{OPT.Max}$ $P_{RES}^{OPT.Max}$) at different $P_{RES}^{Limit\_Up} = q_n.P_{Load}^{rated}$									
	q = 0.50 (292.5 kW)		q = 0.75 (438.8 kW)		q = 1.00 (585 kW)		q = 1.25 (731.3 kW)		q = 1.50 (877.5 kW)	
	$P_{RES}^{OPT.Max}$ [kW]	$E_{storage}^{rated.Max}$ [kWh]	$P_{RES}^{OPT.Max}$ [kW]	$E_{storage}^{rated.Max}$ [kWh]	$P_{RES}^{OPT.Max}$ [kW]	$E_{storage}^{rated.Max}$ [kWh]	$P_{RES}^{OPT.Max}$ [kW]	$E_{storage}^{rated.Max}$ [kWh]	$P_{RES}^{OPT.Max}$ [kW]	$E_{storage}^{rated.Max}$ [kWh]
497.25	48.20	41560	48.74	50000	51.68	50000	53.38	50000	48.93	49530
468.00	79.30	49960	79.30	50000	79.30	50000	79.30	50000	79.30	49980
438.75	121.59	50000	121.59	49960	121.59	50000	121.59	49920	121.59	49970
409.50	160.69	50000	160.69	50000	160.69	50000	160.69	50000	160.69	50000
380.25	214.75	50000	214.75	50000	214.75	50000	214.75	50000	214.75	50000
351.00	274.50	49990	274.50	50000	274.50	50000	274.50	50000	247.50	50000
321.75	292.50	46650	339.63	50000	339.63	50000	339.63	50000	339.63	50000

Their respective polynomial surface fit and unique coefficients and confidence bounds are shown in Figure C- 25and Figure C- 26 in the Appendix. These polynomial surface fits are obtained from Table 6-9 and Table 6-11. Additionally RMSE values of 33.52 and 7.53 are obtained both combination respectively.

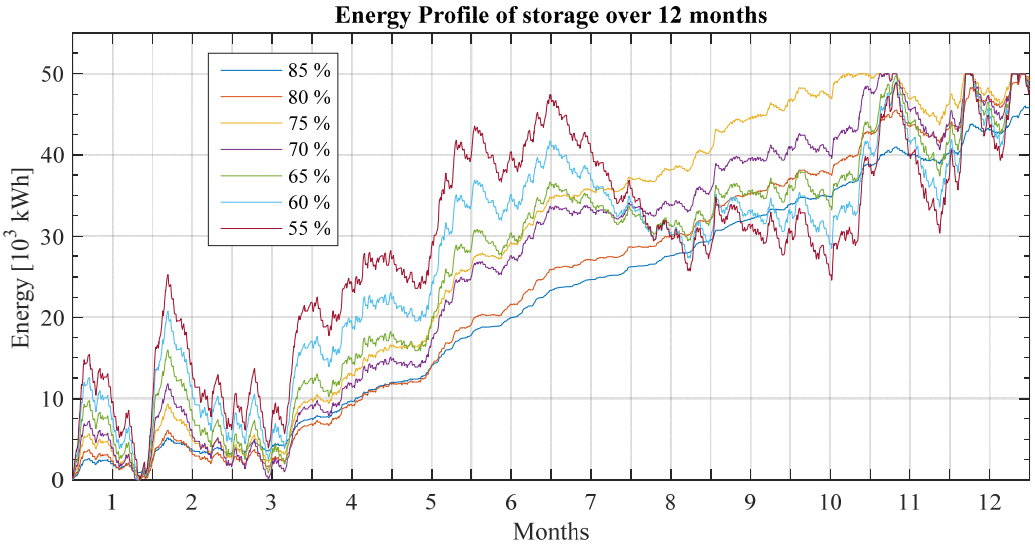

Figure 6-21: Energy profile for storage at different desire maximum demand for Wind power under q = 1.0 at bus Kn0_12

The average unutilized power from both PV – Storage and Wind – Storage system plant and average extra infeed are observed to be the same for all P_{Load}^{ideal} values except P_{Load}^{ideal} =

321.75 kW and from 'q' values starting from 0.75. These observations are made from results in Table 6-10 and Table 6-12.

Table 6-12: Average Loss in power from Wind and average extra power infeed for varying values of desired maximum demand at Kn0_12 for Case 2.

P_{Load}^{ideal} [kW]	Average loss of Wind power and average extra infeed from Utility [kW] at Bus Kn0_12									
	q = 0.50 (292.5 kW)		q = 0.75 (438.8 kW)		q = 1.00 (585 kW)		q = 1.25 (731.3 kW)		q = 1.50 (877.5 kW)	
	Loss	Infeed	Loss	Infeed	Loss	Infeed	Loss	Infeed	Loss	Infeed
497.25	0	0	0	0	0	0	0	0	0	0
468.00	0	0	0	0	0	0	0	0	0	0
438.75	0.20	0	0.20	0	0.20	0	0.20	0	0.20	0
409.50	0.08	0.16	0.08	0.16	0.08	0.16	0.08	0.16	0.08	0.16
380.25	0.06	0.15	0.06	0.15	0.06	0.15	0.06	0.15	0.06	0.15
351.00	0.09	0.09	0.09	0.09	0.09	0.09	0.09	0.09	0.09	0.09
321.75	0	3.15	0.54	0.03	0.54	0.03	0.54	0.03	0.54	0.03

Case 2

The resulting optimal size for a storage system at bus Kn0_12 is the upper limit of the range for both PV – Storage and Wind – Storage system. The optimal sizes for both PV and Wind power capacity are both observed to be lower that lowest proposed P_{Load}^{ideal} under Case 1 (Table 6-13). Three out of the four parameters are to be determined by the sizing process.

Table 6-13: Summary of result for optimal sizing of PV – Storage and Wind – Storage system at bus Kn0_12 under Case 2.

RES Power Source	Optimal Size of $P_{RES}^{rated.Max}$, P_{Load}^{ideal} and $E_{storage}^{rated.Max}$			$P_{RES}^{Loss\_mean}$ [kW]	$P_{network}^{extra\_mean}$ [kW]
	$P_{RES}^{rated.Max}$ [kW]	P_{Load}^{ideal} [kW]	$E_{storage}^{rated.Max}$ [kWh]		
PV Plant	774.18	234.51	50000	10.27	24.20
Wind Power plant	877.43	163.80	50000	20.76	9.27

The trend of not depleting the entire storage capacity for a Wind-Storage system is observed in Figure 6-22 with about 90 % of storage capacity at the end of the 12 month period.

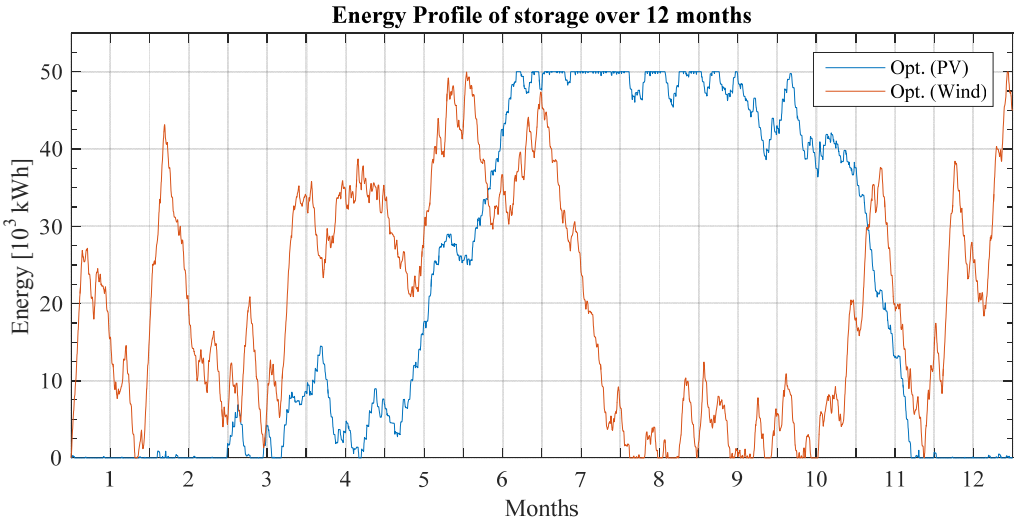

Figure 6-22: Energy profile for storage for optimal size of storage and RES source at bus Kn0_12 for Case 2. Blue is plot of PV-S storage profile, Orang is plot of Wind-S storage profile

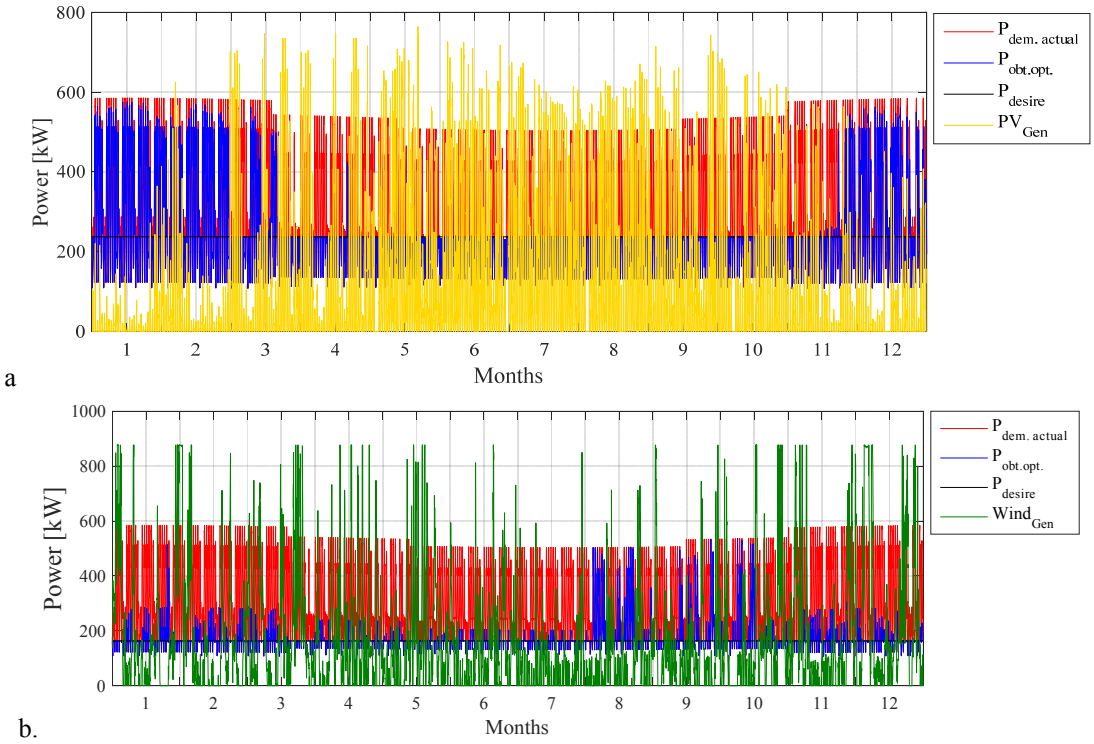

Figure 6-23: Plot of power profiles: Actual load profile (red), Optimal maximum demand utility should support P_{Load}^{ideal} (black), resulting profile of supply from utility (blue), power generation from PV(yellow) in 'a', power generation from Wind Plant(green) in 'b' at bus Kn0_12 for Case 2

PV – Storage system can support extra demand for a period of seven months as shown by profiles in Figure 6-22 and in Figure 6-23 a. Wind – Storage systems can support the system

about 8 months.

Case 3

Under Case 3, Average loses in unused REP reduced by about 67.7 % and 96.6 % to 3.31 kW and 0.76 kW when compared with values under Case 2 for PV and Wind storage systems respectively. The amount of power taken from the network however reduced on the average by 17.77 % and 63.86 % for both Wind-Storage and PV-Storage system.

Table 6-14: Summary of result for optimal sizing of PV – Storage and Wind – Storage system at bus Kn0_12 under Case 3.

RES Power Source	Optimal Size of $P_{RES}^{rated.Max}$, P_{Load}^{ideal} and $E_{storage}^{rated.Max}$				$P_{RES}^{Loss.mean}$ [kW]	$P_{network}^{extra.mean}$ [kW]
	$P_{RES}^{rated.Max}$ [kW]	P_{Load}^{ideal} [kW]	$E_{storage}^{rated.Max}$ [kWh]	$E_{storage}^{rated.Max}$ [kW]		
PV	585	266.67	50000	559.34	3.31	19.90
Wind Power	585	216.99	50000	585.00	0.76	3.35

The storage profiles shown in Figure 6-24 below, shows that storage can support extra needed power for Wind-S system for almost eleven month to a year. On the other hand, the storage can support network for about eight months for PV-S system.

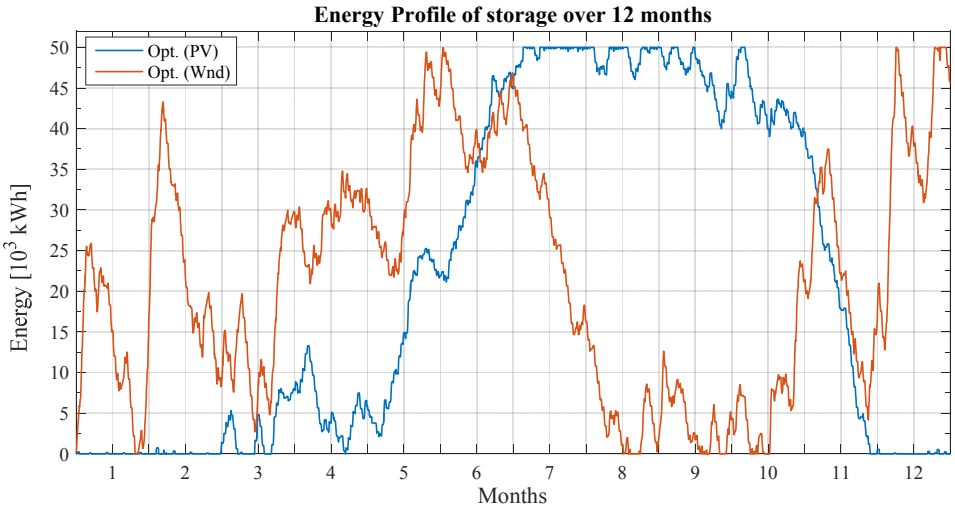

Figure 6-24: Energy profile for storage for optimal size of storage and RES source at bus Kn0_12 for Case 3 Blue is plot of PV-S storage profile, Orang is plot of Wind-S storage profile

6.1.3 Sizing at bus Kn0_13

This bus has a rated installed load capacity of 427.5 kW. The load is made up of residential consumers only. Apart from been lower in magnitude compare to the previous buses, it has different load demand curve when compared with the others. The following are the results per Case.

Case 1

For this case, the focus will be on one set possible set of constraints. This is for q = 1 and $k_{pr.fact}^{m} = 0.70$. Therefore $P_{RES}^{Limit\_Up} = qP_{Load}^{rated}$ and $P_{Load}^{ideal} = k_{pr.fact}^{m} P_{Load}^{rated}$ are 427.5 kW and 299.25 kW. At this bus, the boundary condition is $21 \leq E_{storage}^{\mathrm{OPT}.Max} \leq 37$ MWh. The rated power of storage system remains 300 kW.

Photovoltaic

With the above mentioned parameters, the optimal solution set that resulted for a PV-Storage system is $P_{RES}^{\mathrm{OPT}.Max}$ =242.56 kW and $E_{storage}^{\mathrm{OPT}.Max}$ = 37MWh. This can be seen in Table 6-15. This is arrived at after 2050 iterative steps and returned $P_{RES}^{Loss.mean}$ from PV and $P_{network}^{\mathrm{extra}.mean}$ of 0.21 kW and 0.50 kW respectively (Table 6-16). The values 5.05 MWh and 12.01 MWh are therefore their respectively energy equivalence.

Table 6-15: Optimal Storage Capacities with corresponding optimal PV Power capacity at varying P_{Load}^{ideal} and $P_{RES}^{Limit\_Up}$ at Kn0_13

P_{Load}^{ideal} [kW]	Optimal Storage ($E_{storage}^{rated.Max}$) and PV rated capacity ($P_{RES}^{\mathrm{OPT}.Max}$) at different $P_{RES}^{Limit\_Up} = q_n.P_{Load}^{rated}$									
	q = 0.50 (213.5 kW)		q = 0.75 (320.6 kW)		q = 1.00 (427.5 kW)		q = 1.25 (534.4 kW)		q = 1.50 (641.3 kW)	
	$P_{RES}^{\mathrm{OPT}.Max}$ [kW]	$E_{storage}^{rated.Max}$ [kWh]	$P_{RES}^{\mathrm{OPT}.Max}$ [kW]	$E_{storage}^{rated.Max}$ [kWh]	$P_{RES}^{\mathrm{OPT}.Max}$ [kW]	$E_{storage}^{rated.Max}$ [kWh]	$P_{RES}^{\mathrm{OPT}.Max}$ [kW]	$E_{storage}^{rated.Max}$ [kWh]	$P_{RES}^{\mathrm{OPT}.Max}$ [kW]	$E_{storage}^{rated.Max}$ [kWh]
363.38	213.52	36830	231.19	29470	231.19	27160	231.19	28390	231.19	30490
342.00	213.75	35310	320.63	34240	340.12	34840	320.12	35600	340.12	35310
320.63	213.75	37000	302.84	36990	302.84	37000	302.84	37000	302.84	37000
299.25	213.75	36310	242.56	37000	242.56	37000	242.56	37000	242.56	37000
277.88	213.75	37000	320.63	37000	355.47	36240	377.47	34560	355.47	35560
256.50	213.75	37000	292.49	37000	292.49	37000	292.49	37000	292.49	37000
235.13	213.75	37000	245.83	37000	245.83	36990	245.52	36960	245.82	37000

A closer observation of $P_{RES}^{\mathrm{OPT}.Max}$ values presented in Table 6-15 reveal inconsistencies. This was further evident during the attempt of finding a function that could describe the relationship between variable in the above mentioned table. This effort was not successful for the PV – Storage system.

Table 6-16: Average Loss in power from PV and average extra power infeed for varying values of desired maximum demand at Kn0_13.

P_{Load}^{ideal} [kW]	Average loss of PV power and average extra infeed from Utility [kW] at Bus Kn0_11									
	q = 0.50 (213.5 kW)		q = 0.75 (320.6 kW)		q = 1.00 (427.5 kW)		q = 1.25 (534.4 kW)		q = 1.50 (641.3 kW)	
	Loss	Infeed	Loss	Infeed	Loss	Infeed	Loss	Infeed	Loss	Infeed
363.38	0	0	0	0	0	0	0	0	0	0
342.00	0.01	0.08	0.05	0.01	0.06	0	0.06	0	0.6	0
320.63	0.07	0.26	0.14	0.19	0.14	0.19	0.14	0.19	0.14	0.19
299.25	0.16	0.58	0.21	0.50	0.21	0.50	0.21	0.50	0.21	0.50
277.88	0.320	1.25	0.71	0.86	0.84	0.73	0.84	0.73	0.84	0.73
256.50	0.54	2.18	1.06	1.88	1.060	1.88	1.06	1.88	1.06	1.88
235.13	0.87	3.61	1.09	3.46	1.09	3.46	1.09	3.46	1.08	3.47

Wind

The solution set for the Wind-Storage system for the same $P_{RES}^{Limit\_Up}$ and P_{Load}^{ideal} above is $P_{RES}^{\mathrm{OPT}.Max} = 50.49\,\mathrm{kW}$ and $E_{storage}^{\mathrm{OPT}.Max} = 21750\,\mathrm{kWh}$. This was arrived at after 1950 iterative steps. The resulting values for $P_{RES}^{Loss.mean}$ from Wind Power and $P_{network}^{\mathrm{extra}.mean}$ are 0.05 kW and 0.01 kW respectively. The energies are therefore 0.438 MWh and 0.088 MWh (Table 6-19). The energy values, 12.01 MWh and 0.088 MWh indicates that both systems could not fully support extra demand that was required though some energy produced went unutilized.

The storage systems in both Solar and Wind system arrangements are not depleted at the end of the 12 month period under consideration (Figure 6-25 and Figure 6-26). The plots in Figure 6-25 and Figure 6-26 are observed to have relatively very little activities as greater part of the period had no discharge activities. The PV-S system can support extra demand for nine months whiles a Wind-S system can support up to eleven months of extra demand.

Table 6-17: Optimal Storage Capacities with corresponding optimal Wind Power capacity at varying P_{Load}^{ideal} and $P_{RES}^{Limit\_Up}$ at Kn0_13

P_{Load}^{ideal} [kW]	Optimal Storage ($E_{storage}^{rated.Max}$) and Wind rated capacity ($P_{RES}^{OPT.Max}$) at different $P_{RES}^{Limit\_Up} = q_n.P_{Load}^{rated}$									
	q = 0.50 (213.5 kW)		q = 0.75 (320.6 kW)		q = 1.00 (427.5 kW)		q = 1.25 (534.4 kW)		q = 1.50 (641.3 kW)	
	$P_{RES}^{OPT.Max}$ [kW]	$E_{storage}^{rated.Max}$ [kWh]	$P_{RES}^{OPT.Max}$ [kW]	$E_{storage}^{rated.Max}$ [kWh]	$P_{RES}^{OPT.Max}$ [kW]	$E_{storage}^{rated.Max}$ [kWh]	$P_{RES}^{OPT.Max}$ [kW]	$E_{storage}^{rated.Max}$ [kWh]	$P_{RES}^{OPT.Max}$ [kW]	$E_{storage}^{rated.Max}$ [kWh]
363.38	22.04	36640	19.57	33630	21.89	31730	23.20	36460	18.33	34880
342.00	29.96	37000	29.96	37000	29.96	37000	29.96	37000	29.96	37000
320.63	33.41	37000	33.41	37000	33.41	37000	33.41	37000	33.41	37000
299.25	50.49	36990	50.49	21750	50.49	36920	50.49	29780	50.49	36980
277.88	74.58	32970	74.58	35080	74.58	33330	74.58	32580	74.58	32990
256.50	107.75	37000	107.75	37000	107.75	36960	107.75	36990	107.75	36660
235.13	145.23	37000	145.21	37000	145.21	37000	145.21	37000	145.21	37000

An interpolated surface approximation plot of $P_{RES}^{OPT.Max}$ result in Table 6-15 is present in Figure C- 27 in the Appendix. Result presented in Table 6-17for Wind-Storage system however were consistent. Also in the Appendix of both the interporlated and polynomial surface plots. A function that describes the relationship between the variables in Table 6-17 is shown in equation 6-2.

$$f(x_1, x_2) = c_1 + c_2 x_1 + c_3 x_2 + c_4 x_1^2 + c_5 x_1 x_2 + c_6 x_2^2 + c_7 x_1^3 + c_8 x_1^2 x_2 \ldots + \ldots + c_9 x_1 x_2^2 + c_{10} x_1^4 + c_{11} x_1^3 x_2 + c_{12} x_1^2 x_2^2 \quad (6\text{-}2)$$

Table 6-18: Coefficient and confidence bounds valid for polynomial surface fit in Figure C- 28 and described by (6-2)

Coefficient		Confidence bounds	
		Lower	Upper
C_1	924.7	453.1	1396
C_2	428.5	-821.7	1679
C_3	-5.106	-8.01	-2.203
C_4	-408.9	-1670	851.9
C_5	-1.988	-8.512	4.536
C_6	0.0074	0.0027	0.0121
C_7	119.5	-591.1	830.1
C_8	1.718	-2.07	5.507
C_9	0.00153	-0.00879	0.01184
C_{10}	2.041	-170.5	166.5
C_{11}	-0.416	-1.161	0.3289
C_{12}	-0.0009	-0.00597	0.00424

The unique coefficient and confidence bound are presented in Table 6-18. This polynomial surface approximation plot has RMSE value of 2.42. This is so far the lowest among all the polynomial surface fit plots.

Table 6-19: Average Loss in power from Wind and average extra power infeed for varying values of desired maximum demand at Kn0_13.

P_{Load}^{ideal} [kW]	Average loss of PV power and average extra infeed from Utility [kW] at Bus Kn0_11									
	q = 0.50		q = 0.75		q = 1.00		q = 1.25		q = 1.50	
	Loss	Infeed	Loss	Infeed	Loss	Infeed	Loss	Infeed	Loss	Infeed
363.38	0	0	0	0	0	0	0	0	0	0
342.00	0	0	0	0	0	0	0	0	0	0
320.63	0	0.01	0	0.01	0	0.01	0	0.01	0	0.01
299.25	0.06	0.01	0.05	0.01	0.05	0.01	0.05	0.01	0.05	0.01
277.88	0.15	0	0.16	0	0.15	0	0.15	0	0.15	0
256.50	0.38	0	0.38	0	0.38	0	0.38	0	0.38	0
235.13	0.95	0.14	0.95	0.14	0.95	0.14	0.95	0.14	0.95	0.14

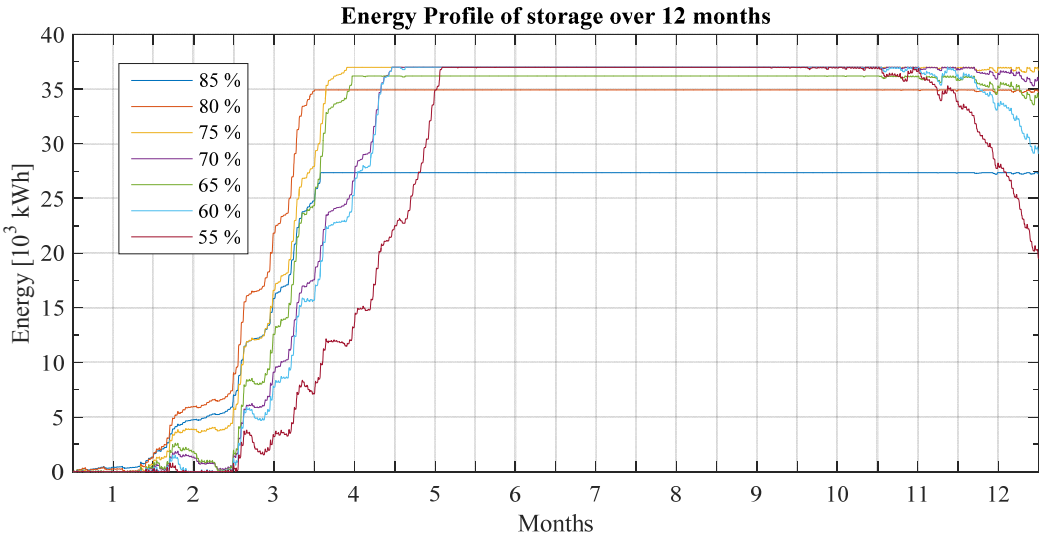

Figure 6-25: Energy profile for storage at different desire maximum demand for PV Power under q = 1.0 bus at Kn0_13 for Case 1

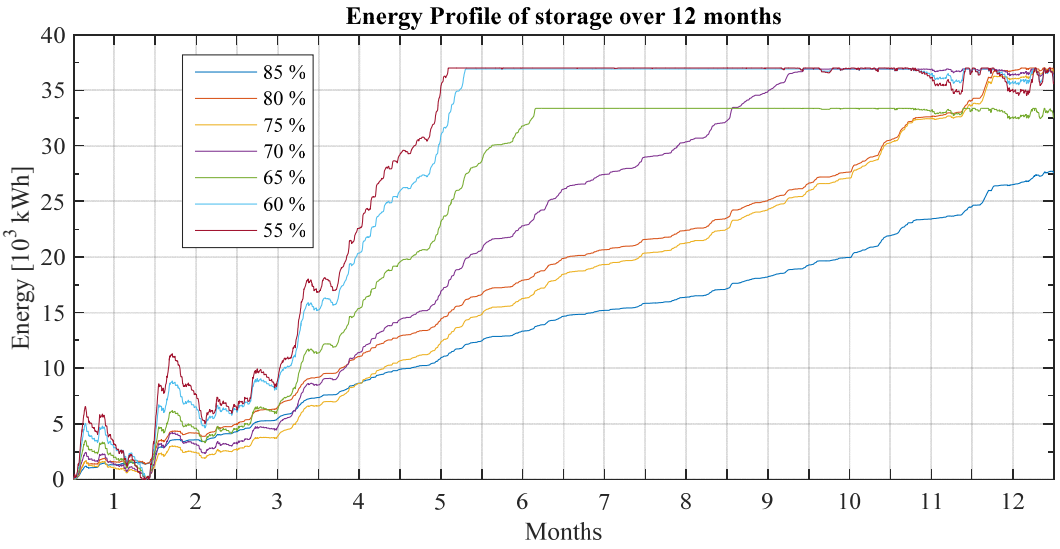

Figure 6-26: Energy profile for storage at different desire maximum demand for Wind Power under q = 1.0 bus at Kn0_13 for Case 1

Case 2

In Table 6-20 is the result of sizing RES-Storage system at bus Kn0_13 based on Case 2. Both results returned the same size for storage system and the RES capacity. Both returned values of P_{Load}^{ideal} that are lower than the minimum P_{Load}^{ideal} under Case 1. Both RES-Storage systems returned average unutilized power as well as extra power drawn from utility. The average unutilized value seen in Wind-Storage system is seen to be higher than in PV-Storage system while the converse is true for average extra power taken from utility. A closer look at Figure 6-27 and Figure 6-28 revels that REP-Storage system can support extra demand six and nine months in the option with PV and Wind power respectively.

Table 6-20: Summary of result for second instance.

RES Power Source	Optimal Size of $P_{RES}^{rated.Max}$, P_{Load}^{ideal} and $E_{storage}^{rated.Max}$			$P_{RES}^{Loss\_mean}$	$P_{network}^{extra\_mean}$
	$P_{RES}^{rated.Max}$ [kW]	P_{Load}^{ideal} [kW]	$E_{storage}^{rated.Max}$ [kWh]	[kW]	[kW]
PV Plant	641.25	77.98	37000	5.91	45.42
Wind Power plant	641.25	81.04	37000	8.94	3.99

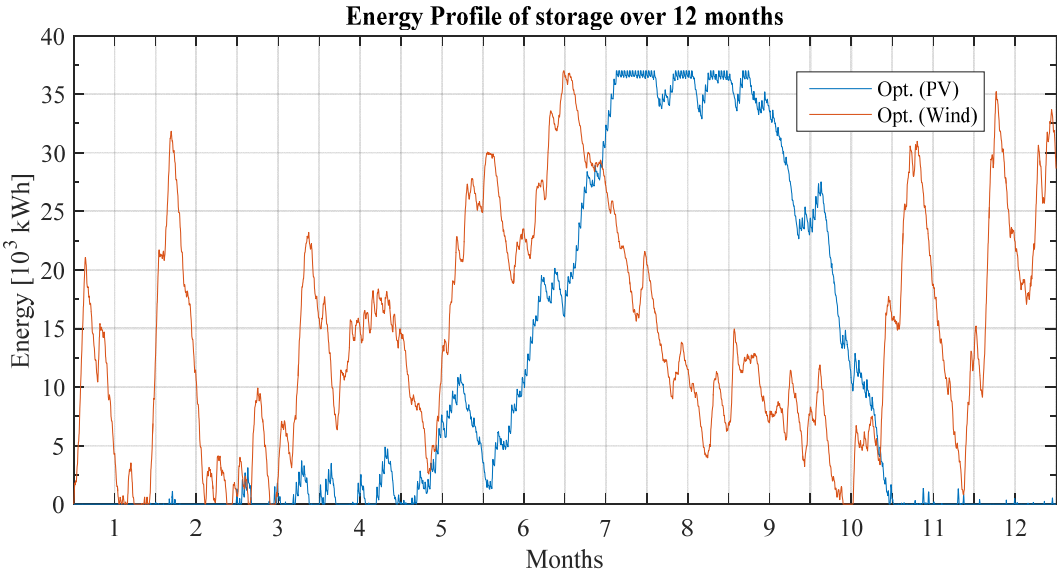

Figure 6-27: Energy profile for storage for optimal size of storage and RES source at bus Kn0_13 for Case 2. Blue is plot of PV-S storage profile, Orang is plot of Wind-S storage profile

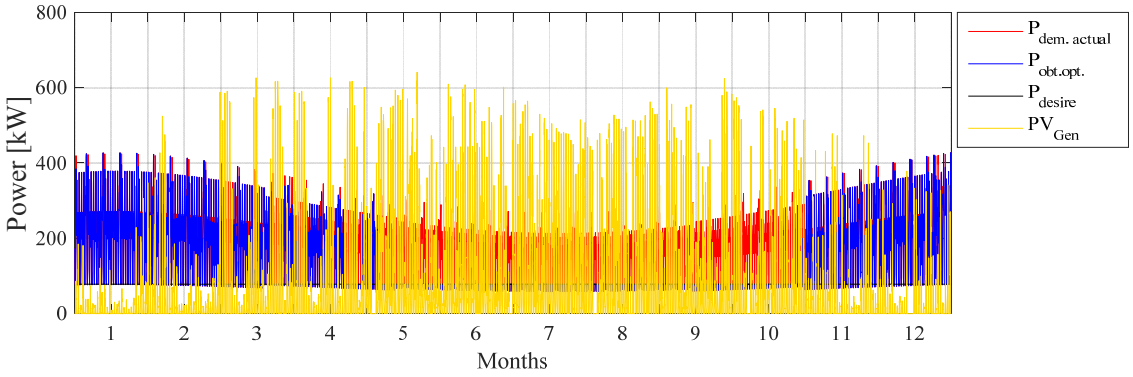

a.

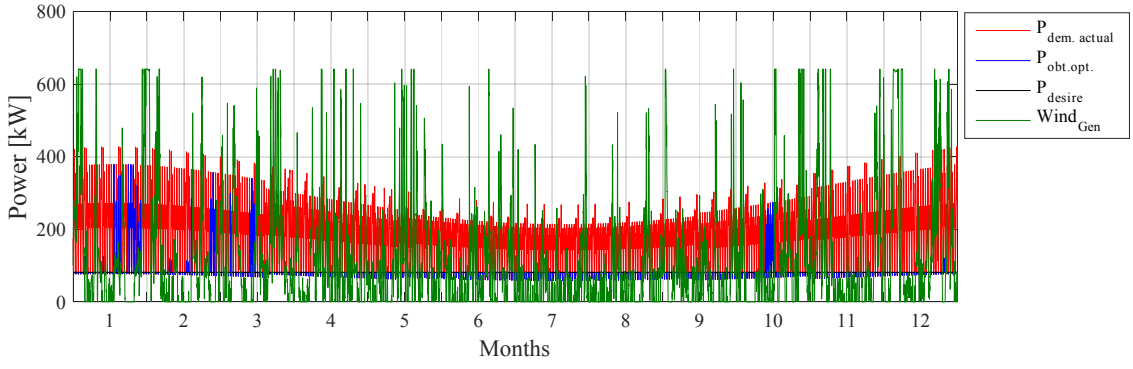

b.

Figure 6-28: Plot of power profiles: Actual load profile (red), Optimal maximum demand utility should support P_{Load}^{ideal} (black), resulting profile of supply from utility (blue), power generation from PV in 'a', power generation from Wind Plant(green) in 'b'

Just as in previous Cases, the storage profile corresponds to the energy production from the respective renewable energy plants. The period or season of the year with high yield in energy production result in the longer period of storage remaining in charged condition and vice versa. The profile of storage from Wind-S system (blue plot in Figure 6-27) is always observed to have more activities of charge and discharge.

Case 3

The result of finding the optimal parameter of RES-S system that be integrated into the network at bus Kn0_13 under Case 3 is shown in Figure 6-21. This is form both PV-S and Wind-S systems. Evaluation for Wind-S system returns a slightly lower storage energy capacity as compared with PV-S system which returned the maximum e upper limit of the boundary of 37 MWh. Comparing results from Case 3 to Case 2 reveal a 8.3 % average increase in power drawn from the utility.

Table 6-21: Summary of result for optimal sizing of PV – Storage and Wind – Storage system at bus Kn0_13 under Case 3.

RES Power Source	Optimal Size of $P_{RES}^{rated.Max}$, P_{Load}^{ideal} and $E_{storage}^{rated.Max}$				$P_{RES}^{Loss.mean}$ [kW]	$P_{network}^{extra.mean}$ [kW]
	$P_{RES}^{rated.Max}$ [kW]	P_{Load}^{ideal} [kW]	$E_{storage}^{rated.Max}$ [kWh]	$P_{storage}^{OPT.Max}$ [kW]		
PV	279.90	203.60	37000	344.65	3.38	6.61
Wind Power	427.5	115.16	33200	427.5	0	4.32

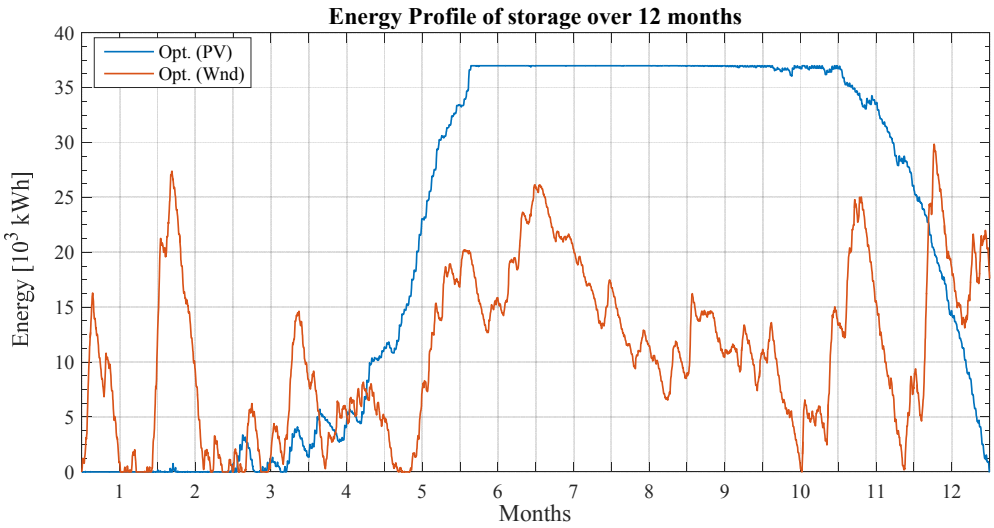

Figure 6-29: Energy profile for storage for optimal size of storage and RES source at bus Kn0_13 for Case 3. Blue is plot of PV-S storage profile, Orang is plot of Wind-S storage profile

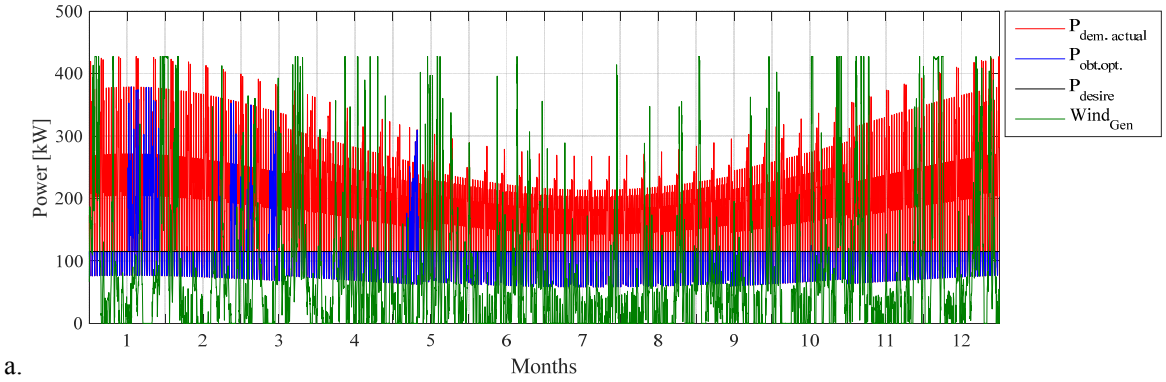

a.

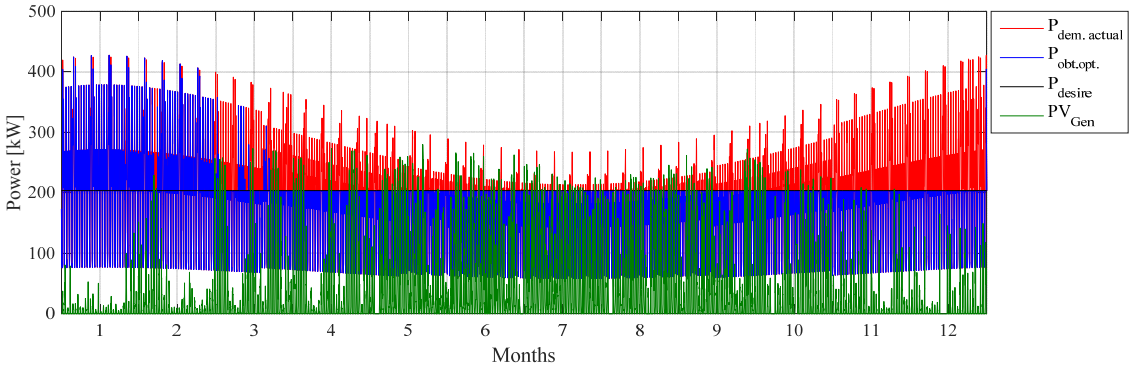

b.

Figure 6-30: Plot of power profiles for Case 3 at bus Kn01_13: Actual load profile (red), Optimal maximum demand utility should support P_{Load}^{ideal} (black), resulting profile of supply from utility (blue), power generation from PV(green) in (a), power generation from Wind Plant (green) in (b)

6.2 Analysis on 30 bus network

Hypothetical REP-S systems are installed at some buses in the 30bus network depicted in Figure 3-1a. The Figure 6-31 shows the network with locations of REP-S systems. The multiple choice of location is with the aim of determining the impact of optimally sized multiple REP-S system with different capacities in an electrical network.

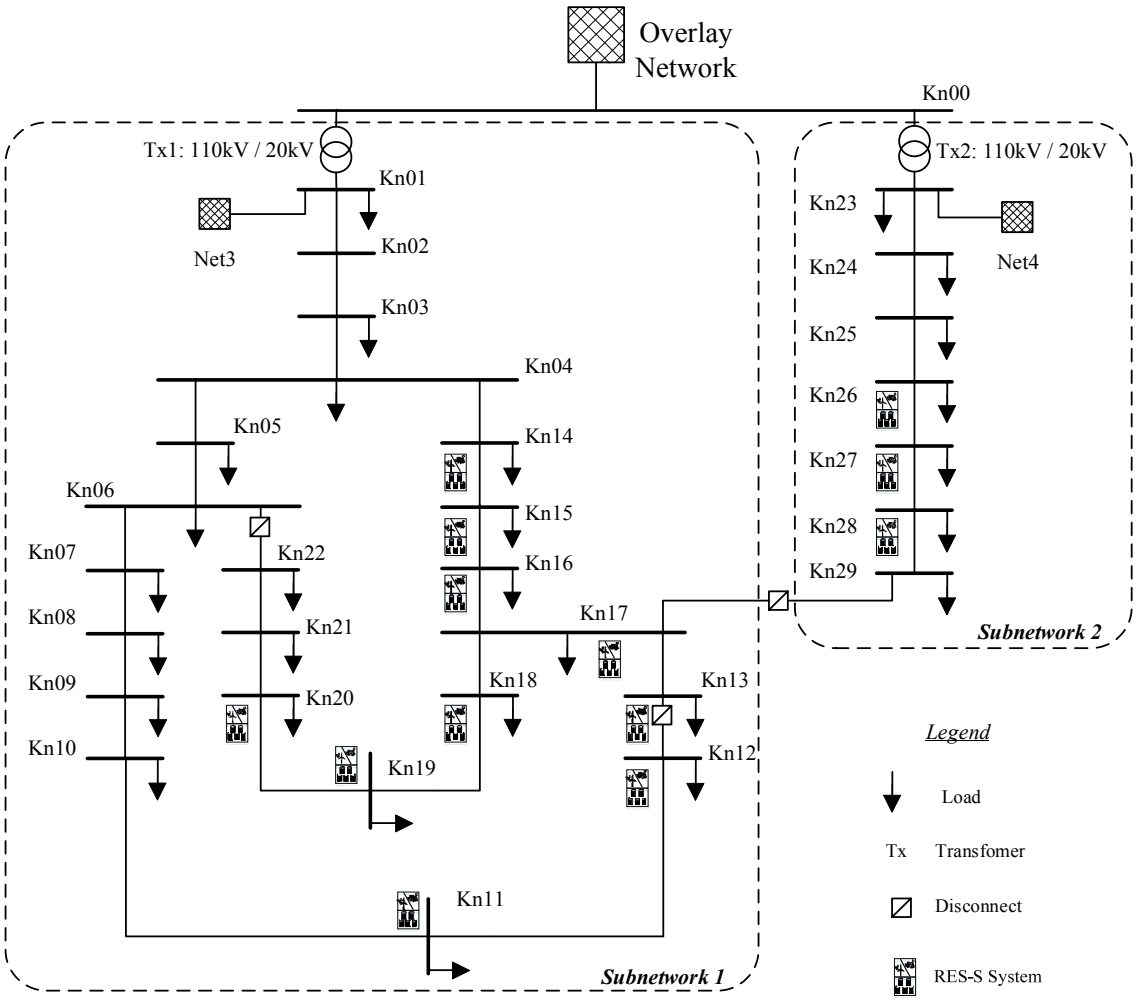

Figure 6-31: Adapted 30 bus network with installed RES-S system at 14 buses.

In the single node analysis, wind-storage system gave a relatively better result. Therefore only Wind-Storage systems was used. Result of the dynamic load flow analysis done on the 30 bus network in section 4.2.2 had voltages at all buses within the acceptable limit as stipulated in DIN IEC 60038. The network was with closed disconnect switch and tap changer set at maximum. This network configuration was therefore adopted. Similar to the analysis with single node network, the voltage profiles and overall current from the utility was compared. All buses in subnetwork 1 where the REP-S are connected are characterised by residential load type while the buses in subnetwork 2 with REP-S are characterised by loads with a mixture of residential and commercial. The overall current flowing through bus Kn00 from the overlay network is observed.

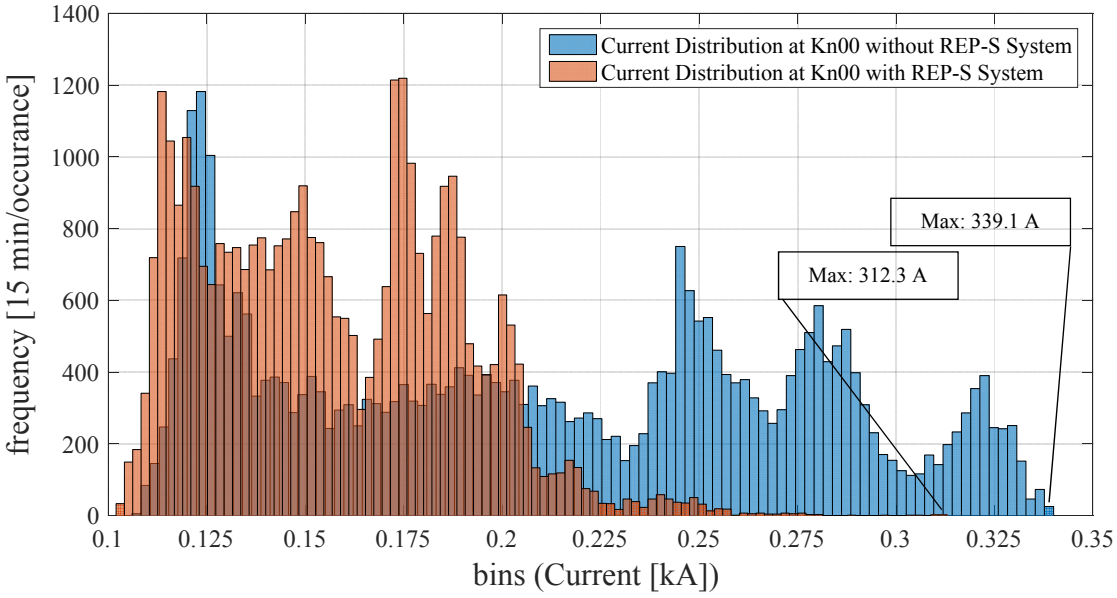

Figure 6-32: Current distribution at bus Kn00 of 30 bus network without and with renewable energy plant-storage system at 15 minutes data time stamps.

For the observation, a frequency distribution plot was made from current measurement made from the year simulation. There are two sets of measurement for 30 bus network without and with the installed REP-S systems. The two distribution plots are compared as shown in Figure 6-32. It can be seen that with introduction of REP-S system the frequency of current values more that about 274 A has reduced. The maximum current draw in both are 339.1 A and 313.3 A for network without RES-S and with REP-S systems. This is about 8 % reduction in instantaneous maximum current. The current drawn on the average are 209.7 A for network without REP-S and 157 A for network with REP-S. This means load demand up to about 52.7 A can be supported by the network. This value is on the primary (110 kV) side of both transformer 1 and 2. Referring this value to the 20 kV side implies about 290 A of extra demand can be supported.

6.3 Effect of REP-Storage System on Study Network

The resulting profiles obtained from the optimal sizing procedures in the previous section is used as the input data for modelled single node network shown in Figure 3-1(a). The RES-Storage system is integrated into study network at each bus as shown in Figure 5-1. That is,

for each Case, the resulting optimally sized RES-Storage system at respective buses are integrated. It is shown in the previous section that each sizing process apart from the optimal sizes also returns expected load profile if RES-Storage system with the resulting size was in the network for the period under consideration. Some of these resulting profiles are the blue plots in Figure 6-1, Figure 6-7, Figure 6-15, Figure 6-23 and Figure 6-28. Therefore the integration of RES-Storage system is by simply using this resulting new load profile which combines Load and RES-Storage systems. A simulation for load flow analysis is then conducted. The aim is to assess the impact of implementing RES – Storage systems with the respective resulting profiles on the study network. For this reason;

- The resulting current loading and flow through system components such as cable and transformers are observed and compared with base case situation where demand at buses were only supplied by utility.
- It is expected to find the extent to which the hosting capacity of the immediate network has been affected.
- The changes in voltage levels with and without the integration of RES – Storage systems that is aimed at supporting the hosting capacity of the network are observed and compared.

In Figure 6-33 is section of new load profile as seen by each bus in Figure 3-1(b) for a PV – Storage system for q = 1 and $k_{pr.fact}^{m}$ = 0.7. With reference to Figure 6-33, PV – Storage system with the said parameters could not support demand above the agreed level. Table C-3 to Table C- 6 in Appendix B shows average, minimum and maximum voltages and currents observed at bus Kn0_11 running single node model with new data load profiles as a result of both PV and Wind Storage systems for all values of q and $k_{pr.fact}^{m}$.

The voltages recorded in Table C- 3 and Table C- 4 for load bus Kn0_11 are observed to be similar to voltages observed for dynamic simulation of the same network whose results are shown in Table 4-6 and as box plot in Figure 4-11. The lowest voltage observed after running simulation with results obtained after optimal sizing is 0.93 pu similar to what is observed in Figure 4-11. A further comparison with voltages at buses Kn0_1 and Kn01 showed similar

trends of similarities.

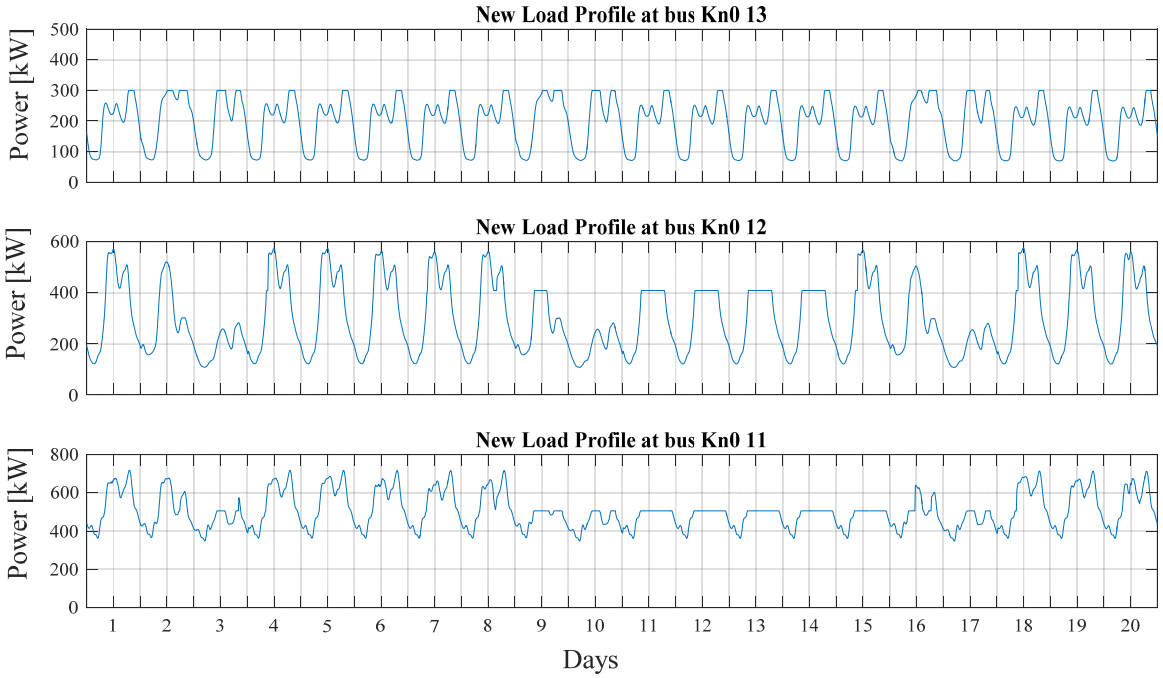

Figure 6-33: New load profile for simulation with single node model for PV – Storage system; q = 1 and $k^{m}_{pr.fact}$ = 0.7.

Voltage levels for integration of Wind or PV presented in Figure 4-13 and Table 4-7 show voltage levels than 1.1 pu. In both plots of Figure 4-13, outliers are observed. These values are due to intermittent sudden high infeed of RES into the network. It be clearly seen that though the integration of PV and Wind at the same rated value of the loads caused the voltages at these buses to reach upper tolerable voltage limit. Maximum hosting capacity based on voltage standard had been reached. However the results on Table C- 3 and Table C- 4 show voltages with acceptable limit even at q values greater than 1. The use of REP – Storage system help maintain voltage within acceptable limits.

In Table 6-22 are results from simulating the model in Figure 5-1 with resulting profiles from sizing RES – System under Case 1 with q = 1 and $k^{m}_{pr.fact}$ = 0.70. That is P^{ideal}_{Load} is predetermined before the sizing. The result return the optimal install capacity for REP and optimal maximum energy capacity of Storage system. On the other hand, Table 6-23 shows the results when simulation is done with resulting profile from result under Case 2. Table 6-24 shows the results of simulating with profile resulting from sizing under Case 3.

Voltages in the above mentioned tables are similar to those in Table 4-6 and within the voltage operating limit as per standard.

Table 6-22: Voltage and Currents at buses for both PV and Wind – Storage System for q = 1 and $k^{m}_{pr.fact}$ = 0.70

PV – Storage						
Bus ID	V_max [pu]	V_min [pu]	V_mean [pu]	I_max [A]	I_min [A]	I_mean [A]
Kn00	1.00	0.99	0.99	55.34	17.58	32.51
Kn01	1.00	0.99	0.99	55.69	17.90	32.83
Kn01_1	1.02	0.96	1.00	2642.7	842.97	1554.30
Kn01_11	1.01	0.94	0.98	1307.0	581.92	826.32
Kn01_12	1.02	0.92	0.98	1012.7	168.35	458.28
Kn01_13	1.02	0.95	0.99	580.65	86.98	274.55
Wind - Storage						
Bus ID	V_max [pu]	V_min [pu]	V_mean [pu]	I_max [A]	I_min [A]	I_mean [A]
Kn00	1.00	0.99	0.99	47.38	17.58	31.84
Kn01	1.00	0.99	0.99	47.71	17.90	32.16
Kn01_1	1.02	0.98	1.00	2262.8	842.97	1522.5
Kn01_11	1.01	0.96	0.98	896.3	581.92	806.15
Kn01_12	1.02	0.94	0.98	999.59	168.35	447.79
Kn01_13	1.02	0.97	1.00	580.65	86.98	274.55

From Table 4-3 and Table 4-4 the total current of all load demand and rated current of transformer are 2816.6 A and 2886.8 A respectively. Simulation of the single node model without any RES infeed produced a maximum instantaneous current of 2664.6 A that can be drawn from the network at bus Kn01_1 during the period of one year under consideration. Bus Kn01_1 is the common point from which all the three load branches off. This meant the network could support addition load of about 220 A. The average instantaneous current that is drawn for this period is 1667.8 A. With the introduction of RES at all buses, maximum instantaneous current values of 2627.4 A and 2664.5 A were recorded for PV and Wind Power integration. Their presence in the network reduces the current that is drawn from the network corresponding to average values of 1374.2 A and 1245.1 A for PV plant and Wind Power respectively. Comparing these average values to the former of 1667.8 A, reveals percentage reductions in current of 17.6 % for PV integration and 26.5 % for integration of Wind Power plants of similar power rating. By virtue of these reduction values, additional demands of 293 A and 442 A can be added at the lower voltage level of the network.

A look at in Table C- 3 and Table C- 4 in the Appendix shows a decrease in the average

current drawn from the network decreasing values of P_{Load}^{ideal} at the same 'q' value. This is mainly due to the fact that decreasing P_{Load}^{ideal} means decreasing dependency on the network which translate into decreasing current drawn. The average current is also observed to reduce as for increasing values of 'q' but from $k_{pr.fact}^{m} = 0.70$.

Table 6-23: Voltages and Currents at buses for both PV and Wind – Storage System: Case 2

PV - Storage						
Bus ID	V_max [pu]	V_min [pu]	V_mean [pu]	I_max [A]	I_min [A]	I_mean [A]
Kn00	1.00	0.99	0.99	55.02	17.58	27.37
Kn01	1.00	0.99	0.99	55.36	17.90	27.69
Kn01_1	1.02	0.96	1.01	2627.1	842.97	1309.4
Kn01_11	1.01	0.94	0.99	1307.4	581.92	753.68
Kn01_12	1.02	0.93	1.00	998.22	168.35	374.18
Kn01_13	1.02	0.95	1.00	673.79	86.98	186.10
Wind - Storage						
Bus ID	V_max [pu]	V_min [pu]	V_mean [pu]	I_max [A]	I_min [A]	I_mean [A]
Kn00	1.00	0.99	1.00	47.68	17.58	21.23
Kn01	1.00	0.99	0.99	48.02	17.90	21.55
Kn01_1	1.02	0.98	1.02	2277.7	842.97	1017.0
Kn01_11	1.01	0.95	1.00	1193.0	581.92	627.77
Kn01_12	1.02	0.94	1.01	892.78	168.35	268.07
Kn01_13	1.02	0.97	1.02	587.11	86.84	124.49

From Table 6-22 the maximum instantaneous and average current values of 2642.7 A and 2262.8 A and then 1554.3 A and 1522.5 A at bus Kn01_1. When compared with the base case, it is observed that the average current drawn from the network reduced by 113.5 A and 145.3 A for PV – Storage System and Wind – Storage System respectively. Similarly the maximum currents seen for the same bus in Table 6-23 and Table 6-24 indicated significant reduction in average current drawn from the utility. Under Case 2 where P_{Load}^{ideal} is also optimally sized, average current drawn from network reduce by 358.4 A (21.5 % of 1667.8 A) and 650.5 A (40 % of 1667.8) for PV – Storage System and Wind – Storage System respectively.

For Case 3, the total average current drawn by all three load at the point of common coupling are 1406.6 A for integrated PV – Storage and 1165.9 A for Wind – Storage system. The estimated reduction in average current compared with case is 261.2 A for PV and 501.9 for wind. Reduction in current drawn from the network due to integration of REP and

REP-Storage system implies the opportunity to add consumer up to the reduced quantity. Both RES and REP-Storage show reduction in current compared with base case.

Table 6-24: Voltage and Currents at buses for both PV and Wind – Storage System: Case 3

PV - Storage						
Bus ID	V_max [pu]	V_min [pu]	V_mean [pu]	I_max [A]	I_min [A]	I_mean [A]
Kn00	1.00	0.99	0.99	54.82	17.58	29.41
Kn01	1.00	0.99	0.99	55.16	17.90	29.73
Kn01_1	1.02	0.96	1.01	2617.7	842.97	1406.6
Kn01_11	1.01	0.94	0.99	1307.1	581.92	581.92
Kn01_12	1.02	0.92	0.99	1002.9	168.35	393.19
Kn01_13	1.02	0.95	1.00	673.79	86.98	255.15
Wind - Storage						
Bus ID	V_max [pu]	V_min [pu]	V_mean [pu]	I_max [A]	I_min [A]	I_mean [A]
Kn00	1.00	0.99	1.00	45.84	17.57	24.36
Kn01	1.00	0.99	0.99	46.18	17.89	24.68
Kn01_1	1.02	0.98	1.01	2189.9	842.55	1165.9
Kn01_11	1.01	0.95	1.00	1186.5	581.50	684.50
Kn01_12	1.02	0.94	1.00	892.80	168.35	320.05
Kn01_13	1.02	0.97	1.01	584.21	86.98	165.56

For instance the overall current observed at bus Kn00 is 34.39 A (Table 4-6), 28.73 A for Solar and 26.03 A for Wind (Table 4-7), 32.51 for base case and with the integration of Solar and wind respectively. Relatively more significant reduction in the current is observed to occur when P_{Load}^{ideal} is optimally sized under Case 2 and Case 3 and not predetermined under Case 1.The summary of average current through single node network for base case and all Case is seen in Table 6-25 and Figure 6-34. Case 2 returned highest reduction in current compared with Case 3. Under Case 2, the rated power of storage system is predefined at each bus while the energy storage capacity is not. The converse rated power is true for Case 3. The converse in that, rated power of storage is optimally sized likewise the energy storage capacity as seen in section 5.2.2. On the basis of current, the ability of the study network to add on more consumers have been improved by the introduction of REP-Storage systems. Since the single node network forms part of the bigger 30 bus network, it follows that substituting the lump load seen in 30 bus network with replicas of the single node network will result in similar proportions in reduction currents flowing from overlay network. This is seen in the result of analysis made in section 6.2 where demand up to about 52.7 amperes (110 kV side) can be supported by the network.

Table 6-25: Summary of Current at buses under all Cases for Solar and Wind

Bus ID	Current_mean [A]						
		With Solar			With Wind		
Bus ID	Base Case	Cond. Set 1	Cond. Set 2	Cond. Set 3	Cond. Set 1	Cond. Set 2	Cond. Set 3
Kn00	34.89	32.51	27.37	29.41	31.84	21.23	24.36
Kn01	35.21	32.83	27.69	29.73	32.16	21.55	24.68
Kn01_1	1667.8	1554.30	1309.4	1406.6	1522.5	1017.0	1165.9
Kn01_11	904.61	826.32	753.68	581.92	806.15	627.77	684.50
Kn01_12	488.69	458.28	374.18	393.19	447.79	268.07	320.05
Kn01_13	280.91	274.55	186.10	255.15	274.55	124.49	165.56

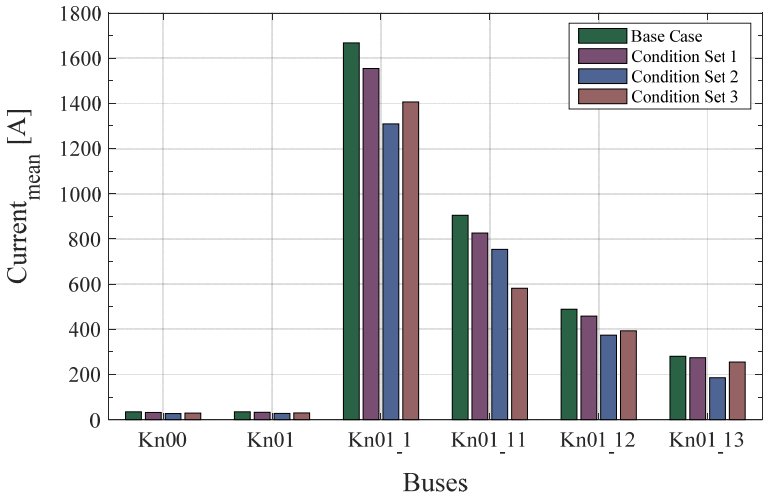

a.

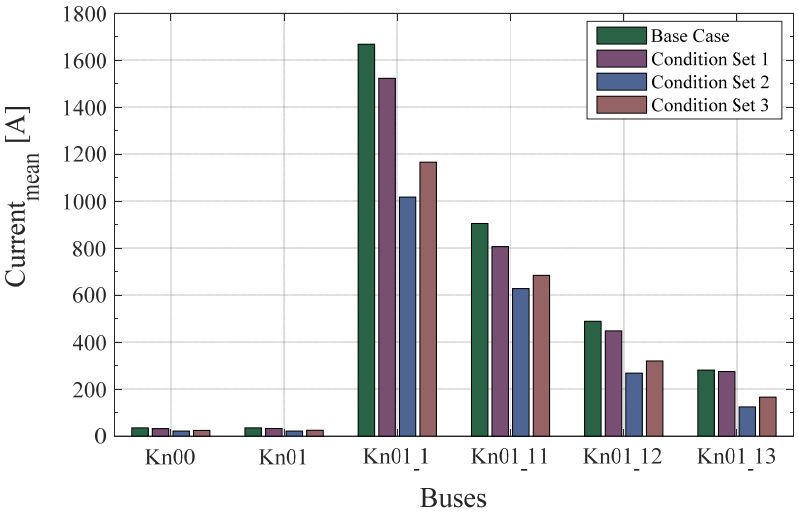

b.

Figure 6-34: Current levels at buses with RES-Storage system for all Cases; a. PV-Storage system, b. Wind-Storage system

The different loads exhibited different characteristics for REP-Storage systems and storage

system as whole. This can be seen in the extra plots provided in the Appendix. This implies the need for location specific analysis and sizing of REP-Storage system. This location should have its unique consumption pattern as well as weather data patterns.

Based on the available data and analysis made, most results of PV-Systems return profiles where some days of the beginning and end of the period under consideration were not covered by the RES-Storage system but by the network. This is observed with mainly with profile for PV-Storage systems. Based on this observed trend, utilities can plan supply to cater for extra demand that may arise at the beginning end of the year. Special tariffs plans could be made out of.

7. Conclusion and Future Work

In this work, a concept of integrating energy from renewable energy plants together with storage system (REP-Storage System) with the aim of supporting electrical networks at the low and medium voltage level is introduced. This is in contrasts with common practice where RES are integrated with the aim of producing as much energy as possible. The success and extent of supporting electrical network is identified to be based on the ability to achieve optimal size of RES and Storage system as a unit.

To start with, the work acknowledged the trends in development of RES industry with financial support schemes, governmental policies. It also acknowledged the developments in storage technologies and data acquisition and storage in the electrical energy distribution industry. RES integration will continue to increase. The levels of fluctuations, intermittencies, loss of energy due to under or over production and priority to keep the network safe and in operation will be expected to increase with the coming online of more energy sources from RE. Emphasis are laid on energy from wind through wind turbines and solar through PV as the main causes of the above mentioned problem as they are dominant in the electrical network. Both were estimated to contribute about 92 % of total installed RES power plants in the 50 Hertz transmission control region. And numbering in total of almost 130000 power plant. The intermittent nature of RES though not desired still contains resources that can be utilized hence the need of a storage system. The energy potential in wind and solar is estimated from some historic data obtained to buttress this point. The different types of storage technologies in existence with varying operating characteristics, telecommunication, advanced control technology and smart metering points to the fact that some if not all the technologies to implement such balancing systems exist. These problems could be solved with storage system which as a basic knowledge could store energy for later use immediate or later use. Future installations of RES especially those in the low voltages level could be installed with Storage systems from the onset but optimally sized with the aim of supporting the hosting network.

The idea of having a REP-Storage system supporting the network starts from the idea that an agreed level of demand is always made available anytime. This means consumption only switch to the RES-Storage system if and only if consumption exceeds the agreed level. And only after the RES-Storage system could not fully cover the extra consumption should there be additional supply from the network. The other variation of this ideas sort to size both the REP-Storage system and level of demand that the network should at all time provide.

In Chapter 5 the criteria and decision steps and option of this idea is described. An objective function to with scripts created from these steps in MATLAB are used runs both assertions of having a predefined agreed level of demand that should be met by utility, or allowing sizing process to find this level together with finding the size of RES-Storage system and optimally sizing storage rated power. For every predefined reference demand that the utility should supply, the solution of the sizing process returned values of the size of RES plant and storage system that could support as much excess demand as possible for the period of one year. Different sets of conditions gave different sets of answer as expected. Infeed from Wind most often than not returned solution that could support excess load for the period. Sizing with PV plant data only returned solution that had storage system not completely empty at the end of the year. This stored energy could be carried on in the following year. The sizing process returned values that were satisfactory. This observation attest the fact that better results will be obtained with more historic data.

Profiles that were generated as expected load demand pattern when used for simulation of modified single node network presented Figure 5-1 gave satisfactory results. It was observed that bus voltages remained with the stipulated tolerance level when simulation of network in Figure 5-1 was run with selected resulting new load profiles of optimal sizing process. Voltage levels were above the upper limit at some buses when simulations were conducted with PV or Wind data together with respective bus load profile. This was an indication that the REP-Storage system did not course and disturbance to that the network. Average currents at buses were observed to be lower when compared to the base case. The highest percentage reduction of average observed was 40 % of base current. This reduction in value is an opportunity to add more consumers to this network.

The sizing under Case 2 and Case 3 returned relatively low values of P_{Load}^{ideal} than

predetermined under Case 1. Case 2 also returned the highest percentage reduction in average current compare with simulation with profiles resulting from predetermined P_{Load}^{ideal}. However their respective resulting load profile and energy profile shows inadequacy in covering excess demand over the period. Extension of this work will be to improve upon the algorithm for sizing in other get more coverage of extra load demand. The optimization function could be extended to include cost evaluation aspect of the sizing. This work could also be extended to further expand the function to include more parameters.

The sizing steps did not consider properties such charge and discharge rates of storage. This work can therefore be extended in other to include characteristics of specific storage types in the sizing process. That is, the constraints variables of the objective function will be increased. Also analysis with data spanning more years should be considered. The effects of trends that are repeated or changing consumption patterns could play major part in sizing. This will make results more reflective of the characteristics of bus under consideration.

The time stamp used in this was standard 15 minutes time interval. The shorter the time interval, the more realistic the data is. Actual measured load data should be used instead of standard load profiles. This analysis and simulation should be conducted with data spanning longer than a year.

Appendix

A. Parameters of Electrical Networks

The table presented below contains the length and current capacities of the cables used in the model of CIGRE 30 bus network seen in Figure 3-1(a).As can be observed, the current loading on the cables are as low as 6 % (Kn10 to Kn11) and as high as about 95 % (Kn01 to Kn02). The low loading

Table A-1: Length of cables in network

	From(Bus)	To(Bus)	Length [km]	Loading [A]	Current Carrying Capacity [A]	Percentage Loading [%]
Subnetwork 1						
	Kn01	Kn02	2.41	1519	1595	95.24
	Kn02	Kn03	2.41	1618	1710	94.62
	Kn03	Kn04	2.41	1437	1595	90.09
	Kn04	Kn05	0.303	705	855	82.46
	Kn04	Kn14	0.487	466	570	81.75
	Kn05	Kn06	0.303	673	855	78.71
	Kn06	Kn07	0.303	357	570	62.63
	Kn06	Kn22	0.325	166	285	58.25
	Kn07	Kn08	0.28	279	570	48.95
	Kn08	Kn09	0.28	248	285	87.02
	Kn09	Kn10	0.28	130	285	45.61
	Kn10	Kn11	0.49	19	285	6.67
	Kn11	Kn12	0.49	44	285	15.44
	Kn13	Kn12	0.236	62	285	21.75
	Kn14	Kn15	0.328	359	570	62.98
	Kn15	Kn16	0.385	235	285	82.46
	Kn16	Kn17	0.385	214	285	75.09
	Kn17	Kn13	1.667	83	285	29.12
	Kn17	Kn18	0.16	102	285	35.79
	Kn19	Kn18	0.16	83	285	29.12
	Kn20	Kn19	0.325	32	285	11.23
	Kn21	Kn20	0.325	52	285	18.25
	Kn22	Kn21	0.325	147	285	51.58
Subnetwork 2						
	Kn23	Kn24	3.916	1519	1595	95.24
	Kn24	Kn25	0.487	1021	1276	80.02
	Kn25	Kn26	0.487	846	957	88.40
	Kn26	Kn27	0.395	674	957	70.43
	Kn27	Kn28	0.395	528	638	82.76
	Kn28	Kn29	2.20	434	638	68.03
Disconnect switch - On	Kn29	Kn17	2.00	292	319	91.54

Table A-2 : Contribution of H0, G0, G3 and L0 to total load demand in network

	Node	Load Types	Active Power per Node out of 60 MW	H0[Norm]	H0[MW]	G3[Norm]	G3[MW]	G0[Norm]	G0[MW]	L0[Norm]	L0[MW]
Subnetwork 1	Kn01	G3	3.04			0.4	3.04				
	Kn03	H0	0.51	0.3	0.51						
	Kn04	H0 + G0	2.77	0.3	1.66			0.2	1.11		
	Kn05	H0	0.63	0.3	0.63						
	Kn06	H0 + G3	3.61	0.3	1.55	0.4	2.07				
	Kn07	H0 + G3	1.92	0.3	0.82	0.4	1.10				
	Kn08	H0	0.74	0.3	0.74						
	Kn09	H0 + G0	2.93	0.3	1.76			0.2	1.17		
	Kn10	H0 + G3	3.73	0.3	1.60	0.4	2.13				
	Kn11	H0	0.63	0.3	0.63						
	Kn12	H0	0.46	0.3	0.46						
	Kn13	H0	0.51	0.3	0.51						
	Kn14	H0 + G3	2.57	0.3	1.10	0.4	1.47				
	Kn15	H0 + G0	3.06	0.3	1.84			0.2	1.23		
	Kn16	H0	0.51	0.3	0.51						
	Kn17	H0	0.71	0.3	0.71						
	Kn18	H0	0.47	0.3	0.47						
	Kn19	H0 + G0	2.88	0.3	1.73			0.2	1.15		
	Kn20	H0	0.47	0.3	0.49						
	Kn21	H0 + G3	2.36	0.3	1.01	0.4	1.35				
	Kn22	H0	0.48	0.3	0.48						
Subnetwork 2	Kn23	G3	3.50			0.4	3.50				
	Kn24	H0 + G0 + L0	3.97	0.3	2.38			0.2	1.59	0.1	0.79
	Kn25	H0 + G3	4.13	0.3	1.77	0.4	2.36				
	Kn26	H0 + L0	4.14	0.3	3.10					0.1	1.03
	Kn27	H0 + G0	3.58	0.3	2.15			0.2	1.43		
	Kn28	H0 + G0	2.31	0.3	1.38			0.2	0.92		
	Kn29	L0 + G0	3.38					0.2	2.25	0.1	1.13
	Total [MW]				**29.99**		**17.02**		**10.85**		**2.96**
	Percentage				**49.32**		**27.98**		**17.84**		**4.86**

In Table A-2, the contribution of the four load types selected for the thesis ae shown. The percentage contribution of each load type are about 49 %(H0), 28 %(G3), 17 %(G0) and 5 %(L0). Table A-3 shows the maximum installed capacity and power factor of load connected at respective buses in Figure 3-1(a).

Table A-3: Maximum installed capacity of network loads of Figure 3-1with corresponding power factors

Bus/Node Numbers	Active Power Demand (Max)	Power factor
01	3,04	0,85
03	0,51	0,95
04	2,77	0,95
05	0,63	0,90
06	3,61	0,95
07	1,92	0,95
08	0,74	0,95
09	2,93	0,95
10	3,73	0,95
11	0,63	0,95
12	0,46	0,95
13	0,51	0,95
14	2,57	0,95
15	3,06	0,95
16	0,51	0,95
17	0,71	0,95
18	0,47	0,95
19	2,88	0,95
20	0,49	0,95
21	2,36	0,95
22	0,48	0,95
23	3,50	0,85
24	3,97	0,95
25	4,13	0,95
26	4,14	0,95
27	3,58	0,95
28	2,31	0,95
29	3,38	0,95

B. Voltage profiles for 30 bus network under base case scenario

The figures in this section show the voltages at all buses of the adopted CIGRE 30 network for load flow conducted under base case condition at 25 %, 50 %, 75 % and 100 % load demand.

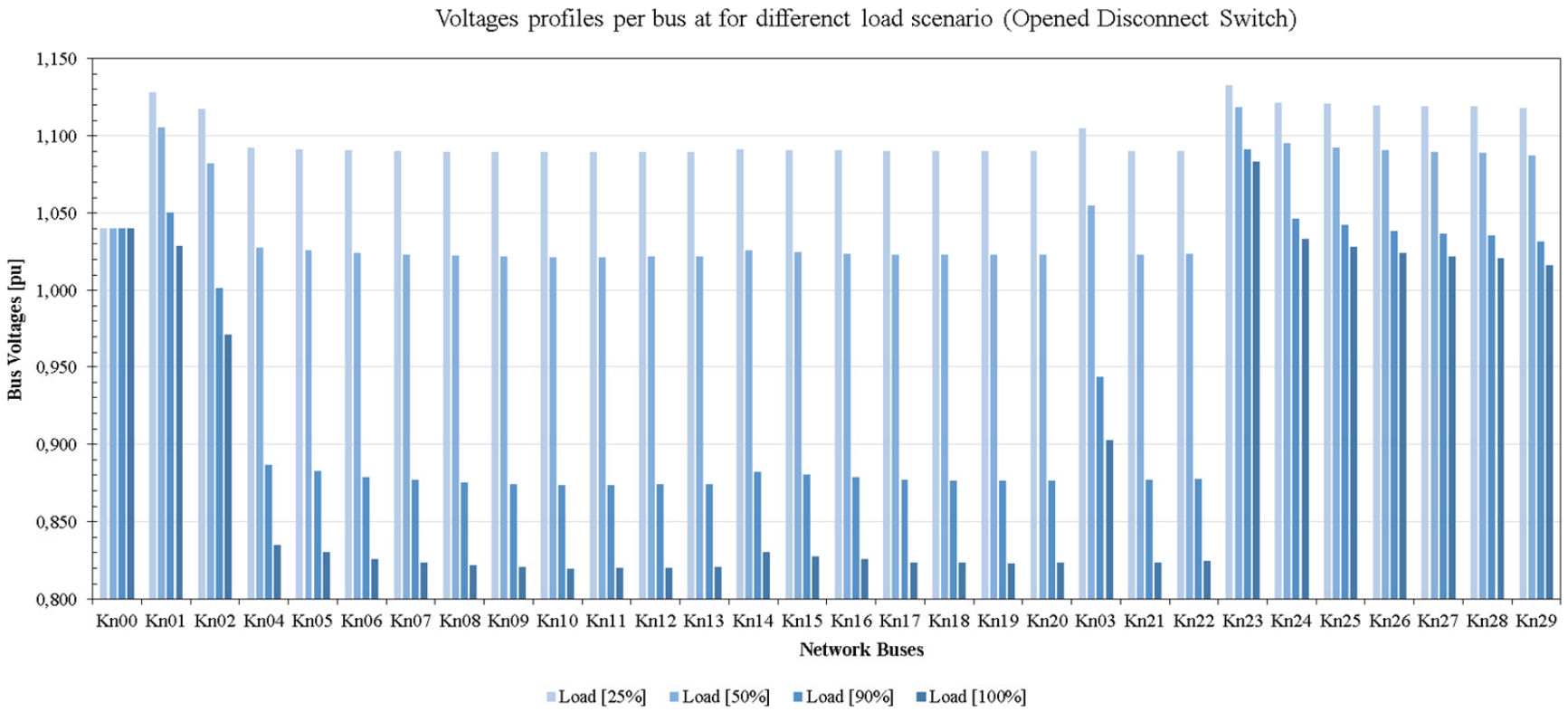

Figure B- 1: Voltage profile of buses under open disconnect switch condition

Plot with opened disconnect switch, is observed to have voltage at some buses below the stipulated allowed level. The converse is true for plot with closed disconnect switch. This is due to the redistribution of current true alternative less limiting paths.

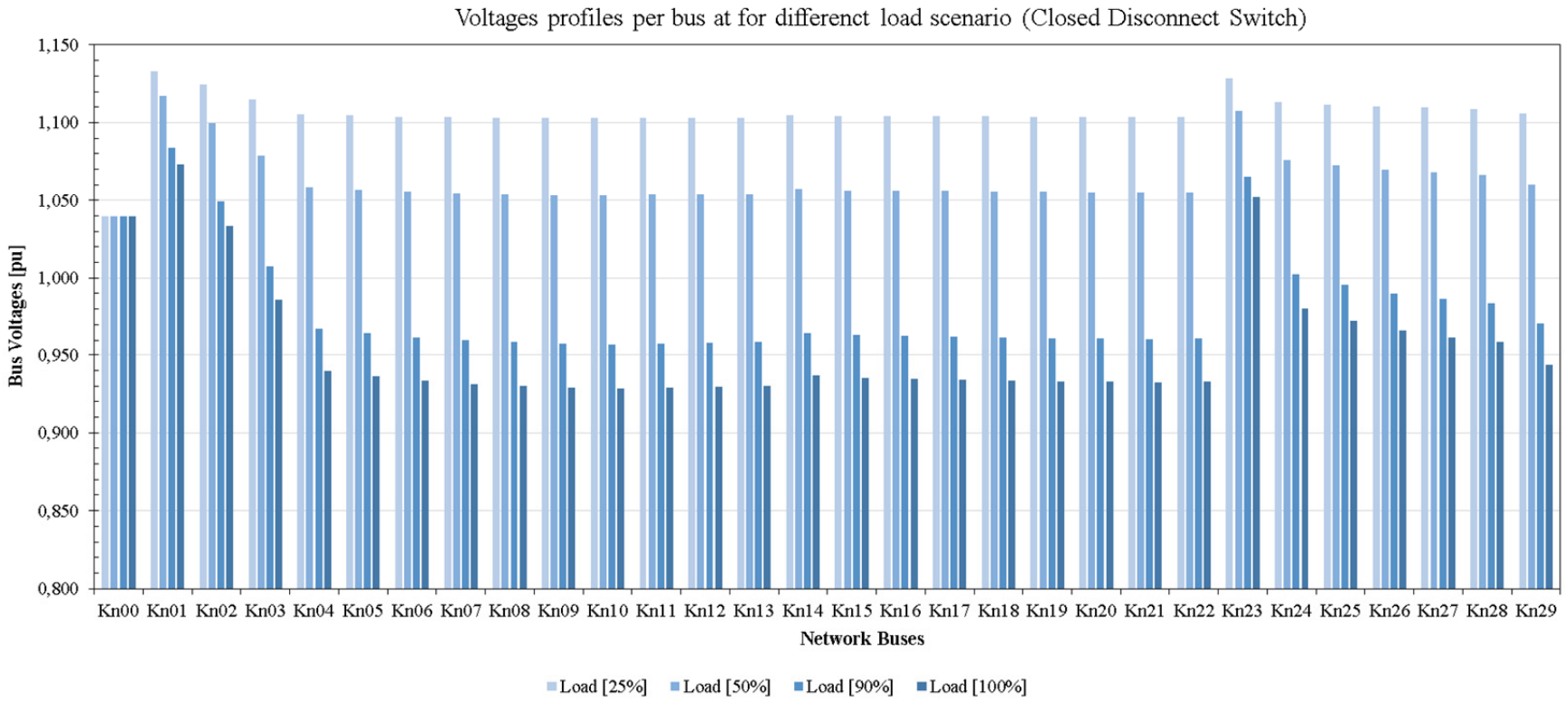

Figure B- 2: Voltage profile of buses under Closed disconnect switch condition

C. Results of REP-Storage System Capacity Sizing

1. Energy Plots for PV Storage System at bus Kn0_11

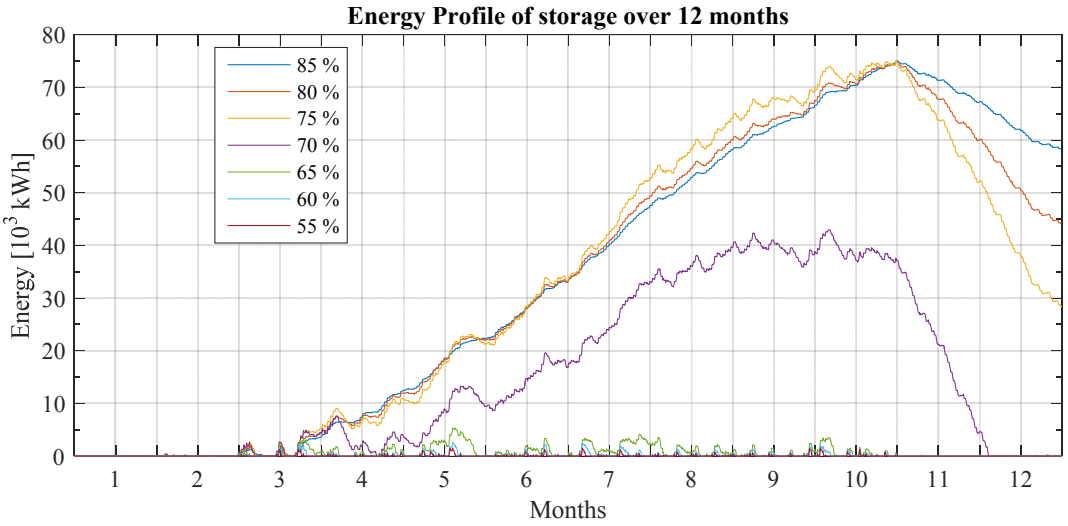

Figure C- 1: Energy profile for PV - Storage system at different desire reference demand for q = 0.5 at bus Kn0_11.

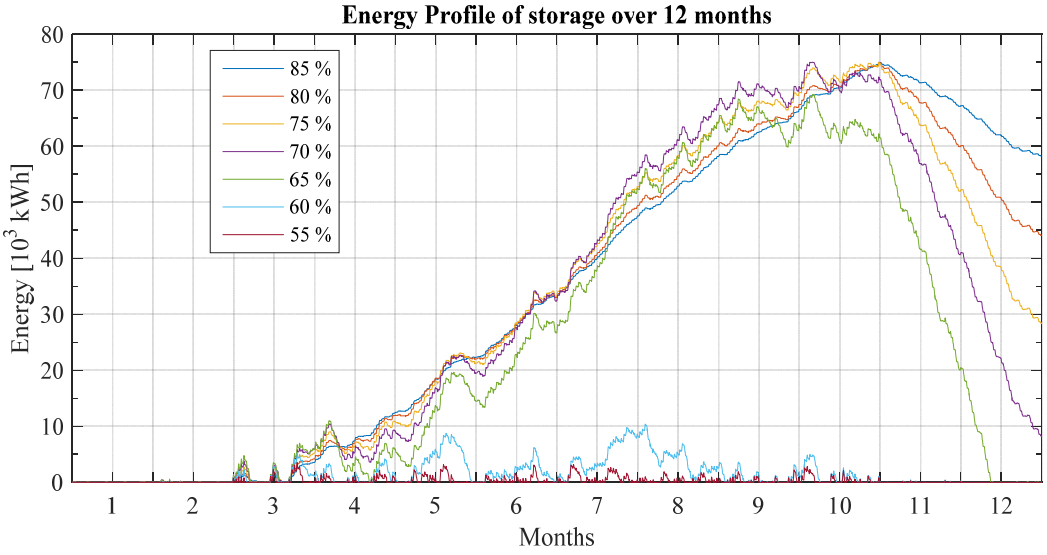

Figure C- 2:Energy profile for PV - Storage system at different desire reference demand for q = 0.75 at Kn0_11

The percentage value markings are equivalent to the factor $k^{m}_{pr.fact}$. That is; $k^{m}_{pr.fact}$ = {0.55, 0.60, 0.65 … 0.85} implies $k^{m}_{pr.fact}$ = {55%, 60%, 65% … 85%}. In effect, the percentages are reflecting the reference demand at specific buses according to $P^{ideal}_{Load} = k^{m}_{pr.fact}.P^{rated}_{Load}$. At Kn0_11 therefore, the reference demands are {397.38 (55%), 433.50(60%), 469.63(65%) …

614.13(85%)} since $P_{Load}^{rated} = 722.5$ kW.

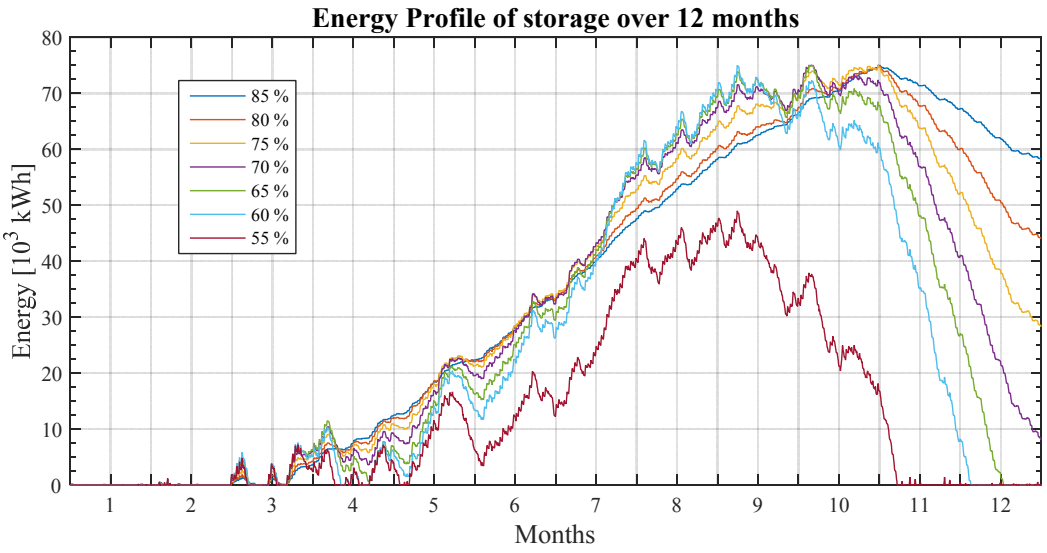

Figure C- 3:Energy profile for PV - Storage system at different desire maximum demand for q=1.25 at Kn0_11

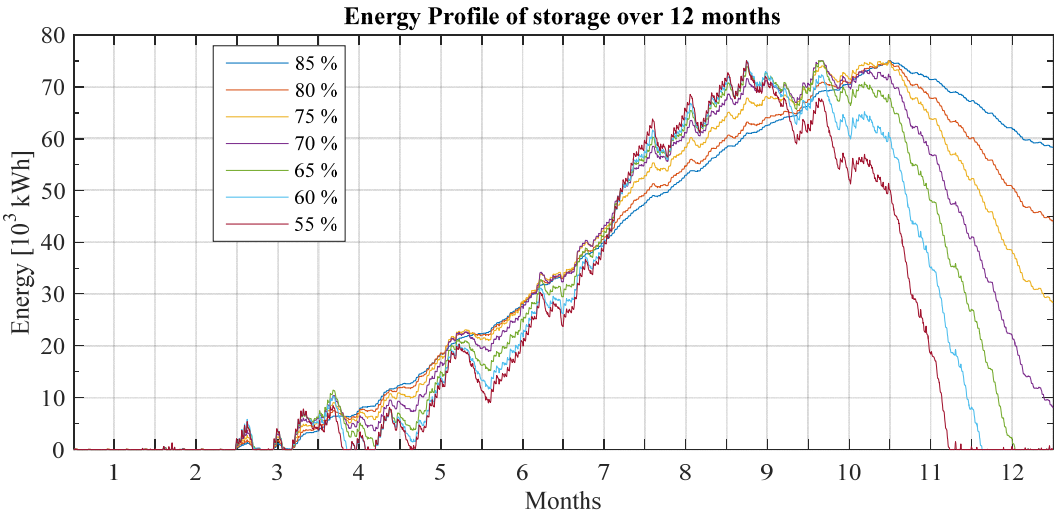

Figure C- 4: Energy profile for PV - Storage system at different desire maximum demand for q = 1.5 at bus Kn0_11.

2. Energy Plots for Wind Storage System at bus Kn0_11

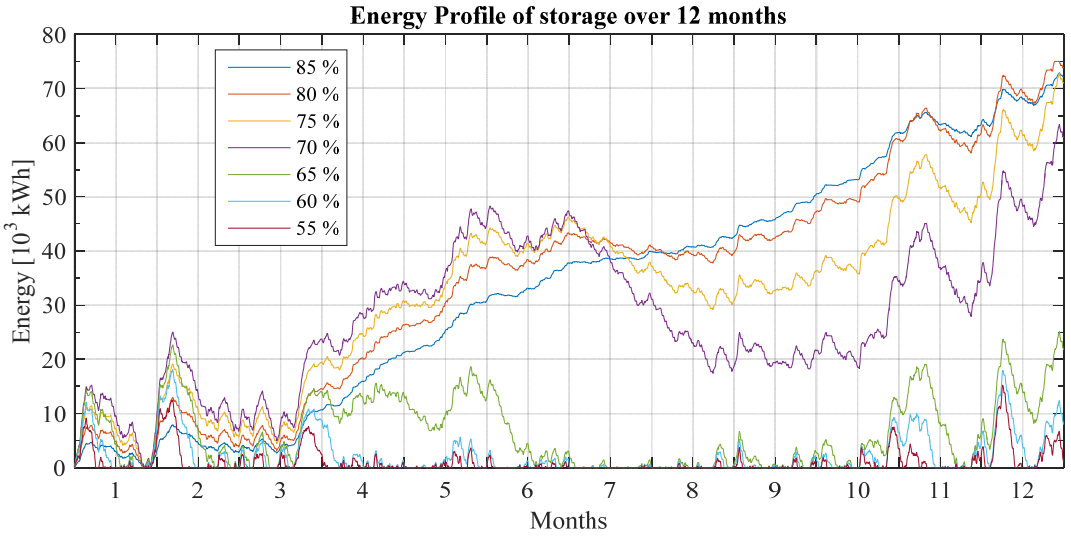

Figure C- 5 : Energy profile for Wind - Storage system at different desire maximum demand for q = 0.5 at bus Kn0_11.

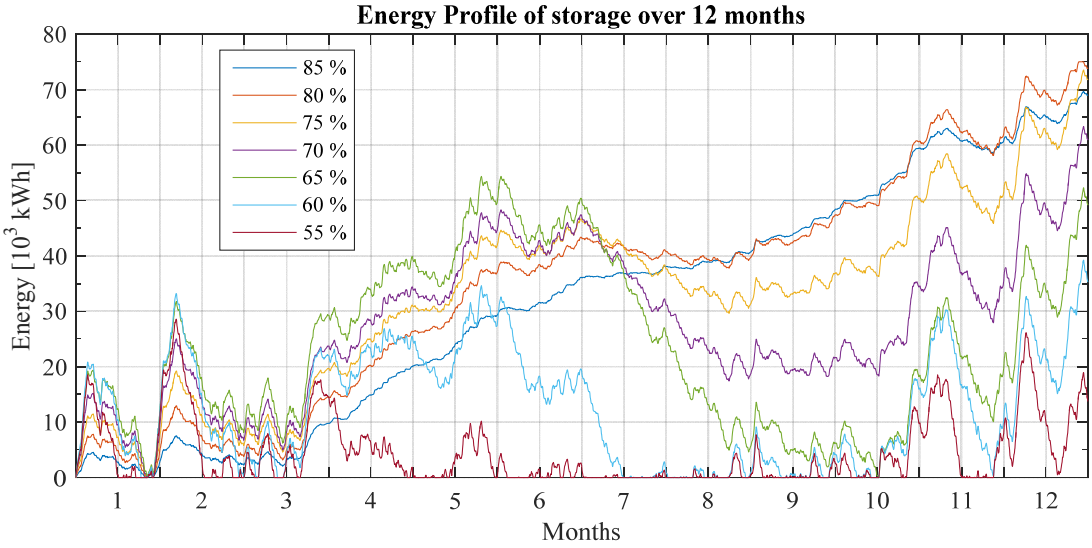

Figure C- 6: Energy profile for Wind - Storage system at different desire maximum demand for q = 0.75 at Kn0_11

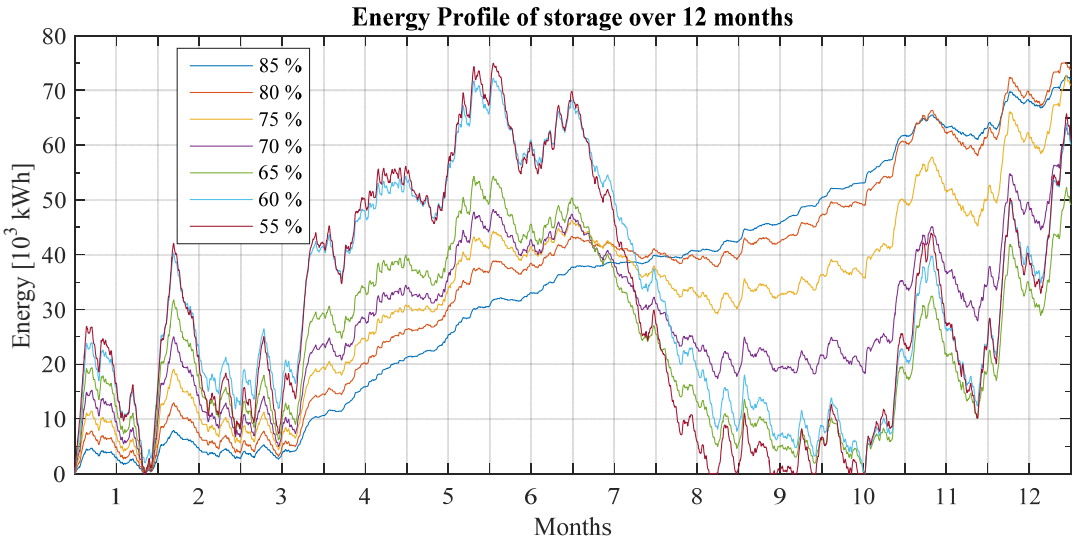

Figure C- 7: Energy profile for Wind - Storage system at different desire maximum demand for q = 1.25 at Kn0_11

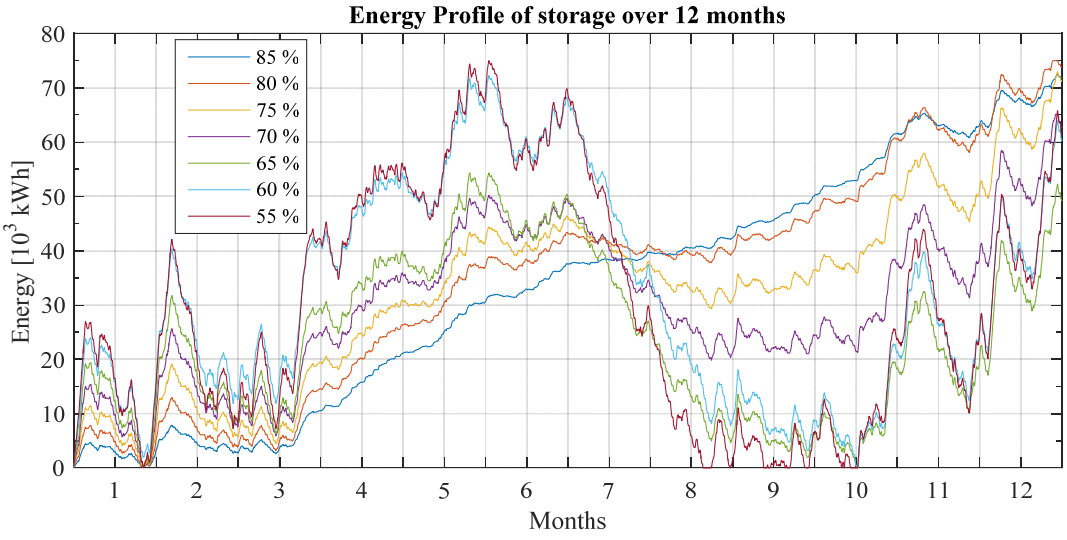

Figure C- 8: Energy profile for Wind - Storage system at different desire maximum demand for q = 1.5 at bus Kn0_11.

3. Energy Plots for PV Storage System at bus Kn0_12

At Kn0_12 therefore, the reference demands are {321.75 (55%), 351.00(60%), 380.25(65%) … 497.25(85%)} since P_{Load}^{rated} = 585 kW.

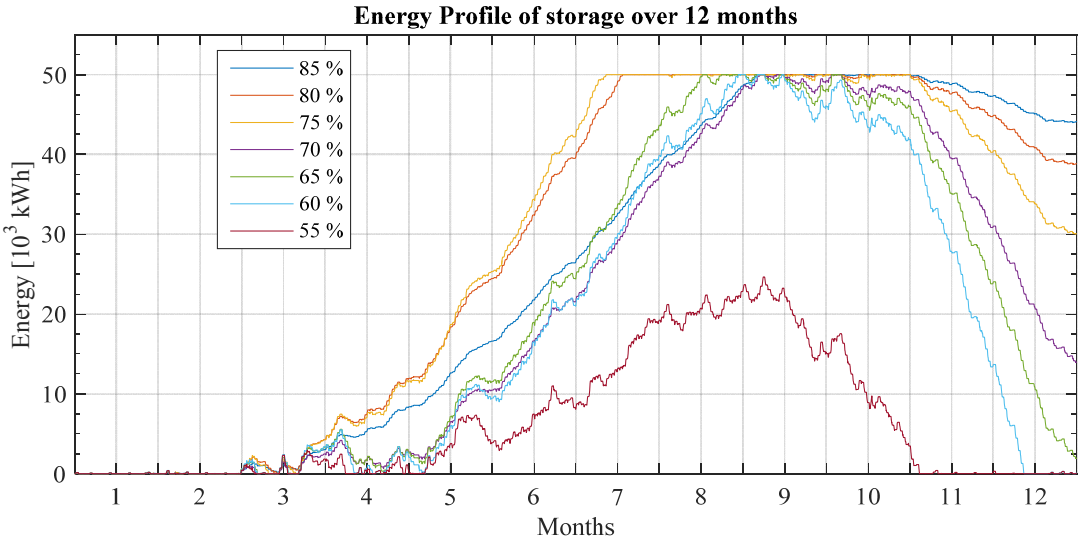

Figure C- 9: Energy profile for PV - Storage system at different desire maximum demand for q = 0.5 at bus Kn0_12

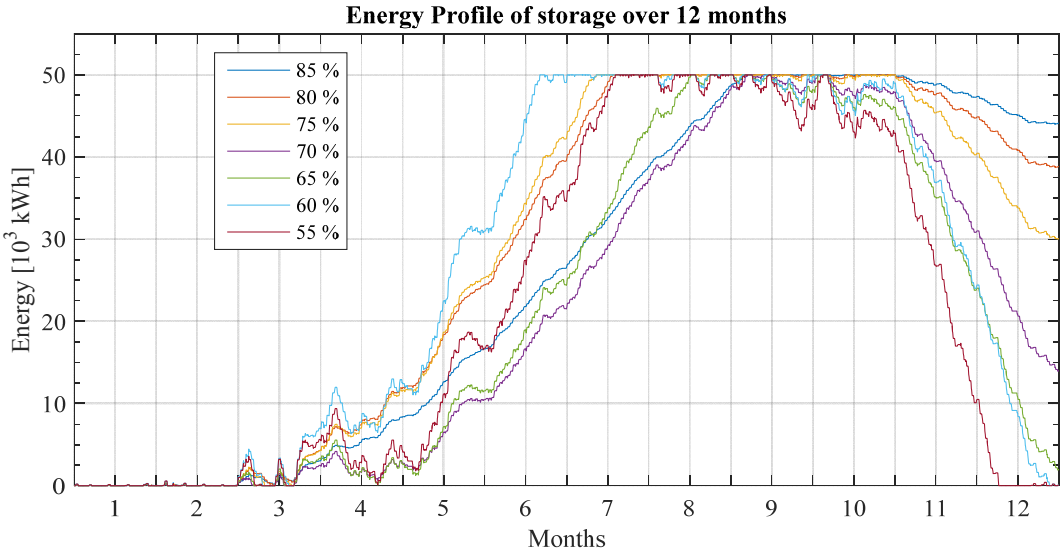

Figure C- 10: Energy profile for PV - Storage system at different desire maximum demand for q = 0.75 at Kn0_12

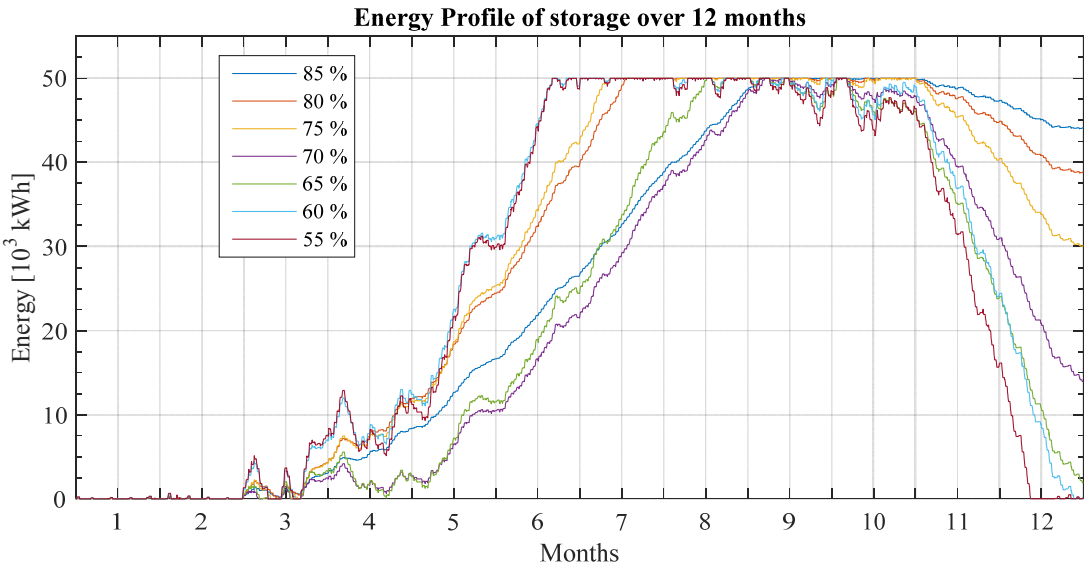

Figure C- 11: Energy profile for PV - Storage system at different desire maximum demand for q = 1.25 at Kn0_12

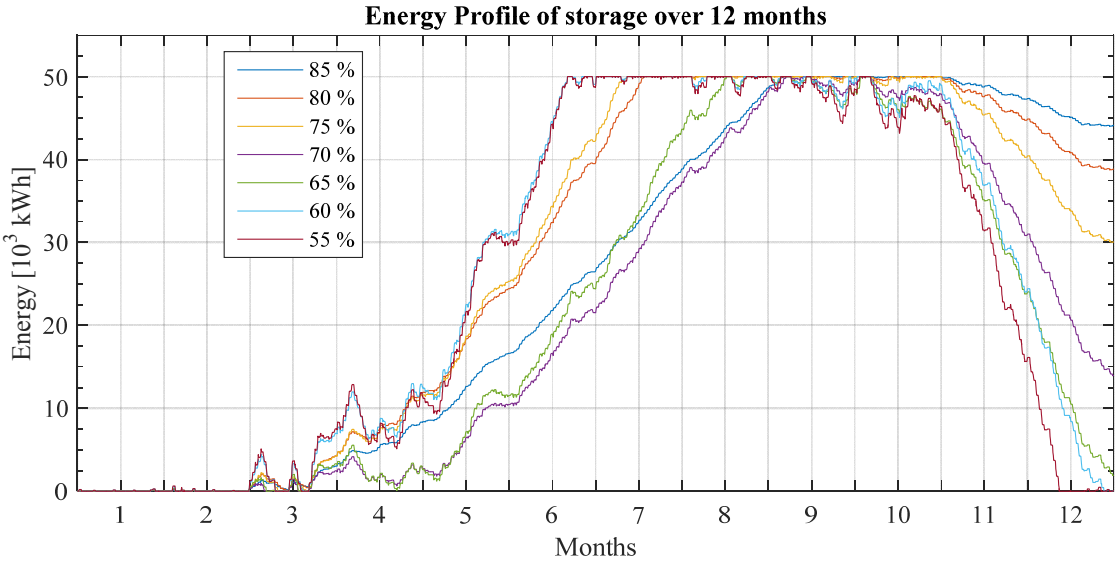

Figure C- 12: Energy profile for PV - Storage system at different desire maximum demand for q = 1.5 at bus Kn0_12

4. Energy Plots for Wind Storage System at bus Kn0_12

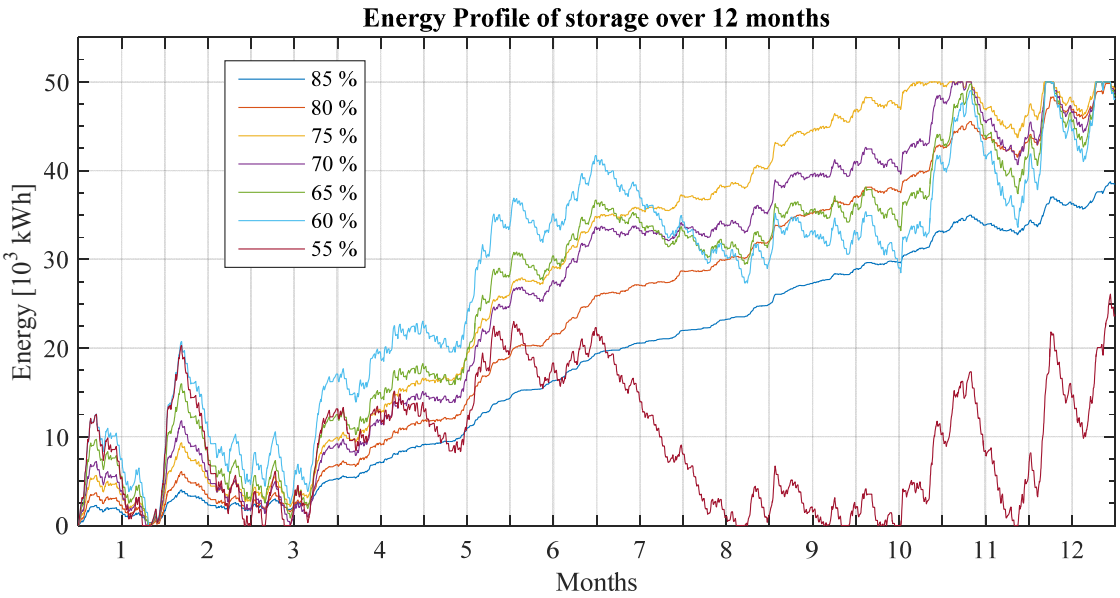

Figure C- 13: Energy profile for Wind - Storage system at different desire maximum demand for q = 0.5 at bus Kn0_12

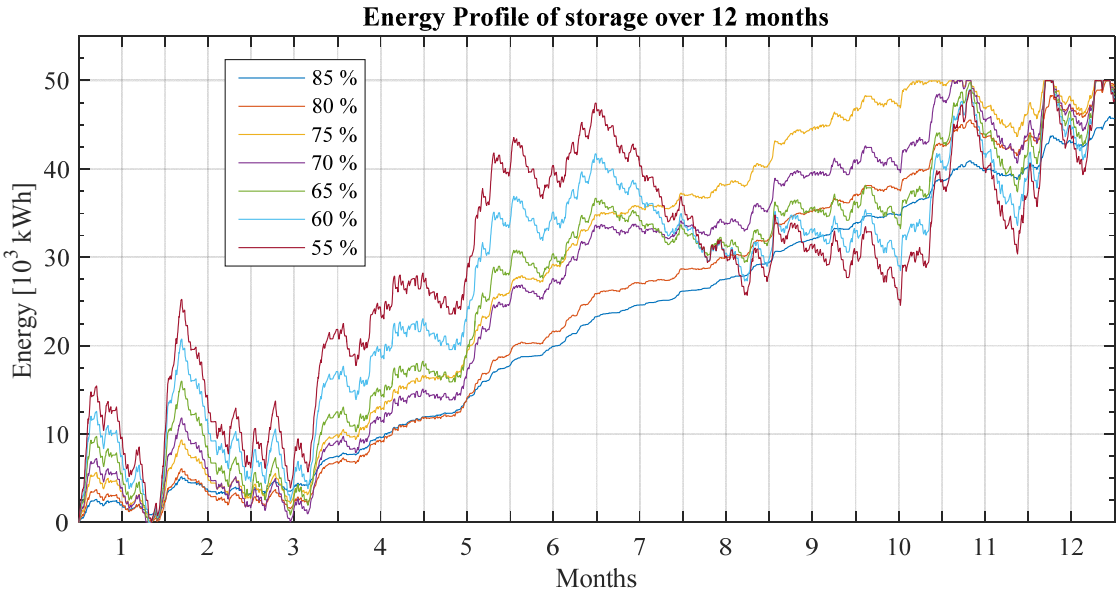

Figure C- 14: Energy profile for Wind - Storage system at different desire maximum demand for q = 0.75 at Kn0_12

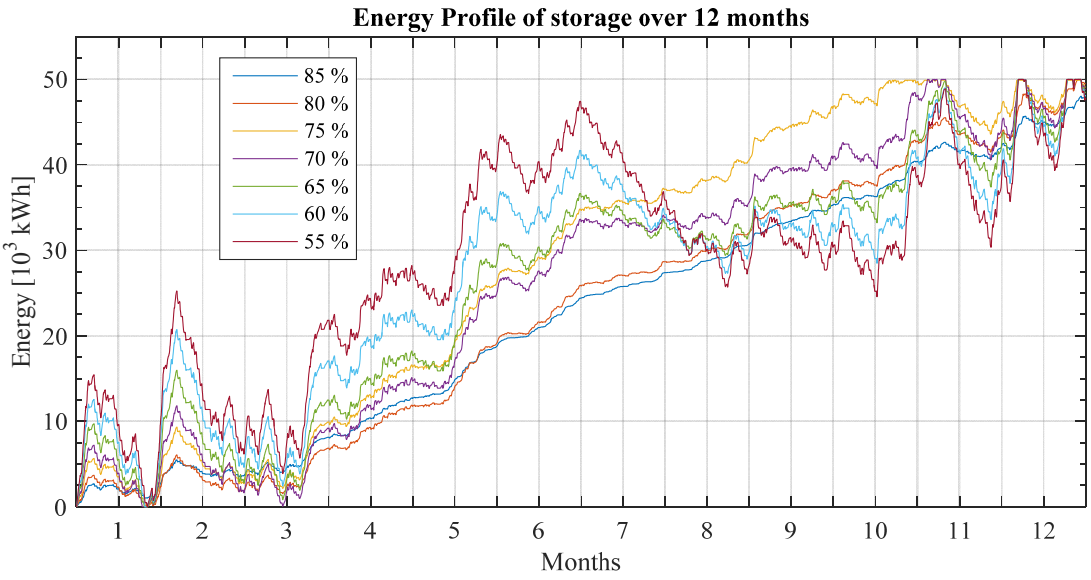

Figure C- 15: Energy profile for Wind - Storage system at different desire maximum demand for q = 1.25 at Kn0_12

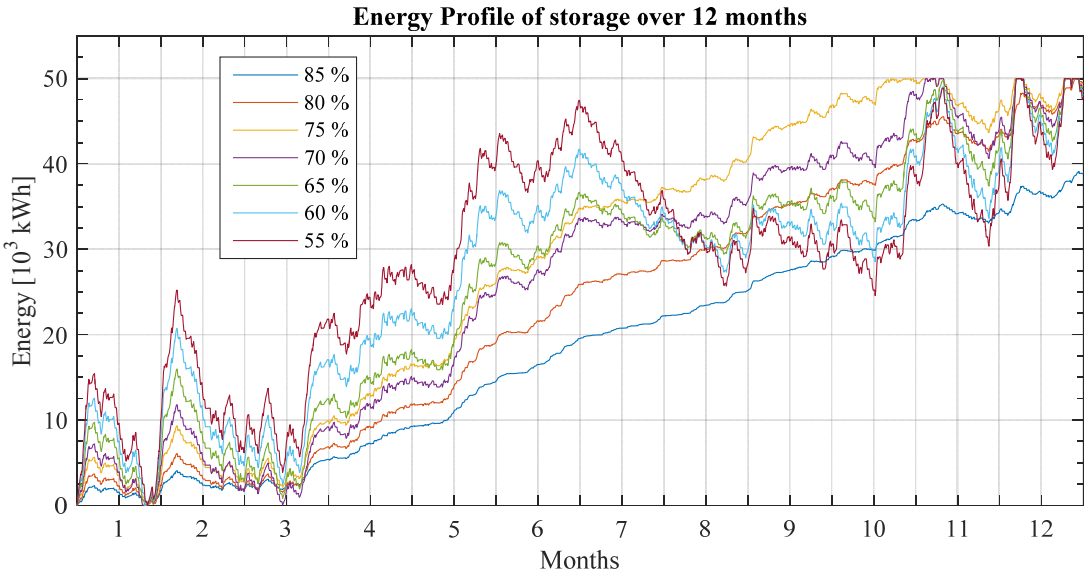

Figure C- 16: Energy profile for Wind - Storage system at different desire maximum demand for q = 1.5 at bus Kn0_12

5. Energy Plots for PV - Storage System at bus Kn0_13

At Kn0_13 therefore, the reference demands are {235.13 (55%), 256.50(60%), 277.88(65%) … 363.38(85%)} since according to $P_{Load}^{rated} = 427.5$ kW.

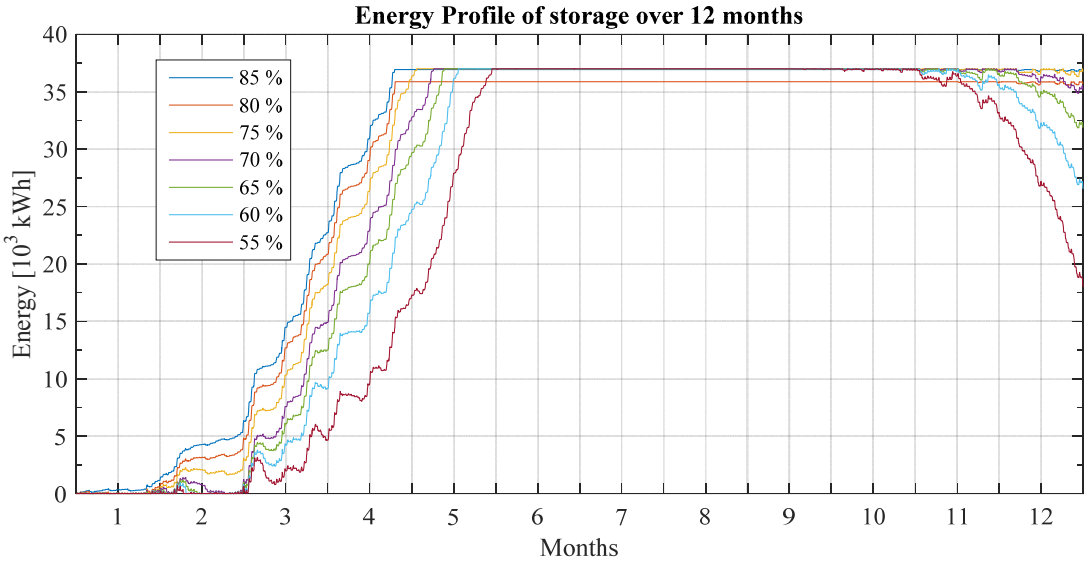

Figure C- 17: Energy profile for PV - Storage system at different desire maximum demand for q = 0.5 at bus Kn0_13

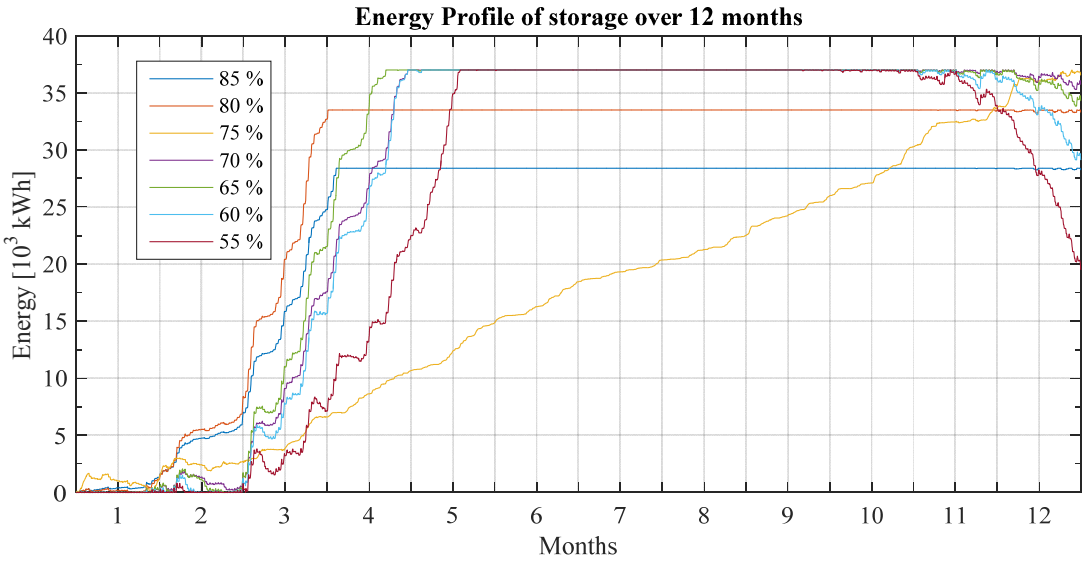

Figure C- 18: Energy profile for PV - Storage system at different desire maximum demand for q = 0.75 at bus Kn0_13

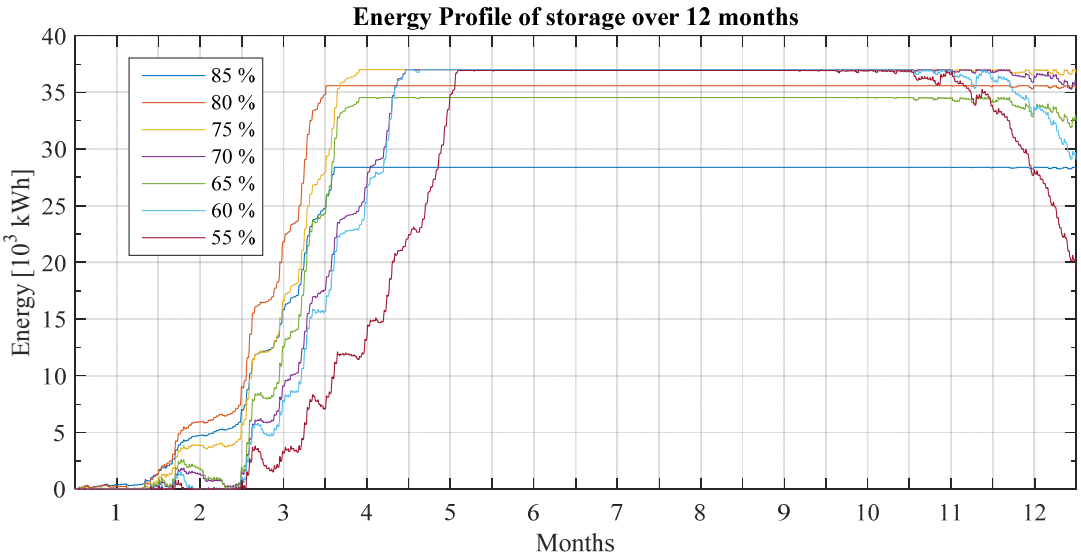

Figure C- 19: Energy profile for PV - Storage system at different desire maximum demand for q = 1.25 at bus Kn0_13

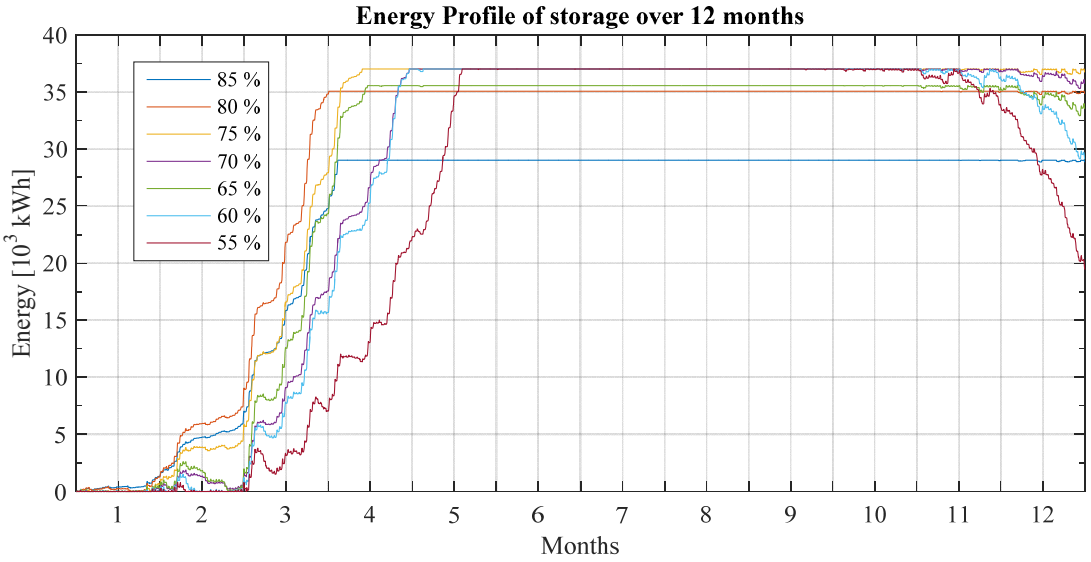

Figure C- 20: Energy profile for PV - Storage system at different desire maximum demand for q = 1.5 bus at Kn0_13

6. Energy Plots for PWind - Storage System at bus Kn0_13

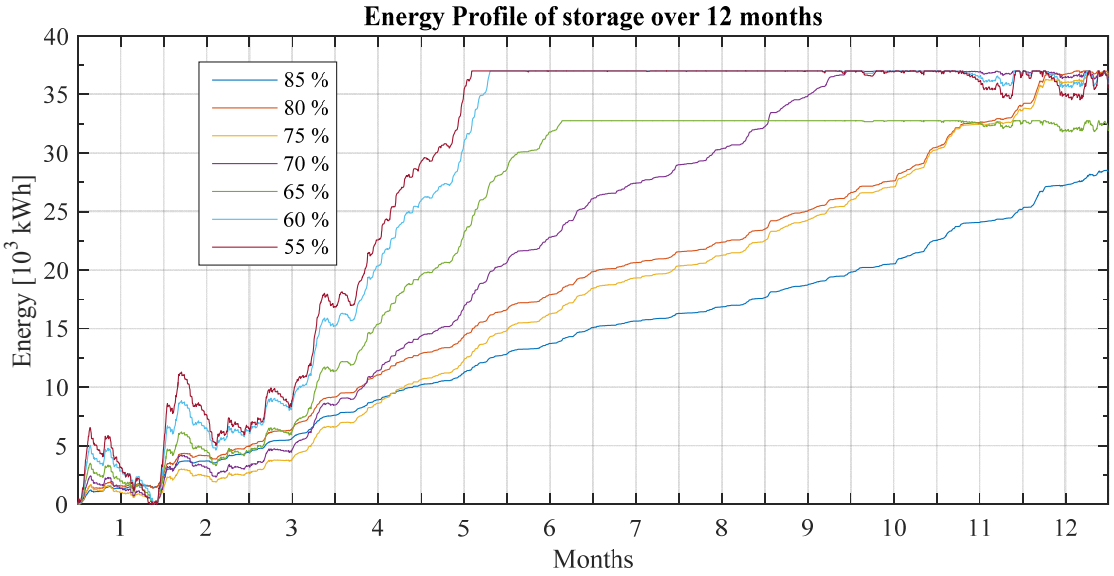

Figure C- 21: Energy profile for Wind - Storage system at different desire maximum demand for q = 0.5 bus at Kn0_13

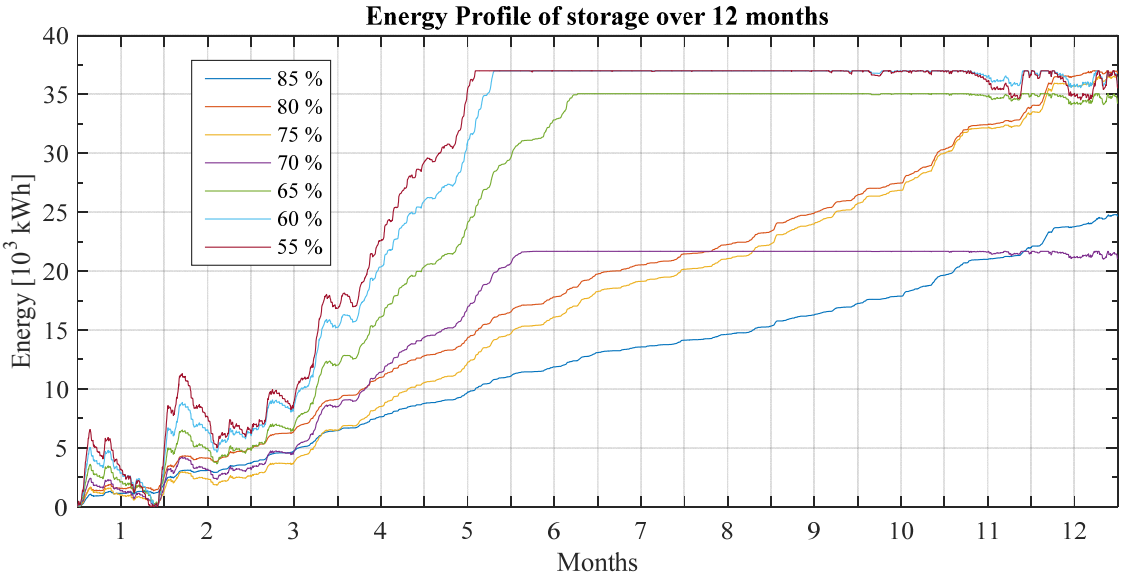

Figure C- 22: Energy profile for Wind - Storage system at different desire maximum demand for q = 0.75 at bus Kn0_13

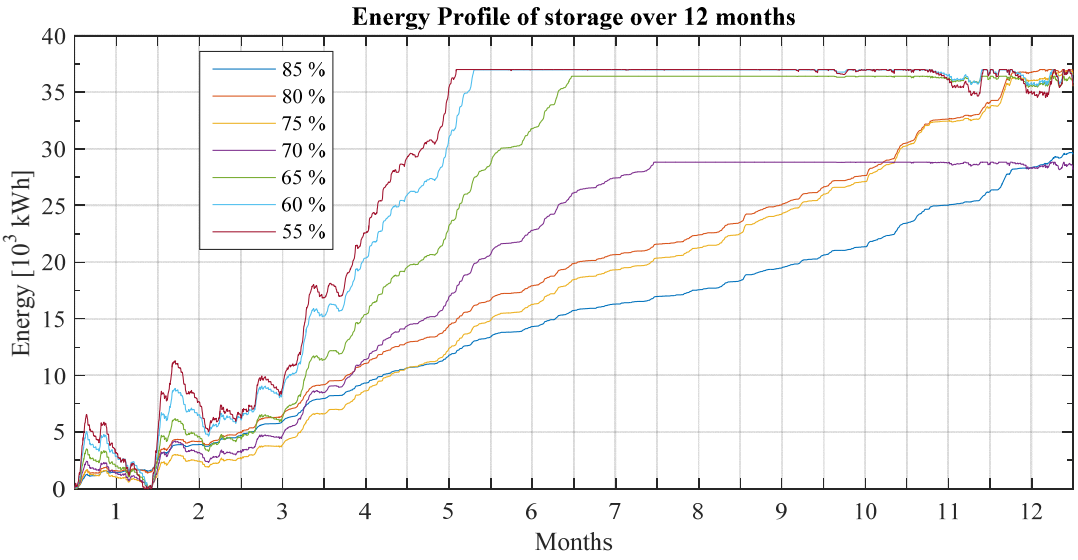

Figure C- 23: Energy profile for Wind - Storage system at different desire maximum demand for q = 1.25 at bus Kn0_13

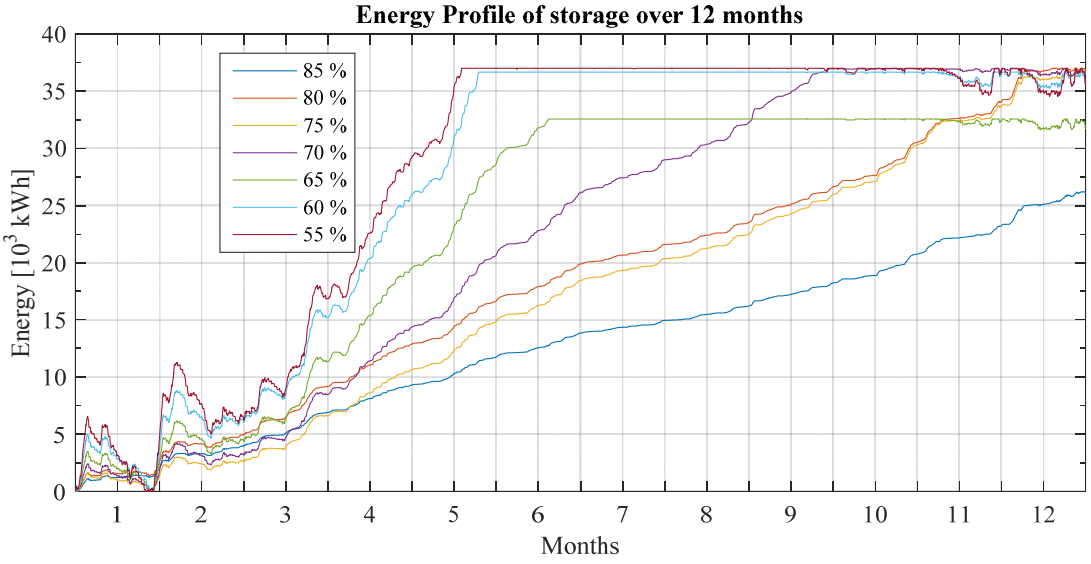

Figure C- 24: Energy profile for Wind - Storage system at different desire maximum demand for q = 1.5 at bus Kn0_13

7. Polynomial Surface Approximation Plots and Coefficeint

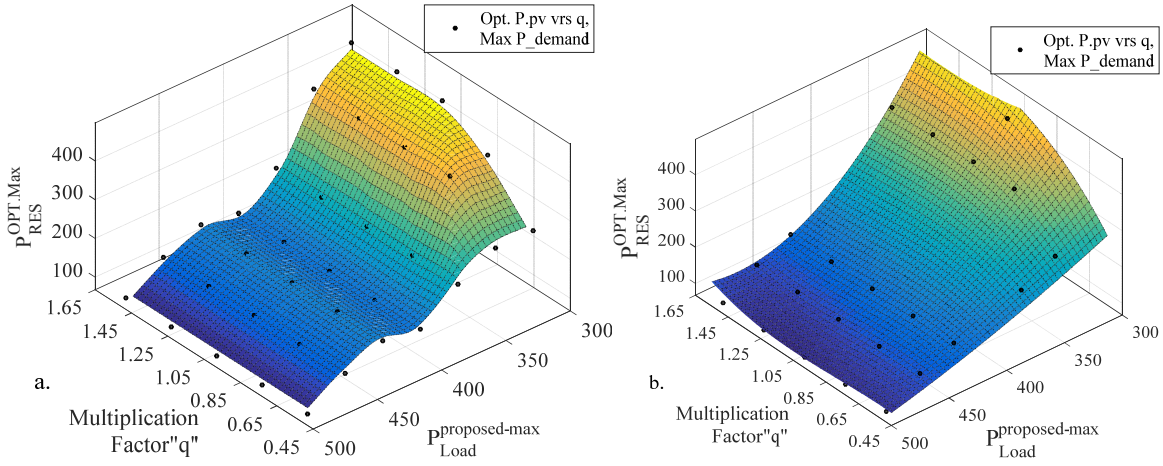

Figure C- 25: Curve fitting plot of $P_{RES}^{OPT.Max}$ versus "q" and fixed P_{Load}^{ideal} for PV – Storage system at bus Kn0_12; (a) is the interpolated surface fit of result in Table 6-9, (b) is the polynomial surface approximation with two variables.

Table C- 1: Coefficient and confidence bounds valid for polynomial surface fit shown in Figure C- 25(b)

Coefficient		Confidence bounds	
		Lower	Upper
C_1	-872	-2971	1227
C_2	4469	1755	7184
C_3	3.801	-6.016	13.6
C_4	-1245	-2780	290.1
C_5	-14.62	-24.5	-4.736
C_6	-0.00387	-0.01566	0.0079
C_7	126.6	-312.6	565.9
C_8	1.902	-0.0017	3.806
C_9	0.01216	0.0010	0.0233

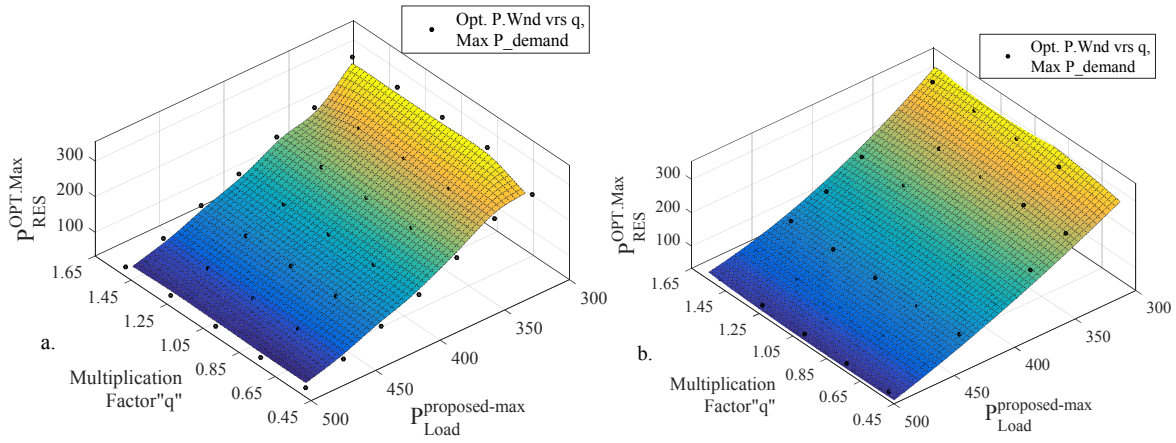

Figure C- 26: Curve fitting plot of $P_{RES}^{\mathrm{OPT}.Max}$ versus "q" and fixed $P_{Load}^{proposed\_\max}$ for Wind – Storage system at bus Kn0_12; (a) is the interpolated surface fit of result in Table 6-11, (b) is the polynomial surface fit with two variables.

Table C- 2: Coefficient and confidence bounds valid for polynomial surface fit in shown in Figure C- 26(b)

Coefficient		Confidence bounds	
		Lower	Upper
C_1	-872	-2971	1227
C_2	4469	1755	7184
C_3	3.801	-6.016	13.6
C_4	-1245	-2780	290.1
C_5	-14.62	-24.5	-4.736
C_6	-0.00387	-0.01566	0.0079
C_7	126.6	-312.6	565.9
C_8	1.902	-0.0017	3.806
C_9	0.01216	0.0010	0.0233

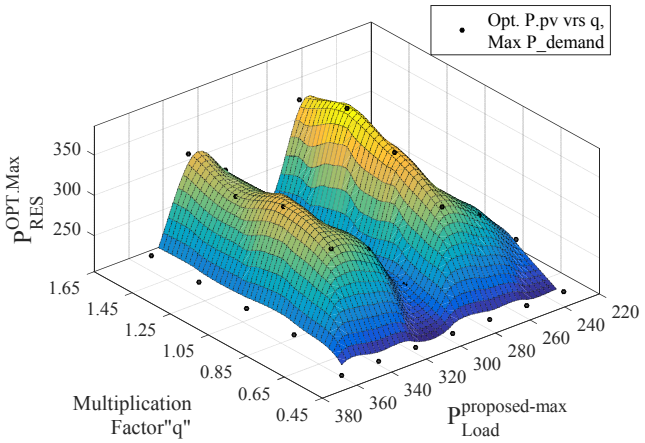

Figure C- 27: Curve fitting plot of $P_{RES}^{OPT.Max}$ versus "q" and fixed P_{Load}^{ideal} for PV – Storage system at bus Kn0_13; interpolated surface fit of result in Table 6-15

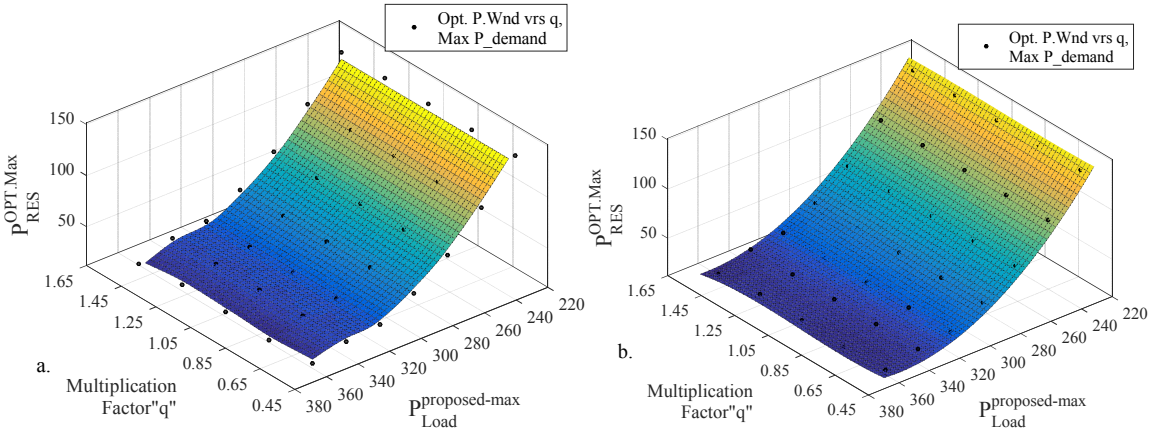

Figure C- 28: Curve fitting plot of $P_{RES}^{OPT.Max}$ versus "q" and fixed P_{Load}^{ideal} for Wind – Storage system at bus Kn0_13; 'a' is the interpolated surface fit of result in Table 6-17, 'b' is the polynomial surface fit with two variables.

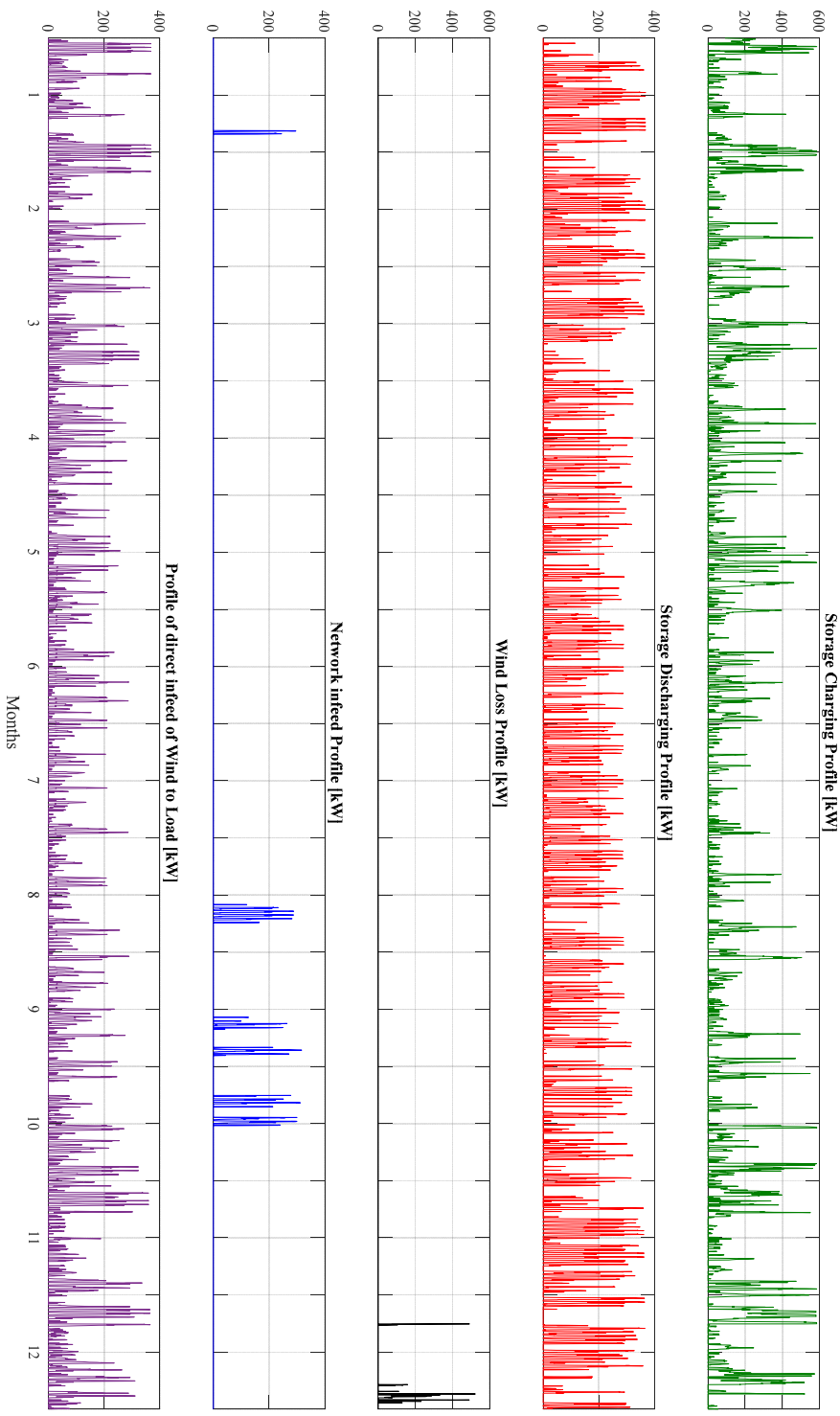

Figure C- 29: Plot of power profiles for Case 3 at Kn0_12: Storage charging in the presence of Wind Power generation (green), Storage discharge in instance of need (red),unutilized power from Wind Power generator at instance of fully charged battery or higher power output than rated power of storage (black), extra needed demand other than agreed P_{Load}^{ideal} supplied by utility (blue), direct supply from Wind Power generator to load when demand exceed P_{Load}^{ideal}

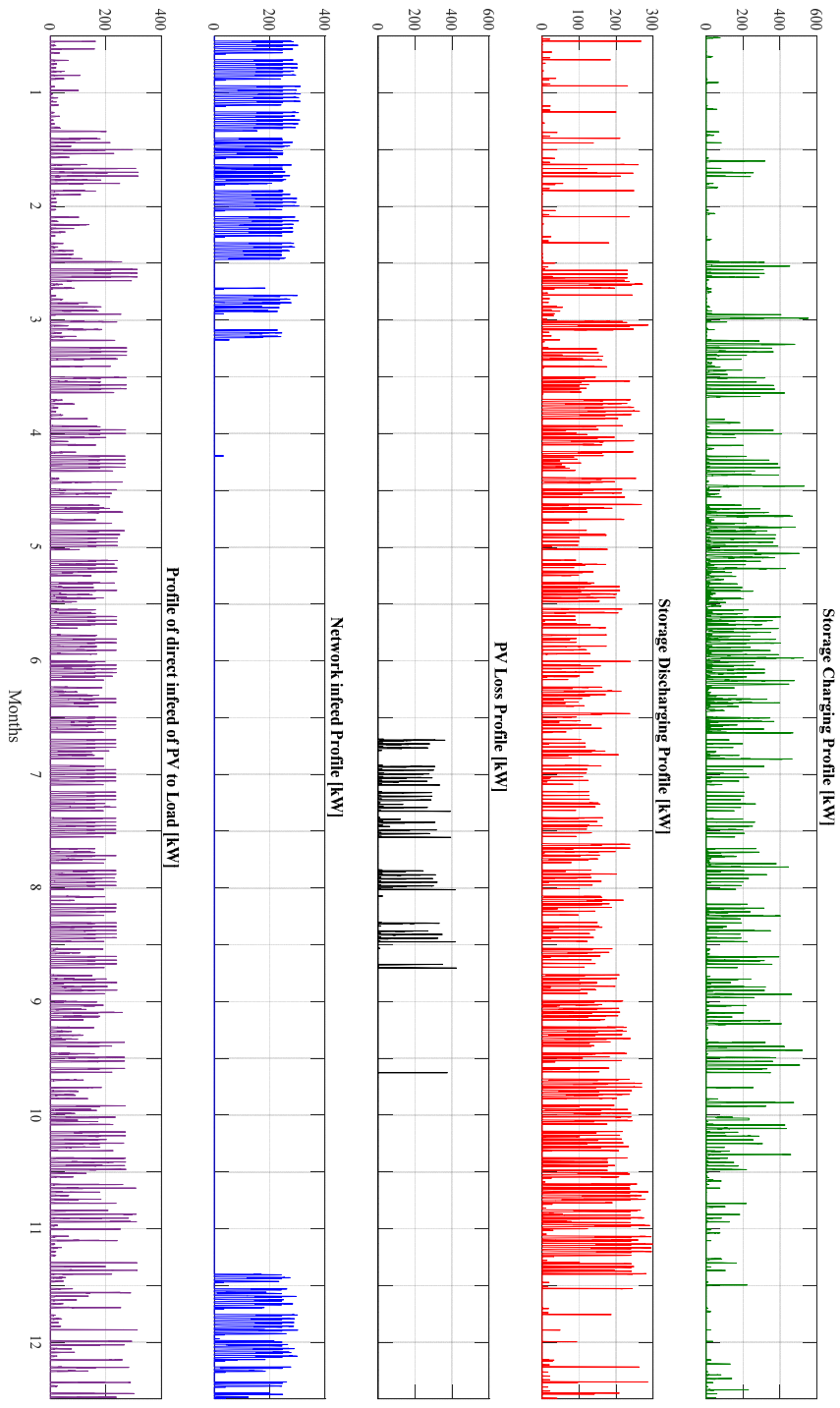

Figure C- 30: Plot of power profiles for Case 2 at Kn0_12: Storage charging in the presence of PV Power generation (green), Storage discharge in instance of need (red), unutilized power from PV Power generator at instance of fully charged battery or higher power output than rated power of storage (black), extra needed demand other than agreed P_{Load}^{ideal} supplied by utility (blue), direct supply from Wind Power generator to load when demand exceed P_{Load}^{ideal}

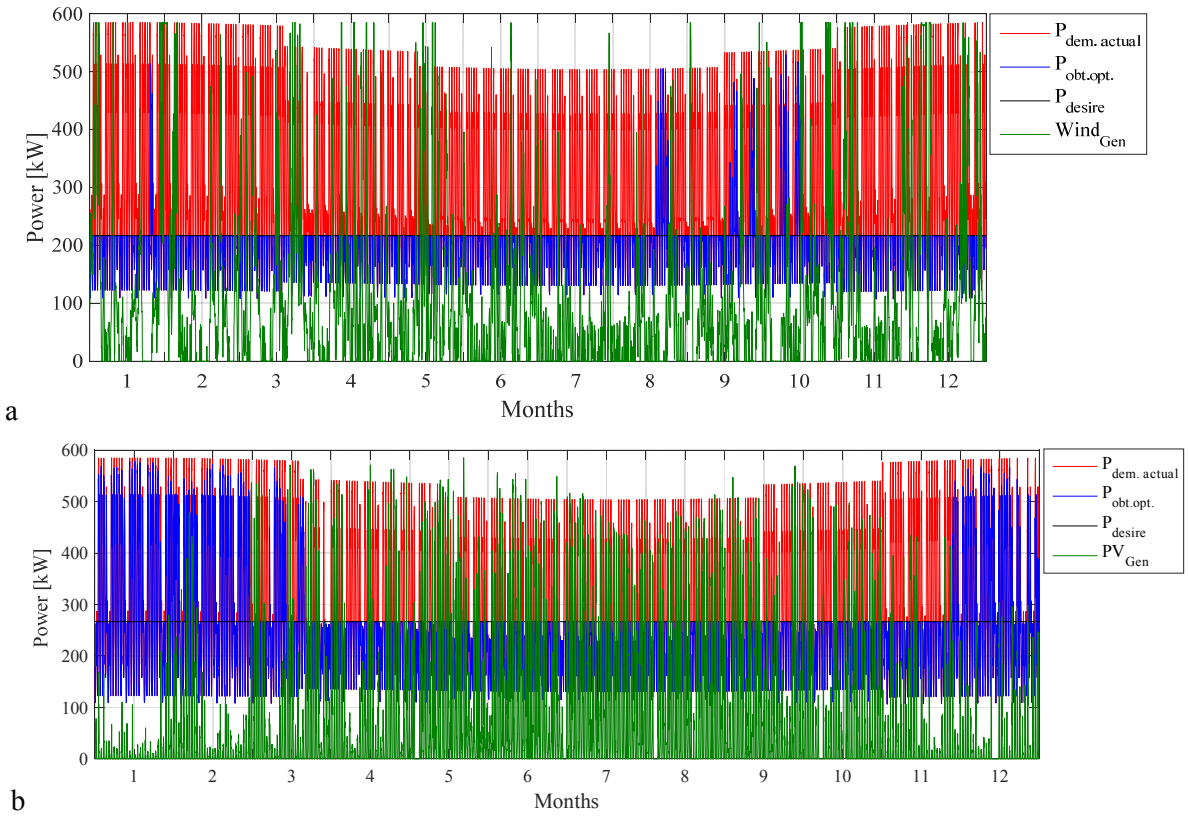

Figure C- 31: Plot of power profiles for Case 3 at bus Kn01_12: Actual load profile (red), Optimal maximum demand utility should support P_{Load}^{ideal} (black), resulting profile of supply from utility (blue), power generation from PV(green) in (a), power generation from Wind Plant (green) in (b)

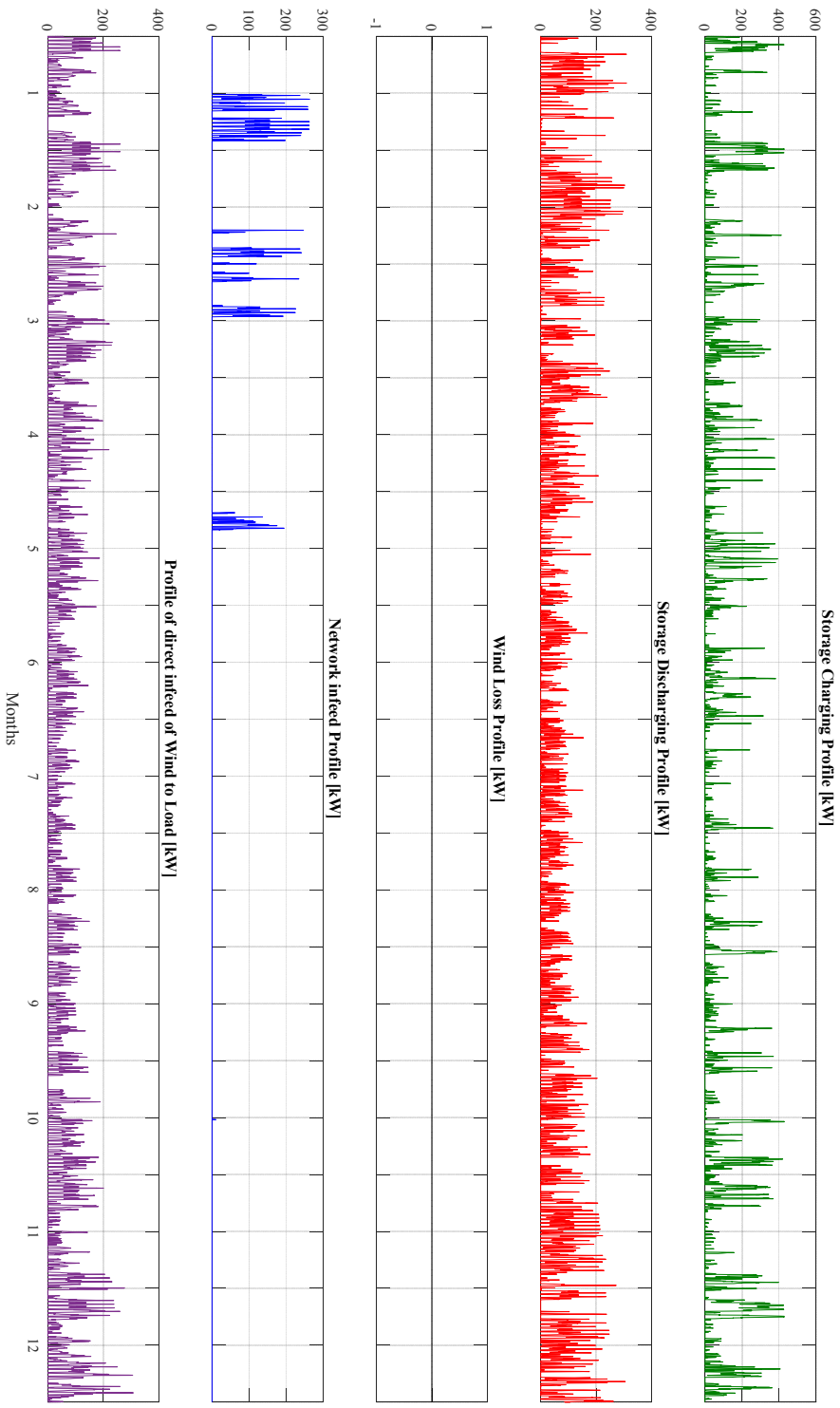

Figure C- 32: Plot of power profiles for Case 3 at Kn0_13: Storage charging in the presence of Wind Power generation (green), Storage discharge in instance of need (red) unutilized power from Wind Power generator at instance of fully charged battery or higher power output than rated power of storage (black), extra needed demand other than agreed P_{Load}^{ideal} supplied by utility (blue), direct supply from Wind Power generator to load when demand exceed P_{Load}^{ideal}

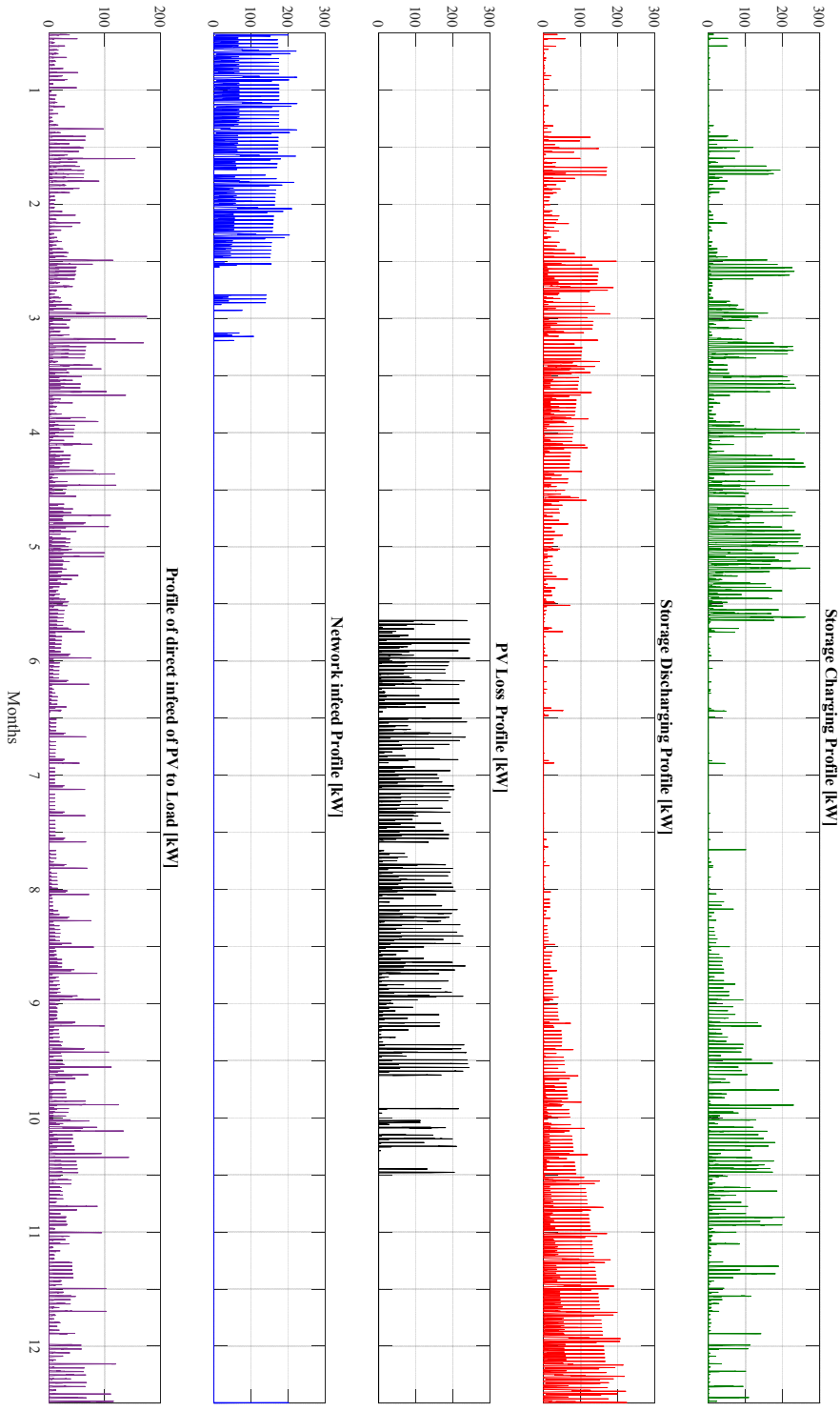

Figure C- 33: Plot of power profiles for Case 3 at Kn0_13: Storage charging in the presence of PV Power generation (green), Storage discharge in instance of need (red), unutilized power from PV Power generator at instance of fully charged battery or higher power output than rated power of storage (black), extra needed demand other than agreed P_{Load}^{ideal} supplied by utility (blue), direct supply from Wind Power generator to load when demand exceed P_{Load}^{ideal}

8. Results of Simulation with Resulting load Profile after Sizing at Kn0_11

Table C- 3: Voltage levels at buses with PV – Storage System at Kn0_11

Bus		Kn0_11			Kn0_1			Kn01		
q	$P_{Load}^{proposed.max}$ [kW]	V_max [pu]	V_min [pu]	V_mean [pu]	V_max [pu]	V_min [pu]	V_mean [pu]	V_max [pu]	V_min [pu]	V_mean [pu]
0.5										
	614.13	1.02	0.93	0.98	1.03	0.96	1.00	1.00	0.99	0.99
	578.00	1.02	0.93	0.98	1.03	0.96	1.02	1.00	0.99	0.99
	541.88	1.02	0.94	0.98	1.03	0.96	1.00	1.00	0.99	0.99
	505.75	1.02	0.94	0.98	1.03	0.96	1.00	1.00	0.99	0.99
	469.63	1.02	0.94	0.98	1.03	0.96	1.00	1.00	0.99	0.99
	433.50	1.02	0.94	0.98	1.03	0.96	1.00	1.00	0.99	0.99
	397.38	1.02	0.94	0.98	1.03	0.96	1.00	1.00	0.99	0.99
0.75										
	614.13	1.02	0.93	0.98	1.03	0.96	1.00	1.00	0.99	0.99
	578.00	1.02	0.93	0.98	1.03	0.96	1.00	1.00	0.99	0.99
	541.88	1.02	0.94	0.98	1.03	0.96	1.00	1.00	0.99	0.99
	505.75	1.05	0.94	0.98	1.05	0.96	1.00	1.00	0.99	0.99
	469.63	1.05	0.94	0.98	1.05	0.96	1.00	1.00	0.99	0.99
	433.50	1.02	0.94	0.98	1.03	0.96	1.00	1.00	0.99	0.99
	397.38	1.02	0.94	0.98	1.03	0.96	1.00	1.00	0.99	0.99
1.0										
	614.13	1.02	0.93	0.98	1.03	0.96	1.00	1.00	0.99	0.99
	578.00	1.02	0.93	0.98	1.03	0.96	1.00	1.00	0.99	0.99
	541.88	1.02	0.94	0.98	1.03	0.96	1.00	1.00	0.99	0.99
	505.75	1.02	0.94	0.98	1.03	0.96	1.00	1.00	0.99	0.99
	469.63	1.02	0.94	0.98	1.03	0.96	1.00	1.00	0.99	0.99
	433.50	1.02	0.94	0.98	1.03	0.96	1.00	1.00	0.99	0.99
	397.38	1.02	0.94	0.98	1.03	0.96	1.00	1.00	0.99	0.99
1.25										
	614.13	1.02	0.93	0.98	1.03	0.96	1.00	1.00	0.99	0.99
	578.00	1.02	0.93	0.98	1.03	0.96	1.00	1.00	0.99	0.99
	541.88	1.05	0.94	0.98	1.05	0.96	1.00	1.00	0.99	0.99
	505.75	1.02	0.94	0.98	1.03	0.96	1.00	1.00	0.99	0.99
	469.63	1.02	0.94	0.98	1.03	0.96	1.00	1.00	0.99	0.99
	433.50	1.02	0.94	0.98	1.03	0.96	1.00	1.00	0.99	0.99
	397.38	1.02	0.94	0.98	1.03	0.96	1.00	1.00	0.99	0.99
1.50										
	614.13	1.02	0.93	0.98	1.03	0.96	1.00	1.00	0.99	0.99
	578.00	1.02	0.93	0.98	1.03	0.96	1.00	1.00	0.99	0.99
	541.88	1.02	0.94	0.98	1.03	0.96	1.00	1.00	0.99	0.99
	505.75	1.02	0.94	0.98	1.03	0.96	1.00	1.00	0.99	0.99
	469.63	1.02	0.94	0.98	1.03	0.96	1.00	1.00	0.99	0.99
	433.50	1.02	0.94	0.99	1.02	1.00	0.97	1.00	0.99	0.99
	397.38	1.02	0.93	0.98	1.03	0.96	1.00	1.00	0.99	0.99

Table C- 4: Voltage levels at buses with Wind – Storage System at Kn0_11

Bus		Kn0_11			Kn0_1			Kn01		
q	$P_{Load}^{proposed.max}$ [kW]	V_max [pu]	V_min [pu]	V_mean [pu]	V_max [pu]	V_min [pu]	V_mean [pu]	V_max [pu]	V_min [pu]	V_mean [pu]
0.5										
	614.13	1.02	0.95	0.98	1.03	0.97	1.00	1.00	0.99	0.99
	578.00	1.02	0.94	0.98	1.03	0.97	1.00	1.00	0.99	0.99
	541.88	1.02	0.95	0.98	1.03	0.98	1.00	1.00	0.99	0.99
	505.75	1.02	0.96	0.98	1.03	0.98	1.00	1.00	0.99	0.99
	469.63	1.02	0.93	0.98	1.03	0.96	1.00	1.00	0.99	0.99
	433.50	1.02	0.94	0.98	1.03	0.96	1.00	1.00	0.99	0.99
	397.38	1.02	0.94	0.98	1.03	0.96	1.00	1.00	0.99	0.99
0.75										
	614.13	1.02	0.94	0.98	1.03	0.97	1.00	1.00	0.99	0.99
	578.00	1.02	0.94	0.98	1.03	0.97	1.00	1.00	0.99	0.99
	541.88	1.02	0.95	0.98	1.03	0.98	1.00	1.00	0.99	0.99
	505.75	1.05	0.96	0.98	1.05	0.98	1.00	1.00	0.99	0.99
	469.63	1.05	0.96	0.99	1.05	0.98	1.00	1.00	0.99	0.99
	433.50	1.02	0.93	0.99	1.03	0.96	1.00	1.00	0.99	0.99
	397.38	1.02	0.93	0.99	1.03	0.96	1.00	1.00	0.99	0.99
1.0										
	614.13	1.02	0.95	0.98	1.03	0.97	1.00	1.00	0.99	0.99
	578.00	1.02	0.94	0.98	1.03	0.98	1.00	1.00	0.99	0.99
	541.88	1.02	0.95	0.98	1.03	0.98	1.00	1.00	0.99	0.99
	505.75	1.02	0.96	0.98	1.03	0.98	1.00	1.00	0.99	0.99
	469.63	1.02	0.96	0.99	1.03	0.98	1.00	1.00	0.99	0.99
	433.50	1.02	0.97	0.99	1.03	0.96	1.00	1.00	0.99	0.99
	397.38	1.05	0.98	1.01	1.05	0.99	1.02	1.00	0.99	0.99
1.25										
	614.13	1.02	0.95	0.98	1.03	0.97	1.00	1.00	0.99	0.99
	578.00	1.02	0.94	0.98	1.03	0.98	1.00	1.00	0.99	0.99
	541.88	1.02	0.95	0.98	1.05	0.98	1.00	1.00	0.99	0.99
	505.75	1.02	0.96	0.98	1.03	0.98	1.00	1.00	0.99	0.99
	469.63	1.02	0.96	0.99	1.03	0.98	1.00	1.00	0.99	0.99
	433.50	1.02	0.97	0.99	1.03	0.98	1.00	1.00	0.99	0.99
	397.38	1.02	0.95	0.99	1.03	0.97	1.00	1.00	0.99	0.99
1.50										
	614.13	1.02	0.95	0.98	1.03	0.97	1.00	1.00	0.99	0.99
	578.00	1.02	0.94	0.98	1.03	0.97	1.00	1.00	0.99	0.99
	541.88	1.02	0.95	0.98	1.03	0.98	1.00	1.00	0.99	0.99
	505.75	1.02	0.96	0.98	1.03	0.98	1.00	1.00	0.99	0.99
	469.63	1.02	0.96	0.99	1.03	0.98	1.00	1.00	0.99	0.99
	433.50	1.02	0.97	0.99	1.02	0.98	1.00	1.00	0.99	0.99
	397.38	1.02	0.95	0.99	1.03	0.97	1.00	1.00	0.99	0.99

Voltages at buses at the various levels of ‘q’ can be seen to be with the acceptable operation limit as stipulated by IEC voltage standard.

Table C- 5: Current at buses with PV- Storage System at Kn0_11

Bus		Kn0_11			Kn0_1		
q	$P_{Load}^{proposed.max}$ [kW]	I_max [A]	I_min [A]	I_mean [A]	I_max [A]	I_min [A]	I_mean [A]
0.5							
	614.13	1307.10	581.92	892.30	2654.70	843.06	1654.90
	578.00	1307.10	581.92	874.88	2652.80	843.06	1636.70
	541.88	1307.10	581.92	852.45	2650.20	843.06	1613.30
	505.75	1307.10	581.92	834.68	2648.50	843.06	1594.90
	469.63	1307.10	581.92	835.14	2648.5	843.06	1595.6
	433.50	1307.10	581.92	835.41	2648.5	843.06	1595.9
	397.38	1307.10	581.92	835.61	2648.50	843.06	1596.20
0.75							
	614.13	1307.10	581.92	892.30	2654.70	843.06	1654.90
	578.00	1307.10	581.92	874.88	2652.80	843.06	1636.70
	541.88	1307.10	581.92	852.45	2650.20	843.06	1613.30
	505.75	1307.10	581.92	827.35	2647.2	843.06	1587.20
	469.63	1307.10	581.92	802.23	2643.7	843.06	1561.20
	433.50	1307.10	581.92	802.21	2643.7	843.06	1561.50
	397.38	1307.10	581.92	802.09	2643.7	843.06	1561.50
1.0							
	614.13	1307.10	581.92	892.30	2654.70	843.06	1654.90
	578.00	1307.10	581.92	874.88	2652.80	843.06	1636.70
	541.88	1307.10	581.92	852.45	2650.20	843.06	1613.3
	505.75	1307.10	581.92	827.35	2647.20	843.06	1587.20
	469.63	1307.10	581.92	800.55	2643.40	843.06	1559.50
	433.50	1307.10	581.92	774.19	2638.90	843.06	1532.30
	397.38	1307.10	581.92	772.64	2638.90	843.06	1531.00
1.25							
	614.13	1307.10	581.92	892.30	2654.70	843..06	1654.90
	578.00	1307.10	581.92	874.88	2652.80	843.06	1636.70
	541.88	1307.10	581.92	852.45	2650.20	843.06	1613.30
	505.75	1307.10	581.92	827.35	2647.20	843.06	1587.20
	469.63	1307.10	581.92	800.55	2643.40	843.06	1559.50
	433.50	1307.10	581.92	772.10	2638.50	843.06	1530.10
	397.38	1307.10	581.92	749.61	2634.10	843.06	1507.10
1.50							
	614.13	1307.10	581.92	892.30	2654.70	843.06	1654.90
	578.00	1307.10	581.92	874.88	2652.80	843.06	1636.70
	541.88	1307.10	581.92	852.45	2650.20	843.06	1613.30
	505.75	1307.10	581.92	827.35	2647.20	843.06	1587.20
	469.63	1307.10	581.92	800.55	2643.40	843.06	1559.50
	433.50	1307.10	581.92	772.10	2638.50	843.06	1530.10
	397.38	1307.10	581.92	739.09	2631.50	843.06	1496.200

Table C- 6: Current at buses with Wind – Storage System at Kn0_11

Bus		Kn01_11			Kn01_1		
q	$P_{Load}^{proposed.max}$ [kW]	I_max [A]	I_min [A]	I_mean [A]	I_max [A]	I_min [A]	I_mean [A]
0.5							
	614.13	1103.50	581.92	886.75	2504.50	843.06	1649.00
	578.00	1202.6	581.92	864.95	2585.80	843.06	1626.20
	541.88	964.69	581.92	864.95	2357.8	843.04	1598.00
	505.75	896.34	581.92	2285.60	2285.6	843.06	1566.40
	469.63	1103.50	581.92	886.75	28695	843.06	1566.40
	433.50	1307.10	581.92	790.32	2658.0	843.06	1548.90
	397.38	1307.10	581.92	790.00	26580	843.06	1548.10
0.75							
	614.13	1228.0	581.92	886.79	2633.8	843.06	1649.10
	578.00	1202.60	581.92	864.95	2585.58	843.06	1626.20
	541.88	964.688	581.92	837.82	2357.80	843.06	1598.00
	505.75	896.34	581.92	807.51	2285.60	843.06	1566.40
	469.63	828.65	581.92	771.08	2214.20	843.06	1528.60
	433.50	1306.40	581.92	745.19	2656.20	843.06	1501.90
	397.38	1307.00	581.92	739.57	2657.00	843.06	1496.40
1.0							
	614.13	1103.50	581.92	886.75	2504.50	843.06	1649.00
	578.00	1202.60	581.92	864.95	2585.80	843.06	1626.20
	541.88	964.69	581.92	837.82	2357.80	843.06	1598.00
	505.75	896.34	581.92	807.51	2285.60	843.06	1566.40
	469.63	828.65	581.92	771.08	2214.20	843.06	1528.60
	433.50	761.60	581.92	727.62	2143.50	843.06	1483.70
	397.38	1306.4	581.92	702.56	2656.6	843.06	1458.00
1.25							
	614.13	1103.50	581.92	886.75	2504.50	843.06	1649.00
	578.00	1202.60	581.92	864.95	2585.80	843.06	1626.20
	541.88	964.69	581.92	837.82	2357.80	843.06	1598.00
	505.75	896.34	581.92	807.51	2285.60	843.06	1566.40
	469.63	828.65	581.92	771.08	2214.2	843.06	1528.60
	433.50	761.60	581.92	727.62	2143.5	843.06	1483.70
	397.38	1200.50	581.92	681.18	2410.3	843.06	1435.90
1.50							
	614.13	1103.50	581.92	886.75	2504.50	843.06	1649.00
	578.00	1202.60	581.92	864.95	2585.80	843.06	1626.20
	541.88	964.69	581.92	837.82	2357.80	843.06	1598.00
	505.75	896.34	581.92	807.51	2285.6	843.06	1566.40
	469.63	828.65	581.92	771.08	2214.20	843.06	1528.60
	433.50	761.60	581.92	727.62	2143.50	843.06	1483.70
	397.38	1200.50	581.92	681.18	2410.3	843.06	1435.90

List of Figures

List of Tables

Reference

[1] K. West, States of Matter; Gases, Liquids and Solids, New York: Infobase Publishing, 2007.

[2] Encyclopaedia Britannica, “Sir Charles Algernon Parsons, British Engineer,” [Online]. Available: https://www.britannica.com/biography/Charles-Algernon-Parsons.

[3] Enerdata Intelligence+consulting, “Global Energy Statistical Yearbook 2015,” 2015. [Online]. Available: https://yearbook.enerdata.net/#energy-primary-production.html. [Accessed 5 February 2015].

[4] International Energy Agency, “International Energy Agency: Statistics: Related Surveys: Monthly Electricity Survey,” [Online]. Available: http://www.iea.org/statistics/relatedsurveys/monthlyelectricitysurvey/. [Accessed 05 03 2015].

[5] J. Vasconcelos, S. Ruester, X. He, E. Chong and J.-M. Glachant, “Electricity Storage: How to Facilitate its Deployment and Operation in the EU,” THINK, Firenze, 2012.

[6] European Union, “DIRECTIVE 2005/89/EC OF THE EUROPEAN PARLIAMENT AND OF THE COUNCIL,” European Union, 2006.

[7] European Union, “Security of supply of electricity,” [Online]. Available: http://eur-lex.europa.eu/legal-content/EN/TXT/?uri=URISERV%3Al27016. [Accessed 2015].

[8] U.S. Energy Information Administration, “International Energy Statistics,” [Online]. Available: http://www.eia.gov/cfapps/ipdbproject/iedindex3.cfm?tid=6&pid=34&aid=12&cid=r3,&syid=2008&eyid=2012&unit=BKWH. [Accessed 5 February 2015].

[9] European Commission, “European Commission Energy,” 2015. [Online]. Available: https://ec.europa.eu/energy/en/statistics/country. [Accessed 06 February 2015].

[10] The European Wind Energy Association, “Wind in Power, 2014 European Statistics,” The European Wind Energy Association, 2015.

[11] European Commission, “Communication from the commission to the European Parliament, the council, the European Economic and Social Committee and the Commitee of the regions, A policy framework for climate and energy in the period

from 2020 to 2030," European Commission, Brussels, 2014.

[12] M. Alghanim and P. Mallick, "Utilization of Smart Grid and Renewable Energy towards a Sustainable Future in Saudi Arabia," in *Internationa Conference on Renewable Energyies and Power Quality*, La Coruna, 2015.

[13] V. Fthenakis, J. E. Manson and K. Zweibel, "The Technical, geographical and economic feasibility for Solar energy to supply the energy needs of the United States," *Energy Policy,* vol. 37, pp. 387 - 399, 2009.

[14] "Master data for EEG generators," 50 Hertz Transmission, 2015. [Online]. Available: http://www.50hertz.com/en/Renewables/Disclosure-of-EEG-data/Master-data-for-EEG-generators. [Accessed 2015].

[15] P. E. Morthorst, H. Auer, A. Garrad and I. Blanco, "The Economics of Wind Power," in *Wind Energy - The Facts*, London, Sterling VA, Earthscan, 2009, pp. 227 - 238.

[16] European Commission, "European Commission guidance for the design of renewable support schemes," European Comission, Brussels, 2013.

[17] J. M. Rodrigues, A. J. Alves, E. G. Doingues and W. P. Calixto, "A Technical and Economical Study of a Photovoltaic System Installed on the Rooftop of a Public Building," in *International Conference on Renewable Energies and Power Quality*, La Coruna, 2015.

[18] Bundesministerium für Wirtschaft und Energie, "Informationsportal Eneuerbare Energien," 2015. [Online]. Available: https://www.erneuerbare-energien.de/EE/Redaktion/DE/Downloads/EEG/eeg_2014_engl.pdf?__blob=publicationFile&v=4. [Accessed 6 February 2015].

[19] R. Moesgaard, H. Chandler, P. Barons and G. Kakema, "The Economics of Wind Power," in *Wind Energy - The Facts; A guide to the technology, economics and future of wind power*, London, Earthscan, 2009, pp. 200 - 258.

[20] European Commission , "European Commission guidance for the design of renewable support schemes," European Commission , Brussels, 2013.

[21] "Erneuerbare Energien - Speicher," KFW Bank aou Verantwortung, 01 2015. [Online]. Available: https://www.kfw.de/Download-Center/F%C3%B6rderprogramme-(Inlandsf%C3%B6rderung)/PDF-Dokumente/6000002700_M_275_Speicher.pdf.

[22] C. Märtel, "KfW Förderung für Batteriespeicher," Solaranlagen-Portal, [Online]. Available: http://www.solaranlagen-portal.com/photovoltaik/stromspeicher/foerderung.

[23] N. Screckovic and G. Stumberger, “The Impact of Photovoltaic Systems on Power losses and voltage profiles in a real medium voltage distribution network,” in *International Conference on Renewable Energies and Power Quality*, La Coruna, 2015.

[24] P. D. Lund, J. Lindgern, J. Mikkola and J. Salpakari, “Review of energy system flexibility measures to enable high levels of variable renewable electricity,” *Renewable and Sustainable Energy Reviews,* vol. 45, no. 5, pp. 785 - 807, 2015.

[25] A. S. Brouwer, M. van den Broek, A. Seebregts and A. Faaij, “Impacts of large-scale Intermittent Renewable Energy Sources on electricity systems and how thes can be modeled,” *Renewable and Sustainable Energy Reviews,* vol. 33, no. 5, pp. 443 - 466, 2014.

[26] Fraunhofer Institute for Solar Energy Systems ISE , “Recent Facts about Photovoltaics in Germany,” Fraunhofer Institute, Feiburg, 2015.

[27] TenneT , “Einspeisemanagement,” TenneT Holding B.V, 2015. [Online]. Available: http://www.tennet.eu/de/en/customers/eegkwk-g/einspeisemanagement/background-of-feed-in-management.html. [Accessed 2015].

[28] SAE IT-Systems, “Renewable energy feed-in management Telecontrol in the SMART Grid,” SAE IT Systems, Köln, 2016.

[29] Bundesverband der Energie- und Wasser- wirtshaft e. V., “Technical Guideline "Generating Plants connected to the medium-voltage network",” Bundesverband der Energie- und Wasser- wirtshaft e. V., Berlin, 2008.

[30] D. J. Glover and M. S. Sarma, Power System Analysis and design, Califonia: Brooks/Cole, 2002.

[31] M. Nick, M. Hohmann, R. Cherkaoui and M. Paolone, “On the optimal placement of distributed storage systems for voltage control in active distributioin networks,” in *2012 3rd IEEE PES International Conference and Exhibition on Innovative Smart Grid Technologies (ISGT Europe)*, Berlin, 2012.

[32] C. Bassar, M. Moss, R. Alvarez, P. Wolf, T. Thien, H. Chen, Z. Cai, M. Leuthold, D. U. Sauer and A. Moser, “Optimal Allocation and Capacity of Energy Storage Systems in a Future European Power System with 100% Renewable Energy Generation,” *Energy Procedia,* vol. 46, pp. 40 - 47, 2013.

[33] W. Z. Chen, Q. B. Li, L. Shi, Y. Luo, D. D. Zhan, N. Shi and K. Liu, “Energy Storage Sizing for Dispatchability of Wind Farm,” in *11th International Conference on Environment and Electrical Engineering (EEEIC)*, Venice, 2012.

[34] “Utility-Scale Smart Meter Deployments: Building blocks of the evolving power

grid," Edison Foundation, Pennsylvania, 2014.

[35] R. v. Gerwen, S. Jaarsma and R. Wilhite, "Smart Metering," July 2006. [Online]. Available: http://www.leonardo-energy.org/sites/leonardo-energy/files/root/pdf/2006/SmartMetering.pdf.

[36] Ernst & Young, "Cost-benefit analysis for the comprehensive use of smart metering," Ernst & Young GmbH, 2013.

[37] X. Luo, J. Wang, D. Mark and C. Jonathan, "Overview of Current development in Electrical Storage Technologies and the application potential in power system operation," *Applied Energy,* vol. 137, pp. 511 - 536, 2014.

[38] International Electrotechnical Commission, "Electrical Energy Storage," International Electrotechnical Commission, Geneva, 2011.

[39] International Renewable Energy Agency, "Battery Storage For Renewables: Market Status and Technology Outlook," International Renewable Energy Agency, Bonn, 2015.

[40] A. K. Barnes, J. C. Balda, A. Escobar-Mejia and S. O. Geurin, "Placement of Energy Storage Coordinated with Smart PV Inverters," 2011.

[41] Y. Liu, W. Du, L. Xiao, H. Wang and J. Cao, "A Method for Sizing Energy Storage System to Increase Wind Penetration as Limited by Grid Frequency Deviations," *IEEE Transactions on Power Systems.*

[42] A. Arabali, M. Ghofrani, M. Etezadi-Amoli and M. S. Fadali, "Stochastic Performance Assessment and Sizing for a Hybrid Power System of Solar/Wind/Energy Storage," *IEEE Transactions on Sustainable Energy,* vol. 5, no. 2, pp. 363-371, 2014.

[43] K. Yang and A. Walid, "Outage-Storage Tradeoff in Frequency Regulation for Smart Grid With Renewables," *IEEE Transactions on Smart Grid,* vol. 4, no. 1, pp. 245 - 252, 2013.

[44] A. K. Barnes, J. C. Balda, A. Escobar-Mejia and S. O. Geurin, "Placement of Energy Storage coordinated with Smart PV inverters," in *2012 IEEE PES Innovative Smart Grid Technologies*, Washington, DC, 2012.

[45] C. D'Adamo, S. Jupe and C. Abbey, "Global survey on planning and operation of active distribution networks - Update of CIGRE C6.11 working group activities," in *20th International Conference and Exhibition on Electricity Distribution - Part 1*, Prague, 2009.

[46] F. Pilo, S. Jupe, F. Silvestro, K. El Bakri, C. Abbey, G. Cekku, J. Taylor, A. Baitch

and C. Carter-Brown, “Planning and Optimisation of Active distribtuion Systems - An overview of CIGRE Working Group C6.19 activities,” in *Integration of Renewables into the Distribution Grid, CIRED 2012 Workshop*, Lisbon, 2012.

[47] X. Luo, J. Wang, M. Dooner and J. Clarke, “Overview of current development in electrical energy storage technologies and the application potential in power system operation,” *Applied Energy,* vol. 137, pp. 511 - 536, 2015.

[48] ECOFYS, “Energy Storage Opportunities and Challenges,” ECOFYS, 2014.

[49] Saft, “Energy Storage Systems-New solutions for a new energy environment,” Saft, Bagnolet, 2012.

[50] A. Inc, “Energy Storage Modules,” 2012. [Online]. Available: https://library.e.abb.com/public/f09413974e2f041cc12579e3004fa562/Energy_Storage_Modules_Brochure_Rev_E.pdf.

[51] S. I. a. C. Sector, “The modular energy storage system for a reliable power supply,” 2014. [Online]. Available: http://www.automation.siemens.com/tip-static/dlc/en/Power-Supply-Solutions/SIESTORAGE_for_Modular_Energy_Storage_System.pdf. [Accessed 2015].

[52] N. Etherden and M. H. J. Bollen, “Increasing the hosting capacity of distribution networks by curtailment of renewable energy resources,” in *IEEE PowerTech*, Trondheim, 2011.

[53] J. Smith, M. Rylander, L. Rogers and R. Dugan, “Maximizing the Benefits and Minimizing the impacts of DERs in an Integrated Grid,” *IEEE Power and Energy Magezine for electric power professionals,* vol. 13, no. 2, pp. 20-29, 2015.

[54] K. Rudion, A. Orths, Z. A. Styczynski and K. Strunz, “Design of Benchmark of Medium Voltage Distribution Network for Investigation of DG Integration,” in *Power Engineering Society General Meeting*, Montreal, 2006.

[55] K. Strunz, “Developing Benchmark Models for Studying the Integeration of Distributed Energy Resources,” in *Power Engineering Society General Meeting, 2006. IEEE*, Montreal, 2006.

[56] F. Schaller, F. Karstädt, O. Warweg and P. Bretschneider, “Modellierung realitätsnaher zukünftiger Referenznetze im Verteilnetzsektor zur Überprüfung der Elektroenergiequalität,” in *Internationaler ETG-Kongress 2011*, Würzburg, November 2011.

[57] S. Jürgen and R. Karl-Heinz, Power System Engineering - Planning, Design and Operation of Power Systems and Equipment, Weinheim: Wiley-VCH Verlag GmbH

& Co. KGaA, 2014.

[58] MITNETZ STROM, "MITNETZ STROM: Netznutzung/Netzzugang," Distribution Network Operator, [Online]. Available: https://www.mitnetz-strom.de/Netzkunden-Center/Download-Center/NetznutzungNetzzugang. [Accessed 13 January 2014].

[59] Deutscher Wetterdienst, Meteorological Data Management and Archiving, [Online]. Available: ftp://ftp-cdc.dwd.de/pub/CDC/observations_germany/climate/hourly/. [Accessed 20 February 2014].

[60] Onipko Rotor Wind Station, "Onipko Rotor," Onipko Rotor, February 2014. [Online]. Available: http://onipko.com/wp-content/uploads/2013/12/Poster.pdf. [Accessed 2015].

[61] E. Hau, Wind Turbines, Heidelberg: Springer, 2013.

[62] R. Gasch and J. Twele, Wind Power Plants, Heidelberg: Springer, 2012.

[63] E. K. P. Chong and S. H. Zak, An Introduction to Optimization, John Wiley and Sons, 2013.

[64] P. Venkataraman, Applied Optimization with Matlab Programming, John Wiley and Sons, 2002.

[65] R. A. Sarkar and C. S. Newton, Optimization Modelling, A practical Approach, Florida: CRC Press, Tylor and Francis Group, 2008.

[66] J. C. Spall, "Stochastic Optimization," in *Handbook on Computational Statistics*, Heidelberg, Springer, 2004, pp. 169-197.

[67] L. A. Hannah, 4 April 2014. [Online]. Available: http://www.stat.columbia.edu/~liam/teaching/compstat-spr15/lauren-notes.pdf. [Accessed 2 May 2015].

[68] J. Momoh A, Electric Power System Applications of Optimization, New York: Marcel Dekker Inc, 2001.

[69] MITNETZ STROM, "MITNETZ STROM: Netznutzung/Netzzugang," Distribution Network Operator, [Online]. Available: https://www.mitnetz-strom.de/irj/go/km/docs/z_ep_em_unt_documents/em/mitnetzstrom/Dokumente/HRV_Anlage_2a_MITNETZ_STROM.pdf. [Accessed 13 January 2014].

[70] T. Yoshida, M. Kato and K. Kashima, "Probabilistic Evaluation Method of Interconnectable Capacity for Wind Power Generation Using Actual Data," in *International Conference on Renewable Energies and Power Quality*, La Coruna, 2015.

[71] A. J. Lamadrid, T. D. Mount and R. J. Thomas, "Scheduling of Energy Storage

Systems with Geographically Distributed Renewables," 2011.

[72] Federal Ministry for Economic Affairs and Energy, "Lighting," Federal Ministry for Economic Affairs and Energy, 2015. [Online]. Available: http://www.efficiency-from-germany.info/ENEFF/Navigation/EN/Energyefficiency/BuildingEfficiency/Lighting/lighting.html. [Accessed 2015].

[73] US Eenergy Information Adminstration, US Eenergy Information Adminstration, April 2015. [Online]. Available: https://www.eia.gov/tools/faqs/faq.cfm?id=99&t=3.

[74] Tesla, Tesla Motors, 2015. [Online]. Available: https://www.teslamotors.com/models. [Accessed 2015].

[75] "Alternative Fuels Data Center," The AFDC is a resource of the U.S. Department of Energy's Clean Cities program, 05 2015. [Online]. Available: http://www.afdc.energy.gov/fuels/electricity_charging_home.html. [Accessed 2015].

[76] P. Bertoldi and B. Atanasiu, "Electricity Consumption and Efficiency Tends in the Enlarged European Union," 2007, Luxembourg, 2006.